2015

Comparison of Hydrologic Model Performance Statistics Using Thiessen Polygon Rain Gauge and NEXRAD Precipitation Input Methods at Different Watershed Spatial Scales and Rainfall Return Frequencies

Amanda E. Tancreto
University of North Florida, n00592251@ospreys.unf.edu

Comparison of Hydrologic Model Performance Statistics Using Thiessen Polygon Rain Gauge and NEXRAD Precipitation Input Methods at Different Watershed Spatial Scales and Rainfall Return Frequencies

by

Amanda E. Tancreto

A thesis submitted to the School of Engineering in conformity with the requirements for the degree of

Master of Science in Civil Engineering

University of North Florida

College of Computing, Engineering, and Construction

2015

The thesis "Comparison of Hydrologic Performance Statistics Using Thiessen Polygon Rain Gauge and NEXRAD Precipitation Input Methods at Different Watershed Spatial Scales and Rainfall Return Frequencies" submitted by Amanda E. Tancreto in partial fulfillment of the requirements for the degree of Master of Science in Civil Engineering has been

Approved by the thesis committee: (Date)

_____ _____

Christopher J. Brown, Ph.D., P.E.
Thesis Advisor and Committee Chairperson

_____ _____

Donald T. Resio, Ph.D., P.E., Committee Member

_____ _____

Peter Bacopoulos, Ph.D., E.I., Committee Member

Accepted for the School of Engineering:

_____ _____

Murat Tiryakioglu, Ph.D., CQE
Director of the School of Engineering

Accepted for the College of Computing, Engineering, and Construction:

_____ _____

Mark A. Tumeo, Ph.D., P.E.
Dean of the College of Computing, Engineering, and Construction

Accepted for the University of North Florida:

_____ _____

John Kantner, Ph.D.
Dean of the Graduate School

ACKNOWLEDGMENTS

I would like to recognize, first and foremost, those that helped in the completion of this thesis work. Without these individuals' contribution, this thesis would not have been possible.

My deepest appreciation goes to my advisor, Dr. Christopher Brown, who provided me with an insurmountable level of support and encouragement throughout my graduate degree and thesis research. Without his vast knowledge, guidance, and motivation, this thesis would not have been possible. I feel extremely fortunate to have been able to work with such a dedicated and knowledgeable professor. I would like to express my sincere gratitude for all his assistance throughout my education at the University of North Florida.

My thesis committee, Dr. Donald Resio and Dr. Peter Bacopoulos, have not only guided me through undergraduate and graduate coursework but also provided me with valuable feedback on my thesis research. Dr. Resio's insightful comments were always thought-provoking and helpful in constantly reviewing research from a new perspective. He is an inspiration in many ways, including his high research standards, past and present research experience, and his plethora of knowledge. Dr. Bacopoulos was one of the most talented teachers I had while working on my graduate degree. He has a gift for teaching which allowed even the most complex material to be understood.

I would also like to acknowledge Thomas Jobes from the St. Johns Water Management District. His vast understanding of the project background enabled me to complete a much more accurate model. I cannot express my appreciation enough for his assistance in data compilation and

processing. I am also grateful to my coworkers and supervisor at the U.S. Army Corps of Engineers for being supportive and understanding during this very busy time in my life.

Finally, I would like to thank my family and friends for their loving words of encouragement throughout my graduate degree. To my boyfriend, Hunter, thank you for all that you do for me. I cannot put into words how much your love, kindness, and patience has helped me through this process. I would like to extend my sincerest appreciation to my parents, Glenn and Linda, for their unwavering support and belief in my abilities.

TABLE OF CONTENTS

LIST OF TABLES

LIST OF FIGURES

ABSTRACT

As hydrological computer modeling software continues to increase in complexity, the need for further understanding of the value of different model input datasets becomes apparent. Frequently used precipitation model input include rain gauge data and next-generation radar–based (NEXRAD) rainfall data. Rain gauge data are usually interpolated across a model domain using various methods including the Thiessen Polygon methodology, which may be data-sparse in some areas and overly data-dense in others. However, rain gauge data are generally very easy to use in hydrologic model development, often requiring little to no data processing. NEXRAD data have the potential to improve hydrologic runoff estimates due to the increased spatial resolution of the data: but has its own issues regarding accuracy, false precipitation indications, and difficulties due to data processing. Previous studies have investigated the value of NEXRAD input versus traditional rain gauge data inputs for hydrologic studies; however, results are inconclusive as to which precipitation source provides more accurate results. Limited work has been done to compare the value of these datasets at multiple spatial scales, especially in Florida, a study area dominated by low topographic drive and sub-tropical weather. In addition, little to no research has been done regarding the value of NEXRAD versus rain gauge data inputs at different rainfall return frequencies. The proposed research will utilize a hydrological rain-runoff model (HEC-HMS) of the Upper St. Johns River Basin, Florida to compare the performance of the two precipitation data input types at various watershed spatial scales and rainfall return frequencies. Statistical analysis of the hydrological model "goodness-of-fit" results will be utilized to assess the watershed scaling and rainfall frequency requirements to

which NEXRAD data provide little to no advantage over standard rain gauges using the Thiessen Polygon method for estimating rainfall totals across a model domain.

Chapter 1

INTRODUCTION

Computer models that simulate hydrologic runoff processes are essential tools for understanding and describing the overall hydrologic cycle within the modeled system for proper flood forecasting. Flooding induced by storm events is of major concern for many parts of the world due to the threat of property damage, infrastructure failure, environmental concerns, economic problems, and in extreme cases loss of life. This makes predicting future flow conditions accurately and effectively a necessity for water resources planning and management. Additionally, these models can be used for important studies such as water management, water quality issues, land use changes, and many other forecasting applications. These models can vary greatly in complexity, normally due to the scale of the model, availability of physical data, and quality and completeness of input data. The success of current model development and subsequent hydrologic prediction lies in the proper selection of model input parameters. Researchers believe spatial and temporal variability of precipitation data are the main source of input data uncertainty when rainfall-runoff models are applied (Diaz-Ramirez et al., 2012). Since precipitation is the main driving mechanism for hydrologic models, selecting the suitable meteorological input dataset for precipitation becomes imperative. A major source of observed precipitation data for most watersheds in the United States (U.S.) is rain gauge data. A commonly used method, the Thiessen Polygon method, calculates the weight of each rain gauge according to the rain gauge location to create a polygon network, and applies the gauge rainfall

quantity over the polygon area. The weights of rain gauges are calculated according to the rain gauge location and mean rainfall estimations are applied to areas as is completed in the Thiessen Polygon method. Unfortunately, rain gauge networks can be somewhat sparse, leading to spatial-temporal averaging over large areas. This has led to the use of satellite-based rainfall products, such as the Next-Generation Weather Radar (NEXRAD) data, in many hydrological modeling applications due to the use of spatially continuous estimations at relatively small resolutions. Although the use of NEXRAD generated precipitation seems to have advantages over the use of gauge-measured precipitation due to its capability to capture the spatial variation of precipitation, it is subject to several sources of error when estimating the amount of actual precipitation (Kalin and Hantush, 2006). Research is needed to determine the circumstances in which NEXRAD will provide better run-off estimates than rain gauge data in hydrologic modeling.

Since the acquisition and application of precipitation data become more time consuming and expensive as the spatial resolution is increased (through the incorporation of NEXRAD data), the determination of the appropriate data source needed to provide satisfactory results in a hydrologic model is critical. Additionally, it is not presently understood how the accuracy of hydrologic models using radar and rain gauge data sources may differ over varying watershed spatial scales and rain fall intensities. This thesis provides original work regarding the relationship of hydrologic run off predication at various watershed scales and rainfall intensities using two types of precipitation input. Previous studies have noted improvements of hydrologic modeling results using a particular precipitation method input over another. However, a majority of the research has concentrated on a limited number of test watersheds, normally with small coverage areas, and large precipitation events. Limited inner comparison of watershed response improvement and its relationship at the spatial scale and rain intensity level has been completed.

The approach of this thesis will be to use the hydrologic model simulation results as an indirect assessment of the precipitation data accuracy. The focus of this research aims to provide a framework that will enable researchers to select the appropriate precipitation input dataset based on rainfall return frequency and model study area size to model rainfall-runoff relations with more efficiency.

The objectives of this thesis include the following: (i) complete a hydrologic HEC-HMS model of the Upper and portions of the Middle St. Johns River Basins that provides accurate rainfall-runoff relations with a high level of efficiency suitable for future study scenarios (ii) perform a comparative assessment of the improvement or decline in performance statistics for the model when using NEXRAD radar precipitation data versus the Thiessen Polygon method to capture the spatial variability of the rainfall distribution at both the local and regional scale (iii) provide a comparison of precipitation inputs using NEXRAD data versus rain gauge data at different return frequency which would add to the understanding of the value of using more accurate, yet more cumbersome input data (e.g. NEXRAD data) for different precipitation return frequencies (iv) provide a literature review of related work to compare research findings, similarities, and differences (v) make recommendations on how to use the results of this study for future model development and suggest areas of further research.

This thesis has been organized into five Chapters. Chapter 1 discusses the introduction to the thesis work. Chapter 2 introduces the types of datasets required for the study and presents a literature review of similar work including research findings, similarities, and differences. Chapter 3 includes details of the project area, background, and model history. Chapter 4 presents the methodology behind the model development. Chapter 5 covers the research results including; (1) a comparison of precipitation inputs for gauge and radar data to determine the resulting bias

and (2) a summary of the hydrologic results of the model and the performance statistics for both precipitation input methods. Finally, Chapter 6 provides the recommendations and conclusions drawn from the research conducted.

Chapter 2

LITERATURE REVIEW

An evaluation of the relevant literature was undertaken focusing upon two research topics: (1) assessment of radar-based versus rain gauge-based precipitation estimations, (2) evaluation of performance for hydrologic model simulations using radar and rain gauge precipitation dataset input.

2.1 Introduction to Rainfall Interpolation Methods

Traditionally, precipitation measurements from rain gauges or meteorological stations have been used as the only reliable source of precipitation in watershed modeling (Kalin and Hantush, 2006). The benefit of rain gauges is their ability to obtain a precise point value for precipitation, with minimal data processing needed for use in hydrologic applications. The limitations of rain gauge measurements stem from maintenance and operational issues such as mechanical or electrical failure, clogging, and measurement error from wind and obstructions such as vegetation or structures. However, the most severe limitation in the reliance on rain gauge technology remains the fact that the rain gauge network cannot supply information about rainfall occurring between the gauges, and as a result, the network may not fully capture rainfall events demonstrating high spatial variability (Huebner et al. 2003; Skinner et al., 2009).

In an effort to use these point measurement locations, areal averaging of measured precipitation amounts is necessary. The issues with estimation of areal averaging rainfall is that the reliability of measurements is dependent on the density, position, distribution and representation ability of

meteorological stations, and the methods applied to the data (Bayraktar, 2005). There are multiple mathematical and statistical methods with varying complexities that can be used to interpolate the areal average rainfall amount. Common methods include the Thiessen Polygon, arithmetic mean, inverse distance weighted method, isohyetal, ordinary and block Kriging methods, polynomial and spline surface interpolation, and many other alternative techniques (Ball and Luk, 1998; Cheng et al., 2010; Ly et al., 2013). One of the most commonly used approaches is the Thiessen Polygon method, which defines an individual area of influence surrounding each gauge using the application of a Thiessen Polygon network. Each polygon is formed by the perpendicular bisectors of the lines joining adjacent gauges and represents areas of effective uniform depth. It is assumed that the gauge data, which was collected at a single point, is representative of the entire Thiessen Polygon. A common problem with the Thiessen Polygon method is having an insufficient number of rain gauges in a network, thereby assuming the areal rainfall is spatially homogeneous over large areas. Previous studies investigating the performance of the Thiessen Polygon method found that for a large scale network, the Thiessen Polygon method gave fairly satisfactory results for monthly rainfall (Tabios et al., 1985). Other studies have shown that the Thiessen Polygon method is inferior to other methods (Kriging method) because it has a lesser ability to represent the spatial structure of the rainfall (Cheng et al., 2012). Failing to consider adequately, the spatial variability of rainfall will lead to errors in the runoff response, timing of peak flow, estimation of model parameters, and overall hydrological model outputs (Ly et al., 2013).

In recent years, the technological advancements for rainfall estimation using radar-based data have increased, presenting the possibility of more accurate rainfall predictions. The NEXRAD data system was initiated in the early 1990s by the National Weather Service (NWS) and consists

of a national network of radars known as the WSR-88D (Weather Surveillance Radar 1988). Currently there are over 160 WSR-88D radars in operation across the United States that are able to locate and follow precipitation within a range of 200 to 400 km. The radars emit short (250 m) pulses of coherent microwave energy which are returned to the radar as backscatter when the energy encounters a precipitation droplet (Pathak et al., 2013). From this the NEXRAD can produce reflectivity, spectrum width, and Doppler velocities (Rendon et al., 2013). The radar rainfall amounts are estimated from the reflectivity-to-rainfall (Z-R) equation because the reflectivity factor (Z) is directly related to the raindrop size distribution. Many empirical Z-R relationships have been developed because different climate conditions and rainfall characteristics can impact raindrop size distributions (Pathak et al., 2013). These empirical Z-R relationships have been routinely applied by the NWS to improve radar rainfall accuracy.

NEXRAD data provides spatially continuous estimations of rainfall at two spatial resolutions, 2 X 2 kilometer $(km)^2$ or 4 X 4 km^2. The precipitation products are categorized into four levels based on the extent of preprocess, calibration, and quality control performed (Sexton et al, 2010; Kang and Merwarde, 2014). In Stage I the Hourly Digital Precipitation is developed by entering reflectivity measurements using a Z-R (reflectivity-rainfall) relationship into the Precipitation Process System algorithm. Stage II is the product of combining stage I data with correction for bias based on a single radar site. Stage III data are a combination of stage II data and multiple weather radars covering a River Forecast Center (RFC) region (of the NWS). Finally, stage IV data combine stage III data with coverage of the entire United States. The most commonly used NEXRAD product is the stage III data because the radar rainfall rates are corrected using multiple surface rain gauges and it undergoes a significant degree of meteorological quality control by trained personnel at individual RFCs (Kang and Merwarde, 2014).

The NEXRAD data product for this study was obtained from the St. Johns River Water Management District (SJRWMD). According to their website they use a NEXRAD contractor that uses rainfall data from the Districts network of 75 rain gauges. Additionally, "The contractor receives WSR-88D NEXRAD radar for several stations from the NWS. The individual radar station data are combined into a radar mosaic that completely covers the SJRWMD territory with an array of pixels (SJRWMD, 2015)." These data are sized in approximately two by two kilometer grids, which cover the SJRWMD project area. The website also explains that the NEXRAD contractor uses proprietary geographic information system (GIS) algorithms to help reduce or eliminate any discontinuities and ground clutter from the mosaic. Finally, "the contractor combines the gauge and radar data to calculate a gauge-radar ratio and applies the ratio in a radar calibration algorithm to derive a gauge-adjusted rainfall dataset" (SJRWMD, 2015). This dataset maintains the high spatial resolution of the radar data but uses the direct measurement volumes estimates from the rain gauges (SJRWMD, 2015).

Due to the indirect nature of radar rainfall measurements, NEXRAD data may be subject to many sources of uncertainty such as radar-based factors (antenna, transmitter, and receiver), ground clutter, anomalous beam propagations, radar beam overshooting, and range effects caused by an increase in beam elevation and degradation of resolution due to beam spreading (Kalin and Hantush, 2006; Habib et al., 2009; Renden et al., 2013). Additionally, one of the largest sources of error can be the chosen Z-R relationship because it is directly related to the amount of precipitation estimated. The impact of radar upon the accuracy of hydrograph forecasts depends upon the spatial, temporal and intensity resolution of the data used which, depending on the level of resolution, may need different levels of quality control to remove data errors (Zhijia et al., 2004).

2.2 Studies Comparing NEXRAD and Rain Gauge Precipitation Measurements

Numerous studies have evaluated and compared various radar-based rainfall estimations to gauge rainfall. These studies emphasize the importance of correctly identifying precipitation values and the possible bias associated with using radar and gauge derived values. Skinner et al. (2009) compared rainfall estimates from a gauge-adjusted, NEXRAD-derived product with precipitation measurement from the South Florida Water Management District (SFWMD) rain gauges. The purpose of the study was to assess the quality of radar-rainfall measurements for different conditions against corresponding rain gauge measurement. The study focused on the Upper and Lower Kissimmee River Basin area (approximately 3000 mi^2) in south Florida. The NEXRAD rainfall data were generated for a 2 km by 2 km grid resolution at the daily time-interval over a four year period. The Kolmogorov-Smirnoff (K-S) test and root-mean-square error (RMSE) statistics were used to compare the rain gauge measurements (treated as the independent variable) and the NEXRAD radar-rainfall values derived from reflectivity measurements. The results show that the precipitation datasets are significantly different; therefore the datasets are derived from different populations. Overall, it was determined that NEXRAD underestimated rainfall with respect to rain gauge data over the study period. Additionally, it was determined that the NEXRAD overestimated small rainfall amounts (less than 0.5 inch) but underestimated large rainfall amounts (greater than 1 inch) when compared to rain gauge values.

Habib et al. (2009) performed a validation analysis of radar-based multisensor precipitation estimation product (MPE) against a dense rain gauge network in southern Louisiana. The MPE estimates were produced by the NWS regional RFC as Stage IV data on a 4 x 4 km^2 mosaicked grid. The study area is approximately 35 km^2 in area and was composed of a total of 13 rain

gauge sites. The rain gauge and radar precipitation data intensities were set to three time scales (hourly, daily, and monthly) over a three year period. The rain gauge network was not used in the development of the MPE data and therefore could be used as an independent dataset for evaluating bias. Multiple continuous statistics were used to quantify the differences between the MPE estimates and the reference dataset. The results showed that the MPE tend to overestimate small rain rates (< 0.5 mm /h or approx. 0.5 in/day) and underestimate large rain rates (> 10 mm/h). Over long time scales (annual) the overall bias between the MPE and rain gauge rainfall is small. However, on an event basis, the bias can reach up to ±25% of the event total rainfall depth during 50% of the events and falls between 50% and 100% for 10% of the events. A detection analysis was also performed to examine the volume of rain that is either missed due to lack of detection or falsely detected in the MPE estimates. The results show that MPE has an overall probability of detection of 0.6–0.82; however, most of the undetected rain is in the low range of rain rates (<0.13 mm/h) and a very good detection (90% and higher) is achieved for high rain rates.

A study conducted by Jayakrishnan et al. (2004) evaluated Stage III WSR-88D precipitation data (4 by 4 km grid) for 24 hour accumulation using data from rain gauges for a study period of five years. The study area is in the Texas-Gulf basin and covers a total area of approximately 468,000 km^2. There are seventeen WSR-88Ds located in the region and 545 weather stations. Comparative statistics including Estimation Bias, Estimation Efficiency (EE), and Root Mean Squared Difference (RMSD) were used. The results showed that NEXRAD consistently underestimated rain when compared to a majority of the rain gauges. The five year total difference was within $\pm$500 mm at 42% of all rain gauges. A majority of the gauge locations

were considered to be of better quality (First Order weather stations of NWS and US Army Corps of Engineers) had an EE above 0.50.

Mazari et al. (2013) compared NEXRAD system digital storm-total precipitation product (DSP) to a network for 50 rain gauges in the Upper Guadalupe River Basin, Texas. The DSP product is a recent product that has a high temporal resolution (4-7 minutes) and spatial resolution (1° × 2 km). The comparisons were conducted for different temporal scale (six minute, one hour, and storm-total accumulation) and different distances from the radars. The results show that the radar underestimates at near and very far ranges (<50 and >160 km), matches well or slightly overestimates at middle ranges (50–100 km), and overestimates at far ranges (100–160 km). The DSP product showed reasonably good rainfall estimations when compared with gauge (correlation coefficient of 0.62 to 0.76) for all time scales. Burcea et al (2012) performed a similar study and determined that the radar data were comparable to rain gauge measurements at a radius of less than 150-160 km. It was also found that in general, the radar was likely to underestimate the gauge precipitation.

The above-mentioned studies are included to address the potential for NEXRAD rainfall measurements to demonstrate bias relative to rain gauge measurements for different rainfall events and for different temporal and spatial scale. The relevant study information and findings are summarized in Table 1. It should be noted that several of the authors found that NEXRAD tends to underestimate rainfall overall or for particular rainfall frequencies. Developments and improvements have been on-going for the NEXRAD precipitation processing during recent years. These efforts focus on reducing and quantifying uncertainty in radar precipitation estimates to improve bias value. Recent advances are generally focused on the effective merging of radar quantitative precipitation estimates (QPE) with other estimates; improvements in radar

technology, particularly dual polarization enhancement, and making operational use of radars other than the WSR-88D; and investigation of better quality control procedures (Pathak et al., 2013). As technology continue to progress, radar-derived rainfall data estimate uncertainty should decrease and overall bias should improve.

Table 1: Literature Review Summary of Studies Comparing NEXRAD and Rain Gauge Precipitation Measurements

Author	Precipitation Methods Compared	Study Area Size/Location	Rainfall Return Freq.	Results
Skinner et al. (2009)	Rain Gauge and Gauge-corrected NEXRAD 2 km X 2 km pixel	Upper and Lower Kissimmee River Basin area (approximately 3000 mi^2) in south Florida	Daily time scale, Four year period	NEXRAD underestimated rainfall with respect to rain gauge data over the study period. NEXRAD overestimated small rainfall amounts (less than 0.5 inch) but underestimated large rainfall amounts (greater than 1 inch) when compared to rain gauge values.
Habib et al. (2009)	Dense rain gauge network and Stage IV data on a 4 x 4 km^2 mosaicked grid	Southern Louisiana, 35 km^2	Three time scales (hourly, daily, and monthly) over a three year period.	MPE tend to overestimate small rain rates (< 0.5 mm /h or approx. 0.5 in/day) and underestimate large rain rates (> 10 mm/h)
Jayakrishnan et al. (2004)	Rain Gauge and Stage III WSR-88D precipitation data (4 by 4 km grid)	Texas-Gulf Basin, 468,000 km^2	Daily time scale, Five year period	NEXRAD consistently underestimated rain when compared to a majority of the rain gauges
Mazari et al. (2013)	Rain Gauge and NEXRAD system digital storm-total precipitation product (DSP)	Upper Guadalupe River Basin, Texas, 3000 km^2	Different temporal scale (six minute, one hour, and storm-total accumulation) for a two year period	The DSP product showed reasonably good rainfall estimations when compared with gauge estimates

2.3 Studies Comparing NEXRAD and Rain Gauge Precipitation Datasets on Hydrologic Model Simulations

Many studies have investigated the effects of precipitation variability on the accuracy of hydrologic model simulations. The two types of precipitation input utilized in this thesis' work are largely different in the areal-averaging and resolution. The potential for improved accuracy of hydrologic model simulations and forecasts using radar data instead of point gauge data has been studied previously, with results often being contradictory. Multiple studies were reviewed with the expectation that covering a variety of modeling platforms, study area sizes and locations, precipitation inputs, and rainfall return frequencies would yield a wide array of results.

Neary et al. (2004) compared the hydrologic simulation results using radar-based and rain gauge precipitation input for a HEC-HMS hydrologic model in two sub-basins of the Cumberland River basin, Tennessee. The study area covers 2,424 km^2, with 20 rain gauges located in the vicinity of the project. Radar estimates were Stage III operational precipitation products of NEXRAD with an hourly accumulation over a 4 X 4 km^2 grid. The study period was defined from 1997 to 2001 with 21 simulation periods ranging from 5 to 37 days. Various statistics were used to compare the differences between radar estimates and rain gauge estimates. The results shows that radar underestimation of gauge rainfall was present during a majority of the simulations. Performance statistics, including streamflow volume bias, root mean square difference, mean normalized peak error, and mean peak timing error were used to compare the HEC-HMS model simulations results to observed streamflow at each sub-basin outlet. It was determined that the NEXRAD data were generally less accurate in predicting the streamflow volumes as compared to gauge-only simulations, although both precipitation inputs failed to reproduce observed flood peaks.

Diaz-Ramirez et al. (2012) evaluated the impact of three different rainfall datasets on Hydrological Simulation Program – Fortran (HSPF) simulations in two coastal catchments located in Alabama. Rain gauge data collected and processed by the U.S. National Oceanic and Atmospheric Administration (NOAA) and U.S. Geological Survey (USGS) along with radar precipitation data derived from NOAA NWS (4X4 km NEXRAD Stage IV time series) were input into the HSPF model to simulate hydrological processes and evaluate streamflow at two gauged subcatchments. The two subcatchments were the Fish and Magnolia Rivers, covering an area of 140.1 km^2 and 46.4 km^2, respectively. The study timeframe spanned from July 01, 2002 to December 31, 2008. The rain gauge data time series were reported as daily but were disaggregated to hourly data to remain consistent with the radar rainfall time series, which were recorded hourly. The Thiessen polygon method was used to weigh the rainfall proportion to each sub-watershed. Annual precipitation values were compared, with NOAA rainfall amounts being consistently higher than the USGS precipitation values (~28%) and radar values (~18%). The following best-of-fit and error index criteria were used to evaluate observed streamflow data versus simulated time series by HSPF: the coefficient of determination, the Nash-Sutcliffe coefficient, the mean relative error, and the root mean square error. The results of the research showed that, in general, the NOAA rainfall datasets were the most consistent in simulating long term daily streamflow and storm events, resulting in better derived flows than radar and USGS rainfall time series. However, the stream flows derived from radar rainfall data were consistent and agreeable for certain flow amounts. USGS rainfall data suffered from several inconsistencies (missing data, low values, and timing delay of peaks) for both subcatchements, and therefore produced high relative errors for a majority of the storm events.

Kalin and Hantush (2006) explored the use of NEXRAD data as an alternative source of precipitation data to rain gauges in a Soil Water Assessment Tool (SWAT) model. The model covered an area of 120 km^2 in the Pocono Creek watershed in Monroe County, Pa. The radar data used in the study was MPE, processed for hourly precipitation. Two precipitation point locations for gauge measurements are available but are located outside the watershed boundary at the daily time scale. A comparison of the NEXRAD estimated precipitation at the local gauge stations was completed with a coefficient of determination ranging from 0.86 to 0.94. The model was calibrated using the gauge data for the period of July 1, 2007 to May 31, 2004. The NEXRAD data were then input into the model. Recalibration was needed because the NEXRAD estimates were greater than estimated from the rain gauges. Validation of the model also occurred during the time period of June 1, 2004 to April 30, 2005. Overall, during calibration the NEXRAD and rain gauge driven model performance statistics were comparable and the simulated hydrographs were similar to the observed flow hydrographs. For the validation period, coefficient of determination and the Nash-Sutcliffe efficiency was higher at the monthly time scale with NEXRAD, but lower at the daily time scale.

Sexton et al. (2010) examined the use of NEXRAD data versus rain gauge data for a small watershed (~ 50km^2) located in the Coastal Plain of Maryland, where no dense rain gauge network was available. The comparison of the precipitation data sets was performed on a SWAT model using data from two rain gauges and three types of NEXRAD data. The three NEXRAD data sets (at 4 x 4 km resolution) included (1) non-corrected (NC), (2) bias-corrected (BC), and (3) inverse distance weighted (IDW) corrected NEXRAD data. Calibration and Validation of the model occurred on a daily basis from 2005 to 2006 (calibration) and Jan 1 to April 15, 2007 (validation). Performance measures included the Nash Sutcliffe, r^2, RMSE and percent bias. The

results show that, in most cases, SWAT estimated stream flow more accurately using NEXRAD precipitation data than rain gauge data. The author states that this is likely due to the fact that the rain gauges were located outside of the watershed. The model also performed best using the NC NEXRAD data during calibration and BC NEXRAD data during validation. Due to the limited number of gauges the BC data did not offer much improvement, especially if radar data were corrected to distant gauges.

Price et al. (2013) investigated whether MPE (Stage IV) NEXRAD data would improve simulation results compared to rain gauge data for four different watershed spatial scales at five time steps. Simulations using SWAT were performed from 2002 to 2010 for the Neuse River basin in North Carolina. The four sub-basin sizes were 21 km^2, 203 km^2, 2,979 km^2 and 10,100 km^2. The temporal scales of analysis were daily, weekly, monthly, quarterly, and annual precipitation and streamflow totals. Separate calibrations were performed for each precipitation data type and for each of the four watersheds. The radar and gauge datasets were compared using pairwise difference of means tests and Spearman rank correlation analyses. The results show that gauge total precipitation was greater than radar total precipitation across the entire study period. However, results also indicated that radar total were greater than gauge data during higher storm events (25-50 mm/day). The results for the SWAT simulations showed that for the smaller basins (21 and 203 km^2), simulations were more accurate using radar precipitation data; where for the largest basin (10,100 km^2) gauge precipitation data produced better results. The medium sized basin (2979 km^2) showed comparable results using both precipitation data types. According to the authors, simulation differences between gauge and radar precipitation data were most apparent at a daily timestep and decreased as timesteps became longer, as a result of averaged positive and negative errors. Additionally, radar-based simulations produced more accurate

results for high flow (95th percentile) events, whereas both datasets underestimated median and low (fifth percentile) flow events.

Looper and Vieux (2012) investigated streamflow prediction accuracy using gauge corrected radar-derived precipitation estimates and gauge observations on a physics-based distributed (PBD) hydrologic model, V*flo.* The study area of Austin, TX covered a combined area of 1205.9 km^2, with smaller sub-basins ranging from 16.5 to 839 km^2. The rain gauge network coverage of 164 gauges was used to correct the radar rainfall (resolution at 1-km). The model was calibrated to four large flood events during the years of 2007-2010. The bias between the radar and rain gauge data showed considerable departure from a perfect agreement between the datasets. The results show that the absolute average difference between radar and gauge measurements (at the gauge location) is 32.1% before and 15.6% after bias adjustment. The *Vflo* simulated hydrographs were compared to USGS observed gauge data by the Nash-Sutcliffe efficiency (NSE) probability distribution and Root Mean Square Error (RMSE). The median NSE for gauge corrected radar data was 0.78 and for gain gauge only the median NSE was -0.51. The RMSE was 0.89 m for gauge correct radar and 1.77 m for gauge only data. It was determined that the rain gauge density was one of the main determinants of forecast accuracy.

As can be seen from the results of the previous studies above, there are mixed conclusions in regards to whether radar-derived precipitation is a better alternative than traditional fixed instrument-based rain gauge data. For many studies, NEXRAD and rain gauge data produced comparable results. Improvements in model streamflow accuracy were generally dependent on rain gauge density and their location relative to the watershed boundaries. Many studies that used multiple gauges inside or near the watershed showed a minimal difference in radar or rain gauge simulation results whereas radar-drive simulations were more accurate in areas with minimal rain

gauge coverage. Table 2 below summarizes the studies of hydrologic models using both radar and rain gauge input data and the associated data that are relevant to this study such as the study area size and rainfall return frequency. A majority of the literature reviewed used the SWAT modeling platform, whereas only one article used HEC-HMS, as was used in this study. The study areas were mainly smaller in size, but some studies included larger sub-basins for analysis. Additionally, many of the studies were performed over varying temporal scales, some performing multiyear analyses instead of single storm events, as was completed in this study. The final analyses of results show that there is no straightforward answer regarding which precipitation input method produces more accurate streamflow estimations in varying sub-basin sizes and rainfall return frequencies.

Table 2: Literature Review Summary for Studies Comparing NEXRAD and Rain Gauge Precipitation Datasets on Hydrologic Model Simulations

Author	**Model Software**	**Precipitation Input Methods**	**Study Area Size/Location**	**Rainfall Return Freq.**	**Results**
Diaz-Ramirez et al. (2012)	HSPF	Rain Gauge (NOAA & USGS) via Thiessen Polygon and NEXRAD Radar	Two basins, Alabama - 140.1 km^2 and 46.4 km^2	Multiyear study-annual rainfall avg. between 1165 mm and 1783 mm depending on basin/precip method	NOAA gauges performed the best, followed by radar precip and then USGS gauges (author believed issues with gauges)
Kalin & Hantush (2006)	SWAT	NEXRAD (MPE) and Rain Gauges	Pocono Creek Watershed, PA 120 km^2	Monthly and Daily simulations (over multi-year period). Validation a 10 yr return period storm occurred	During calibration gauge and NEXRAD data produced similar output results. For validation at the monthly time scale NEXRAD had better performance statistics, at the daily time scale, gauge-driven simulations had slightly better statistics.
Looper & Vieux (2012)	Physics-based distributed Vflo	Rain gauge adjusted radar rainfall and rain gauge	Austin, TX 1205.9 km^2 total with smaller sub-	Hourly, 7-8 Sept 2010, high rainfall ~350 mm	Radar with rain gauges showed more accurate hydrologic prediction for flash flood event

		only	basins ranging from 16.5 to 839 km^2	accumulated over 2 days	
Sexton et al. 2010	SWAT	Rain Gauge and three types of NEXRAD; non-corrected, bias-corrected and inverse distance weighted corrected	Coastal Plain of Maryland, ~50km^2 watershed	Daily simulations for a multi-year period.	NEXRAD data produced comparable and, in most cases, better estimates of flow than rain gauge data. NEXRAD is a viable alternative to rainfall data collected from rain gauges located outside of the watershed
Neary et al. (2004)	HEC-HMS	Rain Gage and Stage III NEXRAD data	Dale Hollow watershed within the Cumberland River basin in Tennessee, 2,424 km^2	Hourly data from 1997 to 2001. 21 simulations performed for period of 5 to 37 days with rainfall ranging from <50 mm to >250 mm	Stage III simulations were generally less accurate in predicting streamflow volume as compared to gauge-only simulations
Price et al. (2013)	SWAT	MPE (Stage IV) NEXRAD and rain gauge data	The Neuse River basin in North Carolina, four different sub-basin sizes; 21 km^2, 203 km^2, 2979 km^2 and 10,100 km^2.	Multiple Temporal scales were analyzed over the 9-year simulation period. Daily precipitation ranged from 0mm to approx. 125 mm.	SWAT simulations with both datasets underestimated median and low flows, whereas radar- simulations were more accurate than gauge- simulations for high flows. Results suggest that Radar data can improve modeling efforts in watersheds with poor rain gauge coverage.

Chapter 3

PROJECT BACKGROUND

3.1 Study Location

The St. Johns River (SJR) is the longest river of Florida, beginning near Florida's Turnpike and flowing north for approximately 310 miles until it discharges into the Atlantic Ocean in northeast Florida. The general topography of the project area is flat, with an average slope of approximately 0.016 ft/mile, which results in a more lacustrine than riverine characteristic (SJRWMD, 2012). It is comprised of multiple sub-basins of various sizes and hydrologic properties that drain toward the flow way of the St. Johns River. Due to its size, the SJR has been divided into major "Basins" by the St. Johns River Water Management District (SJRWMD), a state agency whose work focuses on managing water supply, water quality and natural systems management, and flood protection (SJRWMD, 2012). The Upper St. Johns River Basin (USJRB) is a 4530 km^2 (1750 square mile) basin which acts as the headwaters of the St. Johns River. This Basin this mainly comprised of marsh and agricultural land with multiple storage areas used for flood control and environmental management. Additionally, there are multiple flood control projects within the area which include flood levees and water control structures. The Middle St. Johns River Basin (MSJRB) is downstream of the USJRB and encompasses approximately 3100 km^2 (1200 square miles). It includes a variety of natural land types, but a majority of the basin is comprised of highly urbanized areas, such as the city of Orlando, Florida.

The climate of the central and eastern portion of Florida is mainly humid subtropical. The rainy season extends from June through October, with precipitation within the project area generally being frontal, convective, or tropical in nature. Approximately 70% of Florida's rainfall occurs during the rainy season, with many of storms producing a large amount of rainfall over small time periods and localized areas. The dry season extends from December to April, with November and May acting as transitional months depending on when the wet season begins and ends.

3.2 Hydrologic Model Background

The hydrologic model of the Upper and Middle St. Johns River (SJR) basins in east-central Florida was developed using the U.S. Army Corps of Engineers Hydrologic Engineering Center Hydrologic Modeling System (HEC-HMS). The HEC-HMS version 3.5 hydrologic modeling platform was chosen because it simulates precipitation-runoff processes for a wide range of geographic areas and a variety of watershed sizes. The HEC-HMS program is based on over 30 years of experience with hydrologic simulation software and continues to produce new algorithms and analysis techniques to address emerging hydrologic problems (Scharffenberg et al., 2010). It is a widely recognized and used modeling platform, which can be found in multiple peer-reviewed literature sources.

The HEC-HMS model used in this study was originally developed by the author as part of a larger effort that developed and integrated multiple watershed models to determine the economic valuation of wetlands and capacity for flood storage in the St. Johns River. The flow and stage results of the calibration model were used as input to a Soil and Water Assessment Tool (SWAT) model under development by the University of Central Florida (UCF). That model, in turn, provided flow inputs to an existing hydrodynamic model of the Lower St. Johns River Basin.

Collectively, the three models encompass the entire St. Johns River watershed and permit the evaluation of the interesting research topics mentioned above. This work entitled "St. Johns River Economic Valuation Study" was contracted by the St Johns River Water Management District and is currently under review with publication expected later this year. The model domain for the HEC-HMS model included the entire Upper St. Johns River (USJR) Watershed and a majority of the Middle St. Johns River (MSJR) Watershed, as seen in Figure 1. Due to the highly dynamic nature of the flow patterns within the middle St. Johns River, it was determined that this area may not be modeled adequately using a one-dimensional model. The area of the MSRJ that includes Lake Harney, Lake Jesup, and Lake Monroe may be greatly affected by tailwater conditions and present complex stage-storage relationships. Portions of this area (mainly Lake Jesup) were modeled previously using known stage and discharge rates measured by the U.S. Geological Survey. Because the model cannot correctly compute backwater effects and has difficulties sufficiently modeling the proper stage-storage relationships and subsequent flow rates within these lakes, this portion of the model was removed for the thesis work. The new model domain for the HEC-HMS model can be seen in Figure 2.

The original modeling effort for the St. Johns River Economic Valuation Study included both model calibration and validation. The calibration period simulated the period from August 2 to October 8, 2008 and captured the large rainfall event from Tropical Storm Fay. The validation period was from October 1 to October 14, 2007 and covered a very minimal precipitation event. The rainfall inputs to the model were from rain gauge measurements at a daily time scale. The Thiessen Polygon method was used to distribute rain gauge measurement for the entire study area. The simulated daily flow rates were evaluated against U.S. Geological Survey (USGS) stream flow discharge measurements to determine the accuracy of the run-off simulation results

for the modeled area (USGS, 2014). It became apparent that differences in rainfall intensities and sub-basin catchment sizes caused significant changes in the statistical agreement between simulation data and observed data. It was assumed that one of the largest sources of discrepancy between the calibration and validation data was the quality of precipitation input and the appropriateness of using the Thiessen Polygon method. Since this methodology applies uniform precipitation gauge data over the varying polygon areas, it may not capture the varying concentration and inner variability of the precipitation data, which can cause significant changes in the subsequent runoff amounts within the modeled area. It was determined, during this modeling effort, that further research was needed to conclude if model simulation results could be improved through the use of a more spatially continuous precipitation implementation method (i.e. NEXRAD).

3.3 Simulation Storm Return Frequencies and Sub-basin Spatial Scales

The four simulation events chosen for the study occur during specific timeframes from 2007 to 2011. They were chosen based on the amount of rainfall that occurred, with the intention to cover a variety of return frequencies (also known as recurrence intervals). Also, more recent storm events were chosen based on the overall improvements of radar accuracy that are associated with more up to date technology. Additional bias may or may not have been added if the storm event selected was during a period of inferior radar techniques. Table 3 below describes the return frequencies, at both the 24 hour and 48 hour durations, for the selected simulation events. The values were obtained from the National Oceanic and Atmospheric Administration (NOAA) Atlas 14 Point Precipitation Frequency Estimates for the project area.

Table 3: Average Return Frequency for Selected Simulation Events

Average Return Frequency (Recurrence Interval)		
Storm Event	**24 Hour Duration**	**48 Hour Duration**
Calibration, August 2008	Between 5 and 10 years	Between 10 and 25 years
Validation, October 2007	Much less than 1 year storm	Much less than 1 year storm
Validation, March 2010	Less than 1 year storm	Less than 1 year storm
Validation, October 2011	Between 10 and 25 years	25 year

The smallest rainfall event was in October 2007, which was much less than the one year return frequency. This storm would be more representative of an average wet-season event. The next rainfall event, March 2010, was almost a one year return frequency for some areas of the project. Hourly data were reviewed for some of the sub-basins (from the NEXRAD data) and it was determined that for a 12 hour duration, the rainfall amounts would be approximately a 1 year storm. The simulation events of August 2008 and October 2011 were much larger in magnitude, ranging between a5 year and 25 year return frequency for the 24 hour storm and between 10 year and 25 year return frequency for the 48 hour storm. Therefore the data set is believed to cover multiple return frequencies ranging from less than 1 year up to 25 years for the 24 and 48 hour durations.

The USGS observed gauge measurements occur at multiple different locations within the model. Certain gauge locations are at the outlet of sub-basins, thereby representing the area of the upstream sub-basin(s). Any gauges located within the flow-way of the SJR would be representative of all sub-basins upstream. Therefore, a large array of spatial scales could be analyzed. Table 4 shows the various sub-basins or collection of sub-basins and the surface area they represent.

Table 4: Sub-basin Areas Used in Spatial Analysis of Precipitation Input

Location, Sub-basin (s)	**Total Area**
Fort Drum Creek	121 km^2
Blue Cypress Creek	247 km^2
Jane Green Creek	612 km^2
All Upstream of U.S. 192	2379 km^2
Pennywash Creek	52 km^2
Wolf Creek North	65 km^2
All Upstream of S.R. 520	3303 km^2
All Upstream of S.R. 50	3817 km^2
Upstream Inlet of Lake Harney	5038 km^2
Upstream of Little Econlockhatchee River at Union Park	60 km^2
Upstream of Little Econlockhatchee River at University Blvd.	228 km^2
Upstream of Econlockhatchee River near Oviedo	591 km^2
Upstream of Econlockhatchee River near State Highway 13	702 km^2

Chapter 4

MODEL DEVELOPMENT – HEC-HMS MODEL

The following chapter presents the methodology and thought processes behind the HEC-HMS model development. A calibration model (Aug to Oct, 2008) and three validation models (Sept 2007, Mar 2010, Oct 2011) were developed to represent four different simulation storm events, each with a different rainfall return frequency. Two sets of daily precipitation data were used in the models: rain gauge observations and radar-derived estimates. The models were first calibrated using the rain gauge data for each of four simulation periods with the purpose of trying to produce the best possible hydrologic simulations. The models were then re-run using the NEXRAD derived precipitation inputs. It was decided that minor re-calibration was needed to improve the NEXRAD simulations because of the bias present between the rain gauge and radar precipitation data. The model calibration process largely acts to correct this error or bias in precipitation data via parameter adjustment (Price et al., 2013). Many studies discuss the importance of model recalibration when switching precipitation products (Kruger, 1998; Neary et al., 2004; Kalin and Hantus, 2006; Price et al., 2013). The details of the model development and parameter settings can be found in the subsequent paragraphs.

4.1 Model Domain

HEC-HMS simulates natural and controlled hydrologic conditions in watershed systems and simulates precipitation-runoff processes (Scharffenberg et al., 2010). HEC-HMS utilizes infiltration losses, hydrograph transformations, and hydrologic routing with the option of using

various calculation methods. Additionally, mathematical models for simulating the response of the watershed to precipitation and evapotranspiration are available. Also, the code permits the user to input baseflow into the simulated watershed to model real-world hydrologic functions. The HEC-HMS modeling platform allows the Upper and Middle St. Johns River Basins hydrologic processes to be simulated using one large-scale model with adequate detail to determine the changes in runoff processes due to changes in precipitation input conditions. The HEC-HMS model developed for this study is a derivative of the U.S. Army Corps of Engineers (USACE) and St. Johns River Water Management District (SJRWMD) hydrologic boundaries that have been identified in both previously constructed models (SJRWMD) and models that are currently under development (USACE).

The model domain for the HEC-HMS model includes the entire Upper St. Johns River (USJR) Watershed and a portion of the Middle St. Johns River (MSJR) Watershed, as seen in Figure 2. The model domain covers roughly 5200 square kilometers (2000 square miles with a rain gauge density of approximately 217 km^2/gauge (83sq mi/gauge). The modeled area of the Upper St. Johns River Watershed includes sub-basin delineation from the U.S. Army Corps of Engineers and includes the SJRWMD defined Planning Units of Fort Drum Creek, Blue Cypress Creek, Fellsmere, Jane Green Creek, St. Johns Marsh, Lake Poinsett, Toschatchee, and Puzzle Lake. The modeled area of the Middle Basin includes the Econlockhatchee River Planning Unit, also defined by the SJRWMD. The pertinent SJRWMD detailed planning units used in this modeling effort are shown on Figure 3.

Each planning unit consists of multiple sub watersheds or sub-basins which subdivide each planning unit into more detailed areas for hydrologic modeling purposes. These sub-basins are normally defined by a geographic area of natural orientation or by manmade structures such as

levees or canals that contribute flow to a similar outlet location. The sub-basin delineations for the Upper and Middle St. Johns River were delineated using contours and flow paths as well as the sub-basin shapefiles received from the SJRWMD (T. Jobes, personal communication, 2014). Smaller sub-basins were often combined to form larger sub-basins for ease in modeling calculations and development. This approach was deemed satisfactory since the focus of the research study was on large-scale processes. The sub-basins for the Middle and Upper St. Johns River can be seen in Figure 4.

The Upper St. Johns River Basin sub-basin delineations were developed based on projects completed with the Upper Basin in the project year of 2008. This baseline year for the landuse type was set during the model development for the St. Johns River Economic Valuation Study as 1995. Use of the 1995 base year permitted the model to be used for simulation of a wide array of historic storms, as well as simulate the effects of ongoing landuse change in the watershed. Although a majority of the Upper St. Johns River Basin features were present in 2008, some larger man-made project features, such as the Three Forks Marsh Conservation Area, were not included as they were constructed after the base year. The Middle St. Johns River sub-basin delineation has not changed significantly since 1995 but flow patterns have been altered due to the continued increases in urban development. This has caused disruptions in the historical runoff conveyance due to drainage ditching, retention ponds, and increased impervious areas.

4.2 Model Inputs

4.2.1 Basin Model Manager

As stated above, HEC-HMS can be used to estimate runoff volumes and flow hydrographs from multiple computation parameters and models or methods for approximating these processes. To begin the HEC-HMS model design, a new “Basin Model” was created. It was decided that one

basin model will be used for both the Upper and Middle St. Johns areas to ensure flow is properly conveyed throughout the system without the interruptions of linking multiple basin models.

4.2.1.1 Sub-basin Elements

Within the basin model, the first hydrologic element to be added was the sub-basin element which has no inflow and only one outflow. A sub-basin element was added for each sub-basin identified in the model domain. The sub-basin area must be entered and a Canopy Method or Surface Method should be specified. The Canopy Method is meant to represent the interception of precipitation due to the presence of foliage. This tool leads to decreased precipitation that is available for runoff. In addition, the intercepted precipitation is subject to evaporation between rain events. The Canopy Method was not used in the base HEC-HMS model. The Surface Method represents the interception and accumulation of runoff due to the depressions in the ground and increased infiltration. The Surface Method was also set as none in the HEC-HMS model. Both methods were not included because this form of precipitation interception is accounted for when using the U.S. Department of Agriculture Soil Conservation Survey (SCS) method (1972) and through the assignment of initial abstraction, which will be discussed in further detail later in the report.

HEC-HMS computes outflow by subtracting the losses, transforming excess precipitation, and adding baseflow to the precipitation data that is applied to each sub-basin. The following sections will explain how the various input parameters for the sub-basin element were computed.

4.2.1.1.1 Loss Method

The SCS Curve Number Loss was selected as the Loss Method for each sub-basin in the Upper and Middle St. Johns River modeling effort. The calculation of the curve number, initial

abstraction and percent impervious are all parameters that must be entered as part of the SCS Loss Method in HEC-HMS. The following paragraphs explain the methodology and computational methods for determining these parameters for each sub-basin.

The land use and land cover data were downloaded from the St. Johns River Water Management District (SJRWMD) for the project baseline year 1995 (SJRWMD, 2014). Data were available for each Florida County, and therefore only counties associated with the project area were downloaded. Each data set was imported into ArcGIS as a shape file until the entire project area contained Land Use data. Within each shapefile the land use data were expressed using the Florida Land Use and Cover Classification System (FLUCCS), with over 100 different land cover types included (SJRWMD, 2014). This would suggest a relatively adequate land use representation due to the detailed nature of each land use shapefile. The STATSGO soil group classification data were also imported into ArcGIS as a shapefile. The soil group data express the soil group behavior as an A, B, C, D, or as a dual hydrologic soil group type (T. Jobes, personal communication, 2014).

The "A" soil type has a high infiltration rate and low runoff potential. Class "B" soil has moderate infiltration rates and a moderate rate of runoff. Class "C" soils have low infiltration rates and may contain a layer of soil that impedes the downward movement of water. Class "D" soils have very low infiltration rates and include poorly drained, very silty/clayey/organic soils with a very high rate of runoff. The dual hydrologic classification includes soils that can have an unsaturated and saturated condition. The first letter of a dual classification applies to the undrained condition whereas the second letter is for the drained condition. The drained condition is normally dependent on the soils depth to permanent water table.

The sub-basin delineation was also imported into ArcGIS to allow for a spatial comparison between land use, soil group, and sub-basin area. This was completed within ArcGIS using the "Join" feature based on spatial properties of the datasets. The resulting data set contains each sub-basin with the respective land use codes and soil groups for all coverage area within the sub-basin perimeter.

The Soil Conservation Services (SCS) curve number method was used to estimate the amount of runoff potential from the rainfall event based on the relationship between soil type, land use and hydrologic soil conditions. The hydrologic soil condition is known as the Antecedent Moisture Condition (AMC) which describes the preceding soil moisture before the modeled rainfall event. AMC I is used for basins that have had a low amount of rainfall before the modeled event, whereas AMC III is used for a high amount of rain before the modeled event. AMC II may be considered the average condition and is normally used in modeling applications. Curve numbers representing AMC conditions I and III are calculated by applying adjustment factors to the CN reflecting the AMC II condition, as seen in Equation 1 and Equation 2.

$$AMCI = \frac{4.2 * AMCII}{10 - (0.058 * AMCII)} \qquad \textit{Equation 1}$$

$$AMCIII = \frac{23 * AMCII}{10 + (0.13 * AMCII)} \qquad \textit{Equation 2}$$

The SCS curve number may be related to the potential maximum retention by Equation 3.

$$S = \left(\frac{1000}{CN}\right) - 10 \qquad \textit{Equation 3}$$

S = Potential maximum retention after runoff begins (in)

CN = Curve number

For many modeling applications a certain amount of the precipitation is abstracted immediately due to potential losses. These losses can occur in the form of infiltration into the soil, interception due to foliage, and depression storage due to ponding or surface undulations. In the SCS method these loses were combined and termed Initial Abstraction. The empirical equation used to determine the Initial Abstraction can be seen in Equation 4.

$$I_a = 0.2 * S \qquad \textit{Equation 4}$$

I_a = Initial Abstraction (in)

Using these parameters the runoff depth can be predicted using Equation 5 below.

$$Q = \frac{(P-0.2S)^2}{(P+0.8S)} \qquad \textit{Equation 5}$$

P = Precipitation (in)

Q = Runoff (in)

The runoff curve numbers for the Upper and Middle St. Johns River were determined using previously derived SCS curve numbers for the each Florida Land Use Cover code in AMC II condition (Ayres Associates, 2001; Inwood Consulting Engineers, 2009). Each sub basin is comprised of multiple land uses and soil types so a composite weighted curve number for each sub basin was calculated. Calculations were based on the relative percentages of the land use and soil group classifications within the sub basin. Curve numbers were calculated for the AMC I and AMC III condition as well as the respective initial abstraction for each.

In addition to using the land cover type to determine the curve number, it was also used to calculate the percent impervious. The SJRWMD has correlated FLUCCS to the Hydrological Simulation Program-Fortran (HSPF) land use groups to assign the percent impervious for each

land use code (SJRWMD, 2012). A composite percent impervious was determined for each sub-basin.

4.2.1.1.2 Transform Method

To accurately represent the response of each sub basin to the rain event, a hydrograph for each sub basin based on the time of concentration and lag time must be calculated. The time of concentration is defined as the time it takes water to travel from the hydraulically furthermost point in the watershed to the outlet. The lag time is the time it takes from the center of mass of the rainfall to the peak of the hydrograph. Within the hydrologic modeling platform, the lag time is used to create the resulting hydrographs. A common relationship between lag time and time of concentration is that the lag time is 0.6 of the time of concentration (Mays, 2011).

There are many different formulas available to estimate both the time of concentration and lag time. A common formula is the SCS Watershed Lag Time Equation. It uses parameters such as the flow length, average sub basin slope, and retention based on the curve number to determine the adequate lag. The Natural Resources Conservation Service (NRCS) developed two additional methods similar to the SCS method in the years of 1972 and 1997, which utilized similar parameters (Li et al., 2008; Sharifi et al, 2011). The NRCS also uses a method known as the velocity method where the time of concentration may be calculated using the Manning's kinematic solution for sheet flow, shallow concentrated flow, and open channel flow (U.S. Department of Agriculture Natural Resources Conservation Service, 2010). Since the sub-basins involved in this study mainly have sheet flow and shallow concentrated flow, only these lag time calculation methods were used. A modified version of the Snyder lag time equation was also utilized. This form of the lag equation was originally developed by Snyder but was later revised

by the U.S. Corps of Engineers and U.S. Bureau of Reclamation (City and County of Sacramento, 1996).

The initial lag time designated for each sub-basin within the HEC-HMS model was determined using the average of the lag times calculated from the various equations. The lag time was adjusted during calibration after each sub-basin was analyzed further to ensure that the lag time was sufficient to describe the hydrologic conditions present.

4.2.1.1.3 Baseflow Method

The Baseflow Method represents the runoff of prior precipitation and subsurface volumes for each sub-basin. The main source of baseflow within the model would be the presence of previous precipitation from past rain events that is stored temporarily in the watershed. In many portions of the St. Johns River the flow way has an initial flow rate due to the storage of water within the river channel. Baseflow was used in each modeling simulation to represent this initial flow starting condition. Due to the large number of basins and scale of the model, a constant monthly baseflow was specified. The initial baseflow was approximated between 0 and 0.5 m^3/s for many of the sub-basins and the baseflow separation method was used for those sub-basins that contained discharge gauges (Mays, 2011). The baseflow of sub-basins corresponding to the flowway contained higher baseflow conditions to be representative of the river flow rate. Additionally, baseflow was used to incorporate groundwater and spring discharge, which will be explained in greater detail later in this report. Further modifications to the baseflow estimations were completed during calibration.

4.2.1.2 Reach Elements

A reach element has one or more sources of inflow from another element and computes one combined outflow. It represents a segment of the river or flow way and simulates the movement of water by using a user-selected routing method.

The reach parameters were used to represent the flow way of the Upper and Middle St. Johns River. A reach element was added in the model between each point of inflow from contributing sub-basins. Adding multiple reaches permits the definition of the channel properties between each sub-basin inflow point separately. This is important due to the significant variations in channel width and roughness as the St. Johns channel becomes more defined as it flows north. Reach elements were also included to represent any canals, minor flowways, or if the flow length from the sub-basin outlet to the defined flow path of the St. Johns River was long enough to be significantly influenced by routing.

4.2.1.2.1 Routing Method

The hydrologic routing method chosen for the model was the Muskingum-Cunge Routing Method because it can be used in reaches with a small slope and is based on the conservation of mass and the diffusion representation of the conservation of momentum (Scharffenberg et al., 2010). The Muskingum-Cunge method was chosen based on the following model criteria: minimal observed hydrograph data available in the flow way for calibration, flood wave will enter floodplain, and channel slopes are less than 0.004.

The Muskingum-Cunge Method is based on physical parameters such as the reach length, Manning coefficient, channel geometry, and slope. The routing parameters were measured using GIS software to determine the correct reach length and channel bed slope. Aerial photography and engineering judgment were used to determine the appropriate manning coefficient. The cross

section configuration was set to an 8-point cross section configuration with the geometric properties measured using GIS. The 8-point cross section configuration is used to represent the channel, left and right banks of the channel, and the left and right overbank. It was chosen because it is more representative of floodplain storage because the cross sectional geometry accounts for varying conveyance between the main channel and overbank areas through a varying Manning's n value.

In relation to the St. Johns River, one of the largest issues with routing is properly modeling the flood plain storage. This is especially true in the upper St. Johns River where most of the flow way is a flood plain with heavy vegetation. According to the HEC-HMS manual "Flood flows through extremely flat and wide flood plains may not be modeled adequately as one-dimensional flow (USACE, 2000:88)". To overcome the potential overestimation in flow due to inadequate modeling of storage availability, a loss method may be needed to account for reduction in flow.

4.2.1.2.2 Loss/Gain Method

A reach element can also represent interaction of the flow with the subsurface, flow reductions due to withdrawals, or the bi-directional movement of water. To account for these losses the constant loss/gain method was used because it applies a reduction to the flow by a fixed flow rate and/or a fraction of the flow. The fraction amount reduces the inflow by multiplying the flow rate by the value one minus the fraction. The initial fraction of loss used in the model was between 0 and 0.05 and was used as a tool to help calibrate the model by accounting for the large amount of storage potential in the flow way. In addition specific losses were used for water withdrawals and recharge rates. The calculated monthly average recharge rates to the Upper Floridian Aquifer from drainage wells within the Middle Basin during 1995 to 2006 were 19.6

Mgal/d (Sepulveda et al. 2012). The City of Melbourne also had a water supply withdrawal of 14Mgal/d at Lake Washington.

4.2.1.3 Reservoir Element

A reservoir element has one or more inflow and one computed outflow. It was used in this model for any sub-basin that either had an outlet structure, specified pumping rate, or any obstruction to the flow such as a levee or roadway.

If the reservoir had a specified pumping rate the outflow method was set as an Outflow Curve and the Storage Method was set to Elevation-Storage-Discharge. The Elevation-Storage Function was calculated using ArcGIS for each sub-basin. The Storage-Discharge function was estimated for each sub-basin that discharges using a pump (e.g. agricultural pumping or water transfers). Since many of these pumps are operated at the discretion of the land owner, the discharge values ranged from zero near minimal storage and increased to the maximum pumping rate as storage increased. The Storage-Discharge functions can be refined during calibration to ensure the discharge rate is realistic to what may occur in the field after large precipitation events occur. In many cases, the actual discharge versus time function is unknown since these are not reported to the SJRWMD or no instrumentation exists to measure the discharge. Therefore, the simulated functions used in the model are reasonable estimates using the best available information.

The outlet structures routing method was used for any reservoir that had an outlet structure such as a weir, spillway, or culverts. It was also used if flow was restricted to flow through a certain opening, such as a bridge, due to levees or roadways. Information regarding structure geometry was obtained from the U.S. Army Corps of Engineers and the SJRWMD and was input into the model when necessary. The initial condition was set to inflow=outflow for the beginning of the

simulated but during calibration changes in either initial elevation or storage may be incorporated.

4.2.2 Meteorologic Model Manager

The Meteorologic Model is used to specify the meteorological conditions for the sub-basins. It includes the precipitation method and evapotranspiration for the modeled area.

4.2.2.1 Precipitation Method

4.2.2.1.1 Rain Gauge

The first Precipitation Method selected for the modeling effort was Gauge Weights and input was based on precipitation gauge data. This method uses separate parameter data for each gauge and for each sub-basin in the model. The precipitation gauge data were obtained from point rain gauges from the SJRWMD and South Florida Water Management District (SFWMD). Only gauges that contained, at a minimum, the daily precipitation data for the calibration and validation period were used. Since there is limited precipitation gauges located in or near the project area, the Thiessen polygon method was used for the calibration and validation models. The Thiessen polygon defines an individual area of influence surrounding each gauge and represents an effective uniform depth of precipitation over the model area. Any sub-basin or portion of sub-basin falling within this area is closer to the rain gauge at its center than to any other rain gauge. Therefore, it is assumed that the gauge data, which was collected at a single point, is representative of the entire Thiessen polygon. Thiessen polygons were computed for the entire model domain using GIS and can be seen in Figure 5. ArcGIS was used to determine the relative area of each sub-basin within each Thiessen Polygons. For sub-basins that fell within multiple Thiessen Polygons, a percentage of area per Thiessen Polygon was computed. This was applied in the form of the Depth Weight which assigns a weight to each gauge in proportion to

the area of sub-basin. A Time Weight can also be specified but is set at one for all sub-basins because the precipitation gauge data are to be applied throughout the entire simulation run.

4.2.2.1.2 Radar Data

The second Precipitation Method selected for the modeling effort was also Gauge Weights but input was based on sub-basin coverage area. The input precipitation data for each sub-basin was calculated using the next-generation radar (NEXRAD) radar-based rainfall data. The description of how the NEXRAD data were processed was described earlier in this report. Once the data were processed into the 2 by 2 km grids it was overlain onto the defined sub-basin shapefile in ArcGIS. ArcGIS was used to compute the area-weighted average sub-basin precipitation based on the radar grid coverage. In other words, the area of each radar grid that fell within the defined sub-basin boundary was calculated and had known precipitation value that was associated with that grid. Once all the grid areas were computed, a total are-weighted precipitation value could be applied to that sub-basin. The precipitation data for each sub-basin were then specified as a precipitation gauge within the HEC-HMS model. The gauge weight for each sub-basin was set as one because the precipitation data were to be representative of the entire sub-basin. This allowed Precipitation Method type to remain the same between the two precipitation input types for the HEC-HMS model.

4.2.2.2 Evapotranspiration Method

Evapotranspiration combines the evaporation of water from the ground surface and vegetation. The Evapotranspiration Method is set as monthly average which is designed to work with pan evaporation measurements. The rates selected were based on literature research including the Preliminary Water Control Manual – Upper St. Johns River Basin (USACE, 1991) and journal

articles (Mao et al., 2002). The input evaporation was set the same for each sub-basin and can be seen in Table 5 below.

Table 5: Evapotranspiration Rates

Month	Rate (mm/Month)
January	53.086
February	66.04
March	90.932
April	114.046
May	134.874
June	112.014
July	123.952
August	121.92
September	102.108
October	91.186
November	69.088
December	53.086

4.2.3 Control Specifications

The purpose of the control specification is to designate when the model is to start and stop simulations and what time interval is to be used. The specific start and end date and time was entered to match the set calibration and validation time periods. The time interval was based on the necessary simulation output hydrograph data for downstream modeling applications.

4.2.4 Time-Series Data

The Time-Series Data Manager allows measured gauge data to be incorporated into the model either as an initial condition, boundary condition, or parameter. Two types of Time-Series Data were used for the model, Precipitation Gauges and Discharge Gauges. As stated previously, precipitation input data were obtained from SJRWMD and South Florida Water Management District (SFWMD) rain gauges and NEXRAD radar. Discharge Gauge data were obtained from

the United States Geological Survey (USGS) National Water Information System (USGS Water Resources, 2014). The data were entered manually for each precipitation and discharge gauge with the time interval for each matching that of the calibration and validation periods in one day time increments. The discharge gauge data were applied as observed flow to the specific location in the model that correlated to the real-time location. The discharge gauge data were compared to the hydrograph at these locations to help with the calibration and validations of the model. Different discharge gauge data comparisons are present for the calibration and validation models due to gauge data availability. A complete list of the precipitation gauges and discharge gauges can be seen in Table 6 and 7, respectively. The locations of the precipitation gauges can be seen in Figure 6 whereas the locations of the discharge gauges can be seen in Figure 7.

Table 6: Precipitation Gauges

SJRWMD Gauges	SFWMD Gauges
1230507	GRIFFITH_R
1880101	Rock K_R
1330563	Maxceyn
1103624	Elmax
1510686	Kenans2
250215	S99_R
510206	
590263	
4210749	
5140560	
1500682	
530225	
114047	
2275227	
1483356	
3200347	
11523739	

Table 7: Discharge Gauges

USGS/SJRWMD Gauges
02231342
02231396
02231600
02232000
02232155
02232200
02232400
02232500
02233460
02233473
02233484
02233500
02234000

4.2.5 Paired Data

The Paired Data Manager is used to describe an input function that relates physical processes. The Paired Data used in this model were Storage-Discharge and Elevation-Storage Functions as described earlier in the report. Elevation-Storage functions were measured using LiDAR data in ArcGIS whereas the Storage-Discharge functions were estimated based on the best data available (Jobes, personal communication, 2014).

4.3 Model Boundary Conditions

The modeled area covers roughly 5200 square kilometers (2000 square miles), from the beginning near Florida's Turnpike in the Upper St. Johns River Basin (USJRB) and flowing north until the inlet of Lake Harney in the Middle St. Johns River Basin (MSJRB). Figure 7 shows the modeled area, including natural features and the St. Johns River Flowway boundary. The boundary conditions to the east and west are the hydrologic boundaries defined by the SJRWMD which contribute to the total flow of the St. Johns River, which includes both man-made and natural boundaries. The number of sub-basins containing urban development is higher

within the northern portion of the USJRB and MSJRB due to the various cities within these regions. In addition to precipitation and associated runoff from the defined sub-basins, flow also enters the system through groundwater discharges and point source discharges such as wastewater treatment facilities. Flow exits the system from multiple locations due to the surface water withdrawals, discharges to tide, and power generation. More specifically, the St. Johns River Water Management Area discharges water through the C-54 canal to tide, municipal water is withdrawn at Lake Washington, and surface water is used for recreation irrigation, agricultural supply, commercial and industry self-supply.

A majority of the USJRB area between Florida's Turnpike and U.S. 192 has been divided into a number of storage areas for flood control and storage, as well as for environmental purposes. These sub-basins, which are often surrounded completely by levees, are heavily regulated using pumping stations and water control structures. The flow-way within this area is bound by SJRWMD levees, private levees, and natural upland areas to the west and USACE levee to the east. Between U.S. 192 and S.R. 520, the western sub basins have relatively natural drainage patterns, with the exception of the Taylor Creek Reservoir which contains a control structure. There are areas of significant urbanizations in the coastal sub basins which discharge to the SJR by pumping or through canals. The main flow-way within this section passes through Lake Washington, Lake Winder, and Lake Poinsett and contains private levee systems on both the eastern and western side of the river to protect adjacent land from flooding. From S.R. 520 to the inlet of Lake Monroe, are the final sub-basins which make up the USJRB. The western sub-basins within this area drain naturally into the SJRB with minor interference from features such as roads. The eastern sub-basins are similar to those between U.S. 192 and S.R. 520, with a

majority of the basins containing a percentage of urbanization, retention ponding features, and flow interruption due to multiple highway systems.

The most southern portion of the MSJRB is the Econlockhatchee River watershed which is comprised of natural draining wetlands at the headwater, to more urbanized areas in the western and northern sub-basins. In addition multiple detention ponds exist within this area and act as storage facilities for the stormwater runoff that occurs. The flow path is dominated by the natural topography with elevations being the highest at the headwaters and gradually decreasing until the Econlockhatchee River joins the SJR before Lake Harney.

4.4 Model Assumptions

The model input parameters were estimated using best available data and common engineering practices and logic. Model assumptions were only made when the validity of data was in question or if data measurements had not been taken or were missing. The St. Johns River's natural flow pattern has been greatly altered by human activities over the years; therefore certain sub-basins may not produce runoff similar to that of a natural physical watershed. Examples of this would be runoff being collected or diverted in small canals or ditches, interruption of runoff due to levees, roadways, or other manmade structures, storm drains, sewer systems, groundwater recharge locations, retention ponds and drainage wells. The required input parameter data must take into account these disruptions in the natural flow process and subsequent increases in retention time in order to properly model the hydrologic processes present. In addition, many sub-basins in the Upper St. Johns provide temporary storage of floodwaters or long-term storage for environmental purposes. Many of the sub-basins which form water management areas or water conservation areas are heavily regulated and discharges occur only when water levels reach a certain level within the sub-basin. This is also true for many of the sub-basins which are

currently used for agricultural purposes where water withdrawals and releases are at the discretion of the land owner. Each sub-basin element and its associated loss, transform, and baseflow methods were reviewed and modified to produce a runoff hydrograph that was realistic to the particular physical conditions.

The Upper St. Johns River Basin and portions of the Middle St. Johns River Basin have extremely small channel slopes, are heavily vegetated, contain pervious soils, and have a wide floodplain with flood control storage. These factors can greatly reduce the runoff potential and downstream flow rates. In order to produce outflow hydrographs similar to that of the discharge gauge data, assumptions regarding the model parameters were made to account for the site conditions mentioned above.

4.4.1 Runoff Assumptions

Research has indicated that runoff values in the Upper and Middle St. Johns River are relatively low compared to amount of precipitation received. The "Runoff to Streams in Florida Map Series", FGS Map Series 122 showed that the average rainfall was approximately 48 inches in the St. Johns River over the period of 1951-1980 with an average runoff of only 10 to 20 inches (Rumenik, 1988). In addition, the State of Florida Department of Transportation specifies the normal runoff coefficients used for a Design Storm Return Period of 10 years of less (State of Florida Department of Transportation, 2012). This runoff coefficient is the empirical parameter used to calculate the excess rainfall as a fixed percentage of precipitation. The runoff coefficient for a flat slope (0-2%) ranges from 0.1 to 0.20 for woodlands, from 0.15 to 0.25 for pasture, grass, and farmland, and from 0.3 to 0.6 for bare earth. These values depend on the soil type with sandy soils having a lower runoff coefficients than clay soils but since many areas of the watershed are sandy in nature, may be representative.

Storage in the headwater swamps and river floodplains reduces and delays the flood peaks in downstream areas of the river (KBN Engineering and Applied Sciences, 1993). The longer the water is delayed due to storage attenuation, the more exposure it may have to evapotranspiration and further runoff reduction will occur. To adequately predict downstream hydrographs, the model must account for the historically low runoff rates and the large amount of storage due to the relatively flat topography and presence of intermittent hardwood swamps and marsh areas within the St. Johns River watershed.

Since the precipitation runoff calculated in the HEC-HMS model is directly related to the curve number and initial abstraction, these values were modified slightly to produce more accurate runoff values. As stated previously, the curve number values for the Florida Land Use and Cover Classification System were obtained from different literature sources. The curve number values for the land use cover for wetlands are normally very high due the saturated condition and impervious nature of many wetland systems which causes significant runoff to occur. These values were modified from what is normally found to be more representative of the site conditions of the St. Johns River. Since the wetlands within the project area may experience periods of drying and wetting, a lower composite curve number was used to account for increases in potential surface storage capacity. According to the SJRWMD (2012), wetlands act as a storage attenuation feature, which may correlate to less runoff and a lower overall curve number. The overland flow may occur rapidly within the upland landscape but once it enters the lowlands or wetlands, runoff is stored and discharged over a delayed period (SJRWMD, 2012). Lower curve number values were obtained from additional research, mainly from technical notes written by the SJRWMD, which confirmed lower curve number values may be appropriate (Suphunvorranop, 1985; Di et al., 2010).

Another important factor that influences the overall curve number value for the entire drainage basin is the AMC as discussed previously. According to SCS 1972, the condition can be based on the 5-day antecedent rainfall (Charbonnier et al., 2000). The antecedent rainfall is the total rainfall preceding the runoff event that is under consideration. The SCS also determined the corresponding rainfall limits for each of the AMC classes during the dormant, growing and average season. The calibration storm of Tropical Storm Fay selected for this modeling effort occurred after a relative dry period and many of the sub-basins in the Upper and Middle St Johns River had a 5 –day antecedent rainfall of less than 36mm. This is the limit for the AMC I condition in the growing season and therefore many of the sub-basins may be classified as AMC I with respect the curve number assignment in the model. All sub-basin curve numbers in the model are between the AMC I and AMC II condition, depending on what is most appropriate for the basin under consideration. The sub-basins representing the flow way of the St. Johns River and any reservoir that was saturated within the model was assigned an AMC II or higher due to these areas being partially saturated. Many of the sub-basins were modeled between an AMC I and AMC II due to most sub-basins containing areas of dryer upland and partially saturated lowlands.

Using a reduced curve number value for wetlands and a lower AMC class allowed for a lower composite curve number to be used for each sub-basin. A lower curve number means there is a greater storage potential and higher initial abstraction, which may more accurately represent actual conditions. Since the initial abstraction describes the main loss of precipitation due to infiltration, interception, and depression storage, it is directly related to the runoff generated. To further decrease the amount of runoff, the ratio applied to the potential maximum retention should be increased from 0.2 to a higher value. It is believed this increase in initial abstraction is

reasonable due to the dense vegetation, high depression storage potential, and low runoff values measured. Additionally, the equation of initial abstraction suggested by SCS was justified on the basis of measurements in watersheds less than 10 acres in size and since considerable scatter was present in the data, other studies have used higher initial abstraction ratios than 0.2 (Ponce et al., 1996).

This methodology was also applied to the reach parameters within the model. Due to way the model was set up, the reach parameters represented the flow way of the St. Johns River and therefore storage potential must be incorporated. The Muskingum-Cunge routing method was used to geographically represent each reach, or portion of the St. Johns River flowway. This method calculates the respective lag time as the flow travels up the St. Johns River, but did not reduce the flow rate to the extent that has been naturally observed. Therefore, a Loss Method was incorporated into some of the reaches, depending on the site characteristics present. Loss rates were highest near the beginning of the USJRB and gradually decreased as the SJR stream became more defined and overall saturation increased, resulting in less storage potential. The loss percentages applied were also a function of the length of reach present, with longer reaches having more loss because of increased area for storage. Loss was also incorporated in areas where structures were present. This would include all bridge crossings (U.S. 192, S.R. 520, FL-50, FL-528, FL-46) and culverts S-250 A, B, and C, north of Blue Cypress Lake. The total loss percentage applied to the USJRB and MSJRB was set with the intention of replicating the runoff percentages presented in the "Runoff to Streams in Florida Map Series".

Assumptions regarding the Middle basin, especially in the urbanized areas of the city of Orlando, were made due to the presence of drainage wells that aid in the disposal of excess surface water (Kimrey et al, 1984). Most of the drainage wells provide artificial recharge of the Upper Floridan

Aquifer and provide either direct street and urban drainage or lake-level control. A study completed by CH2M Hill evaluated the runoff coefficient for ten street and urban drainage well areas. It was determined that the average runoff coefficient was 0.578 but ranged from 0.376 to 0.837. The recharge from lake-level control wells was also estimated to be approximately 18.06 inches per year but the observed ranges varied greatly (CH2M Hill, 1997). Based on the findings from these studies and the large runoff coefficients determined, the loss rate for the developed areas surrounding the Orlando area was increased.

4.4.2 Lag Time Assumptions

Once the composite curve number for the proper AMC class was determined it was input into the lag time equations for SCS and NRCS lag time. Using multiple equations for lag time as noted previously in the report led to determination of an upper and lower bound of acceptable lag times for the sub-basins. Lag times were modified at higher or lower values than the average if the sub-basin had extensive drainage structures, retention ponds, or other property that would increase or decrease lag times. All lag times defined within the model were within the upper and lower bound determined by the calculated lag times using the various equations.

4.4.3 Reservoir Parameter Assumptions

The main reservoir parameter assumptions made are for the outlet method used. For sub-basins that contained structures such as culverts or spillways, known geometry was used. The geometric properties came from multiple sources such as USACE, SJRWMD, and Central and Southern Florida project design memorandums (USACE, 1991; Armstrong, 2001; Jobes, Personal Communication, 2014). As was stated previously, all stage-discharge curves were computed to discharge the maximum amount that was feasible due to the pump stations present.

4.4.4 Baseflow Assumptions

The hydrogeology conditions within the Upper and Middle St. Johns River include two primary aquifer systems, the Surficial Aquifer System (SAS) and the Floridan Aquifer System (FAS). The aquifer systems are separated by the Hawthorn Formation confining unit. The Hawthorn Formation varies in thickness across the St. Johns River basin (SJRWMD, 2012). Within the Upper St. Johns River the formation is relatively thick upstream of SR 520 but becomes very thin from SR 520 to SR 40 and within a majority of the middle St. Johns River. In areas where the formation is thick, groundwater discharge is minimal but in areas where the formation is thin or non-existent, groundwater discharge into or out of the FAS can be significant. According to the SJRWMD's St. Johns River Water Supply Impact Study; Groundwater Hydrology (2012), the potentiometric surface of the Upper FAS is above the water table of the SAS which creates a positive head difference and since the Upper FAS is in direct interaction with the river, groundwater can discharge into the river. This discharge occurs mainly through springs and by diffuse seepage.

Groundwater inflow from the FAS was modeled mainly as sub-basin baseflow. Within the study area, much of middle St. Johns River Basin and lower portion of the Upper St. Johns River Basin experience discharge from the FAS in areas surrounding the actual "flowway" of the St. Johns River. In addition, two springs in the Middle basin, Starbuck Spring and Clifton Spring which produce 1 to 10 million gallons per day (mgd) and are incorporated into the baseflow calculations in this area (Florida Geological Survey, 2004).

4.5 Model Calibration

The HEC-HMS model was calibrated and validated using existing observed storm events in the study area. To ensure that the model simulates the proper results and environmental processes,

the model is calibrated to the observed conditions during the period of August 1, 2008 to October 8, 2008, which coincided with landfall of Tropical Storm Fay. The process for calibration includes: 1) establishing the model parameters and determining those that will be changed for calibration, 2) defining the observed values and locations to which the model results should reproduce, 3) determining statistical goals for the model to be considered "calibrated", 4) performing iterative solutions and adjustment of parameters until the calibration goals have been met. The initial calibration of the model was completed using the rain gauge data. Once the model was deemed calibrated, the NEXRAD-derived data were input, as explained in Chapter 3 of this paper.

4.5.1 Calibration Parameters

The model input parameters were presented in section 4.2.1., with particular variables that may need modification to produce a best fit between the model and gauge observations. For the sub-basin parameters, these variables include the lag time, curve number, initial abstraction, and baseflow. Initial values for these parameters include: using the average lag time, average curve number between the AMC I and AMC II condition, initial abstraction at 0.2 of the potential maximum retention, and baseflow values at approximately 0 to 0.5 m^3/s for each sub-basin. As stated previously, multiple lag time equations were used to provide an assumed reasonable range for calibration. The results of the lag time values show the SCS lag time equation having the average lowest calculated lag time whereas the NRCS 1972 or Manning's Kinematic Shallow Concentrated equation had the larger calculated lag times. The curve number was only adjusted based on an assumed AMC because the land use/land type data are expected to be correct, but the moisture content may vary depending on the simulation starting condition. The initial abstraction value was changed depending on the curve number chosen, due to their interrelation

based on the percent of potential maximum retention. The baseflow values were estimated for those basins that are ungauged based on the approximate baseflow from gauged basins, known existing water levels, and any calculated spring flows.

It became apparent that the timing of the peak flow compared well to that of the discharge gauges, but the flow rate was greater than recorded at the gauge. In addition, the flow rates at the beginning of the simulation were too low within the flow way (USGS gauges 02232000 and 02232400), which meant the initial baseflow for the St. Johns was too low. The outflow results for the sub-basins which had discharge gauge data matched relatively well, with only minor modifications to the curve number and lag time to reproduce the gauge results.

The calibration parameter for each reach element was the selected Manning's n value within the Muskingum-Cunge routing method because all other parameters are physically measured. In addition, the loss/gain method will act as a calibration parameter due to the storage potential within the St. Johns flowway.

The reservoir element parameters for calibration include the initial reservoir elevation and outflow curves. Starting water surface elevations for the calibration model reservoirs were based on observed gauge data at locations where observed data were available. Typical water surface elevations, where observed gauge data were not available, were estimated on basin knowledge and elevations relative to the gauged basins. The outflow curve dataare meant to replicate realistic pumping rates for those basins and therefore the storage-discharge rates were modified to improve calibration statistics downstream while maintaining relatively close inflow and outflow rates.

4.5.2 Calibration Locations

The calibration locations are determined by the available discharge data locations as provided by USGS, SJRWMD, and SFWMD during the calibration timeframe. Unfortunately, there are not available discharge data for most of the sub-basins within the Upper and Middle St. Johns River. There are multiple calibration points within the St. Johns River flowway channel. Calibration of these locations will afford the assumption that sub-basins upstream are also relatively calibrated. The locations of the pertinent gauges can be seen in Figure 7, as was mentioned in Section 4.2.4.

4.5.3 Calibration Goals

The primary goal of the calibration process is to match the simulation results to the observed USGS gauge data as closely as possible. The modeled error, as measured by statistical analysis, should be minimized by calibration process. The statistical results will be included later in this report.

4.5.4 Calibration Simulations

Calibration of the model is achieved by running the HEC-HMS simulations, comparing the results to the observed data, adjusting parameter values within their reasonable ranges, and re-simulating until the best possible match is achieved. During this process the optimal or near-optimal values of the specified calibration parameters are identified. The calibration parameters are varied during the initial calibration process in order to develop an indication of parameter sensitivity. Those parameters that seem to produce a relatively close approximation to the observed data remain the same, while other parameters are modified to reproduce the results as closely as possible. This process was repeated multiple times, beginning at the headwater of the St. Johns and moving further downstream (Northern direction) until the simulation data matched relatively well to that of the discharge gauge data. It is an iterative process where parameters for

are changed both on a large scale (multi sub-basin) and small scale (singular sub-basin) basis for the closest calibration match possible.

4.5.5 Calibration Parameter Variation

Preliminary results, at the specified parameters mentioned above, showed a reasonable fit between the model and gauge observations data. The observed hydrograph peaks and shaping matched relatively well but it became apparent the model was overestimating runoff. Runoff was reduced by incorporating a higher rate of initial abstraction (approximately 0.4 for most basins). In addition, curve numbers were decreased for sub-basins believed to have dry starting conditions. Lag time values were also recalculated for any sub-basin if the soil type or infiltration topography was believed to warrant a shorter or longer lag time. The lag times were increased if the time to peak was believed to be disrupted due to structures or man-made storm drainage but were all kept within the originally calculated bounds. The specified baseflow was modified for gauged basins to provide a best-fit match to the days leading up to the storm event to replicate proper starting conditions. The final calibration parameter that was used to match the model and gauge observations was the hydrologic routing Manning's n and loss amounts. Manning's n numbers were modified slightly to ensure the proper lag time between gauge observations within the flow-way. The loss percentage within each reach was also increased or decreased slightly to ensure the proper amount of runoff was being conveyed downstream. The final Manning's n values, Lag time, and initial abstraction values for the calibration run, using rain gauge data as input, can be seen in Appendix A, Figure 1 and Figure 2.

4.6 Model Validation

Three model validation periods were chosen for two purposes: 1. Provide additional validation for the calibrated model 2. Perform comparison of rain gauge and radar data at multiple different

return frequencies. The model is validated to the observed conditions during the periods of October 1, 2007 to October 13, 2007; March 3, 2010 to March 20, 2010; October 1, 2011 to October 28, 2011.

Similar processes to those explained in section 4.5 Model Calibration were used during the model validation effort. The starting parameters of the validation model were the same as those determined in the model calibration. The goal of the validation model were to keep as many parameters the same as the calibration model, with minor changes due to initial starting conditions and basin behaviors due to the differences in initial conditions and rainfall events. It was determined that the different starting conditions would be accounted for by changing the initial abstraction values and baseflow values. Certain sub-basins during the validation runs may be considered AMC I or AMC II condition depending on the precipitation amount received before the simulation began. For these sub-basins, the initial abstraction ratio was modified to a value lower than used in the calibration. In addition, the loss percentage within the flow way of the St. Johns River was altered for the smaller and larger rain events. This is due to the larger loss percentages in the smaller rain events due to a higher storage volume available. In the calibration event and October 2011 validation event, storage was reduced due to the larger rain events occupying most of the overbank storage. The elevated water levels assumed during calibration and October 2011 validation caused lower storage availability because once the flow dominates the overbank section it begins to flow faster and the floodplain conveyance will increase. It has been seen in previous studies that the under low flow conditions the floodplain can act as a storage reservoir with low out of bank flow rates, but the retention potential rapidly decreases as the return period of the storm event increases due to the floodplain approaching the conditions of a conveyance channel due to the elevated water conditions (Wyzga, 1999).

The final validation parameters for all simulations using rain gauge data as input can be seen in Appendix B through D, Figure 1 for the 2007, 2010, and 2011 events, respectively.

4.7 Model Re-calibration Using NEXRAD Data

The model was initially calibrated and validated using the rain gauge data for all four simulation storm events. The NEXRAD precipitation was then input for each of the simulation events, without changing any of the other parameters. Re-calibration of the four periods became necessary in order to match the simulation results to the observed USGS gauge data as closely as possible, as was the original goal of the calibration using the rain gauge data. The only model parameters that were changed were the initial abstraction and loss fraction. The final parameters for all simulations can be seen in Appendix A through D, Figure 2.

Chapter 5

RESULTS

5.1 Comparison of NEXRAD and Rain Gauge Precipitation Measurements

The quality of the radar-rainfall measurements, although continuously advancing, remains largely unknown. It is important to distinguish the relationship between the precipitation datasets, as they have a direct impact hydrologic modeling results. Because the comparison of precipitation input in hydrologic simulation is the main objective of the research, the degree of similarity between the rainfall datasets must be analyzed. Comparative statistics will aid in understanding the potential differences in precipitation values, quality of the radar data, and the overall bias of radar generated rainfall compared to rain gauge rainfall quantities. The two statistical measures employed are the bias (B) and root mean square difference (RMSD), as completed in Neary et al. (2004), Skinner et al. (2009), and Jayakrishnan et al. (2004). The estimation bias (B) is the ratio of the total difference in precipitation between the radar total and rain gauge total to the rain gauge total, as seen in Equation 6.

$$Estimation\ Bias\ (\%) = \frac{Radar_{Total} - Gauge_{Total}}{Gauge_{Total}} * 100 \qquad \textit{Equation 6}$$

The RMSD was calculated to determine the degree of deviation or difference between the radar data predicted to the gauge value, which was actually observed. The RMSD represents the standard deviation of the differences between the predicted radar data and the observed gauge

data. It is used to evaluate the goodness of fit for the study rain gauge and NEXRAD data. The RMSD equation can be seen below in Equation 7.

$$RMSD = \sqrt{\frac{1}{n}\sum_{i=1}^{i=n}(R_i - G_i)^2} \qquad \textit{Equation 7}$$

Where:
G_i and R_i represent the *i*th day precipitation rate of gauge and radar, respectively
n is the sample size of radar and gauge pairs

In previous studies, radar estimates are compared with the corresponding gauge observations (Neary et al., 2004; Habib et al., 2009; Sexton et al., 2010). Comparative statistics are normally performed for the radar pixels (one grid) that contain gauges. As discussed earlier, the NEXRAD data processing uses the gauge observations to adjust, correct, and sometimes replace radar estimates. This causes a lack of independence between the two sets of estimates at these locations (Neary et al. 2004). Therefore, a direct comparison of the 2 by 2 km grid at the corresponding rain gauge data (point data) location may not provide an adequate representation of bias present within the dataset. To quantify the amount of total bias present between the datasets, precipitation inputs of particular sub-basins were chosen as the sampling areas. The sub-basins selected were within the boundaries of a single rain gauge Thiessen polygon area, thus the rain gauge data were applied for the entire sub-basin area. The NEXRAD data for the same sub-basin area were also determined by computing the area-weighted average sub-basin precipitation. This allowed for a direct comparison of precipitation data input for the same sub-basin at identical coverage areas. Additionally, distance measurements were computed from the rain gauge location to the centroid of the sub-basin. This was important because as stated above, bias between the gauge and radar data may be reduced (through radar-gauge correction) at

locations close to the gauges. For this reason, the distance was used to determine if the calculated biases were influenced by gauge location through the use of the coefficient of determination.

It was not the purpose of this comparison to examine, in full detail, the accuracy of the NEXRAD data provided, but to provide insight on the bias that may be present when performing simulations. The sub-basin rainfall data chosen for comparison are believed to be representative of the entire basin as they are located throughout the modeled area. The estimation bias for the total rainfall, per simulation event, can be seen in Table 8.

Table 8: Total Bias between Rain Gauge and NEXRAD data

Total Bias Between Rain Guage and NEXRAD datasets (%)				**Simulation Scenario**			
Subbasin I.D.	**Rain Gauge I.D.**	**NEXRAD I.D.**	**Distance (m)**	**2007**	**2008**	**2010**	**2011**
Evans Grove	1880101	752	12250	29.9%	-5.5%	-5.0%	-24.4%
C54 Retention	510206	1067	2850	-3.5%	5.7%	1.4%	10.6%
Bull Creek	590263	1081	8300	53.3%	-1.1%	-21.1%	-2.9%
St. Johns Tributary 3	100109	1135	3500	28.0%	19.9%	6.0%	19.6%
Cox Creek Upper	530225	1329	4200	18.9%	19.9%	14.8%	-0.6%
Green Branch	11523739	28	1500	24.1%	21.1%	4.6%	-0.8%
S.J.R. Puzzle	1140474	250	16500	-36.1%	5.1%	1.2%	-1.3%

The table illustrates that for seven sub-basins rainfall measurements, the total percent bias can range from -36.1% to 53.3%. The average overall bias for 2007 and 2008 were the greatest at 16% and 9%, respectively. The average bias of 2010 and 2011 was close to zero. An explanation behind this may be that radar estimation accuracy has been continuously increasing over the past few years, resulting in higher quality radar data. The higher values of bias indicate that significant random differences may exist between the radar estimates and the corresponding gauge measurements for many of the sub-basins within the model. Additionally, a majority of the sub-basins show a positive bias which indicates that the NEXRAD data may be overestimating rainfall compared to the corresponding gauge.

The total bias was plotted against the distance from the rain gauge to the centroid of the sub-basin in Figure 8. Linear regression was performed and the associated coefficient of determination is shown in the figure. The data show that the total bias is relatively positive at distances up to 5000 feet, with a much smaller difference in the magnitude of bias than the data points at distances greater than 6000 feet. From this it can be inferred that the absolute value of the bias percentage may increase as the distance from the gauge becomes greater. These results agree with the fact that gauge observations were used in the processing of the radar data, and thus the percent bias is expected to be the smallest near the rain gauge location.

When reviewing the data based on the simulation scenario and magnitude of rain each represents, no noticeable trend in total bias (overestimation or underestimation) is present. Although there is not a strong correlation, all trend lines have a negative slope, thereby showing there is a slight relationship between gauge distance and total bias. This relationship suggests that as the distance of the centroid of the sub-basin increases from the rain gauge, the total radar bias (compared to rain gauge) may become negative. Due to the minimal r^2, no strong correlation can be detected regarding total bias in terms of distance from the rain gauge. Additional measurements would need to be made to come to a clear consensus.

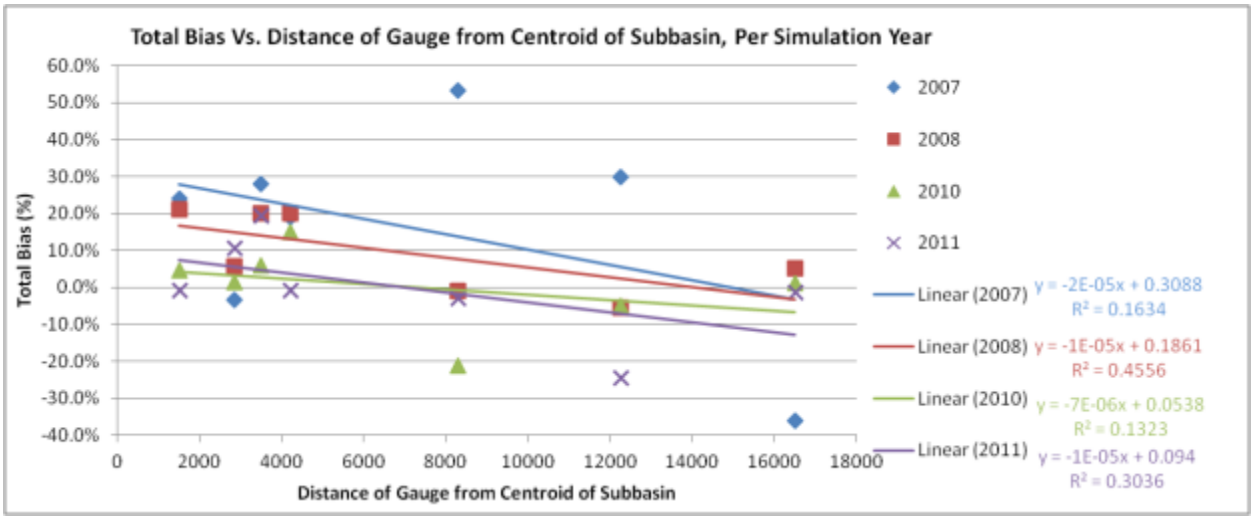

Figure 8. Total Bias vs. Distance of Rain Gauge from Centroid of Sub-basin

The RMSD values can be seen in Table 9. These results help quantify the random differences between the data sets to show the magnitude of error. As can be seen from the table, error up to 0.5 inches was calculated. This error can cause significant implications in hydrologic runoff calculations due to the undesired over- or under-estimation of rainfall amounts. The seven selected rain gauge/NEXRAD locations show relatively similar RMDS values across the four simulation scenarios. The RMSD values calculated for each sub-basin are neither high nor low for a particular simulation scenario or distance. It is interesting to note that during the validation simulation of 2007, the RMSD values were relatively high in relation to the total rainfall for the simulation. This may indicate that the radar data are capturing more of the spatial variability during the storm event, causing higher RMSD values.

Table 9: Total RMSD Between Rain Gauge and NEXRAD Datasets

Total RMSD Between Rain Gauge and NEXRAD Datasets (in.)				Simulation Scenario			
Subbasin I.D.	**Rain Gauge I.D.**	**NEXRAD I.D.**	**Distance (m)**	**2007**	**2008**	**2010**	**2011**
Evans Grove	1880101	752	12250	0.29	0.33	0.17	0.50
C54 Retention	510206	1067	2850	0.15	0.28	0.09	0.26
Bull Creek	590263	1081	8300	0.36	0.26	0.28	0.17
St. Johns Tributary 3	100109	1135	3500	0.10	0.28	0.09	0.30
Cox Creek Upper	530225	1329	4200	0.12	0.20	0.09	0.08
Green Branch	11523739	28	1500	0.14	0.32	0.14	0.08
S.J.R. Puzzle	1140474	250	16500	0.22	0.31	0.11	0.10

A Pairwise difference of median test, the Wilcoxon signed-rank test, was used to determine if the differences in rainfall estimated were statistically significant for each simulation event. The total rainfall for both precipitation input types were compared for each simulation period. This type of statistical test is known as a hypothesis test. They are used to determine if the results of a comparison are statistically significant through the use of a null and alternative hypothesis at a pre-specified level of significance. The null hypothesis for this test states that the medians of the two samples are identical. The significance level is commonly set at 0.05 or 0.01. If the calculated *p*-value is less than the significance level, the null hypothesis is rejected. This statistical test is described in greater detail in the section 5.2 of this report. The results of the Wilcoxon test area shown in Table 10.

Table 10: Wilcoxon Signed-Rank Test Results for the Total Rainfall Measurements, per Simulation

Wilcoxon Signed Rank Test	**2007**		**2008**		**2010**		**2011**	
	Rain Gauge	NEXRAD	Rain Gauge	NEXRAD	Rain Gauge	NEXRAD	Rain Gauge	NEXRAD
Median Value	3.41	3.67	19.48	21.84	4.9	4.86	11.9	12.23
N, number of samples	7		7		7		7	
W test statistic	21		21		16		17	
p value	0.297		0.297		0.813		0.688	

The results show that because the *p*-value is greater than the chosen significance level, the null hypothesis is not rejected. Hence, there is not a significant difference in total rainfall measurements between the rain gauge and NEXRAD datasets.

This analysis helps gain insight on the differences in precipitation input between the radar estimated data and the rain gauge data. The statistical and graphical results were used to characterize the differences and agreements between the rain gauge and radar rainfall values. The results show that at the selected sub-basins, overestimation of radar data was more common than underestimation. A strong correlation was not detected to support a conclusion that the NEXRAD data overestimate or underestimate rainfall for certain return frequency precipitation events.

5.2 Model Performance Evaluation

Having known discharge gauge and simulation data allows a direct comparison to be made to evaluate the performance of the model. This comparison will be completed using three different statistical measures: the coefficient of determination, the Nash-Sutcliffe efficiency coefficient, and the Mann-Whitney Test. These statistics were used to quantitatively compare the hydrologic simulation results to determine which precipitation input method yielded the most accurate results for the various simulations events.

The coefficient of correlation (*r*) measures the strength and direction of the linear relationship between variables of the measured gauge data and simulation data. The calculated *r* value will be between -1 and 1, with 0 representing no correlation. The linear correlation becomes stronger as the *r* value approaches -1 or 1. The coefficient of determination (r^2) gives the variance of the data and assesses a goodness of fit at each calibration point for the model. The equation for r^2 can be seen below in Equation 8. It can help explain the variability of the model and how well

the model may produce results for future predictions. The coefficient of determination is between 0 and 1, with 1 indicating a perfect fit with all variation explained.

$$r^2 = \left(\frac{\sum_{i=1}^{n}(O_i - \bar{O})(S_i - \bar{S})}{\sqrt{\sum_{i=1}^{n}(O_i - \bar{O})^2}\sqrt{\sum_{i=1}^{n}(S_i - \bar{S})^2}} \right)^2 \qquad \textit{Equation 8}$$

Where: O_i is the observed data on the *i*th day
S_i is the simulated data on the *i*th day
$\bar{O}$ and $\bar{S}$ is the observed and simulated mean values, respectively
n is the number of observations

The Nash-Sutcliffe efficiency coefficient (NSE) (Nash and Sutcliffe, 1970) normalized statistic that determines the relative magnitude of the residual variance compared to the measured data variance and indicates how well the plot of the observed data versus the simulated data fits the 1:1 line (Wang et al., 2009). The NSE equation can be seen below in Equation 9.

$$NSE = 1 - \frac{\sum_{i=1}^{n}(O_i - S_i)^2}{\sum_{i=1}^{n}(O_i - \bar{O})^2} \qquad \textit{Equation 9}$$

Where: O_i is the observed data on the *i*th day
S_i is the simulated data on the *i*th day
$\bar{O}$ is the observed mean value
n is the number of observations

The ranges for NSE can vary between -∞ to 1, where: NSE=1 corresponds to a perfect match between discharge data and observed data; NSE=0 shows that the model predictions are as accurate as the mean of the observed data; and -∞<NSE<0 occurs when the observed mean is a better predictor than the model, which indicates unacceptable performance (Wang et al., 2009). The St. Johns River Water Supply Impact Study (2012) completed by the SJRWMD used the Nash-Sutcliffe statistic to explain the calibration performance for their hydraulic model. Following similar methodology, the Nash-Sutcliffe coefficient values will be divided into

intervals which explain performance rating. The intervals are as follows: $0.75 < NSE < 1$ is a "very good" performance rating, $0.65 < NSE < 0.75$ is a "good" performance rating, $0.50 < NSE < 0.65$ is a "satisfactory" performance rating, and $NSE < 0.50$ is an "unsatisfactory" performance rating.

The Wilcoxon signed-rank test is a nonparametric test of hypothesis used to determine whether there is a significant difference between the medians of two related groups. It is an analysis that is useful to determine if the population median-ranks differ between measurements that are repeated, also known as a paired difference test. It can be used as an alternative to the commonly known *t*-test when the data are not normally distributed. The data were determined to be non-normally distributed by the Shapiro-Wilk test. This test utilizes the null hypothesis that the data set is normally distributed. For a majority of the r^2 and NSE results, the *p*-vale was less than the selected alpha level of 0.05, causing rejection of the null hypothesis and assumption of a non-normal distribution.

The calculation of the Wilcoxon signed-rank test involves a *W* test statistic, whose distribution under the null hypothesis (distributions between the pairs are equal) is known. Using the test statistic *W* a z-score and p-value can be calculated. If the p-value calculated is less than the significance level (α), than the groups are statistically significant and the null hypothesis is rejected. The selected significance level for all tests was chosen as 0.05. This test will determine if the resulting NSE and R^2 between the groups of data are statistically significant, that is, there is a distinct difference between the NEXRAD-generated and rain gauge-generated simulation results. If the null hypothesis is rejected then the simulation results are unlikely to have occurred by chance and the simulation results from each precipitation input type do indeed differ.

5.3 Simulation Results

The four simulation runs, representing the different rainfall return frequencies, were completed using two different rainfall input types. The simulation runs were first calibrated to the rain gauge data input. The results for each simulation are in the subsequent sections. The NEXRAD data were then input into the different simulations and the model was rerun without changing any parameters. These results are known as the "NEXRAD (un-calibrated)". Based upon the results presented in section 5.1, bias between the rain gauge data and NEXRAD data is present, causing an overall change in the input of rainfall to the model. As stated previously, multiple researchers have stressed the importance of re-calibrating the model due to the changes in precipitation data source (Neary et al., 2004; Kalin et al., 2006; Price et al., 2013). Therefore, it was determined to perform additional calibration to see if the effort would result in an improvement of the results. These results are known as the "NEXRAD (calibrated)".

The final statistical results are presented on a per simulation basis, with a comparative framework designed to determine which precipitation input yielded more accurate results. Simulation events using NEXRAD data that outperform simulations using gauge data will suggest that, at the return frequency representative of the event, radar data improve model accuracy. Additionally, statistical comparisons and results for the two precipitation input methods at various sub-basin scales are discussed. All simulation results are shown graphically in Figures in Appendices A thru D. These figures show the discharge flow rate in cubic meters per second (CMS) versus time/date for the simulation data. The USGS observed streamflow is plotted against the simulated flow for each precipitation input type. The rain gauge precipitation input and the NEXRAD data (before and after model recalibration) are plotted separately to remain uncomplicated for ease of evaluation.

5.3.1 Calibration, August 2008 to October 2008 Simulation Results

The calibration performance results for the August 2008 to October 2008 simulation event for both the rain gauge precipitation and radar-derived precipitation inputs can be seen in Appendix A. Figures 3 thru 15. These figures show that, at a majority of the discharge gauge locations, the un-calibrated NEXRAD data highly over estimated flow rates. This would suggest that the NEXRAD data overestimated rainfall amounts when compared to the rain gauge data. Once minor recalibration was completed, the calibrated NEXRAD flow rates were comparable to the rain gauge flow rates.

The coefficient of determination results are shown in Table 11. The model was calibrated to the 2008 simulation event with a high level of accuracy, as can be inferred from the high r^2 values. The r^2 values are above 0.75 for all precipitation input methods which suggests a strong goodness of fit between the simulation results and observed data. An increase in the r^2 value of the NEXRAD calibrated and un-calibrated data occurred at six locations, remained the same at two locations, and decreased at five locations.

Outcomes of the two precipitation input methods were compared using the Wilcoxon signed-rank test. Median r^2 values were 0.89 for the rain gauge and 0.9 for the NEXRAD (calibrated) data. The distributions between the two groups did not differ significantly ($W=34.5$, $z=0.13$, $p=0.917$). The high *p* value shows that the models performance using the rain gauge and NEXRAD data is similar and the null hypothesis that the distributions are equal should not be rejected. Even though the NEXRAD data improved r^2 values at more locations than the rain gauge data, the overall improvement of r^2 values is not great enough to say with certainty that NEXRAD produces an improvement in model accuracy.

Table 11: Coefficient of Determination Values for All Precipitation Input Types during the 2008 Calibration Model

Coefficient of Determination Simulation Event From Aug 2008 to Oct 2008		***Rain Gauge***	***NEXRAD (Uncalibrated)***	***NEXRAD (Calibrated)***
Location	**Gauge**	r^2	r^2	r^2
Fort Drum Creek	USGS 02231342	0.89	0.91	0.93
Blue Cypress Creek	USGS 02231396	0.89	0.91	0.90
Jane Green Reservoir	USGS 02231600	0.91	0.90	0.90
U.S. Highway 192	USGS 02232000	0.88	0.90	0.89
Pennywash Creek	USGS 02232155	0.86	0.88	0.87
Wolf Creek North	USGS 02232200	0.87	0.87	0.87
State Highway 520	USGS 02232400	0.98	0.98	0.98
State Highway 50	USGS 02232500	0.95	0.91	0.93
Inlet of Lake Harney	USGS 02234000	0.93	0.91	0.91
Little Econlockhatchee River at Union Park	USGS 02233460	0.85	0.91	0.91
Little Econlockhatchee River at University Blvd.	USGS 02233473	0.89	0.92	0.92
Econlockhatchee River near Oviedo	USGS 02233484	0.90	0.79	0.80
Econlockhatchee River near State Highway 13	USGS 02233500	0.87	0.78	0.78

The results from the Nash-Sutcliffe efficiency statistical analysis can be seen in Table 12. The model performance measures during the calibration period show a strong agreement between the simulated and observed streamflow. For the rain gauge and NEXRAD calibrated simulations, all NSE coefficients are above 0.75 which is considered a "very good" performance. The un-calibrated NSE results improved at one three locations, stayed the same at one location and decreased at nine locations. Improvements in NSE values using NEXRAD calibrated data occurred at four locations, stayed the same at four locations, and decreased at five locations. Median NSE values were .86 for the rain gauge and .88 for the NEXRAD (calibrated) data. The Wilcoxon signed-rank test determined that the distributions between the two groups did not differ significantly (W=325, z=0.297, p=0.797). There is a high probability that the distributions between the data sets are equal. Both Wilcoxon sign-rank test *p* values suggest that there is no

significant improvement of simulated streamflow values when using the NEXRAD data as compared to the rain gauge data.

Table 12: Nash-Sutcliffe Efficiency Values for All Precipitation Input Types during the 2008 Calibration Model

Nash-Sutcliffe Coefficient Simulation Event From Aug 2008 to Oct 2008		***Rain Gauge***	***NEXRAD (Uncalibrated)***	***NEXRAD (Calibrated)***
Location	**Gauge**	**NSE**	**NSE**	**NSE**
Fort Drum Creek	USGS 02231342	0.85	0.90	0.93
Blue Cypress Creek	USGS 02231396	0.84	0.58	0.84
Jane Green Reservoir	USGS 02231600	0.90	0.88	0.89
U.S. Highway 192	USGS 02232000	0.86	0.81	0.87
Pennywash Creek	USGS 02232155	0.79	0.61	0.79
Wolf Creek North	USGS 02232200	0.87	0.87	0.87
State Highway 520	USGS 02232400	0.98	0.90	0.98
State Highway 50	USGS 02232500	0.94	0.76	0.92
Inlet of Lake Harney	USGS 02234000	0.90	0.86	0.88
Little Econlockhatchee River at Union Park	USGS 02233460	0.83	0.89	0.89
Little Econlockhatchee River at University Blvd.	USGS 02233473	0.86	0.87	0.88
Econlockhatchee River near Oviedo	USGS 02233484	0.89	0.74	0.77
Econlockhatchee River near State Highway 13	USGS 02233500	0.85	0.66	0.77

Overall, the model performs well using both precipitation input types. The NEXRAD un-calibrated model simulation results demonstrate a decline in model performance, as can be seen from the decrease in r^2 and NSE values. When reviewing the hydrograph results in Appendix A, figures 3 thru 15 it becomes apparent that the NEXRAD precipitation input was much higher than the rain gauge precipitation input due to the large increase in runoff. Once the model parameters were re-calibrated to the NEXRAD data, the statistical performance increased to values similar to the rain gauge data input. These results reiterate the importance of proper precipitation input due to the possible difference in magnitude of runoff values.

The statistical analysis results show that at a frequency of approximately 5 to 10 year-24 hour duration rainfall, no significant improvement or decline in model streamflow accuracy is present.

5.3.2 Validation, October 2007 Simulation Results

The validation performance results for the October 2007 simulation event for both the rain gauge precipitation and radar-derived precipitation inputs can be seen in Appendix B, Figures 3 thru 15. Similar to the 2008 calibration results, the un-calibrated NEXRAD data produced higher flow rates than the observed discharge gauge data for a majority of locations.

The results for the coefficient of determination are shown in Table 13. The r^2 values differ significantly depending on the discharge location, with a majority of locations showing relatively low correlation (closer to zero than one). The NEXRAD r^2 values were compared against the rain gauge r^2 values to determine improvement or decline. The r^2 improves at five locations for the un-calibrated NEXRAD data and at seven locations when using the calibrated NEXRAD data. The r^2 value decreases at eight and five locations for the NEXRAD un-calibrated and NEXRAD calibrated data, respectively. Finally, the r^2 remained the same at only one location for the calibrated NEXRAD data. Those locations which showed improvement increased the overall average r^2 value from 0.39 to 0.63, which is a favorable increase in performance. The median r^2 values were calculated as 0.53 and 0.7 for the rain gauge and NEXRAD (calibrated) data, respectively. The Wilcoxon signed-rank test calculated W value was 55 and a p value of 0.233 was determined, thus the null hypothesis can only be rejected at an alpha value of 0.23, which is higher than the specific alpha value of 0.05.

Table 13: Coefficient of Determination Values for All Precipitation Input Types during the 2007 Validation Model

Coefficient of Determination Simulation Event Oct 2007		***Rain Gauge***	***NEXRAD (Uncalibrated)***	***NEXRAD (Calibrated)***
Location	**Gauge**	r^2	r^2	r^2
Fort Drum Creek	USGS 02231342	0.49	0.62	0.70
Blue Cypress Creek	USGS 02231396	0.52	0.82	0.63
Jane Green Reservoir	USGS 02231600	0.64	0.73	0.87
U.S. Highway 192	USGS 02232000	0.90	0.89	0.88
Pennywash Creek	USGS 02232155	0.11	0.00	0.55
Wolf Creek North	USGS 02232200	0.29	0.89	0.86
State Highway 520	USGS 02232400	0.48	0.25	0.30
State Highway 50	USGS 02232500	0.95	0.91	0.89
Inlet of Lake Harney	USGS 02234000	0.72	0.32	0.60
Little Econlockhatchee River at Union Park	USGS 02233460	0.16	0.23	0.23
Little Econlockhatchee River at University Blvd.	USGS 02233473	0.53	0.52	0.56
Econlockhatchee River near Oviedo	USGS 02233484	0.85	0.80	0.81
Econlockhatchee River near State Highway 13	USGS 02233500	0.82	0.80	0.82

The results for the NSE values are in Table 14. Many of these locations had little to no correlation (negative values), as determined by NSE value, when using rain gauge data as the precipitation input method. Additionally, the NEXRAD data caused a decrease in NSE values at every location except two, when the model was un-calibrated. Once the NEXRAD data simulation was recalibrated, an improvement over the rain gauge NSE values was observed at ten locations. The use of the NEXRAD data allowed significant improvement at many of these locations. The use of NEXRAD data only caused the NSE to decrease at three locations, with the comparative magnitude of change being relatively small. The median values for the NSE values were -.06 and 0.53 for the rain gauge and NEXRAD (calibrated) data, respectively. The calculated *W* value was 81 with a *p*-value of 0.01. This shows that a statistically significant difference of median is present at the alpha level of 0.05. In fact, the *p*-value shows significance at the lower alpha level of 0.01. Therefore, from the results it can be inferred that the NEXRAD

calibrated data simulations estimate flow more accurately than the rain gauge simulations for rainfall return frequencies less than 1 year 24 hours.

Table 14: Nash-Sutcliffe Efficiency Values for All Precipitation Input Types during the 2007 Validation Model

Nash-Sutcliffe Coefficient Simulation Event Oct 2007		***Rain Gauge***	***NEXRAD (Uncalibrated)***	***NEXRAD (Calibrated)***
Location	**Gauge**	**NSE**	**NSE**	**NSE**
Fort Drum Creek	USGS 02231342	0.33	0.48	0.65
Blue Cypress Creek	USGS 02231396	-0.06	-2.76	0.11
Jane Green Reservoir	USGS 02231600	0.41	0.30	0.81
U.S. Highway 192	USGS 02232000	0.74	0.59	0.72
Pennywash Creek	USGS 02232155	-1.27	-1.78	0.14
Wolf Creek North	USGS 02232200	-0.11	0.33	0.77
State Highway 520	USGS 02232400	-1.00	-5.29	-1.25
State Highway 50	USGS 02232500	0.67	-0.34	0.53
Inlet of Lake Harney	USGS 02234000	-0.47	-1.37	0.21
Little Econlockhatchee River at Union Park	USGS 02233460	-2.44	-2.36	-0.72
Little Econlockhatchee River at University Blvd.	USGS 02233473	-2.86	-2.21	-0.30
Econlockhatchee River near Oviedo	USGS 02233484	0.57	0.36	0.58
Econlockhatchee River near State Highway 13	USGS 02233500	0.19	0.15	0.74

The validation results for October 2007 have relatively low overall r^2 and NSE values, when compared to other 2008 simulation results. Reasons for this may be the large differences in order of magnitude of precipitation during the simulation runs for the 2008 calibration and 2011 validation periods (e.g. high return frequency precipitation event) and the 2007 validation period (very low return frequency precipitation event). Due to the minimal amount of precipitation received during the validation period, runoff values are very sensitive to the initial abstraction rate, curve number, and lag time parameters. Explanation of all possible discrepancies in flow rate measurements will be described later in this report. As can be seen from the Figures 3 to 15 within Appendix B, many of the gauges had changes in discharge rates of fewer than 5 cms.

Visually, the NEXRAD calibrated data shows improvement over the rain gauge data at many of the discharge gauge locations.

5.3.3 Validation, March 2010 Simulation Results

The validation performance results for the March 2010 simulation event for both the rain gauge precipitation and radar-derived precipitation inputs can be seen in Appendix C, Figures 3 thru 15. The un-calibrated NEXRAD simulations indicate that streamflow values are roughly equal to the discharge gauge data in some locations, while overestimating flow in other locations. There was greater agreement between the un-calibrated NEXRAD data and discharge gauge data during the March 2010 simulation than the previously mentioned 2007 and 2008 simulations.

The results for the coefficient of determination are shown in Table 15. A majority of the rain gauge r^2 results were close to one, showing a strong relationship between the simulated and observed streamflow data. The NEXRAD data produced very similar r^2 results to the rain gauge data, therefore minimal recalibration of the NEXRAD data was performed. The range of r^2 values between the three data sets is less than 0.06, reinstating that the simulations were in strong agreement across precipitation inputs, with and without re-calibration. For the r^2 values, improvements for the NEXRAD data occurred at five locations for the un-calibrated simulation and three locations for the calibrated simulation. The calibrated NEXRAD data had a decrease in the r^2 at six locations and stayed the same at two locations. The un-calibrated NEXRAD data decreased at five locations and stayed the same at one location. The median values for both the rain gauge and NEXRAD (calibrated) data for r^2 was 0.9. The Wilcoxon signed-rank test *W* value was 29.5 and the *p* value was calculated as 0.41, which suggests that there is not a significant difference between the rain gauge and NEXRAD calibrated distributions. The *p*

value, although not close to the normal significant levels of approximately 0.05 or 5% is relatively low compared to the results of the August 2008 Calibration model.

Table 15: Coefficient of Determination Values for All Precipitation Input Types during the 2010 Validation Model

Coefficient of Determination Simulation Event March 2010		***Rain Gauge***	***NEXRAD (Uncalibrated)***	***NEXRAD (Calibrated)***
Location	**Gauge**	r^2	r^2	r^2
Fort Drum Creek	USGS 02231342	0.89	0.91	0.91
Blue Cypress Creek	USGS 02231396	0.91	0.92	0.90
Jane Green Reservoir	USGS 02231600	0.94	0.95	0.95
U.S. Highway 192	USGS 02232000	0.96	0.94	0.93
Pennywash Creek	USGS 02232155	0.85	0.90	0.85
Wolf Creek North	USGS 02232200	0.86	0.81	0.86
State Highway 520	USGS 02232400	0.97	0.91	0.96
State Highway 50	USGS 02232500	0.95	0.92	0.92
Inlet of Lake Harney	USGS 02234000	0.95	0.95	0.93
Little Econlockhatchee River at Union Park	USGS 02233460	N/A	N/A	N/A
Little Econlockhatchee River at University Blvd.	USGS 02233473	N/A	N/A	N/A
Econlockhatchee River near Oviedo	USGS 02233484	0.90	0.89	0.89
Econlockhatchee River near State Highway 13	USGS 02233500	0.65	0.68	0.67
*N/A denotes USGS gauge data that was not available				

The NSE Coefficient results are shown in Table 16. The NSE values show the model performed very well (NSE > 0.75) at all locations, besides one, for the rain gauge and NEXRAD data. Similar to the r^2 results, the rain gauge and NEXRAD NSE values show a high level of agreement between simulation and observed data. Improvements of NSE values occur at four locations for the un-calibrated and calibrated model. The NSE values were equal at one location for un-calibrated NEXRAD and three locations for the calibrated NEXRAD. A decrease in NSE occurred at six locations for un-calibrated NEXRAD and four locations for the calibrated NEXRAD.

The median value for the rain gauge NSE values was 0.85 whereas the NEXRAD (calibrated) was 0.86. The Wilcoxon *W* was 29 and the *p* value was 0.484. The datasets show there is

relatively low probability of equal median values. The results suggest that there is no significant improvement of streamflow values using the NEXRAD data over the rain gauge data.

Table 16: Nash-Sutcliffe Efficiency Values for All Precipitation Input Types during the 2010 Validation Model

Nash-Sutcliffe Coefficient Simulation Event March 2010		***Rain Gauge***	***NEXRAD (Uncalibrated)***	***NEXRAD (Calibrated)***
Location	**Gauge**	**NSE**	**NSE**	**NSE**
Fort Drum Creek	USGS 02231342	0.85	0.86	0.86
Blue Cypress Creek	USGS 02231396	0.86	0.82	0.86
Jane Green Reservoir	USGS 02231600	0.91	0.94	0.94
U.S. Highway 192	USGS 02232000	0.98	0.97	0.97
Pennywash Creek	USGS 02232155	0.85	0.68	0.84
Wolf Creek North	USGS 02232200	0.83	0.74	0.83
State Highway 520	USGS 02232400	0.96	0.91	0.94
State Highway 50	USGS 02232500	0.93	0.88	0.91
Inlet of Lake Harney	USGS 02234000	0.87	0.87	0.88
Little Econlockhatchee River at Union Park	USGS 02233460	N/A	N/A	N/A
Little Econlockhatchee River at University Blvd.	USGS 02233473	N/A	N/A	N/A
Econlockhatchee River near Oviedo	USGS 02233484	0.79	0.80	0.84
Econlockhatchee River near State Highway 13	USGS 02233500	0.24	0.42	0.44
*N/A denotes USGS gauge data that was not available				

The model performance statistics indicate a high level of performance during the simulation event for both the rain gauge and NEXRAD data input. Only one location had an unsatisfactory NSE and r^2 value. Visual observations of the results show that the duration of the peak is too short. The observed flow rate may be influenced by downstream tailwater conditions, which cannot be modeled adequately with the HEC-HMS modeling platform. It is important to note that the NEXRAD data significantly improved the NSE value at this location.

5.3.4 Validation, October 2011 Simulation Results

The validation performance results for the October 2011 simulation event for both the rain gauge precipitation and radar-derived precipitation inputs can be seen in Appendix D, Figures 3 thru 13. The r^2 results for the October validation period are shown in Table 17. Similar to the March 2010 simulation, only minor recalibration was needed after the NEXRAD data was input. The

un-calibrated NEXRAD data produce r^2 values that were in many instances close to or equal to the rain gauge r^2 values. The calibrated NEXRAD produced r^2 values that were higher at four locations, lower at five locations, and the same at two locations. The median r^2 values were 0.94 and 0.93 for the rain gauge and NEXRAD (calibrated) results. The Wilcoxon signed-rank test *p* value was determined to be 0.828 with a W test statistic of 24.5. The distributions of the two results did not differ significantly. This implies that the rain gauge and NEXRAD data produce similar streamflow results, with neither input producing more accurate results.

Table 17: Coefficient of Determination Values for All Precipitation Input Types during the 2011 Validation Model

Coefficient of Determination Simulation Event October 2011		***Rain Gauge***	***NEXRAD (Uncalibrated)***	***NEXRAD (Calibrated***
Location	**Gauge**	r^2	r^2	r^2
Fort Drum Creek	USGS 02231342	0.83	0.77	0.77
Blue Cypress Creek	USGS 02231396	0.80	0.80	0.80
Jane Green Reservoir	USGS 02231600	0.76	0.74	0.78
U.S. Highway 192	USGS 02232000	0.98	0.97	0.97
Pennywash Creek	USGS 02232155	0.74	0.76	0.76
Wolf Creek North	USGS 02232200	0.82	0.82	0.84
State Highway 520	USGS 02232400	0.99	0.99	0.98
State Highway 50	USGS 02232500	0.94	0.94	0.93
Inlet of Lake Harney	USGS 02234000	0.95	0.95	0.95
Little Econlockhatchee River at Union Park	USGS 02233460	N/A	N/A	N/A
Little Econlockhatchee River at University Blvd.	USGS 02233473	N/A	N/A	N/A
Econlockhatchee River near Oviedo	USGS 02233484	0.94	0.95	0.95
Econlockhatchee River near State Highway 13	USGS 02233500	0.96	0.95	0.95
*N/A denotes USGS gauge data that was not available				

The NSE results can be seen in Table 18.The model performed relatively well at all locations, with a majority of NSE values showing very good performance. The NERAD un-calibrated and calibrated NSE results showed improvement over the rain gauge NSE values at six locations. A decrease in NSE values for the NEXRAD data occurred at four locations and remained the same at one location. The median value for the rain gauge NSE data was 0.93 and the NEXRAD (calibrated) median NSE value was 0.89. The Wilcoxon signed-rank test *p* value was determined

to be 0.326 with a *W* test statistic of 38. Again, this shows that the rain gauge and NEXRAD data inputs produce comparable results, with similar median flow rate values. Similar to the March 2010 NSE Wilcoxon results, the p-value is not as high as the August 2008 test. The Wilcoxon test shows a relatively low significance level of 32.6%, but it should be noted the median value is higher for the rain gauge data than the NEXRAD results.

Table 18: Nash-Sutcliffe Efficiency Values for All Precipitation Input Types during the 2011 Validation Model

Nash-Sutcliffe Coefficient Simulation Event October 2011		***Rain Gauge***	***NEXRAD (Uncalibrated)***	***NEXRAD (Calibrated***
Location	**Gauge**	**NSE**	**NSE**	**NSE**
Fort Drum Creek	USGS 02231342	0.67	0.72	0.72
Blue Cypress Creek	USGS 02231396	0.72	0.74	0.74
Jane Green Reservoir	USGS 02231600	0.59	0.61	0.64
U.S. Highway 192	USGS 02232000	0.98	0.97	0.97
Pennywash Creek	USGS 02232155	0.64	0.69	0.69
Wolf Creek North	USGS 02232200	0.80	0.82	0.83
State Highway 520	USGS 02232400	0.99	0.98	0.98
State Highway 50	USGS 02232500	0.94	0.82	0.89
Inlet of Lake Harney	USGS 02234000	0.93	0.95	0.94
Little Econlockhatchee River at Union Park	USGS 02233460	N/A	N/A	N/A
Little Econlockhatchee River at University Blvd.	USGS 02233473	N/A	N/A	N/A
Econlockhatchee River near Oviedo	USGS 02233484	0.94	0.94	0.94
Econlockhatchee River near State Highway 13	USGS 02233500	0.95	0.94	0.94

5.4 Model Simulation Results at Different Spatial Scales

The model performance measures were compared across simulation events for both individual sub-basins and at locations downstream of multiple sub-basins. Individual sub-basins are labeled by the sub-basin name whereas locations for multiple sub-basins contain the word “upstream” as to be representative of all sub-basins upstream of that location. This is true for many locations within the St. Johns River and the Econlockhatchee River, where many sub-basins contribute to the discharge location used for comparison.

To determine if NEXRAD data input produced more accurate results at particular sub-basin scales, the r^2 and NSE performance evaluations for all simulations were compared. This was accomplished by subtracting the rain gauge r^2 and NSE value from the associated NEXRAD r^2 and NSE value. Positive results suggest that the NEXRAD data is an improvement over the rain gauge data at that sub-basin location, whereas negative results would suggest the opposite is true. The results for the relative improvement or decline of NEXRAD r^2 and NSE values for the different sub-basin sizes can be seen in Tables 19 and 20, respectively.

Table 19: Relative Improvement or Decline of NEXRAD r^2 Values for Different Sub-basin Sizes

Relative Improvement (+) or Decline (-) for NEXRAD r^2 values over Rain Gauge r^2 values					
Location, Sub-basin (s)	**Total Area**	**August 2008 NEXRAD - Rain Gauge r^2 Values**	**October 2007 NEXRAD - Rain Gauge r^2 Values**	**March 2010 NEXRAD - Rain Gauge r^2 Values**	**October 2011 NEXRAD - Rain Gauge r^2 Values**
Fort Drum Creek	121 km^2	0.04	0.21	0.02	-0.06
Blue Cypress Creek	247 km^2	0.01	0.11	-0.01	0
Jane Green Creek	612 km^2	-0.01	0.23	0.01	0.02
All Upstream of U.S. 192	2379 km^2	0.01	-0.02	-0.03	-0.07
Pennywash Creek	52 km^2	0.01	0.44	0	0.02
Wolf Creek North	65 km^2	0	0.57	0	0.02
All Upstream of S.R. 520	3303 km^2	0	-0.18	-0.01	-0.01
All Upstream of S.R. 50	3817 km^2	-0.01	-0.06	-0.03	-0.01
Upstream of Inlet of Lake Harney	5038 km^2	-0.02	-0.12	-0.02	0
Upstream of Little Econlockhatchee River at Union Park	60 km^2	0.06	0.07	N/A	N/A
Upstream of Little Econlockhatchee River at Univserity Blvd.	228 km^2	0.03	0.03	N/A	N/A
Upstream of Econlockhatvhee River near Oviedo	591 km^2	-0.1	-0.04	-0.01	0.01
Upstream of Econlockhatvhee River near State Highway 13	702 km^2	-0.09	0	0.02	-0.1

Table 20: Relative Improvement or Decline of NEXRAD NSE Values for Different Sub-basin Sizes

Relative Improvement (+) or Decline (-) for NEXRAD NSE values over Rain Gauge NSE values					
Location, Sub-basin (s)	**Total Area**	**August 2008 NEXRAD - Rain Gauge NSE Values**	**October 2007 NEXRAD - Rain Gauge NSE Values**	**March 2010 NEXRAD - Rain Gauge NSE Values**	**October 2011 NEXRAD - Rain Gauge NSE Values**
Fort Drum Creek	121 km^2	0.08	0.32	0.01	0.05
Blue Cypress Creek	247 km^2	0	0.17	0	0.02
Jane Green Creek	612 km^2	-0.01	0.4	0.03	0.05
All Upstream of U.S. 192	2379 km^2	0.01	0.02	-0.01	-0.01
Pennywash Creek	52 km^2	0	1.41	-0.01	0.05
Wolf Creek North	65 km^2	0	0.88	0	0.03
All Upstream of S.R. 520	3303 km^2	0	-0.25	-0.02	-0.01
All Upstream of S.R. 50	3817 km^2	-0.02	-0.14	-0.02	-0.05
Upstream of Inlet of Lake Harney	5038 km^2	-0.02	0.68	0.01	0.01
Upstream of Little Econlockhatchee River at Union Park	60 km^2	0.06	1.72	N/A	N/A
Upstream of Little Econlockhatchee River at Univserity Blvd.	228 km^2	0.02	2.56	N/A	N/A
Upstream of Econlockhatvhee River near Oviedo	591 km^2	-0.12	0.01	0.05	0
Upstream of Econlockhatvhee River near State Highway 13	702 km^2	-0.08	0.55	0.2	-0.01

A comparative analysis based on these results was performed for three different sub-base size groups; small, medium, and large. The purpose of this analysis was to determine if, at certain sub-basin sizes, the NSE or r^2 values would show improvement during the various simulation runs. The six smaller sub-basin sizes (less than 250 km^2) either remain the same or show an improvement in the r^2 and NSE during all or a majority of the simulation runs. The average differences (between r^2 and NSE values) across simulation events show an improvement for all the small sub-basin sizes. For the three medium sub-basin sizes (250 $km^2 < x < 1000$ km^2) the results are mixed. Some sub-basins show improvement, while others show decline in the NSE and r^2 values, depending on the simulation event. The four large sub-basins (over 1000 km^2) show a decline in r^2 values for almost all of the simulation runs, whereas only two sub-basins show a decline in NSE values.

To determine if the performance statistics at the selected sub-basin sizes is significantly different for the NSE and r^2 values, the Wilcoxon signed-rank test was used. The r^2 and NSE values were compared across all simulations events at the three sub- basin size groupings (small, medium, large).

Comparison for the small sub-basin group occurred at six sub-basins with four sub-basins having results for four simulations and two sub-basins having results for only two simulations. This resulted in a sample size of 20 measurements each for the rain gauge and NEXRAD. Median r^2 values for the small sub-basins were determined to be .84 for the rain gauge and .86 for the NEXRAD, respectively. The *W* test statistic was 124 and the *p* value was calculated at 0.002 for r^2. Median NSE values were 0.795 and 0.81 for the rain gauge and NEXRAD values, respectively. The *W* test statistic was 118.5 and the p value was calculated as 0.0002 for the NSE. The null hypothesis is then rejected at the 0.05 significance level, for both performance measures, which suggests a high probability that the two distributions differ. Due to the computed *p* value, median values, and previously computed improvement of r^2 and NSE results, it can be inferred that at smaller sub-basin sizes the NEXRAD data performs better.

The medium sized sub-basin comparison occurred at three sub-basin locations, resulting in 12 samples each of rain gauge and NEXRAD r^2 values. Median r^2 values for the rain gauge and NEXRAD data were .89 and .85, respectively. The *W* test statistic was 36 with a *p* value of 0.818. The NSE median values were 0.82 for the rain gauge and 0.78 for the NEXRAD data. The *W* test statistic was 12.5 with a *p* value of 0.719. Since the p values are much higher than the significance level of 0.05 or 5%, the null hypothesis cannot be rejected. There is no statistical significance suggesting that the distributions between the datasets are different, and thus the NEXRAD data input does not improve r^2 and NSE values at the medium sub-basin size.

The large sub-basin size comparison was completed at four locations, resulting in a sample size of 16 for each precipitation input type. The median r^2 value for the rain gauge data was 0.95 whereas for the NEXRAD data is was 0.925. The *W* test statistic was determined to be 97 with a *p* value of 0.003. The median values were .915 and .885 for the rain gauge and NEXRAD data, respectively. The *W* test statistic was 83 with a *p* value of 0.05. Since the *p* value is equal to the significance level, the null hypothesis should not be rejected. This *p* value is very close to rejecting the null hypothesis thus suggesting that the rain gauge data may produce more accurate results than the NEXRAD data. The datasets are showing that difference in the median values is close to being statistically significant; with one form of precipitation input producing more accurate results. The *p* value, higher median value, and previously determined decline in results when using NEXRAD data would suggest that rain gauge data produces more accurate results at the large sub-basin scale.

5.5 Calibration and Validation Discrepancies

As can be seen from the runoff vs. observed data hydrograph results, different points within the model show different degrees of agreement. There are multiple explanations as to why the calibration and validation results have some level of error as compared to the observed data.

The difference of scale (return frequency) for the storm events is significant. The calibration storm event of Tropical Storm Fay and validation storm event in October 2011 produced historic rainfall totals within the SJR basin whereas the validation storm event of 2007 was a very minor storm. As stated previously, the return frequencies range from much less than the 1 year – 24 hour rainfall event to between a 10 and 25 year – 24 hour rainfall event as defined by Technical Paper No. 40, Rainfall Frequency Atlas of the United States (U.S. Department of Commerce, 1961). Creating a model that is sensitive enough to capture small rain events posed challenges

due to the large domain size of the model. The spatial variability of rainfall represents the dominant effect in the production of runoff; as the spatial variability increases, so does the significance of appropriate rainfall characterization (Ly et al., 2013). It may also be true the further model detail needs to be added to the smaller sub-basins within the HEC-HMS in order to better simulate small precipitation events.

The Thiessen polygon methodology applies uniform precipitation gauge data over a substantial area, which may cause significant over or underestimation of rainfall within the modeled area. When reviewing the precipitation gauge data, different gauges in adjacent geographical areas can have highly inconstant rainfall amounts. For example, gauge 510206 recorded a precipitation of 3.2 inches on October 3, 2007 whereas the nearby gauge 540106, recorded only 2.2 inches on this date. Also, when reviewing the rain gauge data for certain events (namely 2007 and 2010) it can be concluded that the rainfall is concentrated in certain areas with an uneven distribution. The temporal variability has a great impact on peak flows at a small scale because the Thiessen polygon method will either underestimate or overestimate total rainfall. When basin averages are used to distribute rainfalls from storms with varying concentration, the flow forecasts can be incorrect. For smaller storm events this varying concentration and inner variability present can cause significant changes in the local precipitation and subsequent runoff amounts within the modeled area. Since the precipitation amounts are minimal for the 2007 validation event, small scale changes in the precipitation applied to the model can have large scale effects in the performance statistics. As the scale increases, the importance of spatial rainfall decreases and distribution of catchment response time, rather than spatial variability of rainfall, becomes the dominant factor governing runoff generation (Ly et al., 2013). The 2008 calibration event and 2011 validation event had much higher precipitation amounts and gauge recordings were

comparable throughout most of the model domain. Also, both the 2008 and 2011 storm systems had very large, wide spread coverage of similar rainfall intensities and distributions. Due to the large amount of precipitation, discrepancies of one to two inches during these large rain event periods may not be noticeable in the runoff calculations, whereas significant changes would occur in the runoff of small rainfall periods.

The possible errors associated with NEXRAD data have been explained throughout this report. For the simulation periods, discrepancies may occur based on simulation year because NEXRAD data estimation accuracy has been continuously improving over the past few years. The 2007 and 2008 data may be less accurate than the 2010 and 2011 data. Additionally, radar may over or underestimate rainfall rates depending on rainfall frequency and distance relative to the target (rainfall droplets).

Different hydrologic runoff processes become important at different spatial scales and processes that are imperative to properly model small scale events may not be important at large scales. Uncertainty arises when simplifications and approximations are introduced into the model through regional parameter estimation. Although the model was created using the best data available, sub-basin properties were often averaged over large areas thereby creating spatial homogeneity that may not be representative of actual conditions. Due to the large scale of the model, spatial averaging became necessary and many properties were averaged based on the sub-basin delineation, which is relatively large for many sub-basins. Finer resolutions may be needed to capture the smaller peaks and fluctuations in discharge rates for certain simulations. In addition it may be necessary to perform catchment subdivision and additional channel routing for the larger sub-basins for adequate runoff values for smaller storm events.

This includes the land use and land type data, which depending on its location within the sub-basin, can significantly impact runoff intensities and times. Each land use and land type data has a direct relation to different SCS curve number values, thereby directly impacting the hydrologic response of the watershed. It should also be noted that the methodology incorporating the SCS method can lead to errors due to its lack of physical reality in the development of the equation but instead is based off an empirical rainfall-runoff relationship and soil-vegetation-land complex. Previous studies have shown that the effects of the CN variation decrease as the rainfall depth increases, such as for the large storm event of Tropical Storm Fay (Bondelid et al., 1982). The SCS curve number procedure was developed for estimating streamflow volume generated by larger rain storms. Therefore, the intensity and duration of the validation storm may not be adequate enough for proper SCS runoff estimation practices. A main weakness of the SCS curve number method is that the relationship parameters are discrete rather than continuous. This can readily be seen in the initial abstraction values which are not readjusted over time as natural processes such as evaporation and infiltration change catchment storage values. This was observed during the 2007 validation results due to the storm event containing two peaks with little to no rainfall in between. The initial abstraction amount reduces the runoff significantly for the first precipitation event whereas the second event produces greater than measured runoff values. In an area such as the St. Johns River, evaporation is high and run off is low, especially during low flow events, and therefore different methodology consisting of a nonlinear continuous variation of storage may be needed.

The AMC specified for each sub-basin may also cause model run-off value discrepancies due to its direct impact on the SCS curve number value chosen. Many of the sub-basins were computed using a curve number value in between the AMC I and AMC II condition but could vary from

these approximations. The AMC condition is watershed dependent and therefore each sub-basins initial condition may need to be analyzed further for proper AMC estimation.

Other sources of error may include parameters initially estimated based on best available data. This would include the storage-discharge functions for sub-basins that have pump stations, flow patterns of developed areas that include storm drainage structures and retention ponds, and the constant monthly baseflow estimates. To improve these areas of the model, more information must be gathered regarding the pumping schedule, normal discharge amounts, and frequency for which pumping occurs. During the larger storm event, pumping rate volumes were minimal compared to the magnitude of the precipitation and subsequent rainfall the project area received. This is the opposite for the 2007 and 2010 validation period where pumping rates of 1 to 2 cms could cause noticeable changes in the flow rates downstream. In addition, more detailed modeling is necessary to capture the inconsistency present in highly developed areas where non-natural discharges may occur due to complex drainage systems. Urbanization in areas can cause significant changes in the timing and frequency of peak flows that are difficult to estimate using the SCS methodology. The baseflow method may need to be changed within the model from constantly monthly, to a more complex baseflow method to capture the detailed interaction between surface water and groundwater hydrology. Also, the model is currently unable to properly model the flow-ways ability to storage and slowly release flow over time. This may be able to be remediated through a more complex baseflow method or additional storage-discharge functions through the model.

A final source of error is the uncertainty associated with measured streamflow discharge gauge data. Many of the USGS gauge measurements are made from a water-stage recorder and/or an acoustic velocity meter. Water depth measurement devices are normally converted to a

streamflow rate with a predetermined stage-discharge relationship based on channel geometry near the gauge. According to Harmel et al., 2006, a main source of uncertainty of measured streamflow for natural channels is the possible change in channel dimensions, which would change the stage-discharge relationship. Also, measurement of flow velocity can introduce uncertainty due to turbulence. Research compilation completed by Harmel et al.(2006) shows that under average conditions, the direct discharge method can have a $\pm$6% uncertainty, the stage-discharge relationship for a stable channel can have $\pm$ 10% uncertainty, and a continuous stage measurement float recorder can have $\pm$ 2% uncertainty. USGS also states that the gauges "may differ from individual measurements because of changes in tidal influence, wind, or other factors." Individual gauges, such as the Wolf Creek gauge include specific remarks for the surface-water records which state that the records are poor and the discharge is affected at times by variable backwater from the St. Johns River headwaters (USGS, 2009). Although it is difficult to determine the specific error associated with each gauge, recognizing that there is are uncertainty limits associated with the gauge data is important. "Models should be expected to produce output within the uncertainty limits inherent in measured data, not to produce outputs with low deviation from measured data" (Harmel et al., 2006).

5.6 Sensitivity Analysis

The model simulation results are not equally sensitive to all input parameters for the model. To determine which input parameters are the most sensitive, two types of sensitivity analysis were completed. The first sensitivity analysis was performed for only the 2007 and 2008 simulation events, as it was originally part of the original model development during the "St. Johns River Economic Valuation Study". The purpose of the first sensitivity analysis was to provide an overall understanding of the model sensitivity to input parameters using visual comparison. The

second sensitivity was performed for all simulation events, with more detailed numerical comparisons. The purpose of the second sensitivity is to determine how sensitive the model is to rainfall inputs versus parameter inputs.

5.6.1 Sub-basin Parameter Sensitivity

The first sensitivity analysis was conducted for the sub-basin parameters, which are responsible for most of the variability during the computation of runoff values; curve number (C.N.), initial abstraction (I.A.), and lag time. The technique that was adopted for the sensitivity analysis was to vary each input parameter the same relative percentage for all sub-basins while keeping the other sub-basin parameters constant, with the same values used during the 2008 calibration and 2007 validation periods. A sensitivity analysis was not performed on the additional simulation events of 2010 and 2011 because the 2007 and 2008 events already represent a high and low rainfall event. It is believed the sensitivity analysis results of the 2007 and 2008 simulations will be representative of all simulation events.

The sensitivity analysis was performed by increasing and decreasing the sub-basin parameters by 10 percent. This percentage was applied consistently for all sub-basins within the model. Therefore, six different model runs were completed and compared to the original 2008 calibration and 2007 validation run results. The sensitivity analysis was performed and measured at four different gauge locations within the model. These locations included; Fort Drum Creek, Jane Green Reservoir, State Highway 520, and Econlockahatchee near Oviedo. These locations were chosen based on varying watershed sizes and relative areas upstream of the measurements to ensure different magnitudes of flow were captured for sensitivity analysis comparisons. Other parameters such as the base flow and relative loss percentages were not included in the sensitivity analysis due to their linear relationship with runoff production.

To determine the sensitivity, the simulation flow rate results were compared for the three different sensitivity parameters. This was completed using a visual comparison as well as computing the relative overall difference between simulations. Examples of the sensitivity analysis for the 2008 calibration and 2007 validation can be seen in Figures 9 through 14.

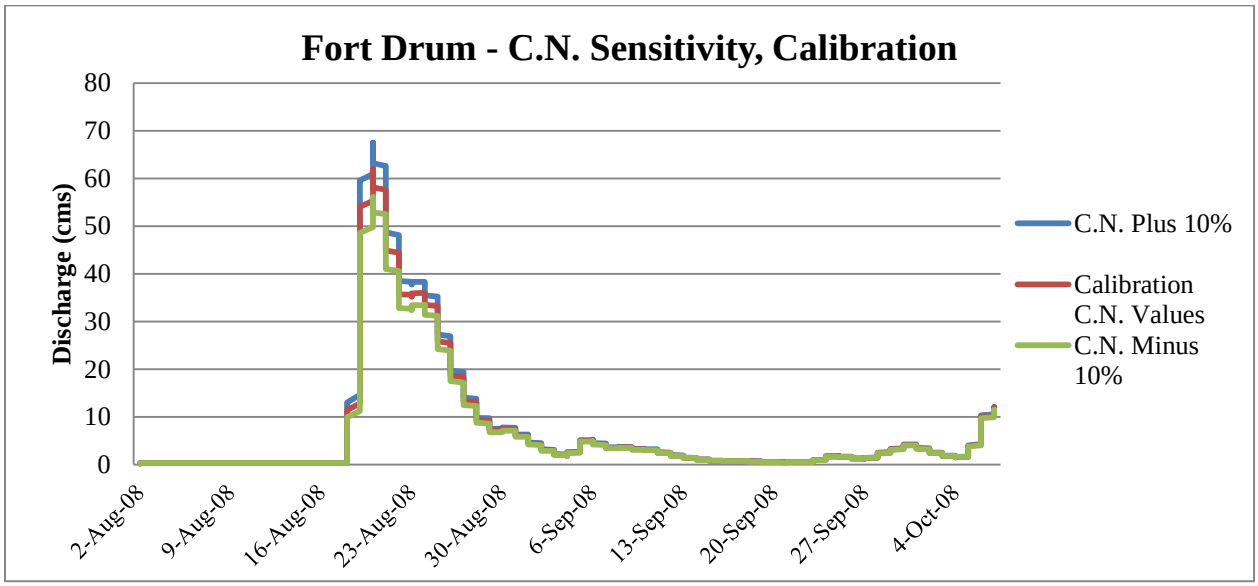

Figure 9. Fort Drum, Curve Number Sensitivity Analysis for Calibration

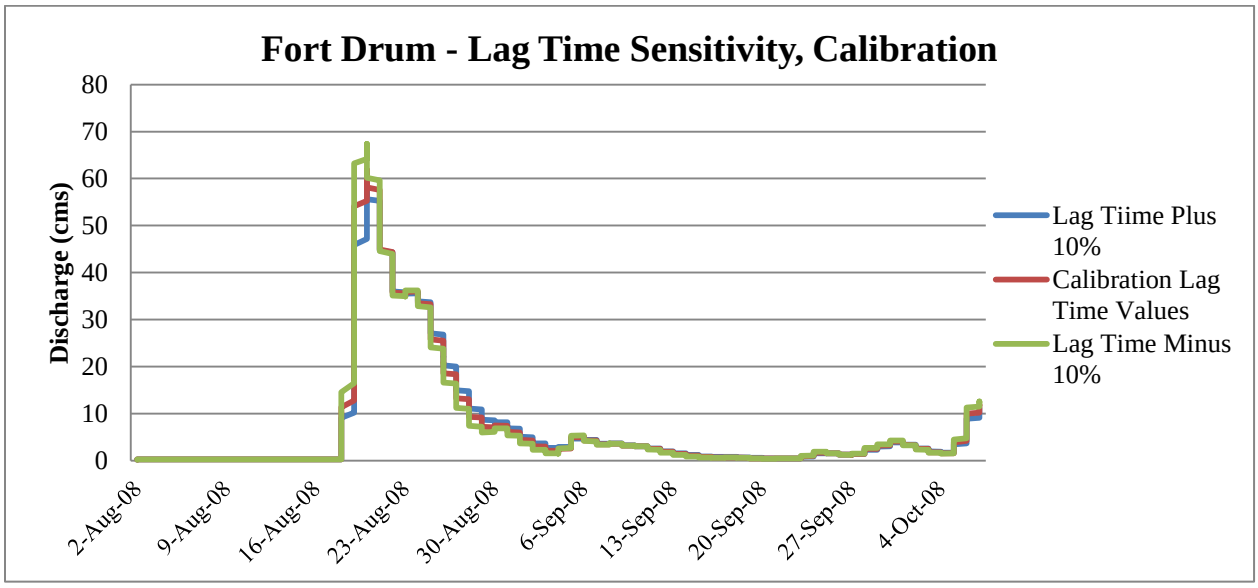

Figure 10. Fort Drum, Lag Time Sensitivity Analysis for Calibration

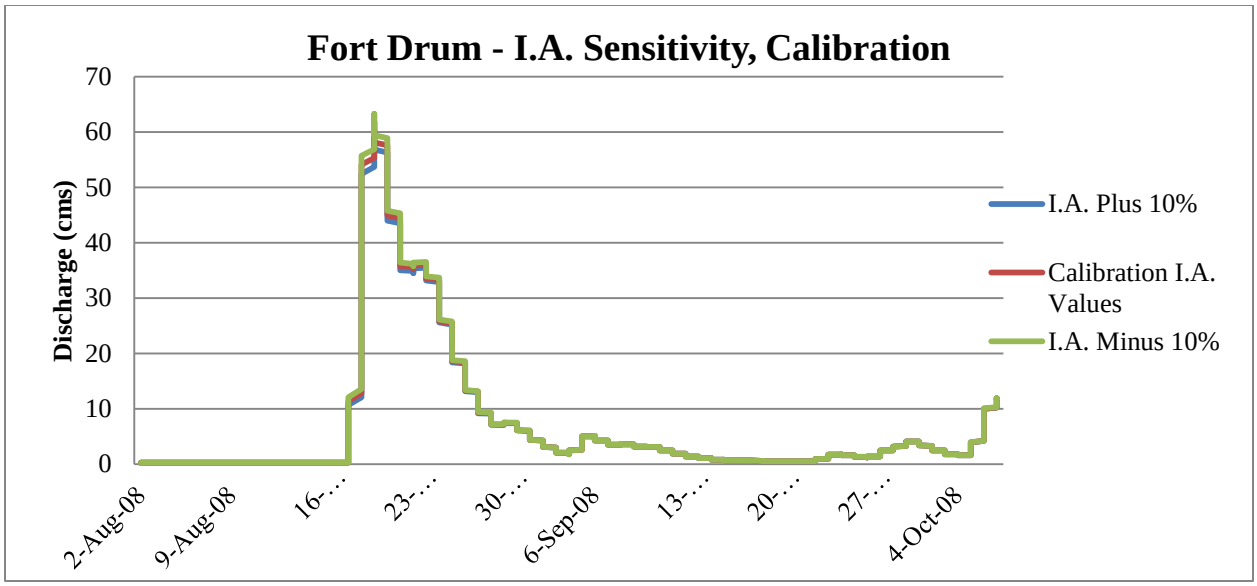

Figure 11. Fort Drum, Initial Abstraction Sensitivity Analysis for Calibration

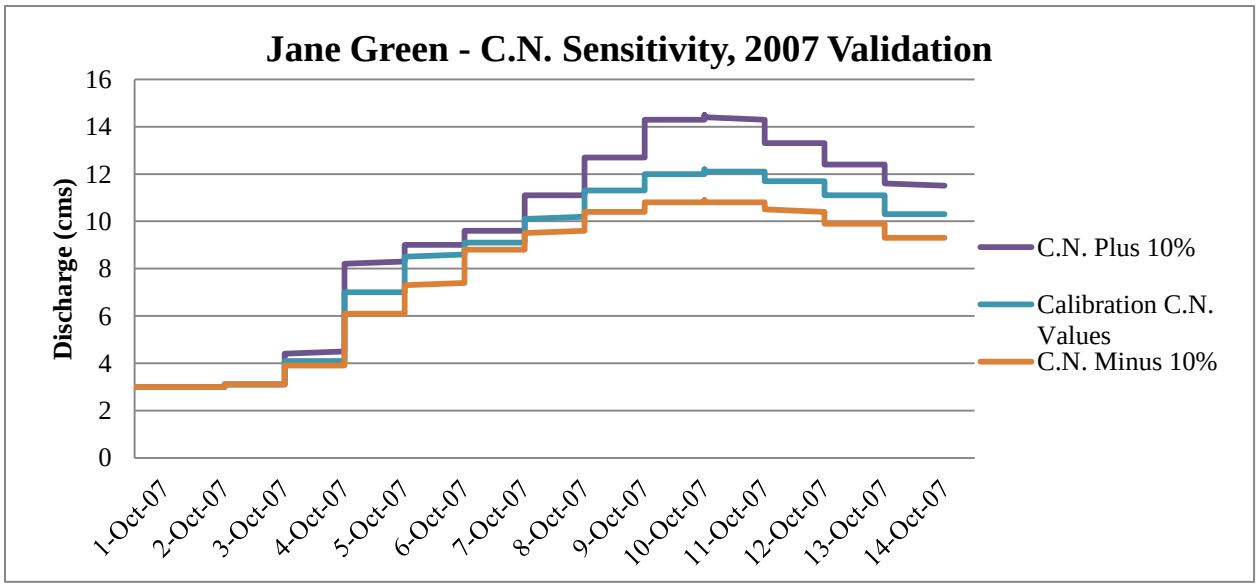

Figure 12. Jane Green, Curve Number Sensitivity Analysis for 2007 Validation

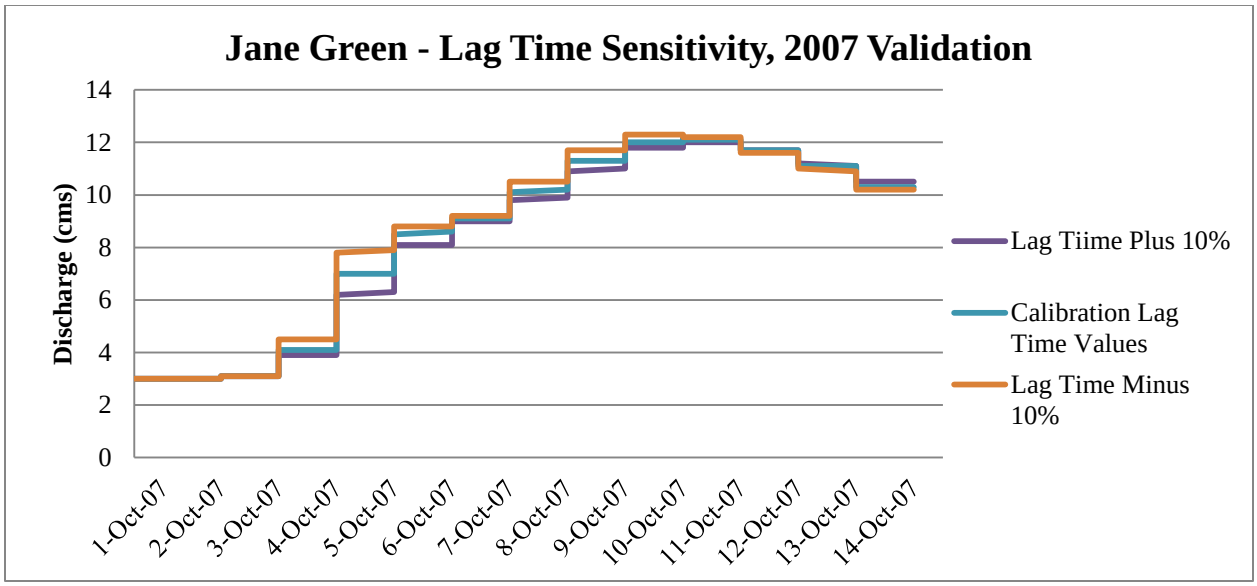

Figure 13. Jane Green, Lag Time Sensitivity Analysis for 2007 Validation

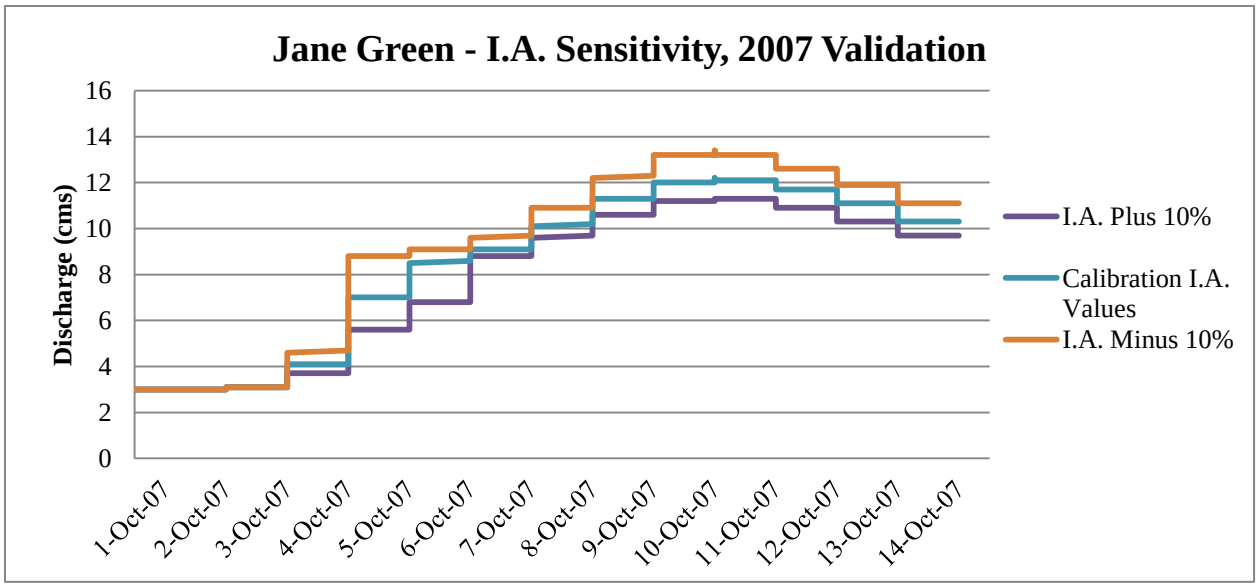

Figure 14. Jane Green, Initial Abstraction Sensitivity Analysis for 2007 Validation

The results of the 2008 calibration sensitivity analysis show that the model is the least sensitive to the initial abstraction amounts (lowest change in flow rates) and the most sensitive to curve number values (highest change in flow rates). Increase or decreases in lag time had effects on the timing and magnitude of peaks but not to the extent of the curve number changes. For the 2008

calibration period the trend of the curve number and lag time being the most sensitive and initial abstraction being the least sensitive seems to be true for all gauge locations. For the 2007 validation period, the changes in the initial abstraction and lag time for the smaller sub-basins produced more noticeable changes in the outflow hydrograph. The larger sub-basins seemed to follow a similar trend to that of the 2008 calibration run sensitivity analysis. Therefore, from the sensitivity analysis it can be inferred that at smaller flow rates, the initial abstraction parameter can be sensitive but for larger flow events it is less sensitive. This also seems true of lag time values but with a higher level of sensitivity. The curve number and lag time parameter are similar in sensitivity between both models, each having the ability to change peak flow values substantially.

5.6.2. Sub-basin Parameter Sensitivity at Different Sub-basin Sizes and Rainfall Frequencies

The second sensitivity analysis was used to determine, at different sub-basin sizes and rainfall precipitation frequencies, which parameter is the most influential on streamflow values. Two initial simulation runs were completed using two different magnitudes of rainfall, 3 inches and 9 inches, each occurring over a one day time period. All model parameters remained the same between these initial runs, the only difference was the precipitation. Next, the model parameters for lag time were changed by $\pm$ 25% and each simulation was re-run. Finally, the lag time was returned to the initial value and the curve number was changed by $\pm$ 25%. Initial abstraction was not modified because the results of the first sensitivity analysis suggested it was less influential on flow values. Three different sub-basins were chosen for comparison, each representing small to large spatial values. The sub-basins selected were Pressley Ranch South (10.99 km^2), Jim Creek (65.56 km^2) and Jane Green Crabgrass Creek (185.15 km^2). This sensitivity analysis was performed using as many consistent model parameters as possible, to reduce outside influence.

The initial abstraction, percent impervious, and curve number were set to the same values for all three sub-basin sizes. Although the initial abstraction and percent impervious were not changed during the simulation runs, as they do have an effect on the computed flow rate and therefore were kept consistent. The curve number of 76 was selected as the starting condition for all three sub-basins. This helped reduce error associated with applying a different magnitude of change for each curve number value. For example, if the beginning curve number of one sub-basin was relatively low, the percent change would also be low, whereas a higher starting curve number would produce a higher change. The change of $\pm$ 25% applied to the curve number value allows for the appropriate range of 57 to 95 to be tested. This range is consistent with the curve number values used within the model simulations. It is important to note that this range in curve numbers describes many different land use types. For instance, a curve number of 57 would describe wood or forested land whereas a curve number of 96 would be a paved road. The lag times were different for all sub-basins because they are a function of the sub-basin size and thus had to remain different to represent the sub-basin size.

Table 21 below illustrates the sub-basin sizes and the respective change in parameters for each simulation run.

Table 21: Sub-basin Parameter Inputs for the 3 Inch and 9 Inch Rainfall Simulations

Sub-basin Name	**Pressley Ranch South**	**Jim Creek**	**Jane Green Crabgrass Creek**
Area (sq km)	10.99	65.56	185.15
Initial Curve Number	76	76	76
+25% Curve Number	95	95	95
-25% Curve Number	57	57	57
Initial Lag Time (min.)	896	2700	3500
+25% Lag Time (min.)	1120	3375	4375
-25% Lag Time (min.)	672	2025	2625

Changing the two model parameters at the various sub-basin sizes and precipitation frequencies adds to the understanding of influence of each input parameter (rainfall, lag time, or curve number) on the model results. For the first analysis, the resulting peak flow rates of each simulation were compared, as seen in Table 22.

Table 22: Peak Flowrate Values for the 3 Inch and 9 Inch Precipitation Input

Peak Flowrate of Each Subbasin (cms) for the 3 Inch and 9 Inch Rainfall Input	**Initial**	**+25% Lag Time**	**-25% Lag Time**	**+25% Curve Number**	**-25% Curve Number**
Pressley Ranch South, 3 Inch	1.4	1.2	1.8	2.8	0.9
Jim Creek, 3 Inch	3.6	3.1	4.4	6.6	2.4
Jane Green Crabgrass Creek, 3 Inch	8.7	7.6	10.5	15.3	6
Pressley Ranch South, 9 Inch	10.4	8.8	12.8	13.4	7.6
Jim Creek, 9 Inch	24.4	19.8	31.4	31.5	17.6
Jane Green Crabgrass Creek, 9 Inch	54.3	44.4	70.4	70.5	39.6

From the table it is inferred that certain parameters affect the peak flow rate more or less severely depending on the sub-basin size and rainfall intensity. Understandably, an increase in the rainfall, by a magnitude of three, causes the greatest influence on stream flow peak values. The only change between the initial simulations was the magnitude of rainfall ($\pm$300%), and therefore it is interesting to note that the resulting relative change in peak flow rates had a much larger magnitude of change. This would suggest that the model is very sensitive to rainfall amounts, and even small errors in rainfall input can be magnified by the computed flow rate values.

To add to the understanding of how the parameter change flow rates, the percentage of change in the resulting peak flow rate of each simulation was compared, as seen in Table 23. The sensitivity of the model may be described in the relative percent change in peak flow rates, with higher sensitivity being associated with a greater percent change. The percentage change was calculated by the following equation, Equation 10.

$$\% \, Change = \frac{V_{parameter} - V_{initial}}{V_{initial}} \qquad \textit{Equation 10}$$

Where $V_{parameter}$ and $V_{initital}$ represent the peak flow rate values at each parameter change and initial simulation, respectively.

Table 23: Percentage Change in Peak Flow Rates from Initial Simulation to Parameter Change Simulation

Percent Change in Peak Flowrate from Initial Simulation to Parameter Change Simulation	**+25% Lag Time**	**-25% Lag Time**	**+25% Curve Number**	**-25% Curve Number**
Pressley Ranch South, 3 Inch	-14.3%	28.6%	100.0%	-35.7%
Jim Creek, 3 Inch	-13.9%	22.2%	83.3%	-33.3%
Jane Green Crabgrass Creek, 3 Inch	-12.6%	20.7%	75.9%	-31.0%
Pressley Ranch South, 9 Inch	-15.4%	23.1%	28.8%	-26.9%
Jim Creek, 9 Inch	-18.9%	28.7%	29.1%	-27.9%
Jane Green Crabgrass Creek, 9 Inch	-18.2%	29.7%	29.8%	-27.1%

For the 3 inch rainfall input, the sensitivity is greatest at the smallest sub-basin and decreases in sensitivity with sub-basin size for all parameter changes. For the 9 inch rainfall input, it seems that the sub-basin size does not influence the percent increase or decrease of peak flow as greatly as the 3 inch simulation. Additionally, for the 9 inch rainfall input, a consistent pattern of percent change is not present across sub-basin size. This would suggest that during small rain events, flow rates may be the most sensitive to parameter changes at small spatial scales. As rainfall inputs increase, sensitivity across spatial scales may become less dominant. A change in the curve number parameter causes the greatest increase or decrease in flow rates when compared to the initial flow rate values, across both rainfall events and sub-basin scales. Comparing the results of both rainfall intensities shows that the smaller rainfall event is more sensitive to the changes in curve number values, as can be seen by the greater overall percent change. A decrease in lag time of 25% increased the peak flow to a similar amount to that of the +25%

curve number for the 9 inch rainfall. Stream flow peaks did not share this trend for the 3 inch rainfall, which suggests a decrease in lag time may be more sensitive at higher rainfall rates.

The percent change of peak flow rates results were also compared across rainfall input amounts, as shown in Table 24.

Table 24: Percent Change in Peak Flow Rates From 3 Inch to 9 Inch Precipitation Input

Percentage Change in Peak Flow Rates from 3 to 9 Inch Input	**Initial**	**+25% Lag Time**	**-25% Lag Time**	**+25% Curve Number**	**-25% Curve Number**
Pressley Ranch South	643%	633%	611%	379%	744%
Jim Creek	578%	539%	614%	377%	633%
Jane Green Crabgrass Creek	524%	484%	570%	361%	560%

The results from this sensitivity analysis show that for all runs, except the -25% lag time, the smallest sub-basin is the most susceptible to changes in rainfall input, as can be seen by the largest percentage of change between peak flow rates. The "initial" model run shows the percentage change between the 3 and 9 inch precipitation inputs with no increase or decrease in parameters. The initial run provides a basis for comparison for the simulations where parameters were changed. An increase in percent change from the "initial" value would suggest that the model is more sensitive to the parameter change when precipitation values are increased. This sensitivity is seen as the largest increase of percent change in peak flow values. A decrease would imply that the model is less sensitive to the parameter change and therefore the resulting variation in peak flow rates would have greater reliance on the differences of the precipitation input.

The smallest sub-basin (Pressley Ranch South) shows that a decrease in curve number causes greater sensitivity in the modeling results when precipitation is increased. For the middle (Jim Creek) and large (Jane Green Crabgrass Creek) sub-basins, a decrease in curve number or lag

time would also increase the sensitivity across precipitation input. All sub-basins showed a decrease in sensitivity when the lag time or curve number was increase by 25%. It is also interesting to note that an increase in curve number caused a much lower percent change than the other parameter changes. The resulting percent change begins to approach the overall difference of precipitation (±300%). Compared to the initial values, a low curve number and lag time value may cause the greatest percent change difference in stream flow results for different rainfall intensities whereas high curve number and lag times may dampen the effects of precipitation input frequencies. To aid in the understanding of how the peak flow rates differ, Figure 15 illustrates an example of the percent change for a selected sub-basin and parameter change.

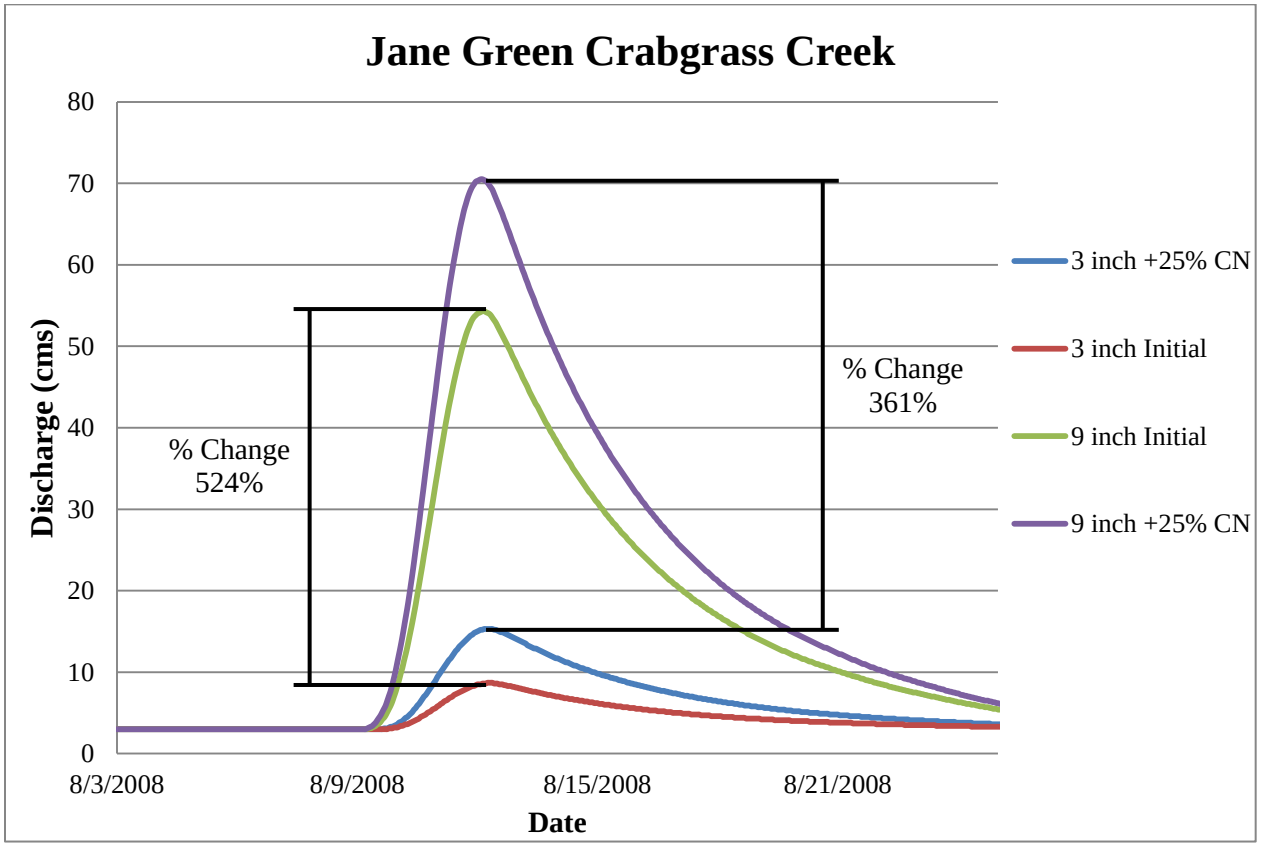

Figure 15. Jane Green Crabgrass Creek Peak Flow Rate Comparison

The results of this sensitivity analysis show that for small sub-basins with low curve numbers, significant changes in peak runoff values may occur due to differing precipitation inputs. Medium and large sized sub-basins that have low curve numbers or lag times will also produce larger percent changes in peak runoff values at differing precipitation input values. All sub-basin sizes that have a high curve number and lag time will produce a less overall percent change in peak flow rates across precipitation input values.

Chapter 6

CONCLUSIONS AND RECOMMENDATIONS

This thesis presents a comparison of HEC-HMS hydrologic simulation performance using rain gauge and NEXRAD precipitation input at varying spatial scales and rainfall return frequencies for the Upper and Middle St. Johns River. In addition to the comparative model performance analysis, total bias between NEXRAD and rain gauge data within the study location was investigated. Precipitation measurements arguably have the most critical influence on the model performance, thus the need for quality data input is apparent. Comparing hydrologic simulation results using radar and rain gauge input aids in identifying the thresholds for maximum gain when using the more cumbersome, but finer-resolution radar data. This research provided guidance for both spatial scale and rainfall return frequency scenarios for which the use of radar data would yield more accurate hydrologic results.

Calibration and validation of a HEC-HMS hydrologic model of the Upper and Middle St. Johns River Basins was completed for four storm simulation periods, each representing a different rainfall return frequency. The calibration period occurred from August 2008 to October 2008 and represented a return frequency of 5 to 10 year-24 hour duration. The validation period occurred in October 2007, March 2010, and October 2011 with return frequencies of less than 1 year- 24 hour duration, approximately 1 year- 24 hour duration, and 10 to 25 year-24 hour duration, respectively. These return frequencies were chosen because they represent a wide array of storm events that may occur within the project area, from one the largest events on record (October 2011) to a small event that is common throughout the year (October 2007).

The HEC-HMS model was first calibrated using precipitation data from rain gauges located within or near the watershed boundary. As an alternative precipitation input source, NEXRAD data was obtained. The data, provided by the SJRWMD, is 2 X 2 km WSR-88D NEXRAD radar data that has been gauge-adjusted from the network of rain gauges within the SJRWMD territory. Rain gauge and NEXRAD precipitation estimates were compared at seven locations within the model domain. The evaluation showed that NEXRAD total precipitation was greater than gauge total precipitation for a majority of the sub-basins, but this positive bias was not statistically significant (alpha of 0.05) for any event. A scatter plot of relative bias versus the measurement distance from the rain gauge station was used to calculate the linear regression correlation coefficient. The poor degree of correlation indicates there is not a strong relationship between total measured bias and distance from the rain gauge point location. RMSD values did not show improvement or decline in estimation efficiency during a particular simulation event or distance from the rain gauge. Given the fact that systematic bias may be present within the NEXRAD data, efforts were directed towards minor re-calibration of the model parameters which had acceptable ranges, which compensated for the difference in precipitation input.

Model performance was evaluated both visually and statistically against observed hydrograph data from USGS. The model performance measures, Nash–Sutcliffe efficiency and coefficient of determination, were used to quantitatively compare the NEXRAD and rain gauge hydrologic simulations to the observed USGS discharge data. Additionally, a statistical hypothesis test, the Wilcoxon Signed-Rank Test was used to evaluate the difference in model performance results for the two precipitation input types. Overall, the calculated NSE and r^2 values for the 2008, 2010, and 2011 simulations were similar and very promising (majority were > 0.75), indicating the model predicts streamflow values with a high level of accuracy for both NEXRAD and rain

gauge data input. The Wilcoxon Signed-Rank Test results confirm that no significant improvement or decline in model streamflow accuracy is present when using NEXRAD data input for rainfall return frequencies of approximately 1 year-24 hour and greater. The 2007 r^2 and NSE rain gauge simulation results indicate a wide range of agreement between the simulated and observed data, with a majority of the values showing a weak relationship or unacceptable model performance. The NEXRAD precipitation data performed better than the rain gauge data at predicting the magnitude and timing of the peak, as reflected in the higher r^2 and NSE values. A statistically significant difference of median is present (at the alpha level of 0.05). Thus, the NEXRAD data were shown to produce more accurate streamflow simulation results for rainfall return frequencies less than 1 year-24 hours. The model performance measures were compared across simulation events for multiple spatial scales. NEXRAD data produced more accurate simulated streamflows values for the small sub-basin or watershed areas (less than 250 km^2); neither NEXRAD nor rain gauge results show consistent improvement or decline in accuracy of the streamflow values for the medium sized sub-basin or watershed areas (250 $km^2 < x < 1000$ km^2); and rain gauge data produced more accurate simulated streamflow values for the large sub-basin or watershed areas (over 1000 km^2). The difference in median for the small and large sub-basin performance statistics were statistically significant.

The results of this study suggest that at small spatial scales and low return frequencies, NEXRAD data may produce more accurate streamflow estimations. Given that the performance of radar data in this study, it may be inferred that the spatial averaging of rain gauge Thiessen polygon data provides similar or more accurate rainfall estimations for large spatial scales and higher rainfall frequencies. This could be an indication of the spatial resolution of the rain gauges not capturing the spatial variability of smaller storm systems, which may be more convecitve in

nature. Additionally, smaller spatial scales show a high level of sensitivity to rainfall input, thus the need for the higher spatial resolution of the NEXRAD data. It is important to note that the results of this study are conditioned on the modeling platform and precipitation data used.. Many important factors should be analyzed before a precipitation input is selected such as; the spatial and temporal scale of the model, rain gauge data avaialability (coverage), quality of radar data, rainfall event, and model structure and spatial discretization. The conclusions of this study are not comprehensive of all watersheds, and thus care should be taken when assessing the results of this study for use in future modeling efforts. Further research should concentrate on identifying the rainfall return frequency threshold for which NEXRAD data may provide more accurate results for varying temporal scales. All simulation periods analyzed in this research were for a daily time period, over a relatiely short duration. Introducing radar data at the hourly time scale may further improve model performance statistics, thus suggesting improvement of NEXRAD simulation results at certain return frequencies. Additionally, further research on model spatial discretization and its relation to streamflow accuracy at different spatial scales is needed. Due to the realtive size of the model domain, the spatial discretization was relatively coarse for this project. Therefore, a full range of model benefits, including improvements in model accuracy, may not have been realized.

FIGURES

Figure 1. Overall Study Area of SJR and Location of HEC-HMS Model

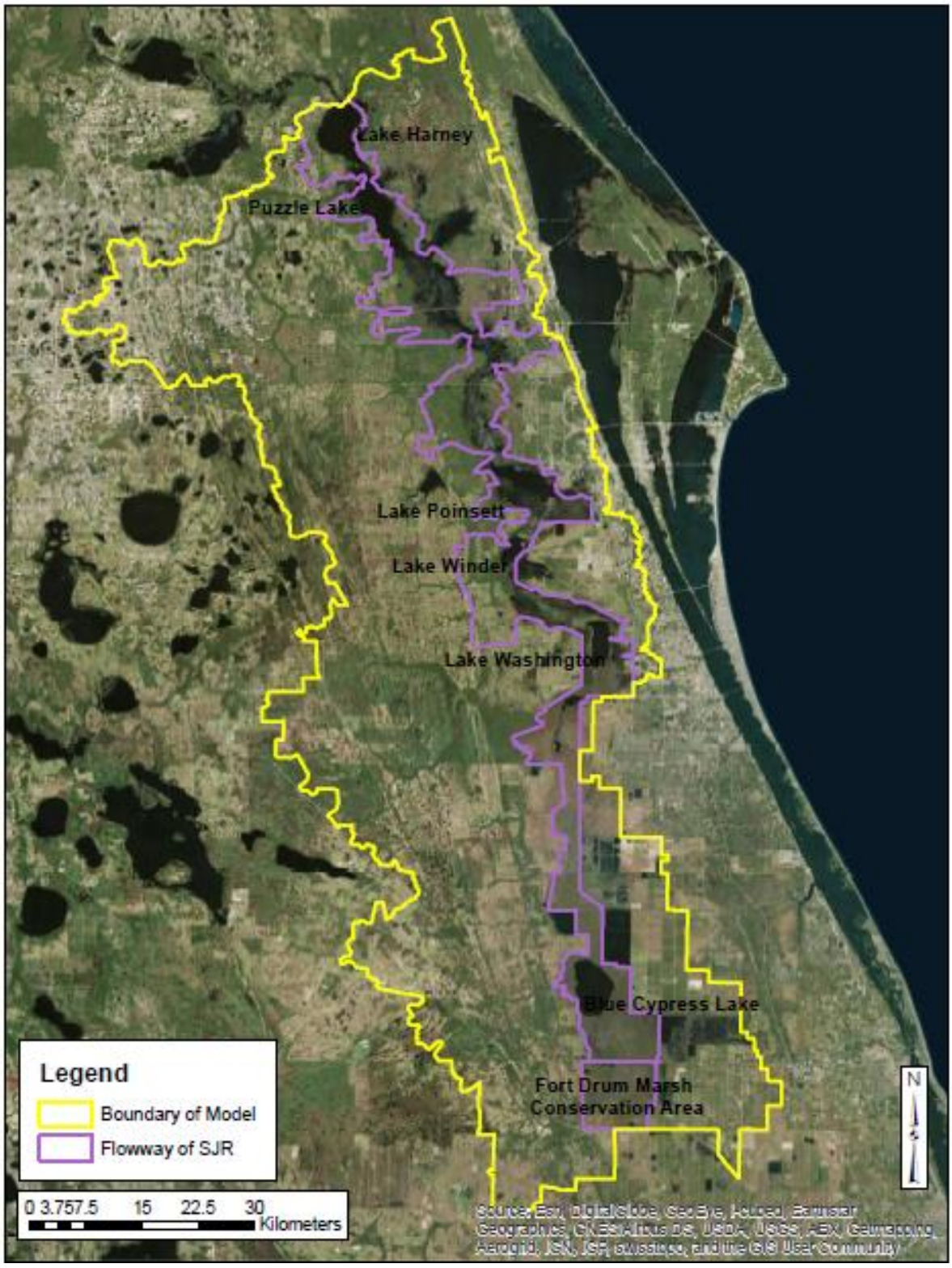

Figure 2. Model Boundary and St. Johns River Flowway

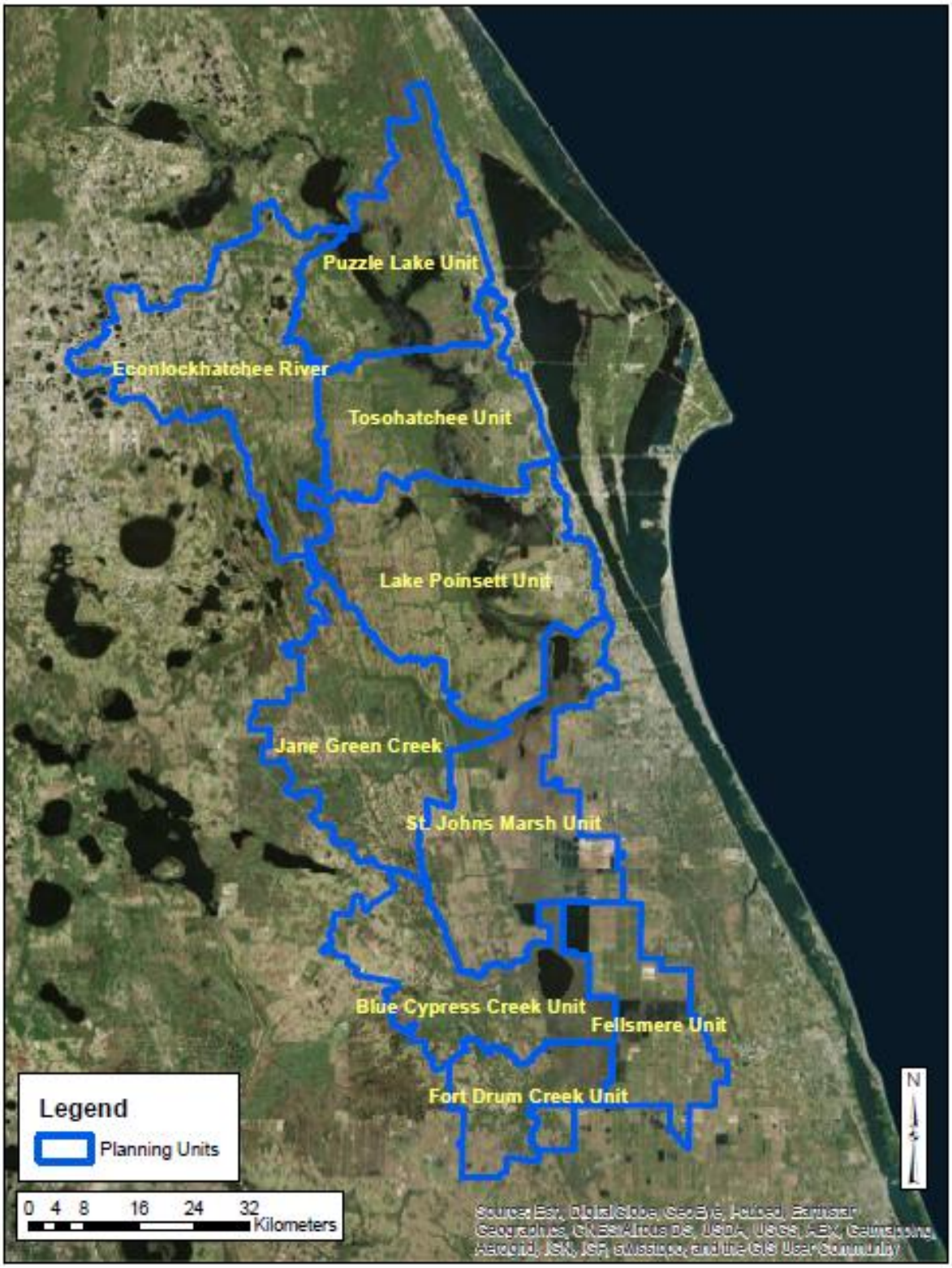

Figure 3. Planning Units

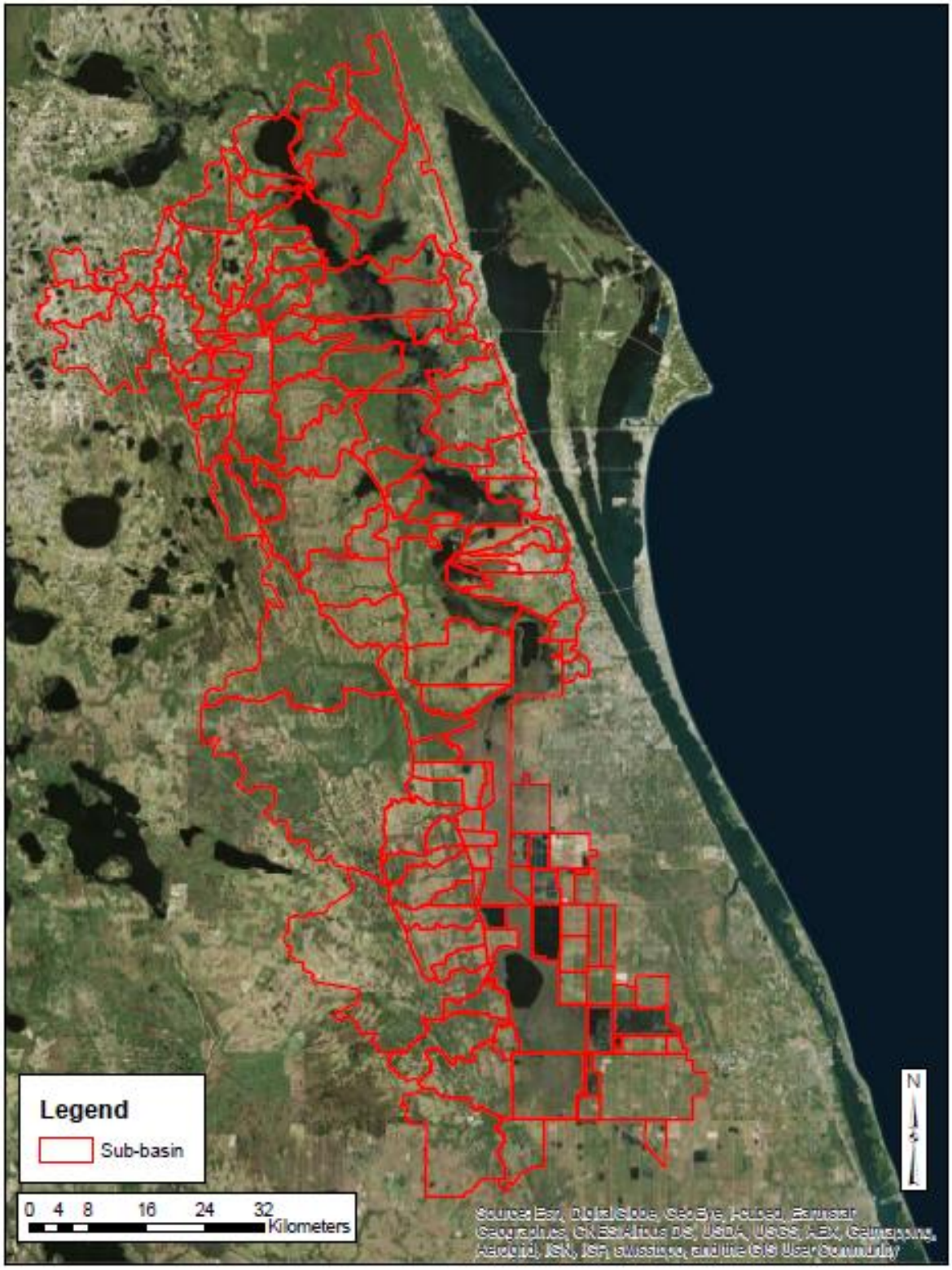

Figure 4. Modeled Sub-basins

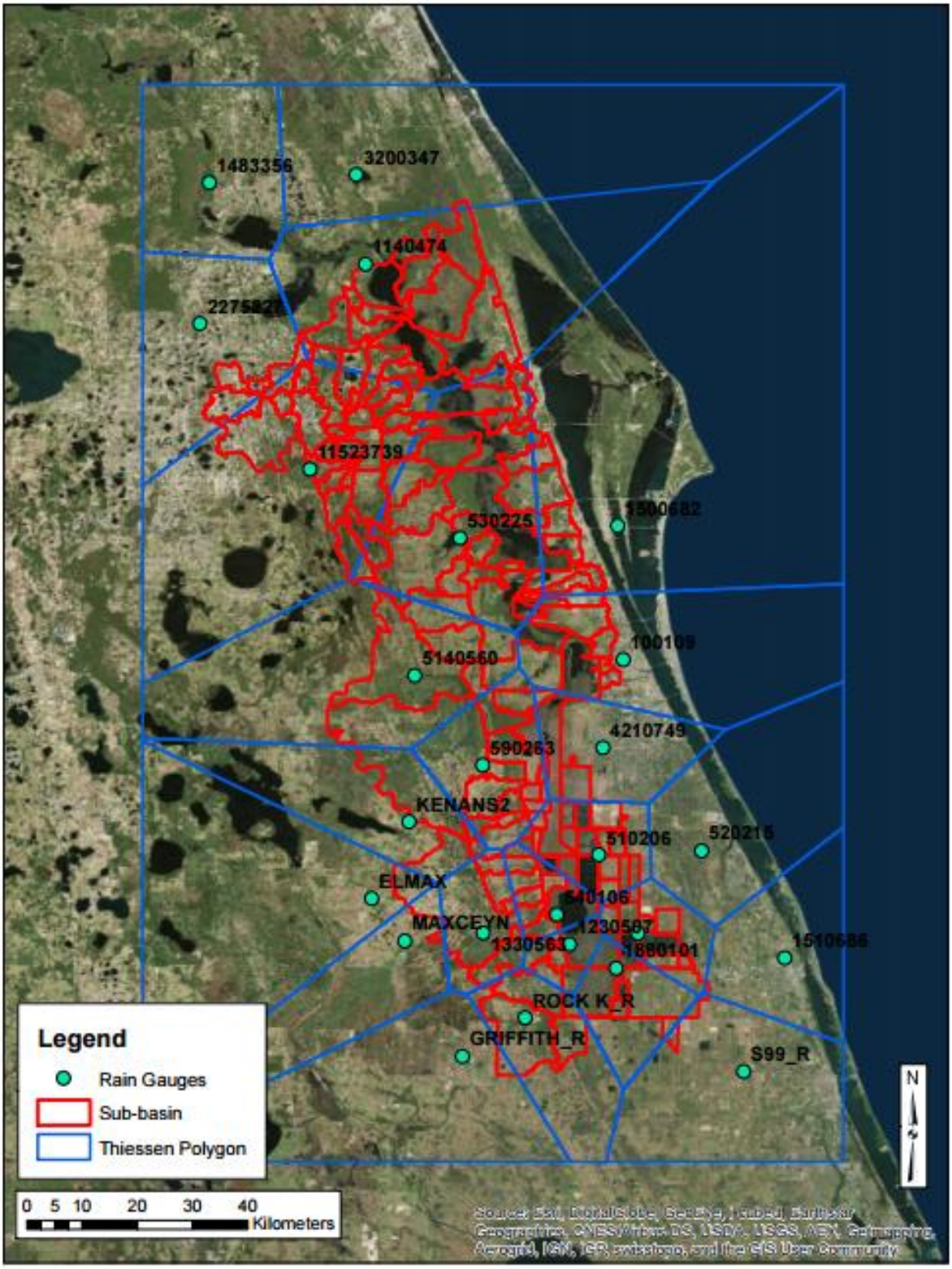

Figure 5. Thiessen Polygon

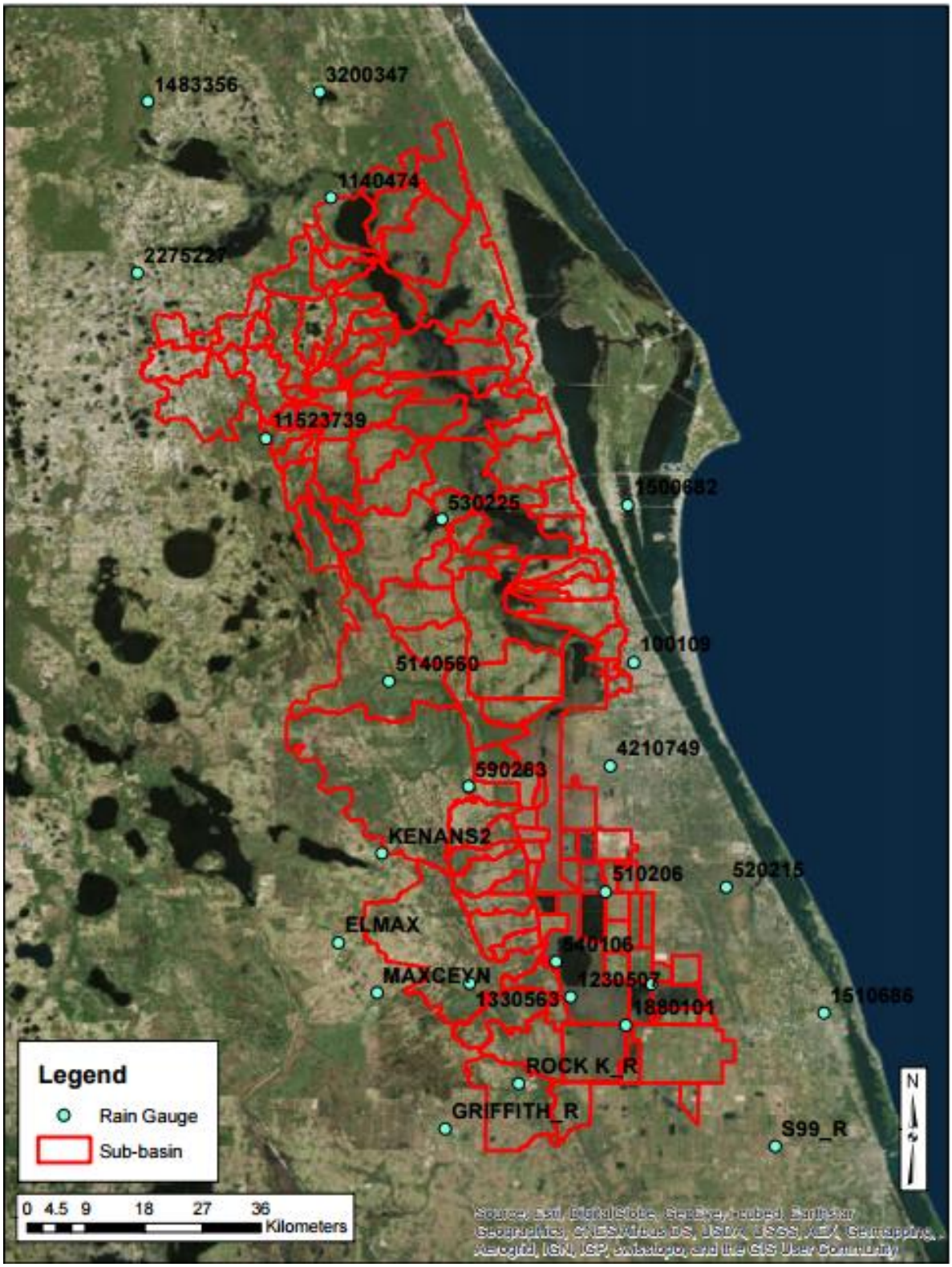

Figure 6. Rain Gauge Locations

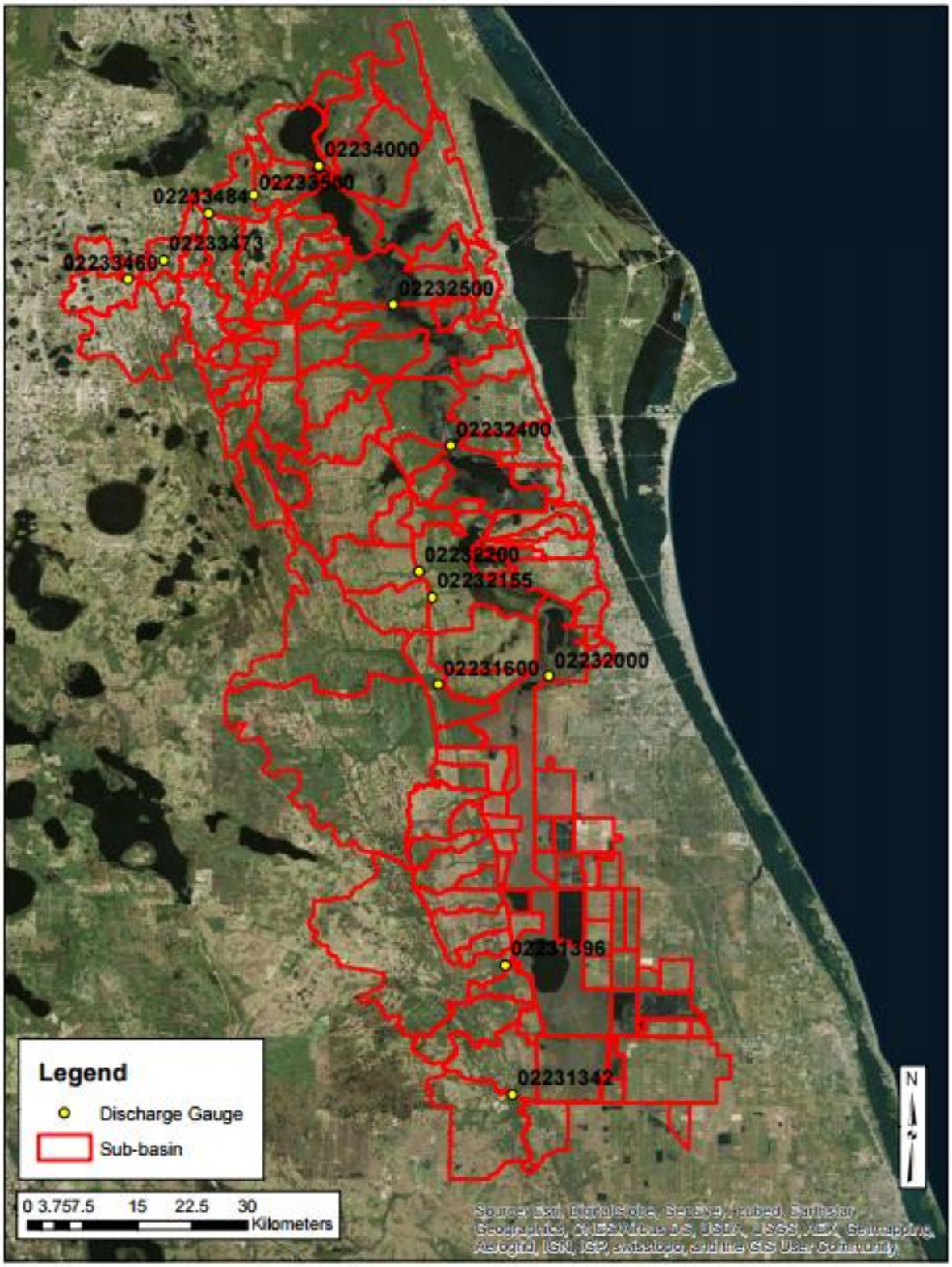

Figure 7. Discharge Gauge Locations

APPENDIX A

August 2008 to October 2008 Calibration Model Results

Subbasin	I. A. (mm)	C. N.	Lag Time (min.)	Subbasin	I. A. (mm)	C. N.	Lag Time (min.)
Barney Green	42	72	1560	Lake Poinsett Rainfall North	17	83	3300
Barry Groves	24	81	2646	Lake Poinsett Rainfall South	37	74	3450
BC East Rainfall	14	88	3351	Lake Price Outlet	47	68	1000
BCMCA Rainfall	27	79	7500	Lake Proctor	81	51	550
BC West Rainfall	23	82	1700	Lake Wash 1 Rainfall	15	87	5900
Bird Lake Combined	30	78	1800	Lake Wash 2 Rainfall	15	87	3850
Bird Lake Ditches	31	78	1200	Lake Wash 3 Rainfall	15	87	3900
Bithlo Branch	26	80	650	Lake Wilson Outlet	27	79	2361
Blue Cypress Creek	55	65	3500	Lake Winder Rainfall	22	83	5800
Broadmoor Marsh	32	76	1370	Little Creek	38	72	2000
Bull Creek	36	75	1300	Little Econlock River	51	66	2000
Buscombe Creek	15	87	1000	Little Econlock Tributary	43	70	2100
C25 Ext	43	71	2130	Long Branch	23	75	650
C54 Retention Area	10	92	1163	Mary A Groves	15	87	715
Cabbage Slough	31	76	2300	Mary A Groves Res Rain	29	79	500
Caine Farms	18	85	1250	Mary A Groves Restoration	6	95	574
Christmas Creek	14	89	1500	Mary A Rainfall	37	74	1400
Clark Lake Outlet	30	78	3100	Mills Creek	27	80	1550
Cocoa Canals	21	84	2500	Mitchell Creek	15	88	1285
Cowpen Branch	28	79	750	Moccasin Isl 1	40	73	7600
Cox Creek Lower	41	71	1400	Moccasin Isl 2	17	86	3000
Cox Creek Res Rainfall	41	73	990	Moccasin Isl 3	21	83	2500
Cox Creek upper	30	78	1800	Moccasin Isl 4	26	80	2000
Crane Strand Drain	55	68	1500	Moccasin Isl 5	35	75	1800
Cross Triangle	32	77	1900	Moccasin Isl 6	47	69	3300
Delespine Grant	34	76	1400	Padgett Branch	28	79	2405
Delta Farms	64	63	1240	Pennywash Creek	40	75	1350
Delta Farms Res Rain	20	84	735	Pressley Ranch	40	73	1282
Deseret 1	10	91	720	Pressley Ranch South	33	76	869
Deseret 2	21	84	662	Rdd Primary Canal	33	76	1650
Deseret East	24	81	1525	Roberts Branch	30	77	1600
Deseret Farms	40	73	2240	Rockledge	50	68	2129

Figure 1 - Calibration Parameters for August 2008 to October 2008 Simulation Event with Rain Gauge and NEXRAD (not re-calibrated) Input

Subbasin	I. A. (mm)	C. N.	Lag Time (min.)	Subbasin	I. A. (mm)	C. N.	Lag Time (min.)
Deseret Farms South	41	72	1400	Rollins Ranch	40	73	955
Econlock 1	35	73	1600	Rollins South A	41	72	1143
Econlock 2	40	70	1600	Rollins South B	40	73	1143
Econlock 3	53	65	2500	Rollins South C	40	73	1143
Econlock 4	44	70	2150	Sartori East	40	73	1459
Econlock 5	50	67	1700	Sartori Farms	16	87	1797
Econlock River Swamp	56	64	3000	Savage Creek	16	87	1000
Econlock River Trib 1	36	74	1000	Second Creek	27	80	1700
Econlock River Trib 2	36	74	1000	Sixmile Creek	26	80	2000
Evans Grove	31	77	1190	Sixmile Restoration Area	35	75	1131
FDMCA Rainfall	27	79	2770	Sixmile Tributary	26	80	745
FF PS1	36	75	1970	SJR Cone	20	84	2100
FF PS2	36	75	1720	SJR Harney	12	89	1650
FF PS3	18	85	1265	SJR Puzzle	12	92	2500
FF PS4	34	76	1525	SJR State Road 46	29	79	1300
FF PS5	15	87	875	SJR State Road 50	20	84	3300
FF PS6	38	74	1751	SJWMA Rainfall	40	73	1681
FF PS7	33	76	1593	SN Knight (Kenansville)	16	86	130
Fort Drum Creek	58	66	2400	South Lake Outlet	35	75	1200
Fourmile Creek	45	74	3000	St Johns Imp Dis	37	74	7054
Goupher Slough	19	85	2074	St Johns Imp Dis Res Rain	37	74	1516
Green Branch	32	76	650	St Johns Trib 1&2	21	83	2500
JG Bull Creek	54	66	3000	St Johns Trib 3	17	86	850
JG Crabgrass Creek	57	64	3500	St Johns Trib 7	23.5	82	1300
JG Creek	39	73	2984	St Johns Trib 9	38	74	3500
JG Tributary	37	74	2563	Taylor Creek	23	82	1600
Jim Creek	32	77	2700	Taylor Creek Res Rainfall	41	72	2511
Jim Creek North	41	72	1800	Tenmile Creek	41	72	2272
Jim Green Creek	33	76	2125	Tootoosahatchee Creek	38	74	1500
Joshua Creek	19	84	2200	Tucker Rainfall	34	76	669
King Street	36	75	2200	Turkey Creek	38	73	1150
Knight Creek	13	89	1483	Underhill Slough	17	86	836
Lake Berge Outlet	44	70	1000	Union Park Canal	55	69	1600
Lake Hell n Blazes	41	72	1200	Wolf Creek	68	66	1400
Lake Irma Outlet	60	68	1200	Wolf Creek North	30	77	1500

Figure 1 continued - Calibration Parameters for August 2008 to October 2008 Simulation Event with Rain Gauge and NEXRAD (not re-calibrated) Input

Subbasin	I. A. (mm)	C. N.	Lag Time (min.)	Subbasin	I. A. (mm)	C. N.	Lag Time (min.)
Barney Green	42	72	1560	Lake Poinsett Rainfall North	25	83	3300
Barry Groves	24	81	2646	Lake Poinsett Rainfall South	37	74	3450
BC East Rainfall	14	88	3351	Lake Price Outlet	47	68	1000
BCMCA Rainfall	35	79	7500	Lake Proctor	81	51	550
BC West Rainfall	23	82	1700	Lake Wash 1 Rainfall	20	87	5900
Bird Lake Combined	30	78	1800	Lake Wash 2 Rainfall	20	87	3850
Bird Lake Ditches	36	78	1200	Lake Wash 3 Rainfall	25	87	3900
Bithlo Branch	26	80	650	Lake Wilson Outlet	32	79	2361
Blue Cypress Creek	80	60	3500	Lake Winder Rainfall	30	83	5800
Broadmoor Marsh	32	76	1370	Little Creek	38	72	2000
Bull Creek	36	75	1300	Little Econlock River	51	66	2000
Buscombe Creek	15	87	1000	Little Econlock Tributary	43	70	2100
C25 Ext	43	71	2130	Long Branch	23	75	650
C54 Retention Area	10	92	1163	Mary A Groves	15	87	715
Cabbage Slough	31	76	2300	Mary A Groves Res Rain	29	79	500
Caine Farms	18	85	1250	Mary A Groves Restoration	6	95	574
Christmas Creek	14	89	1500	Mary A Rainfall	37	74	1400
Clark Lake Outlet	30	78	3100	Mills Creek	27	80	1550
Cocoa Canals	25	84	2500	Mitchell Creek	15	88	1285
Cowpen Branch	28	79	750	Moccasin Isl 1	40	73	7600
Cox Creek Lower	41	71	1400	Moccasin Isl 2	17	86	3000
Cox Creek Res Rainfall	41	73	990	Moccasin Isl 3	21	83	2500
Cox Creek upper	30	78	1800	Moccasin Isl 4	26	80	2000
Crane Strand Drain	50	68	1500	Moccasin Isl 5	35	75	1800
Cross Triangle	32	77	1900	Moccasin Isl 6	47	69	3300
Delespine Grant	34	76	1400	Padgett Branch	28	79	2405
Delta Farms	64	63	1240	Pennywash Creek	70	65	1350
Delta Farms Res Rain	20	84	735	Pressley Ranch	40	73	1282
Deseret 1	10	91	720	Pressley Ranch South	33	76	869
Deseret 2	21	84	662	Rdd Primary Canal	33	76	1650
Deseret East	24	81	1525	Roberts Branch	30	77	1600
Deseret Farms	40	73	2240	Rockledge	50	68	2129

Figure 2- Re-Calibration Parameters for August 2008 to October 2008 Simulation Event with NEXRAD Input

Subbasin	I. A. (mm)	C. N.	Lag Time (min.)	Subbasin	I. A. (mm)	C. N.	Lag Time (min.)
Deseret Farms South	41	72	1400	Rollins Ranch	40	73	955
Econlock 1	35	73	1600	Rollins South A	41	72	1143
Econlock 2	40	70	1600	Rollins South B	40	73	1143
Econlock 3	53	65	2500	Rollins South C	40	73	1143
Econlock 4	44	70	2150	Sartori East	40	73	1459
Econlock 5	50	67	1700	Sartori Farms	16	87	1797
Econlock River Swamp	56	64	3000	Savage Creek	16	87	1000
Econlock River Trib 1	36	74	1000	Second Creek	32	80	1700
Econlock River Trib 2	36	74	1000	Sixmile Creek	26	80	2000
Evans Grove	31	77	1190	Sixmile Restoration Area	35	75	1131
FDMCA Rainfall	27	79	2770	Sixmile Tributary	26	80	745
FF PS1	36	75	1970	SJR Cone	20	84	2100
FF PS2	36	75	1720	SJR Harney	12	89	1650
FF PS3	18	85	1265	SJR Puzzle	12	92	2500
FF PS4	34	76	1525	SJR State Road 46	29	79	1300
FF PS5	15	87	875	SJR State Road 50	32	84	3300
FF PS6	38	74	1751	SJWMA Rainfall	40	73	1681
FF PS7	33	76	1593	SN Knight (Kenansville)	16	86	130
Fort Drum Creek	30	66	2400	South Lake Outlet	35	75	1200
Fourmile Creek	45	74	3000	St Johns Imp Dis	37	74	7054
Goupher Slough	19	85	2074	St Johns Imp Dis Res Rain	37	74	1516
Green Branch	32	76	650	St Johns Trib 1&2	21	83	2500
JG Bull Creek	66	66	3000	St Johns Trib 3	23	86	850
JG Crabgrass Creek	65	64	3500	St Johns Trib 7	23.5	82	1300
JG Creek	39	73	2984	St Johns Trib 9	38	74	3500
JG Tributary	37	74	2563	Taylor Creek	28	82	1600
Jim Creek	37	77	2700	Taylor Creek Res Rainfall	47	72	2511
Jim Creek North	52	72	1800	Tenmile Creek	41	72	2272
Jim Green Creek	33	76	2125	Tootoosahatchee Creek	43	74	1500
Joshua Creek	19	84	2200	Tucker Rainfall	34	76	669
King Street	41	75	2200	Turkey Creek	38	73	1150
Knight Creek	13	89	1483	Underhill Slough	17	86	836
Lake Berge Outlet	44	70	1000	Union Park Canal	50	69	1600
Lake Hell n Blazes	41	72	1200	Wolf Creek	68	66	1400
Lake Irma Outlet	60	68	1200	Wolf Creek North	35	77	1500

Figure 2 continued- Re-Calibration Parameters for August 2008 to October 2008 Simulation Event with NEXRAD Input

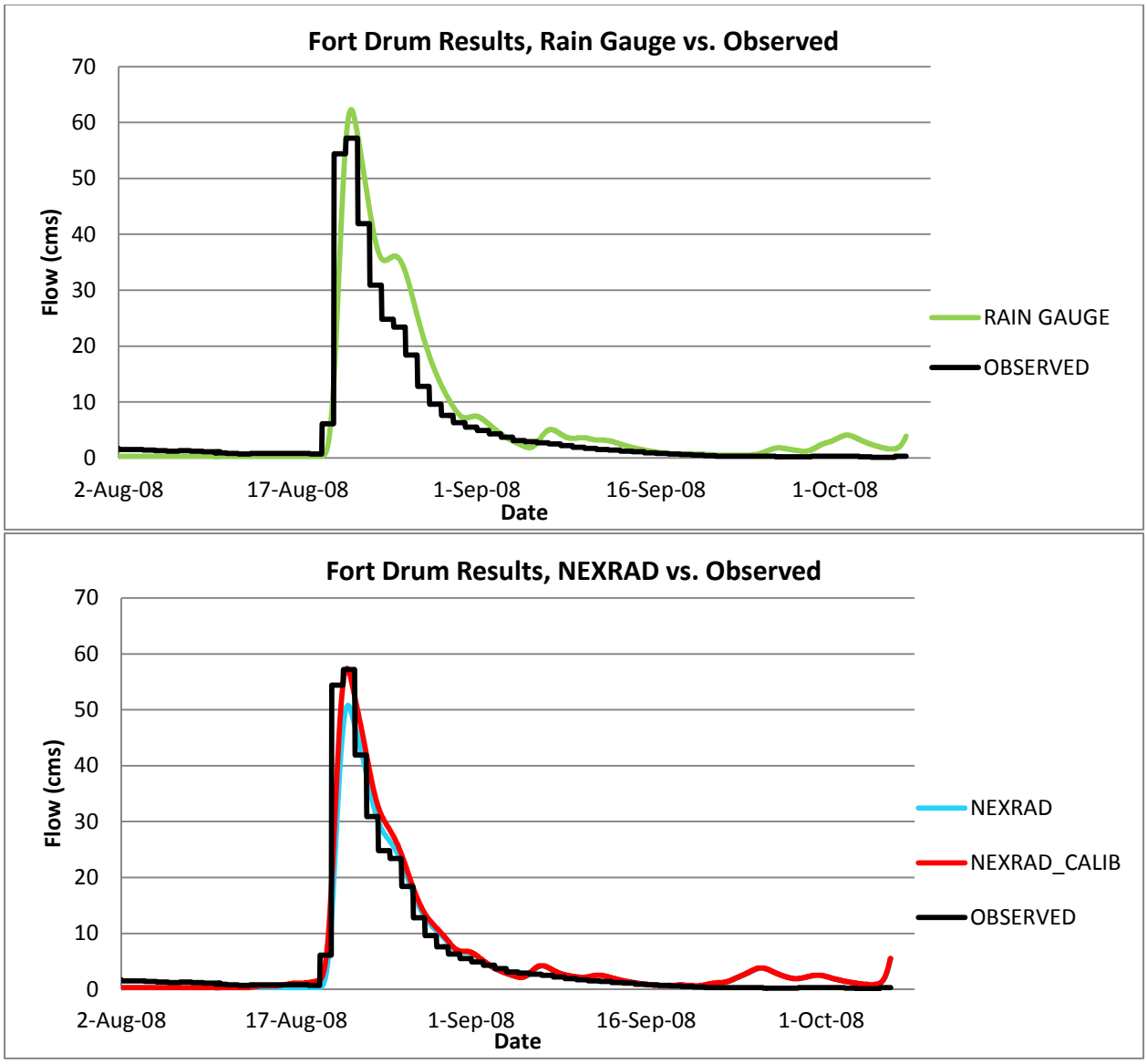

Figures 3a and 3b - Ft. Drum Creek Calibration Results, USGS Gauge 02231342

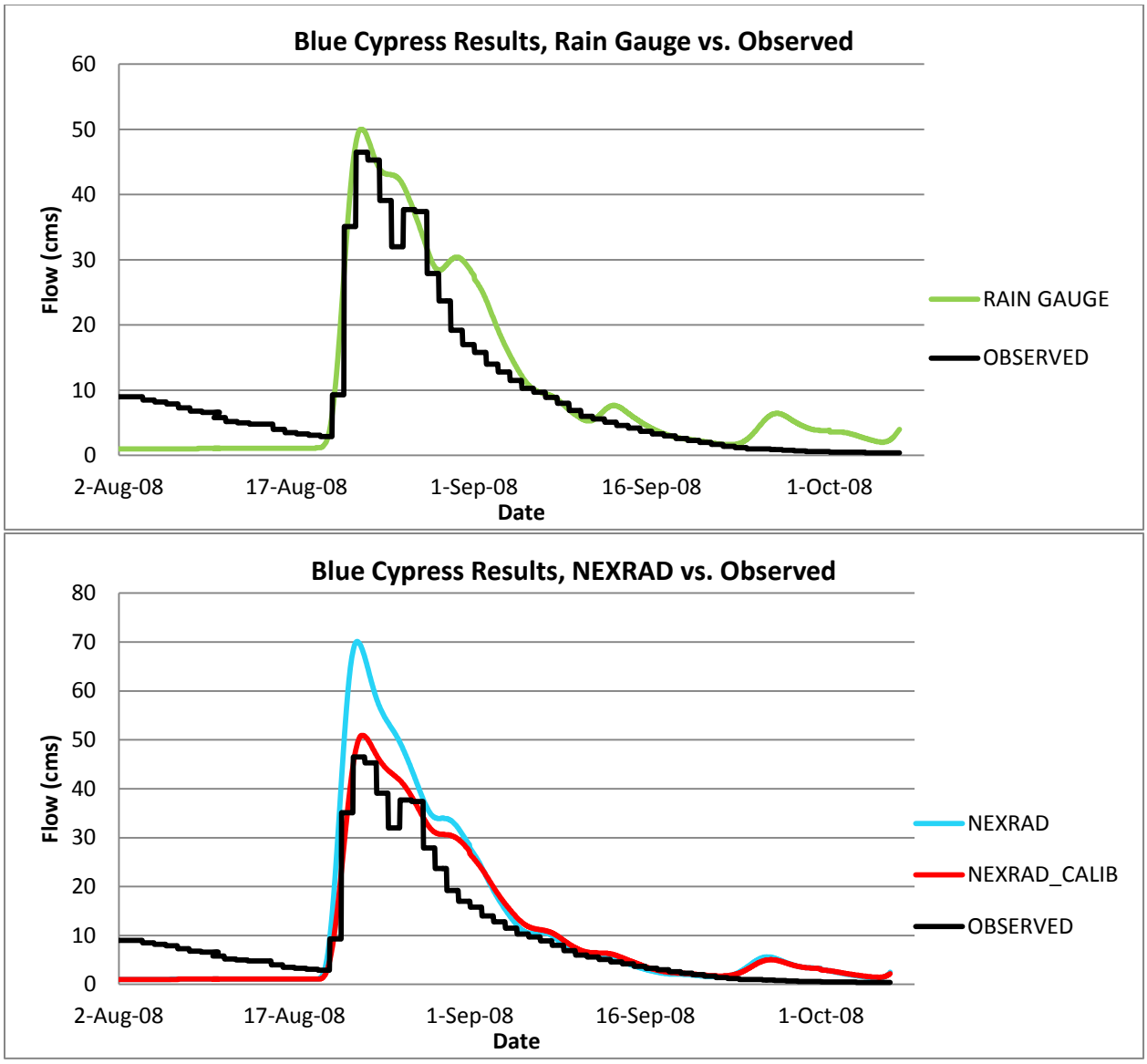

Figures 4a and 4b - Blue Cypress Creek Calibration Results USGS Gauge 02231396

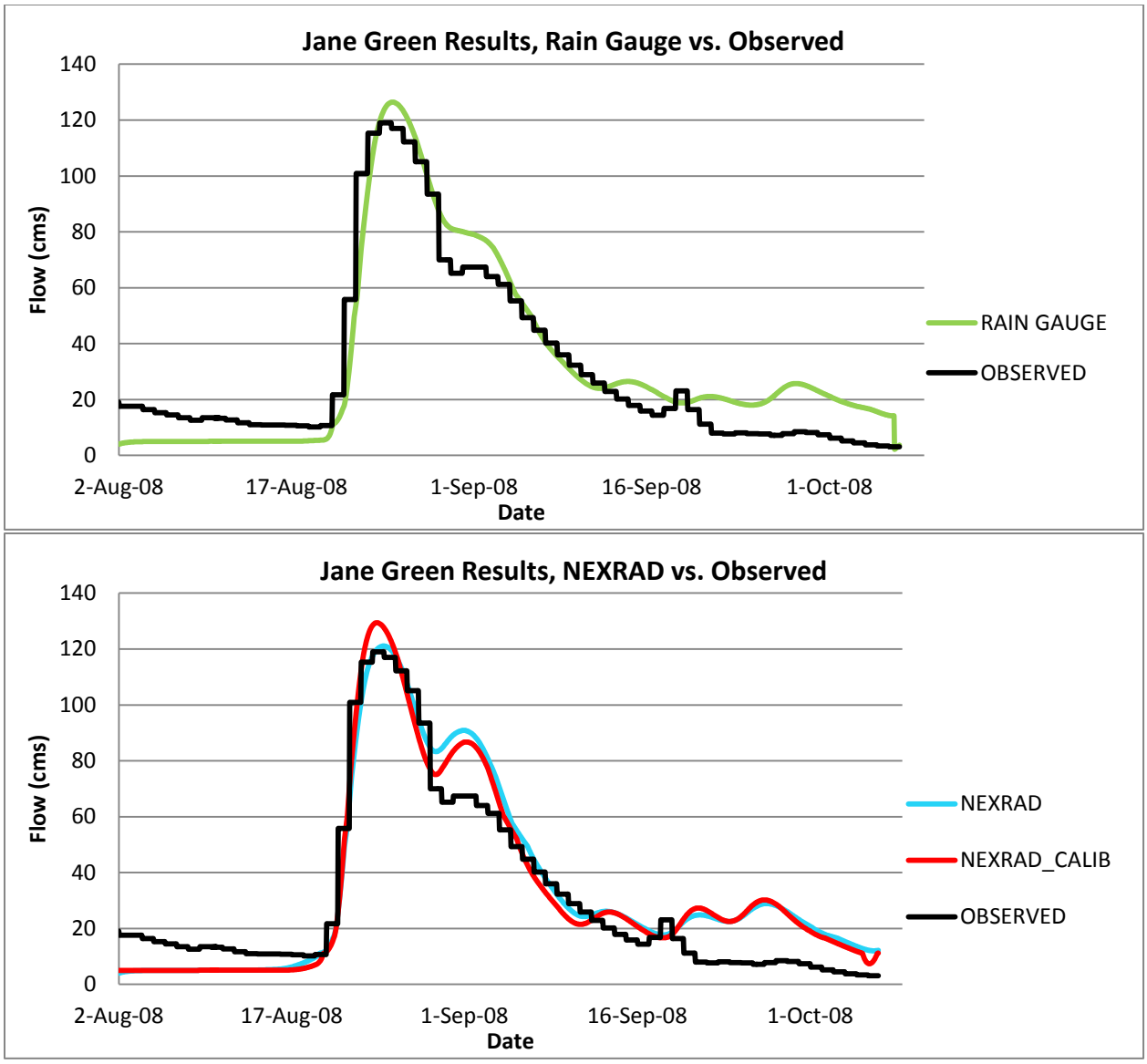

Figures 5a and 5b - Jane Green Reservoir Calibration Results USGS Gauge 02231600

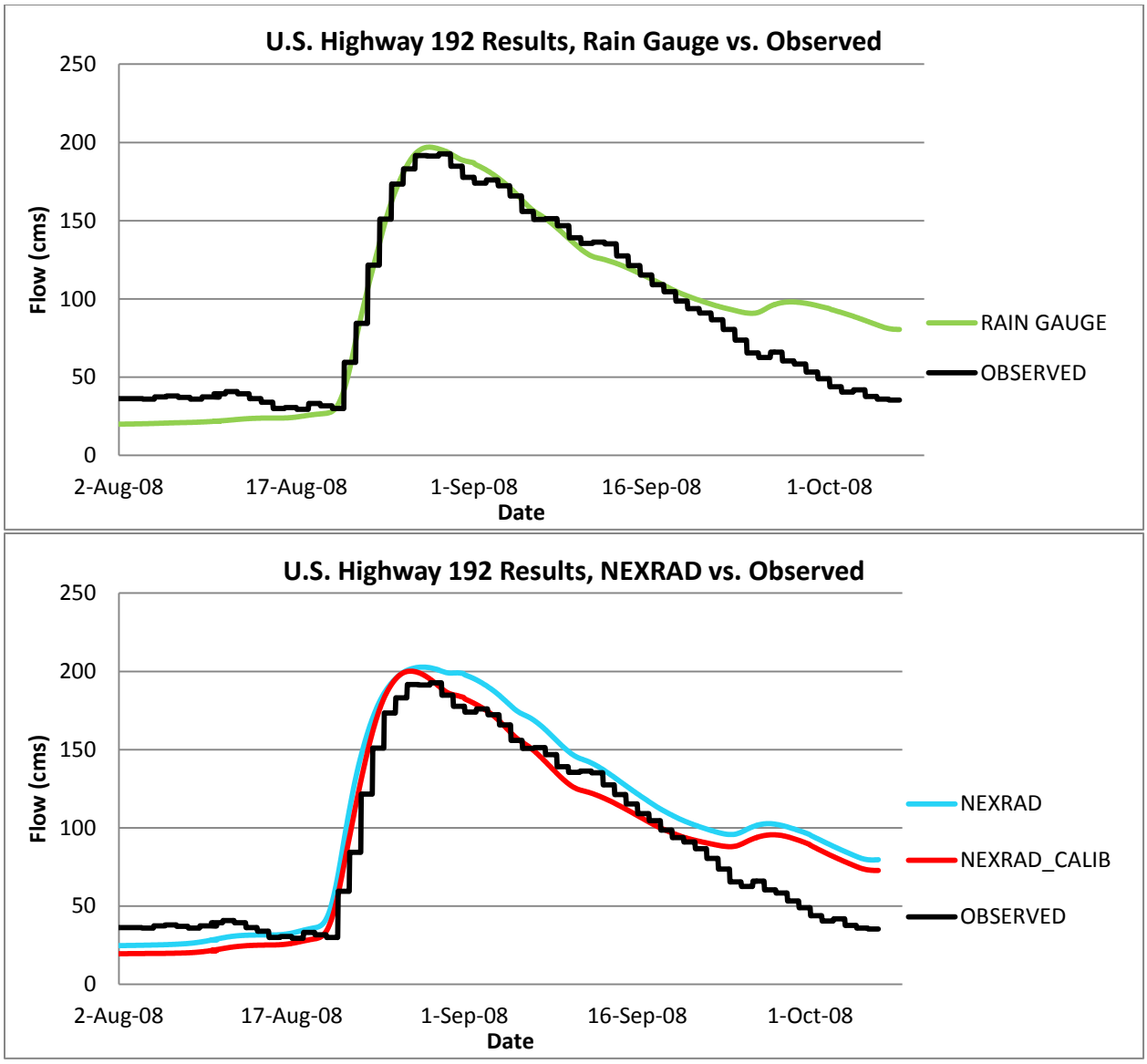

Figures 6a and 6b - St. Johns River at U.S. Highway 192 Calibration Results USGS Gauge 02232000

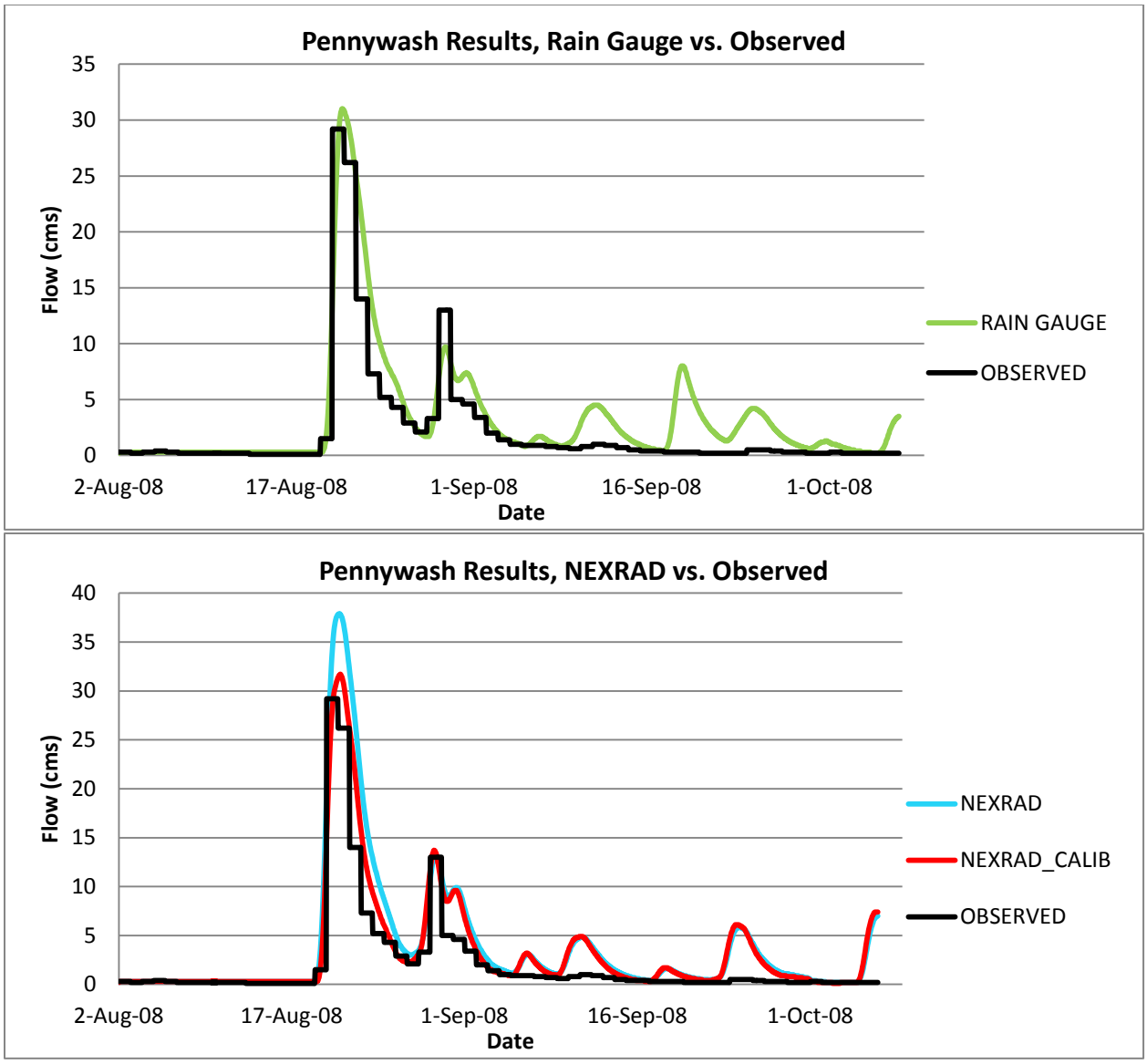

Figures 7a and 7b - Pennywash Creek Calibration Results USGS Gauge 02232155

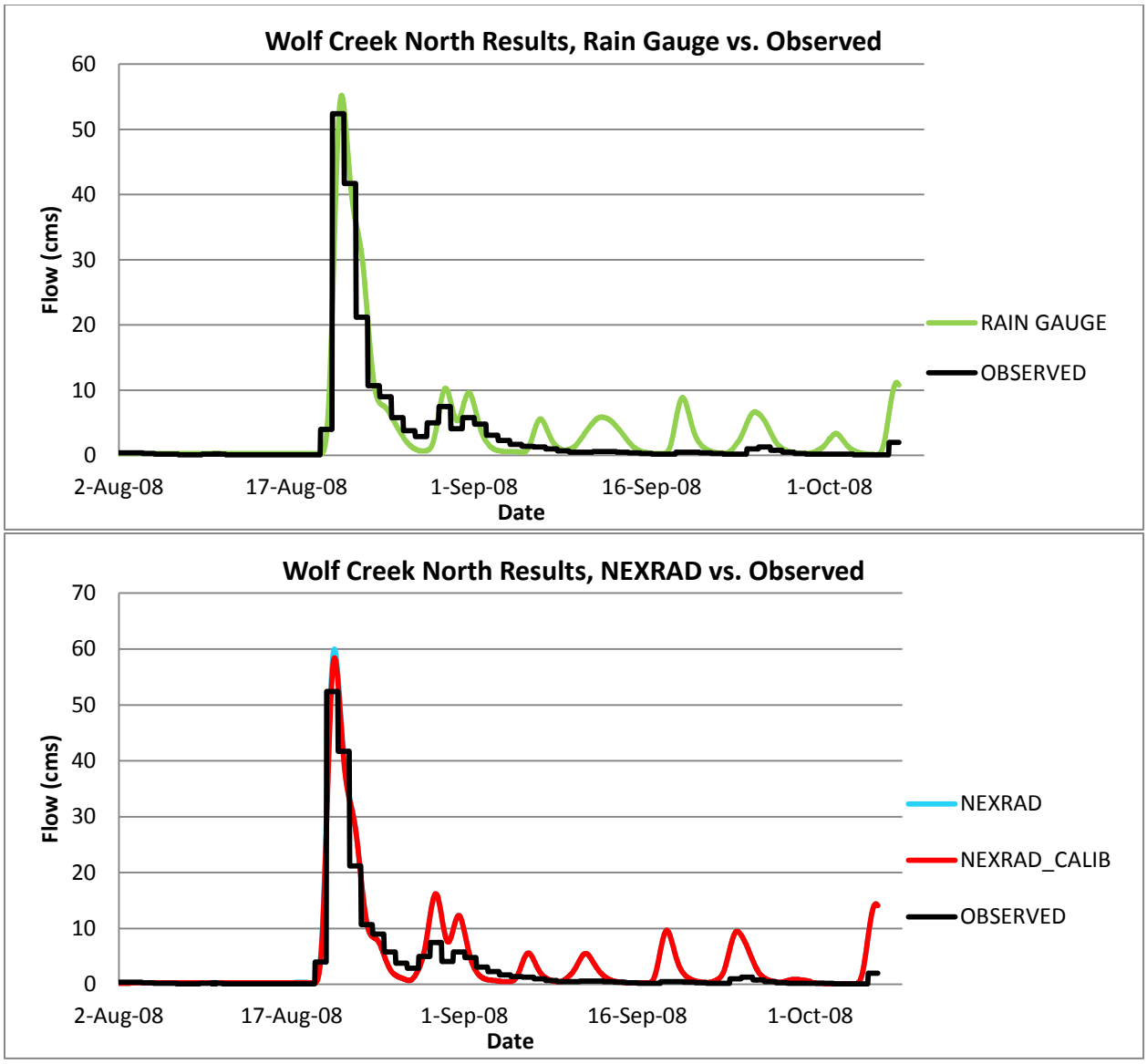

Figures 8a and 8b - Wolf Creek North Calibration Results USGS Gauge 02232200

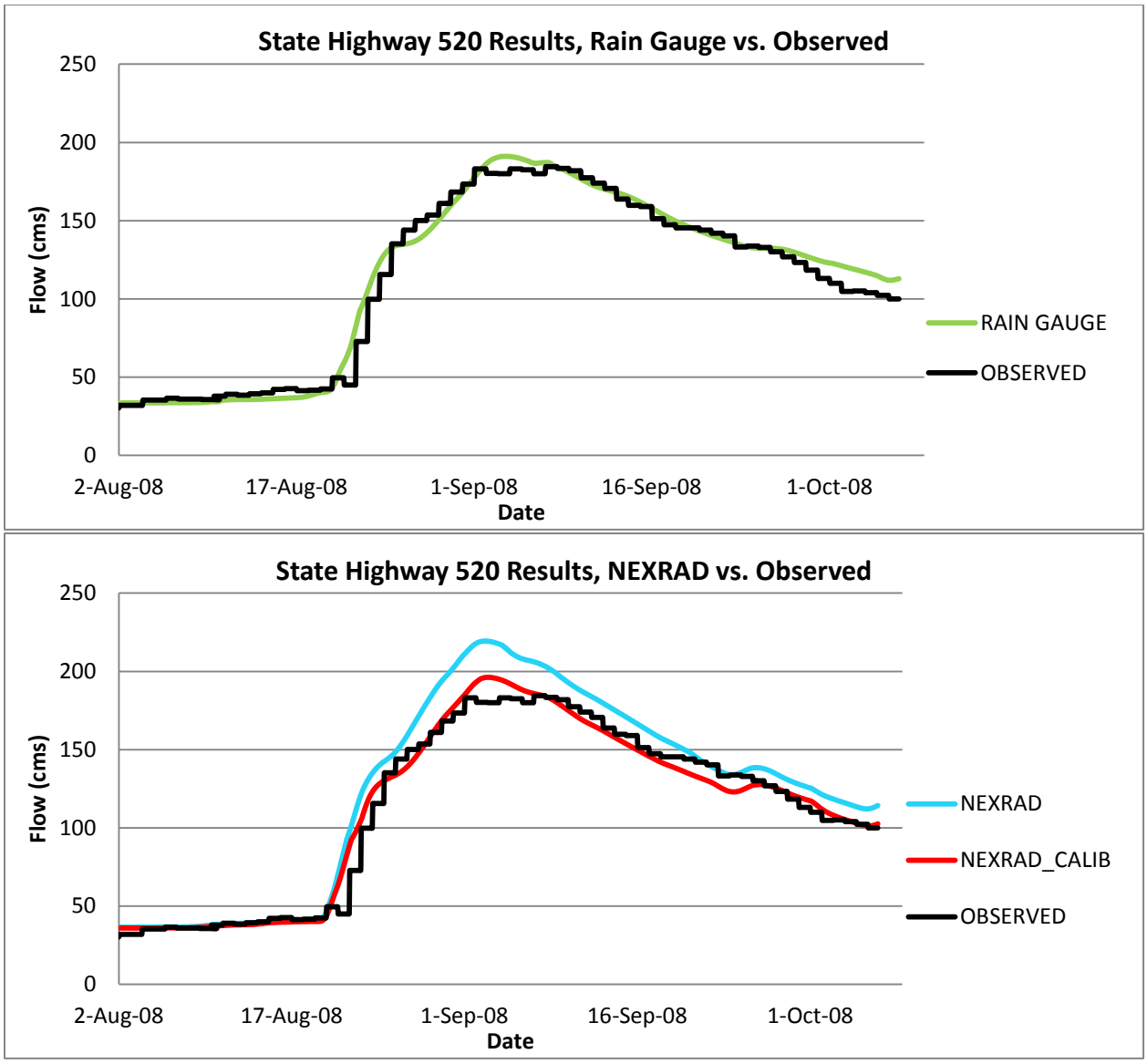

Figures 9a and 9 b - St. Johns River at State Highway 520 Calibration Results USGS Gauge 02232400

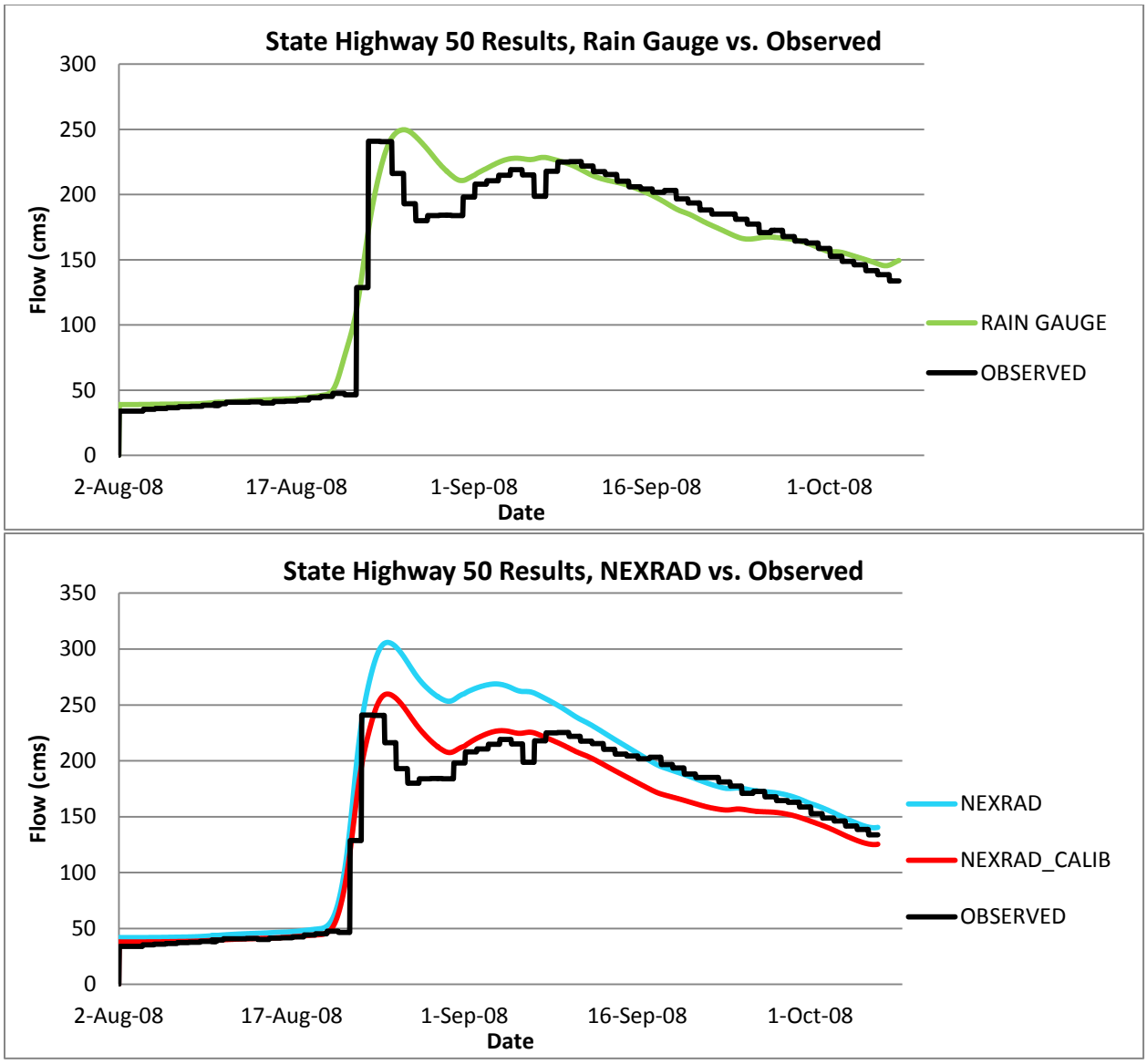

Figures 10a and 10b – St. Johns River at State Highway 50 Calibration Results USGS Gauge 02232500

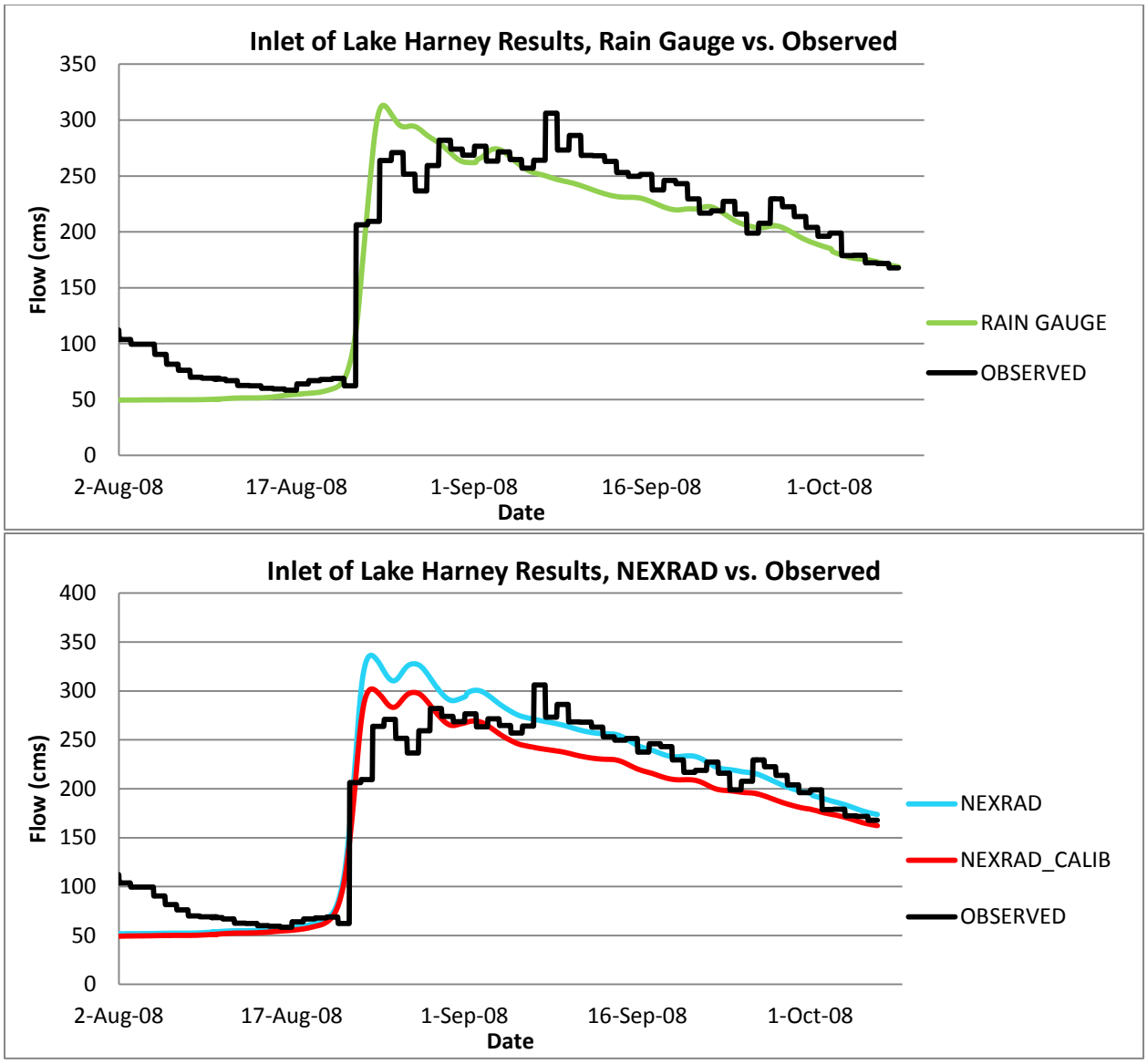

Figures 11a and 11b - St. Johns River at Inlet of Lake Harney Calibration Results USGS Gauge 02234000

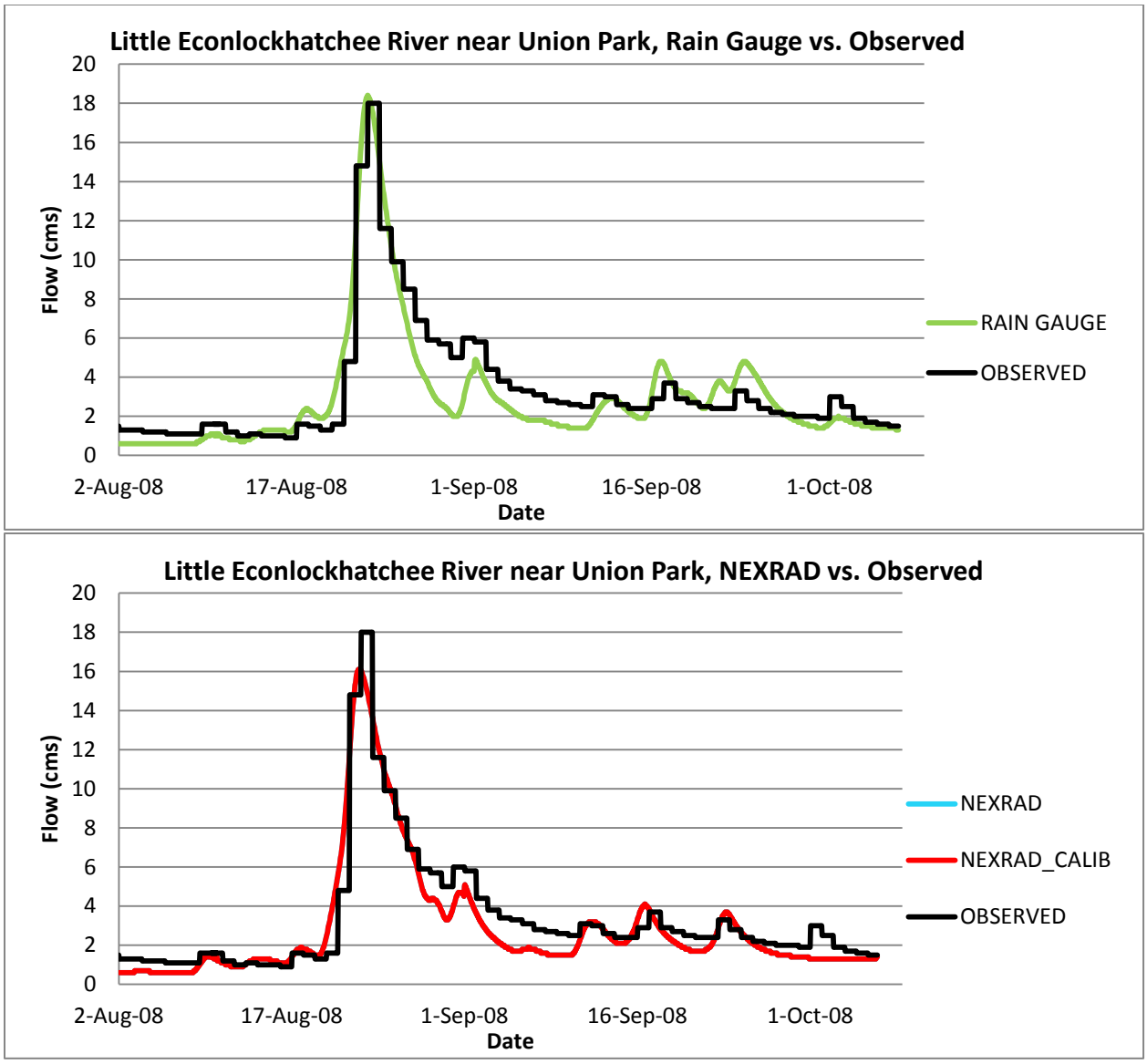

Figure 12a and 12b – Little Econlockhatchee River near Union Park Calibration Results USGS Gauge 02233460

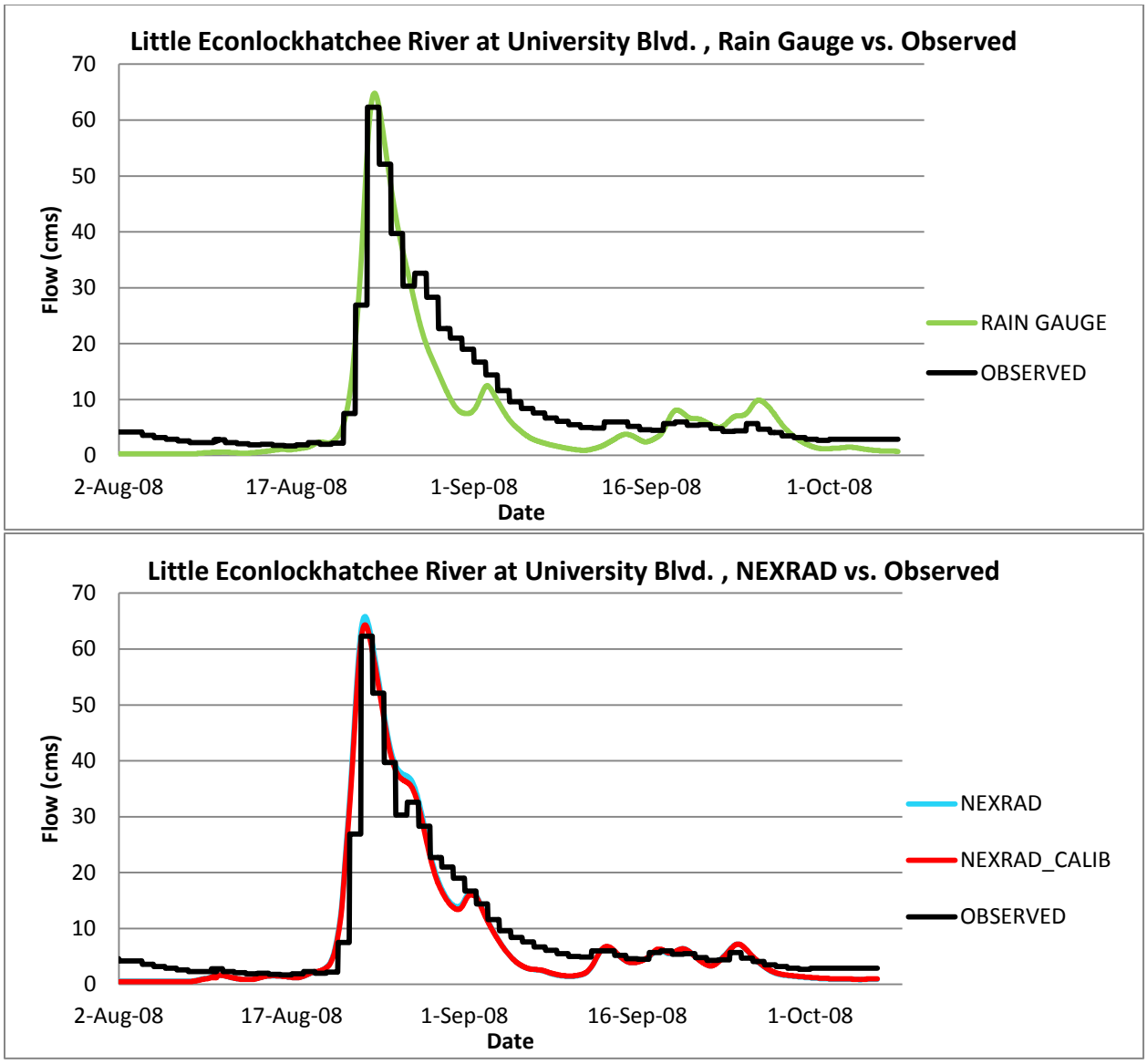

Figure 13a and 13b – Little Econlockhatchee River at University Blvd. Calibration Results
USGS Gauge 02233473

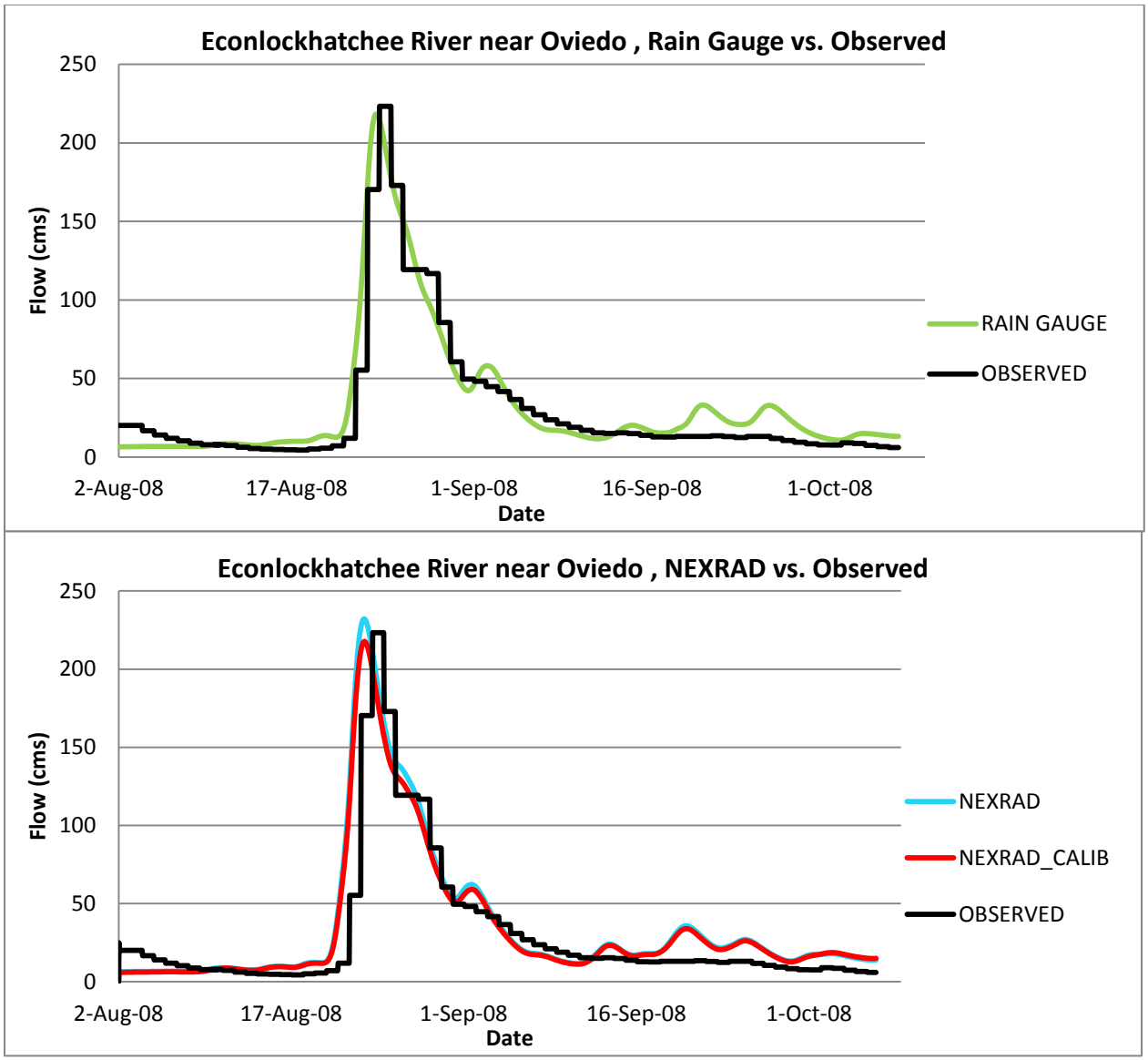

Figure 14a and 14b – Econlockhatchee River near Oviedo Calibration Results USGS Gauge 02233484

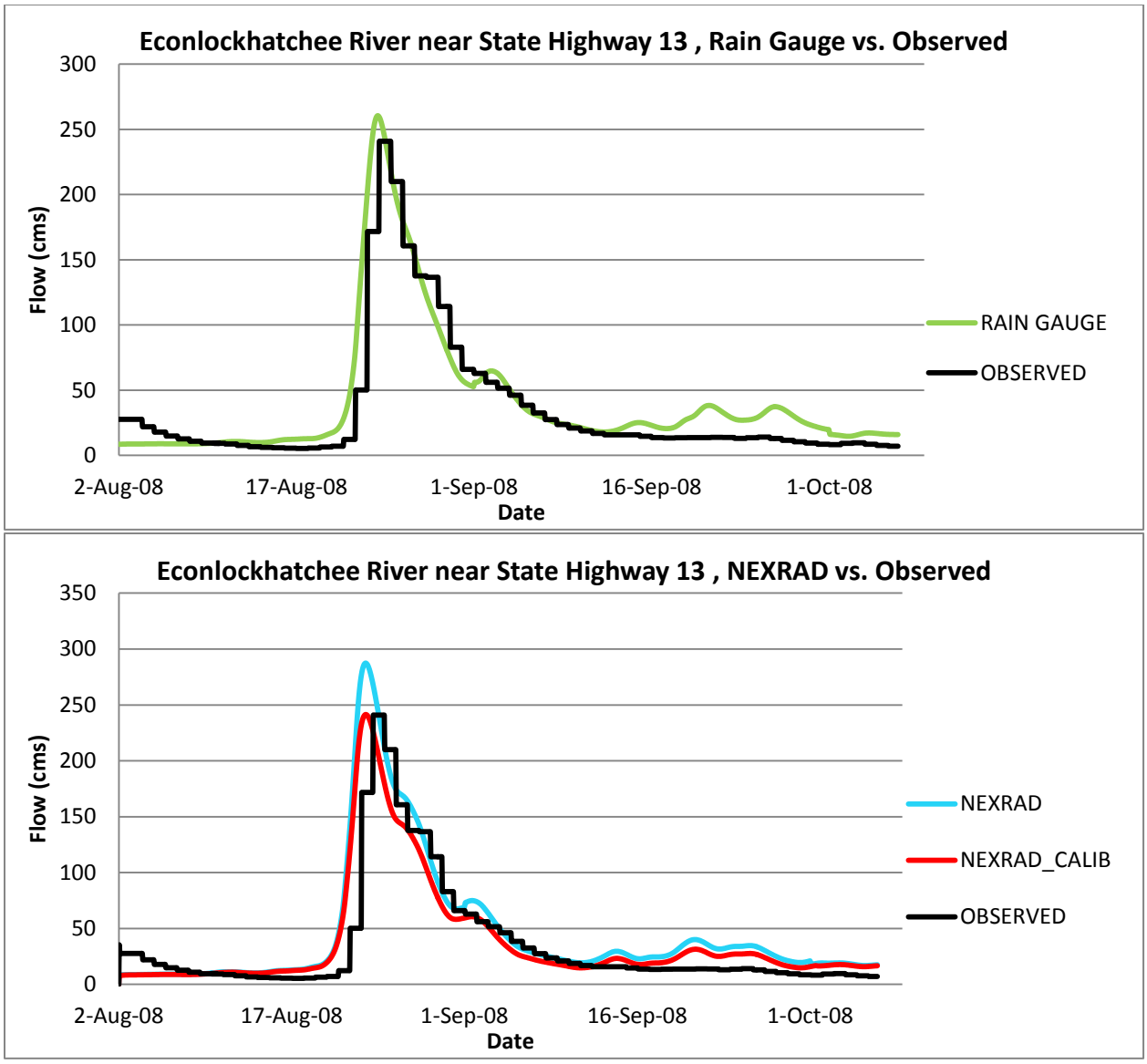

Figure 15a and 15b – Econlockhatchee River near State Highway 13 Calibration Results USGS Gauge 02233500

APPENDIX B

October 2007 Validation Model Results

Subbasin	I. A. (mm)	C. N.	Lag Time (min.)	Subbasin	I. A. (mm)	C. N.	Lag Time (min.)
Barney Green	42	72	1560	Lake Poinsett Rainfall North	17	83	3300
Barry Groves	24	81	2646	Lake Poinsett Rainfall South	37	74	3450
BC East Rainfall	14	88	3351	Lake Price Outlet	47	68	1000
BCMCA Rainfall	20	79	7500	Lake Proctor	81	51	550
BC West Rainfall	23	82	1700	Lake Wash 1 Rainfall	13	89	4500
Bird Lake Combined	30	78	1800	Lake Wash 2 Rainfall	10	89	3850
Bird Lake Ditches	31	78	1200	Lake Wash 3 Rainfall	13	89	2900
Bithlo Branch	26	80	650	Lake Wilson Outlet	27	79	2361
Blue Cypress Creek	31	65	3500	Lake Winder Rainfall	17	86	5800
Broadmoor Marsh	32	76	1370	Little Creek	38	72	2000
Bull Creek	36	75	1300	Little Econlock River	51	66	2000
Buscombe Creek	15	87	1000	Little Econlock Tributary	43	70	2100
C25 Ext	43	71	2130	Long Branch	23	75	650
C54 Retention Area	10	92	1163	Mary A Groves	15	87	715
Cabbage Slough	31	76	2300	Mary A Groves Res Rain	296	79	500
Caine Farms	18	85	1250	Mary A Groves Restoration	6	95	574
Christmas Creek	14	89	1500	Mary A Rainfall	37	74	1400
Clark Lake Outlet	30	78	3100	Mills Creek	27	80	1550
Cocoa Canals	21	84	2500	Mitchell Creek	15	88	1285
Cowpen Branch	28	79	750	Moccasin Isl 1	40	73	7600
Cox Creek Lower	41	71	1400	Moccasin Isl 2	17	86	3000
Cox Creek Res Rainfall	41	73	990	Moccasin Isl 3	21	83	2500
Cox Creek upper	30	78	1800	Moccasin Isl 4	26	80	2000
Crane Strand Drain	55	68	1500	Moccasin Isl 5	35	75	1800
Cross Triangle	32	77	1900	Moccasin Isl 6	47	69	3300
Delespine Grant	34	76	1400	Padgett Branch	28	79	2405
Delta Farms	64	63	1240	Pennywash Creek	48	65	1350
Delta Farms Res Rain	20	84	735	Pressley Ranch	40	73	1282
Deseret 1	10	91	720	Pressley Ranch South	33	76	869
Deseret 2	21	84	662	Rdd Primary Canal	33	76	1650
Deseret East	24	81	1525	Roberts Branch	30	77	1600
Deseret Farms	40	73	2240	Rockledge	50	68	2129

Figure 1 - Calibration Parameters for October 2007 Simulation Event with Rain Gauge and NEXRAD (not re-calibrated) Input

Subbasin	I. A. (mm)	C. N.	Lag Time (min.)	Subbasin	I. A. (mm)	C. N.	Lag Time (min.)
Deseret Farms South	41	72	1400	Rollins Ranch	40	73	955
Econlock 1	35	73	1600	Rollins South A	41	72	1143
Econlock 2	40	70	1600	Rollins South B	40	73	1143
Econlock 3	53	65	2500	Rollins South C	40	73	1143
Econlock 4	44	70	2150	Sartori East	40	73	1459
Econlock 5	50	67	1700	Sartori Farms	16	87	1797
Econlock River Swamp	56	64	3000	Savage Creek	16	87	1000
Econlock River Trib 1	36	74	1000	Second Creek	27	80	1700
Econlock River Trib 2	36	74	1000	Sixmile Creek	26	80	2000
Evans Grove	31	77	1190	Sixmile Restoration Area	35	75	1131
FDMCA Rainfall	27	79	2770	Sixmile Tributary	26	80	745
FF PS1	36	75	1970	SJR Cone	20	84	2100
FF PS2	36	75	1720	SJR Harney	12	89	1650
FF PS3	18	85	1265	SJR Puzzle	12	92	2500
FF PS4	34	76	1525	SJR State Road 46	29	79	1300
FF PS5	15	87	875	SJR State Road 50	20	84	3300
FF PS6	38	74	1751	SJWMA Rainfall	40	73	1681
FF PS7	33	76	1593	SN Knight (Kenansville)	16	86	130
Fort Drum Creek	10	75	2400	South Lake Outlet	35	75	1200
Fourmile Creek	45	74	3000	St Johns Imp Dis	37	74	7054
Goupher Slough	19	85	2074	St Johns Imp Dis Res Rain	37	74	1516
Green Branch	32	76	650	St Johns Trib 1&2	21	83	2500
JG Bull Creek	37	72	3000	St Johns Trib 3	17	86	850
JG Crabgrass Creek	50	64	3500	St Johns Trib 7	22	82	1200
JG Creek	39	73	2984	St Johns Trib 9	38	74	3500
JG Tributary	37	74	2563	Taylor Creek	20	82	1600
Jim Creek	32	77	2700	Taylor Creek Res Rainfall	41	72	2511
Jim Creek North	41	72	1800	Tenmile Creek	41	72	2272
Jim Green Creek	33	76	2125	Tootoosahatchee Creek	38	74	1500
Joshua Creek	19	84	2200	Tucker Rainfall	34	76	669
King Street	36	75	2200	Turkey Creek	38	73	1150
Knight Creek	13	89	1483	Underhill Slough	17	86	836
Lake Berge Outlet	44	70	1000	Union Park Canal	55	69	1600
Lake Hell n Blazes	41	72	1200	Wolf Creek	68	64	1400
Lake Irma Outlet	60	68	1200	Wolf Creek North	15	76	1500

Figure 1 continued - Calibration Parameters for October 2007 Simulation Event with Rain Gauge and NEXRAD (not re-calibrated) Input

Subbasin	I. A. (mm)	C. N.	Lag Time (min.)	Subbasin	I. A. (mm)	C. N.	Lag Time (min.)
Barney Green	42	72	1560	Lake Poinsett Rainfall North	25	83	3300
Barry Groves	24	81	2646	Lake Poinsett Rainfall South	34	74	3450
BC East Rainfall	14	88	3351	Lake Price Outlet	55	68	1000
BCMCA Rainfall	20	79	7500	Lake Proctor	60	51	550
BC West Rainfall	23	82	1700	Lake Wash 1 Rainfall	13	89	4500
Bird Lake Combined	30	78	1800	Lake Wash 2 Rainfall	10	89	3850
Bird Lake Ditches	25	78	1200	Lake Wash 3 Rainfall	13	89	2900
Bithlo Branch	26	80	650	Lake Wilson Outlet	27	79	2361
Blue Cypress Creek	50	60	3500	Lake Winder Rainfall	17	86	5800
Broadmoor Marsh	32	76	1370	Little Creek	38	72	2000
Bull Creek	36	75	1300	Little Econlock River	58	66	2000
Buscombe Creek	15	87	1000	Little Econlock Tributary	48	70	2100
C25 Ext	43	71	2130	Long Branch	23	75	650
C54 Retention Area	10	92	1163	Mary A Groves	15	87	715
Cabbage Slough	31	76	2300	Mary A Groves Res Rain	29	79	500
Caine Farms	18	85	1250	Mary A Groves Restoration	6	95	574
Christmas Creek	14	89	1500	Mary A Rainfall	37	74	1400
Clark Lake Outlet	30	78	3100	Mills Creek	27	80	1550
Cocoa Canals	21	84	2500	Mitchell Creek	15	88	1285
Cowpen Branch	28	79	750	Moccasin Isl 1	40	73	7600
Cox Creek Lower	41	71	1400	Moccasin Isl 2	17	86	3000
Cox Creek Res Rainfall	41	73	990	Moccasin Isl 3	21	83	2500
Cox Creek upper	35	78	1800	Moccasin Isl 4	26	80	2000
Crane Strand Drain	55	68	1500	Moccasin Isl 5	35	75	1800
Cross Triangle	32	77	1900	Moccasin Isl 6	47	69	3300
Delespine Grant	34	76	1400	Padgett Branch	28	79	2405
Delta Farms	64	63	1240	Pennywash Creek	38	65	1350
Delta Farms Res Rain	20	84	735	Pressley Ranch	40	73	1282
Deseret 1	10	91	720	Pressley Ranch South	33	76	869
Deseret 2	21	84	662	Rdd Primary Canal	33	76	1650
Deseret East	24	81	1525	Roberts Branch	30	77	1600
Deseret Farms	40	73	2240	Rockledge	50	68	2129

Figure 2- Re-Calibration Parameters for October 2007 Simulation Event with NEXRAD Input

Subbasin	I. A. (mm)	C. N.	Lag Time (min.)	Subbasin	I. A. (mm)	C. N.	Lag Time (min.)
Deseret Farms South	41	72	1400	Rollins Ranch	40	73	955
Econlock 1	35	73	1600	Rollins South A	41	72	1143
Econlock 2	50	60	1600	Rollins South B	40	73	1143
Econlock 3	53	65	2500	Rollins South C	40	73	1143
Econlock 4	44	70	2150	Sartori East	40	73	1459
Econlock 5	50	67	1700	Sartori Farms	16	87	1797
Econlock River Swamp	56	64	3000	Savage Creek	16	87	1000
Econlock River Trib 1	36	74	1000	Second Creek	27	80	1700
Econlock River Trib 2	36	74	1000	Sixmile Creek	26	80	2000
Evans Grove	31	77	1190	Sixmile Restoration Area	35	75	1131
FDMCA Rainfall	27	79	2770	Sixmile Tributary	26	80	745
FF PS1	36	75	1970	SJR Cone	20	84	2100
FF PS2	36	75	1720	SJR Harney	12	89	1650
FF PS3	18	85	1265	SJR Puzzle	12	92	2500
FF PS4	34	76	1525	SJR State Road 46	29	79	1300
FF PS5	15	87	875	SJR State Road 50	25	84	3300
FF PS6	38	74	1751	SJWMA Rainfall	40	73	1681
FF PS7	33	76	1593	SN Knight (Kenansville)	16	86	130
Fort Drum Creek	3	75	2400	South Lake Outlet	35	75	1200
Fourmile Creek	45	74	3000	St Johns Imp Dis	37	74	7054
Goupher Slough	19	85	2074	St Johns Imp Dis Res Rain	37	74	1516
Green Branch	32	76	650	St Johns Trib 1&2	21	83	2500
JG Bull Creek	45	72	3000	St Johns Trib 3	17	86	850
JG Crabgrass Creek	50	64	3500	St Johns Trib 7	22	82	1200
JG Creek	39	73	2984	St Johns Trib 9	38	74	3500
JG Tributary	37	74	2563	Taylor Creek	25	82	1600
Jim Creek	37	77	2700	Taylor Creek Res Rainfall	41	72	2511
Jim Creek North	41	72	1800	Tenmile Creek	41	72	2272
Jim Green Creek	33	76	2125	Tootoosahatchee Creek	38	74	1500
Joshua Creek	19	84	2200	Tucker Rainfall	34	76	669
King Street	36	75	2200	Turkey Creek	38	73	1150
Knight Creek	13	89	1483	Underhill Slough	17	86	836
Lake Berge Outlet	48	70	1000	Union Park Canal	55	69	1600
Lake Hell n Blazes	41	72	1200	Wolf Creek	68	64	1400
Lake Irma Outlet	60	68	1200	Wolf Creek North	15	76	1500

Figure 2 continued- Re-Calibration Parameters for October 2007 Simulation Event with NEXRAD Input

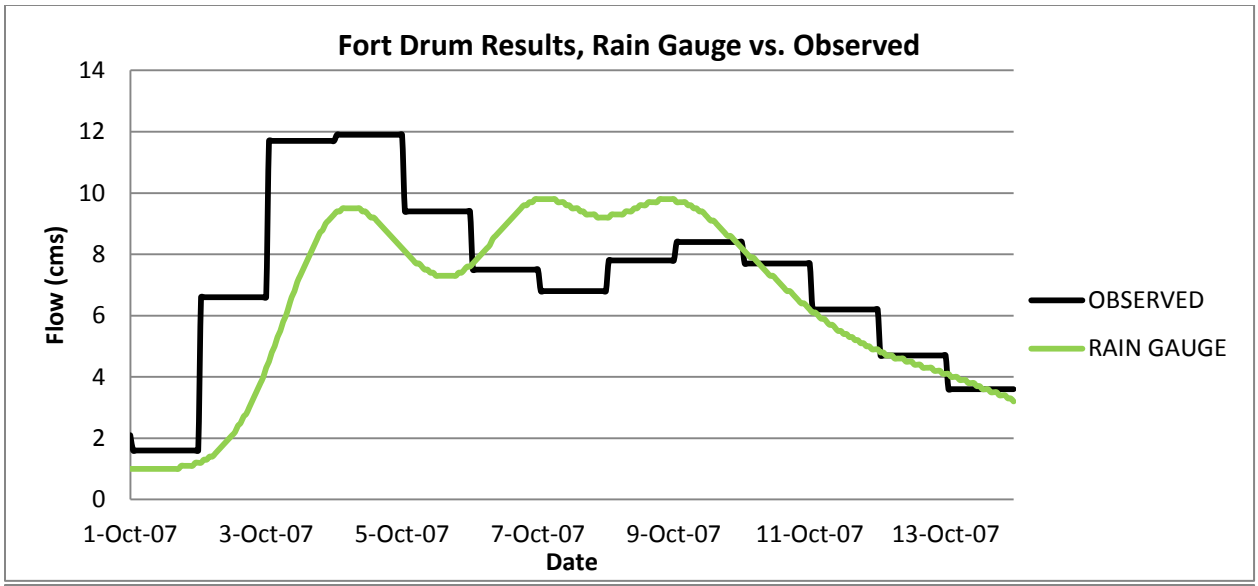

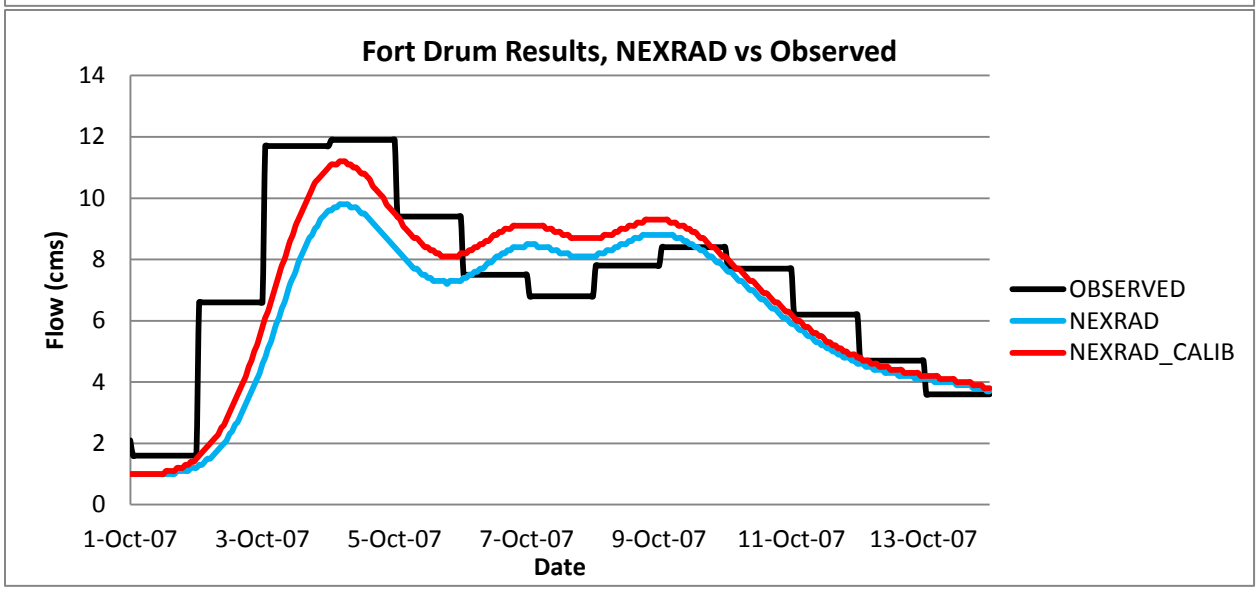

Figures 3a and 3b - Ft. Drum Creek 2007 Validation Results, USGS Gauge 02231342

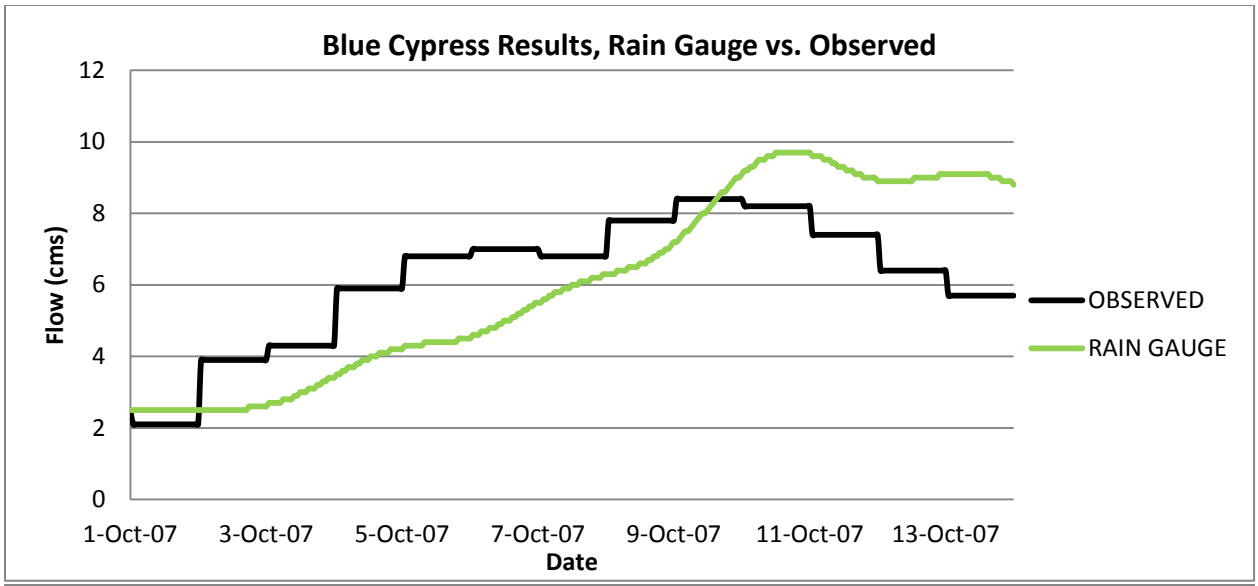

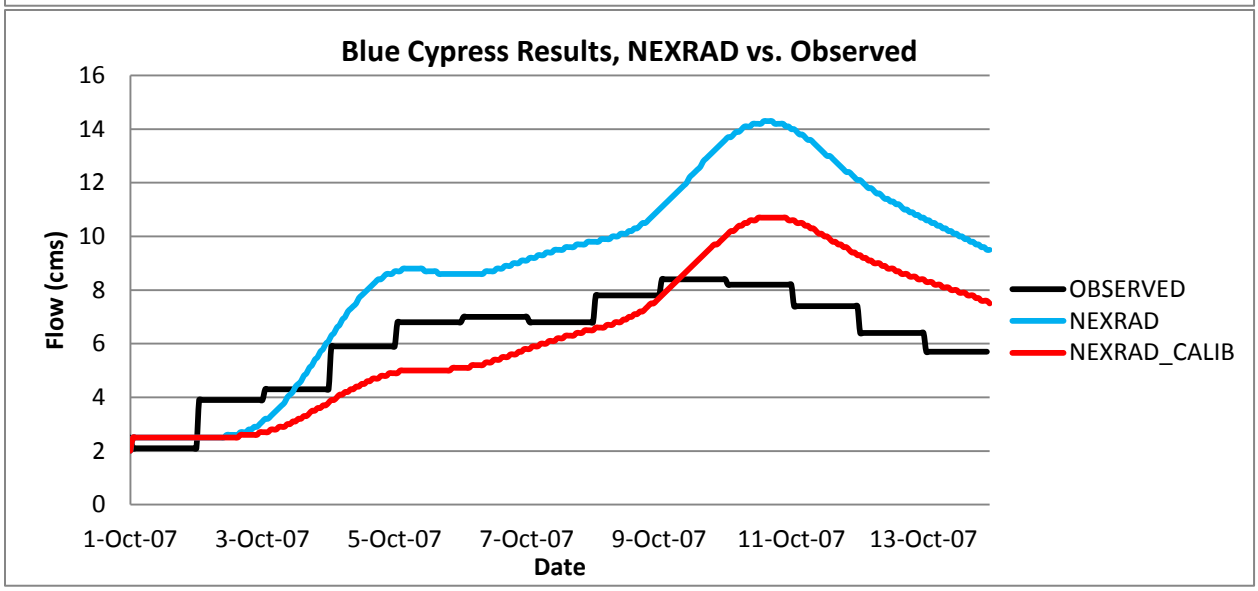

Figures 4a and 4b - Blue Cypress Creek 2007 Validation Results USGS Gauge 02231396

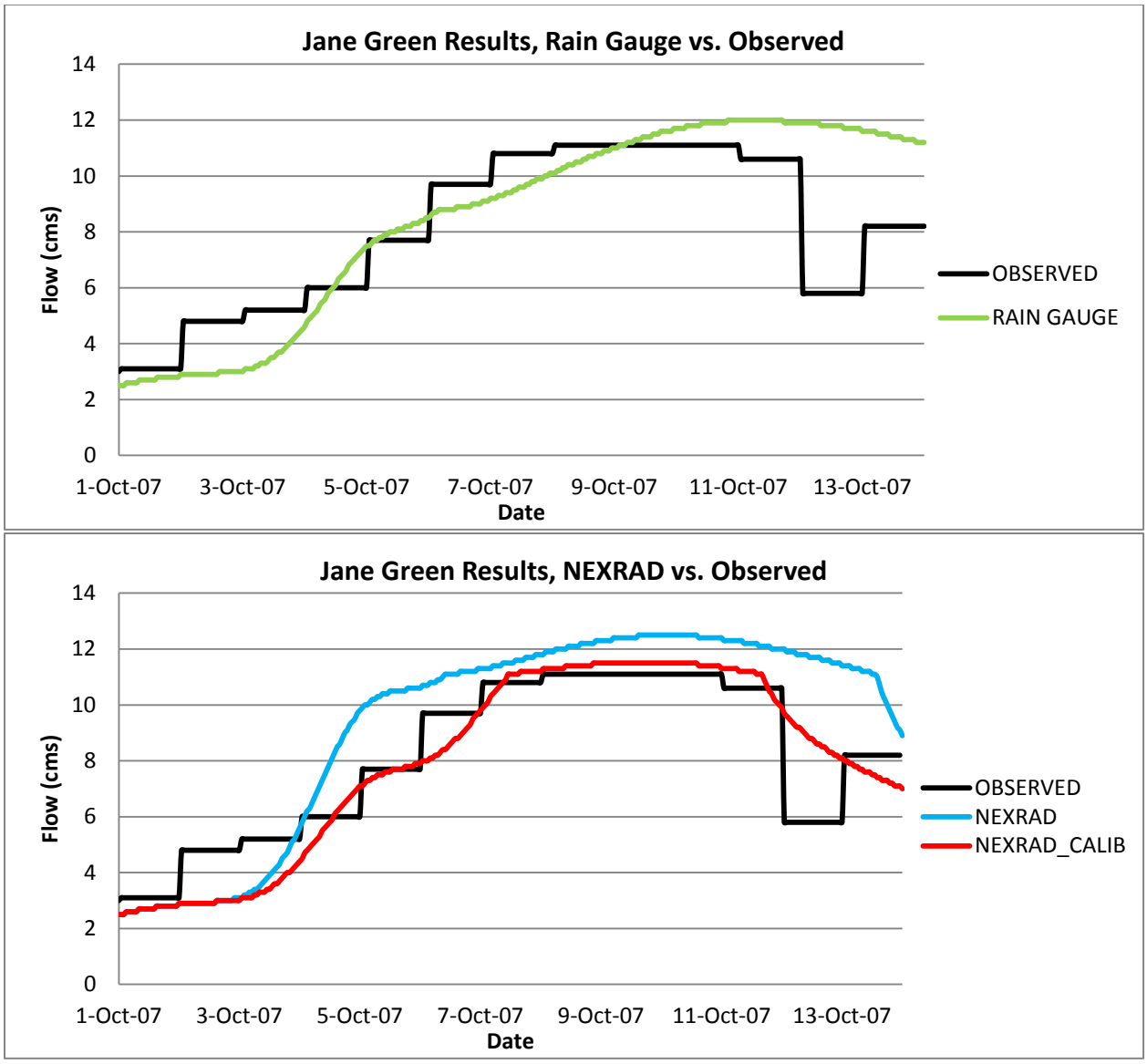

Figures 5a and 5b – Jane Green Reservoir 2007 Validation Results USGS Gauge 02231600

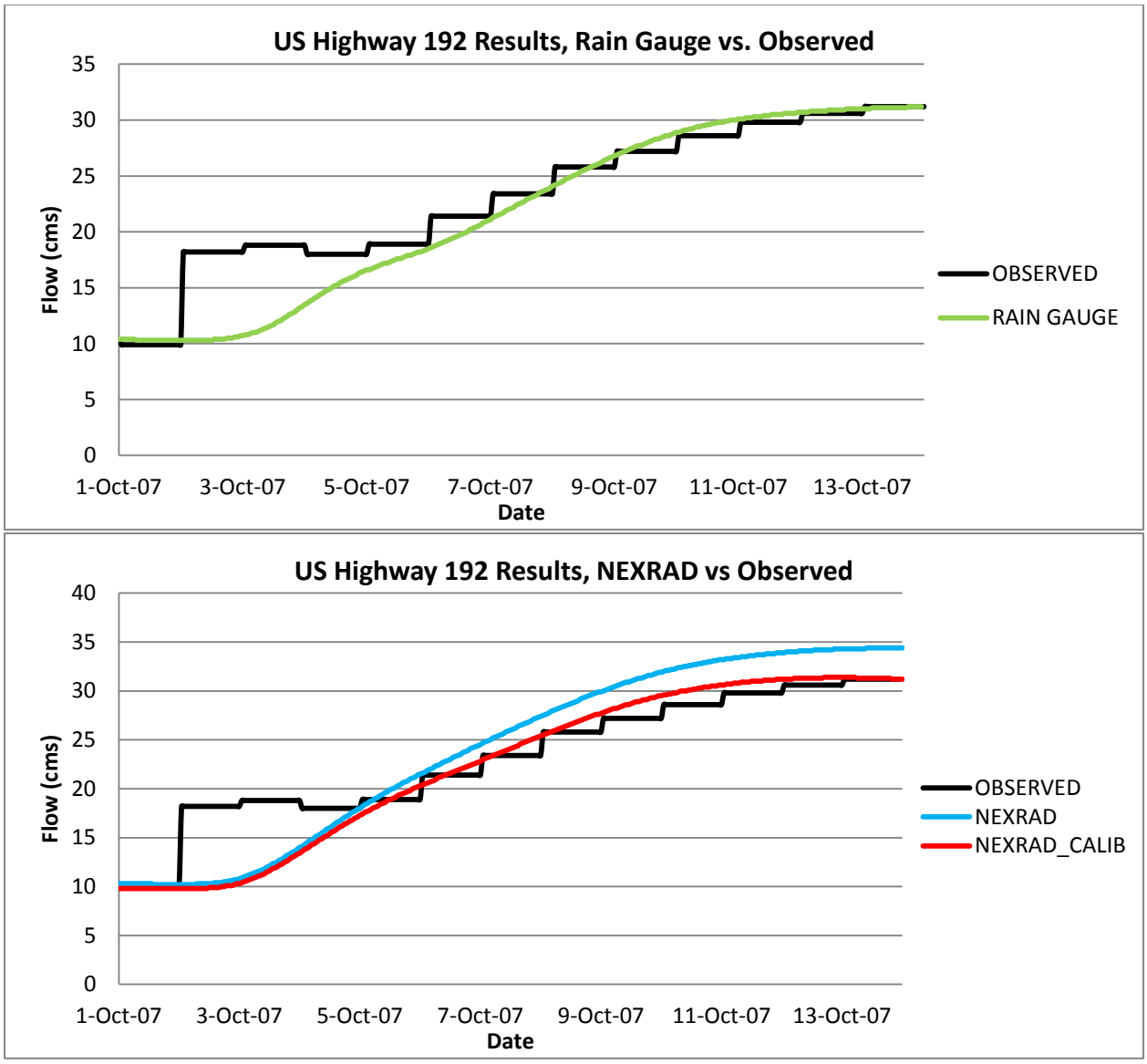

Figures 6a and 6b – St. Johns River at U.S. Highway 192 2007 Validation Results USGS Gauge 02232000

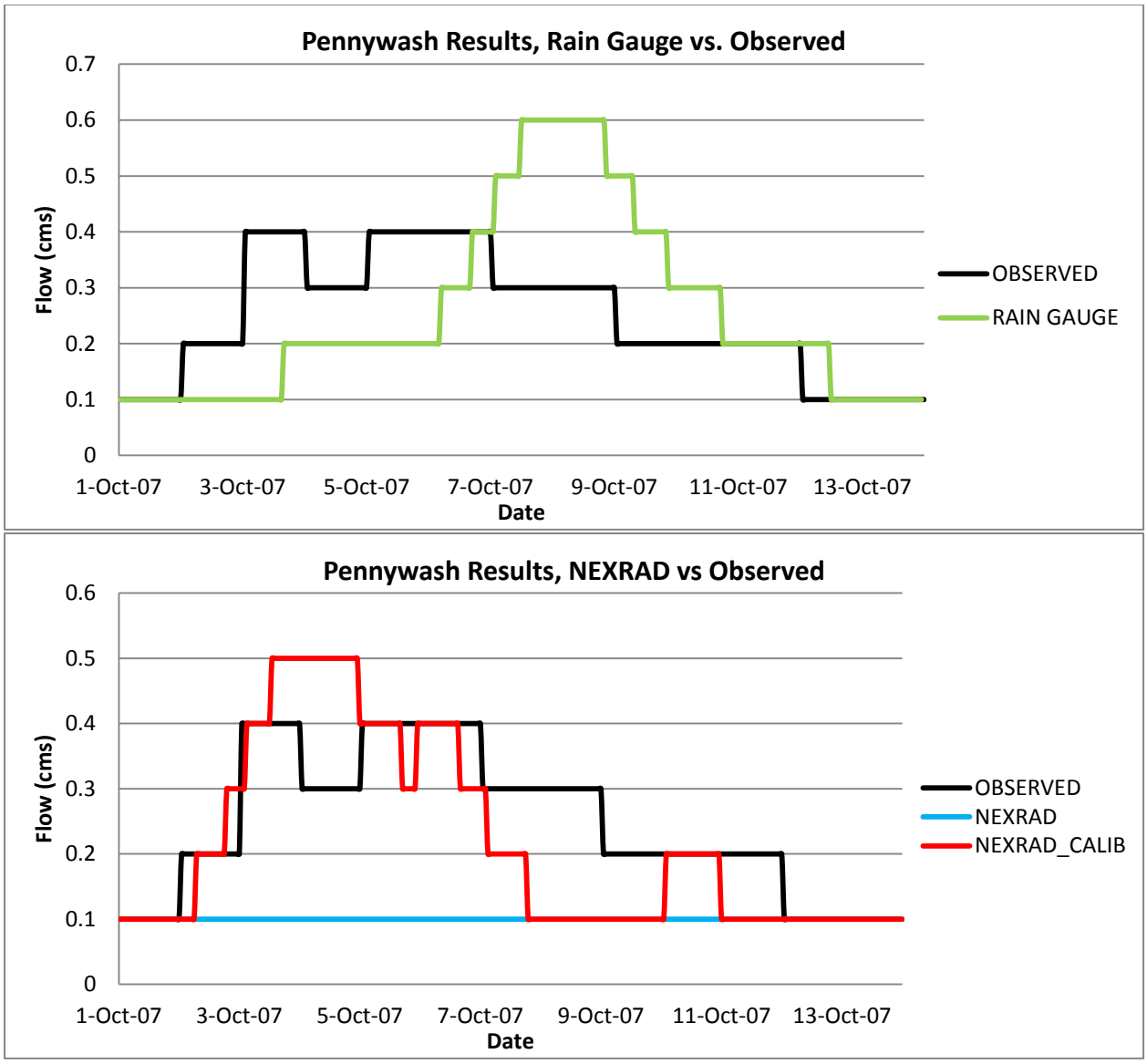

Figures 7a and 7b – Pennywash Creek 2007 Validation Results USGS Gauge 02232155

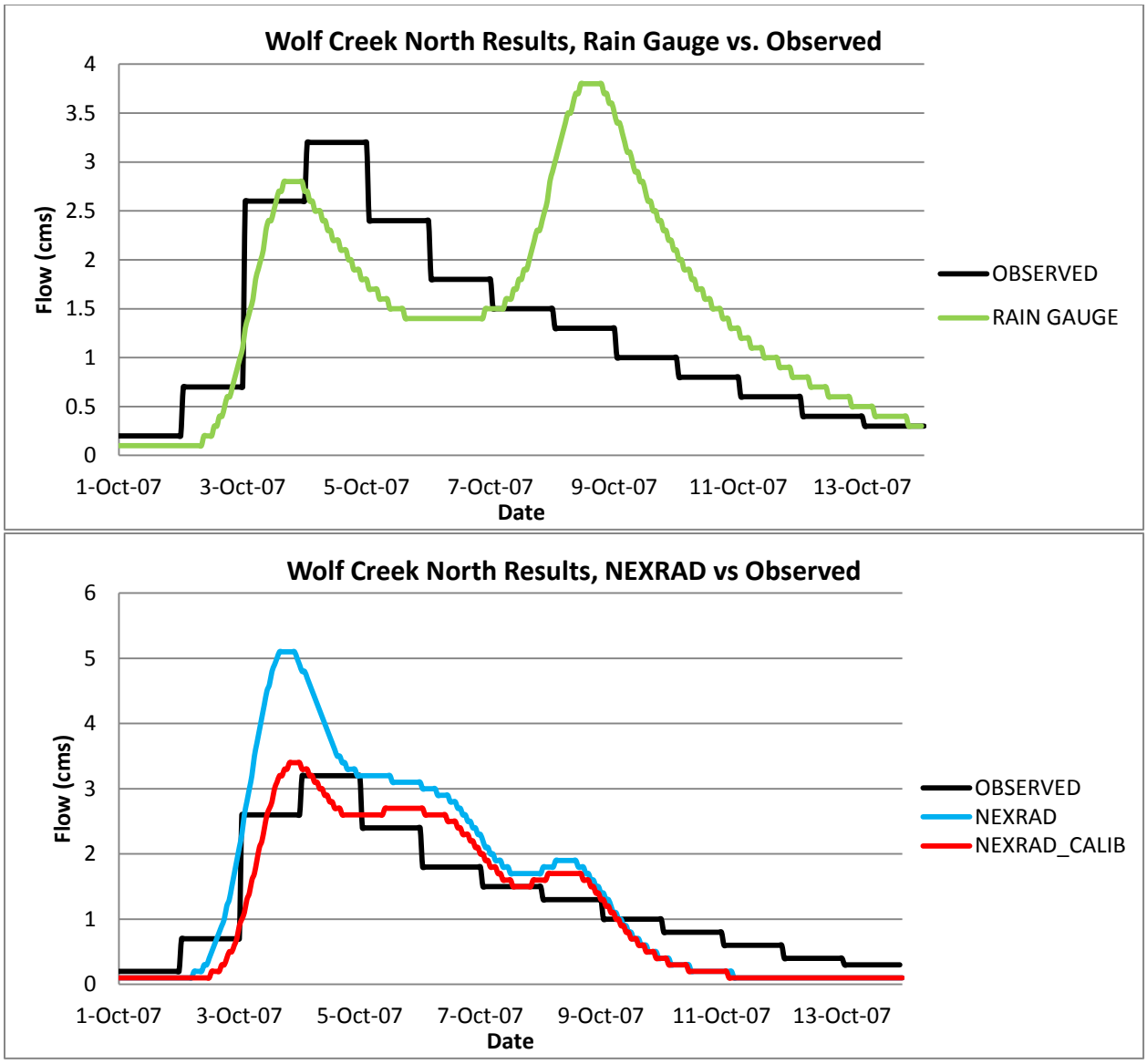

Figures 8a and 8b – Wolf Creek North 2007 Validation Results USGS Gauge 02232200

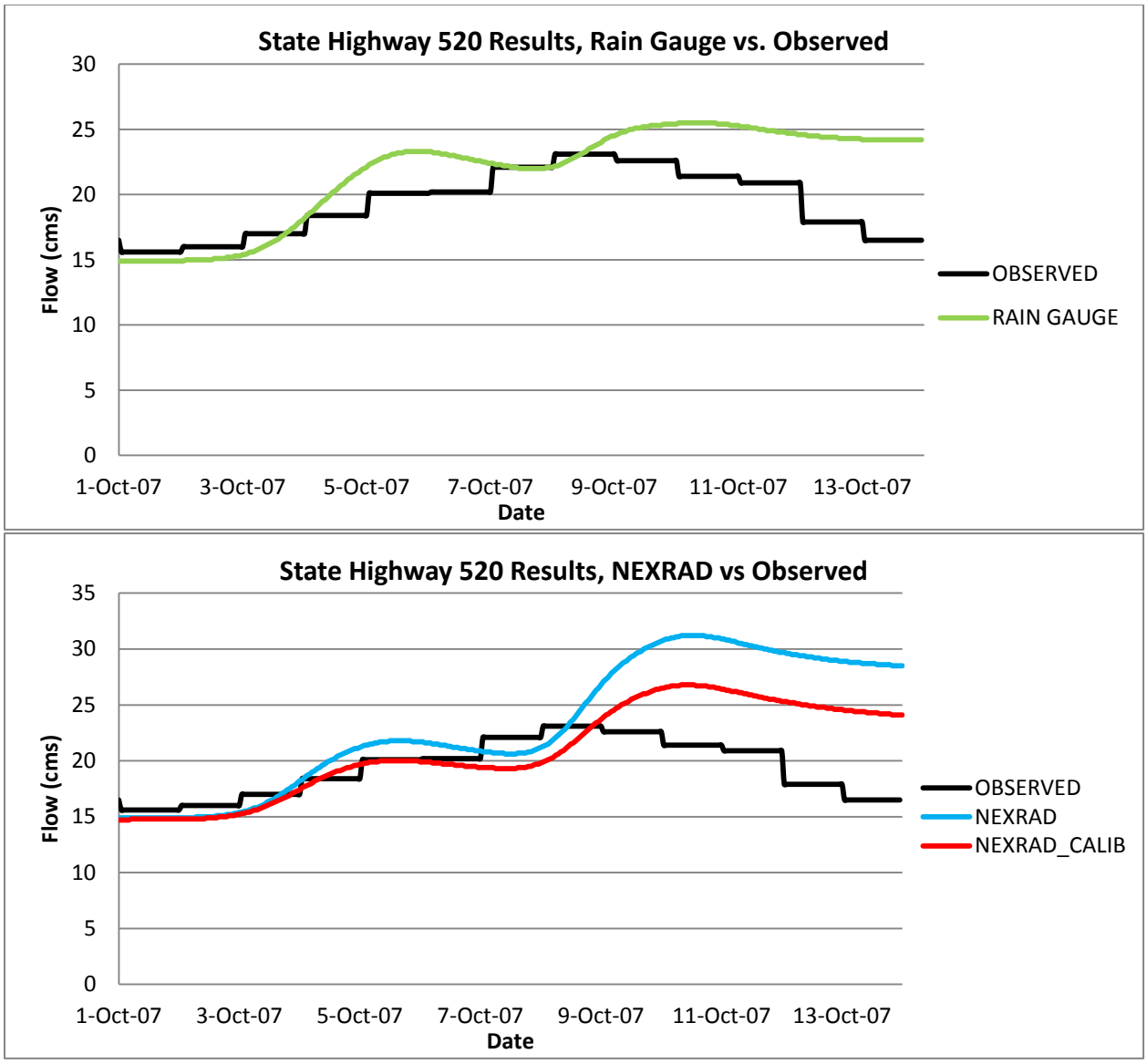

Figures 9a and 9b – St. Johns River at State Highway 520 2007 Validation Results USGS Gauge 02232400

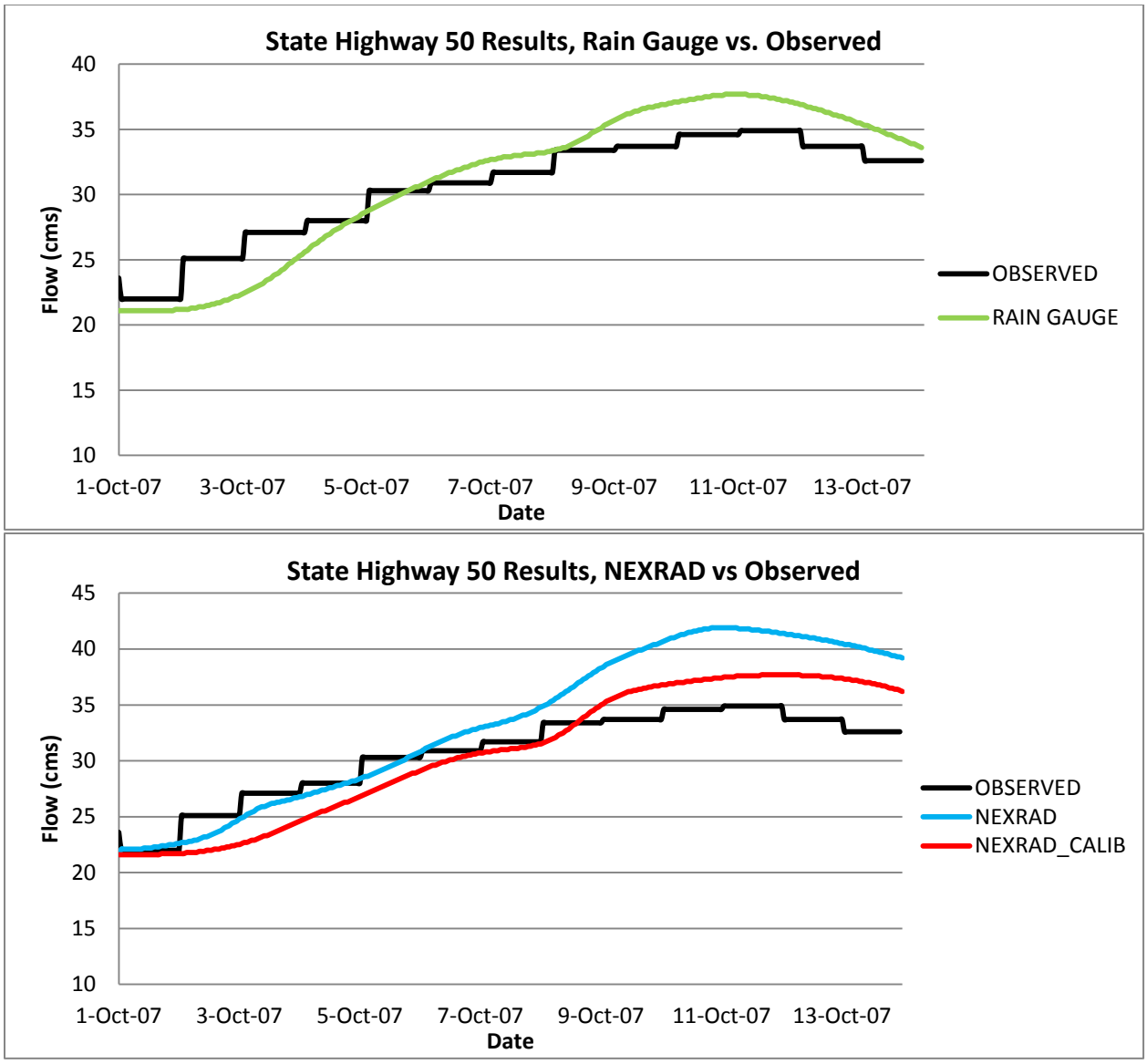

Figures 10a and 10b - St. Johns River at State Highway 50 2007 Validation Results USGS Gauge 02232500

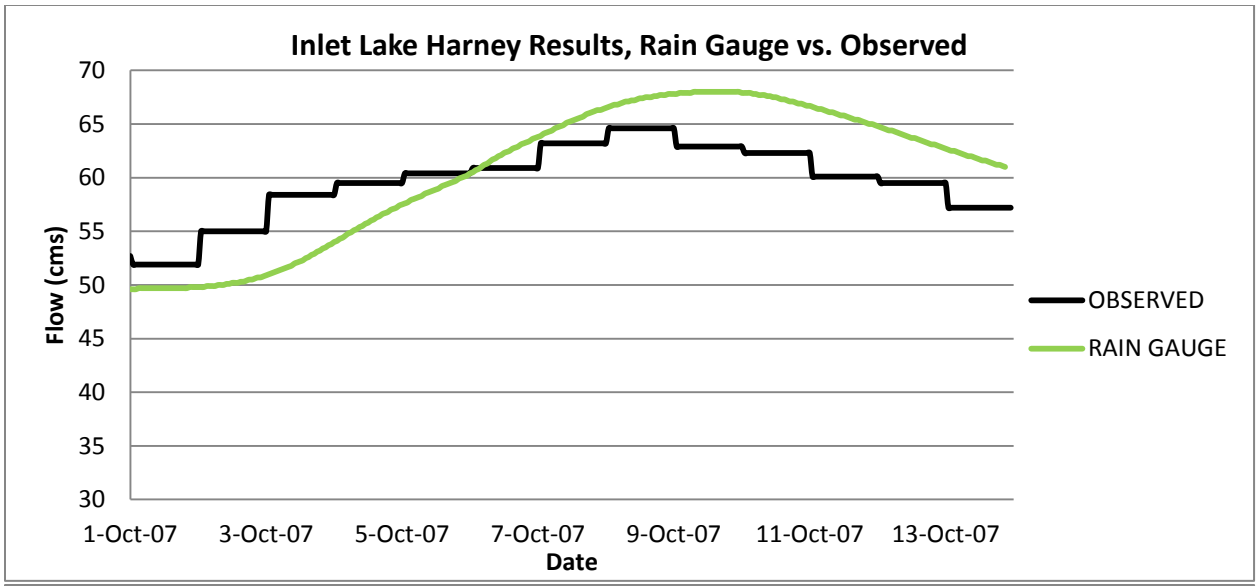

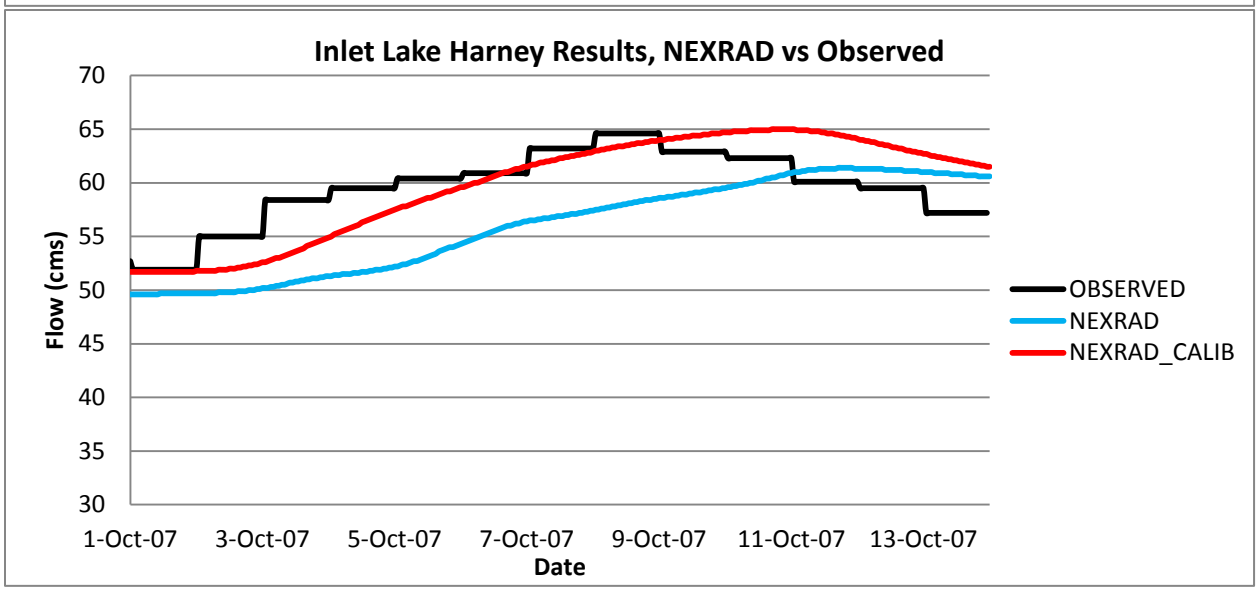

Figures 11a and 11b - St. Johns River at Inlet of Lake Harney 2007 Validation Results USGS Gauge 02234000

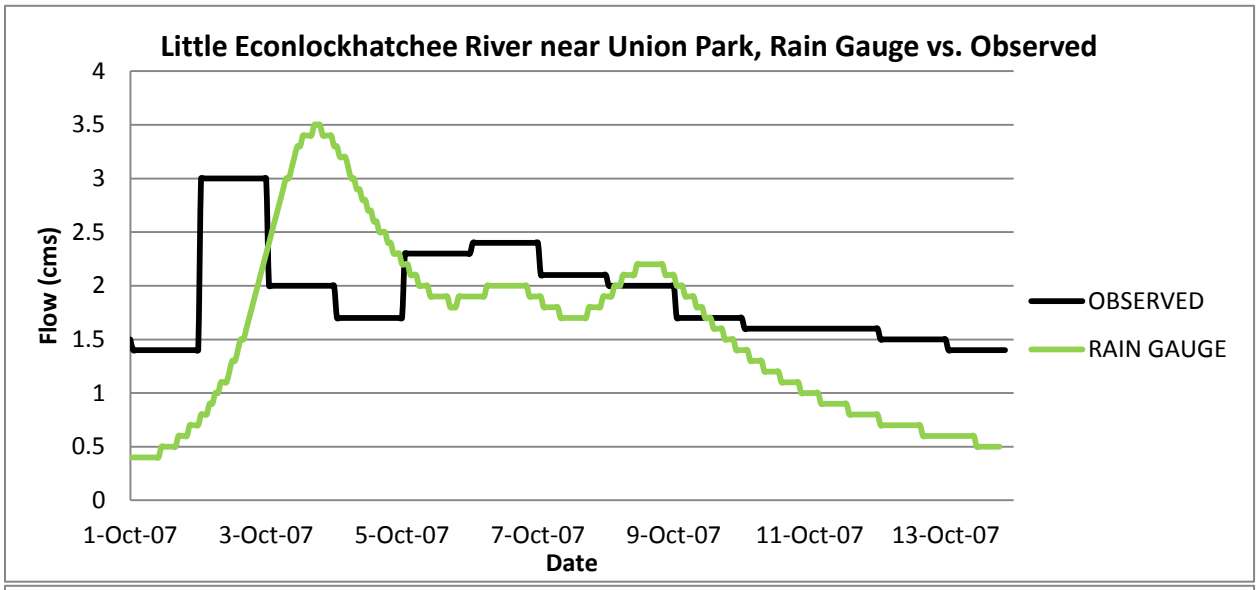

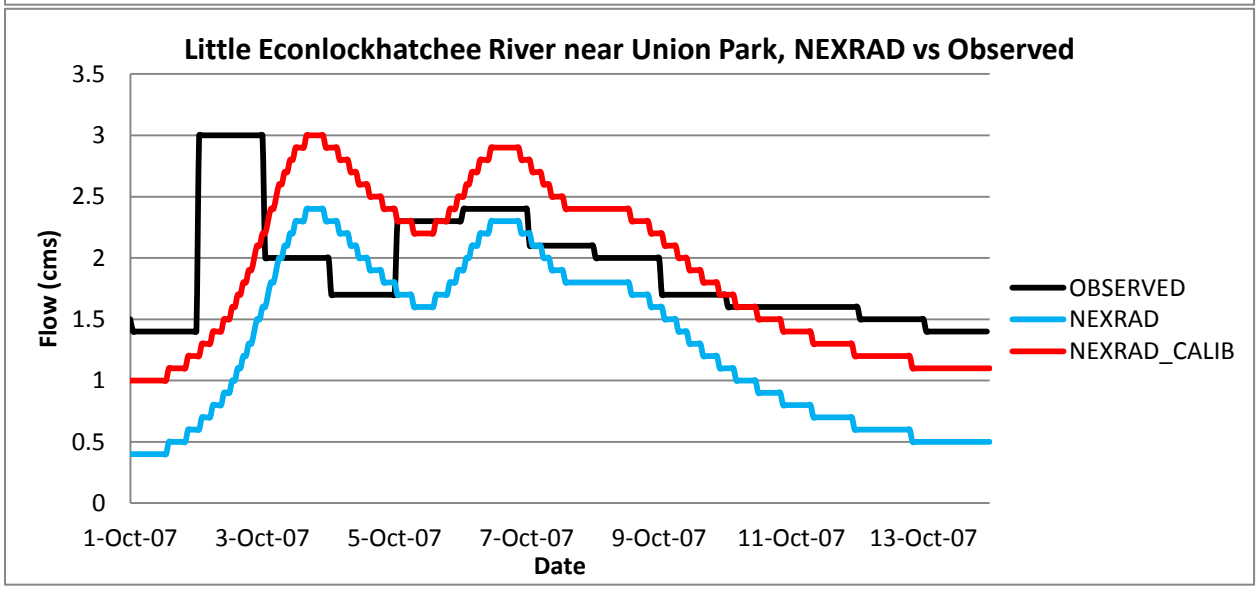

Figures 12a and 12b - Little Econlockhatchee River near Union Park 2007 Validation Results
USGS Gauge 02233460

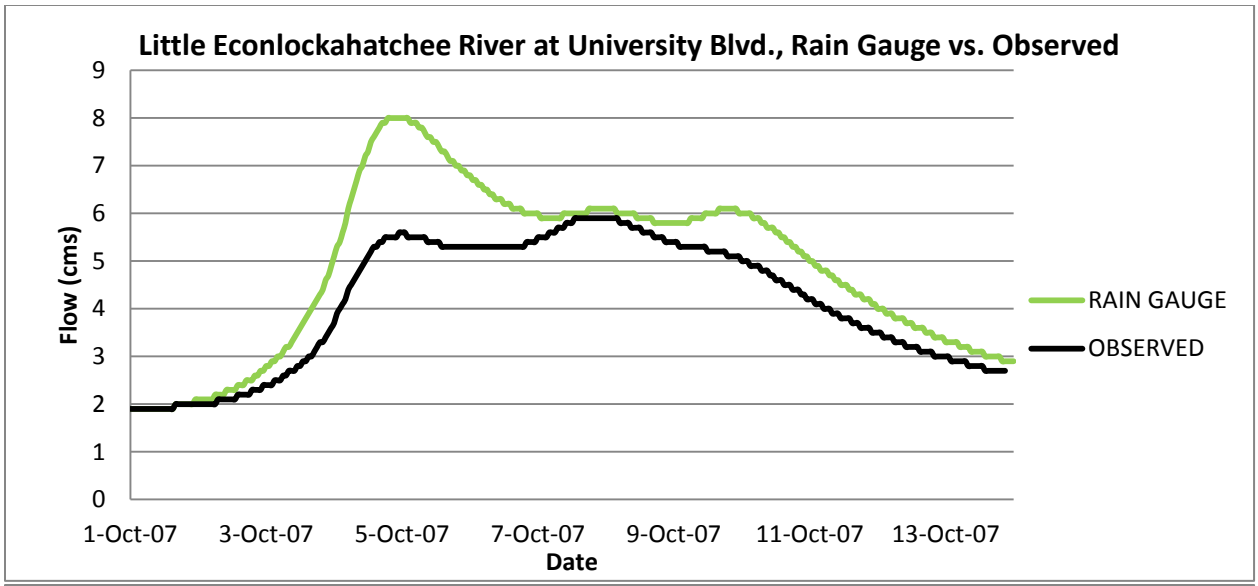

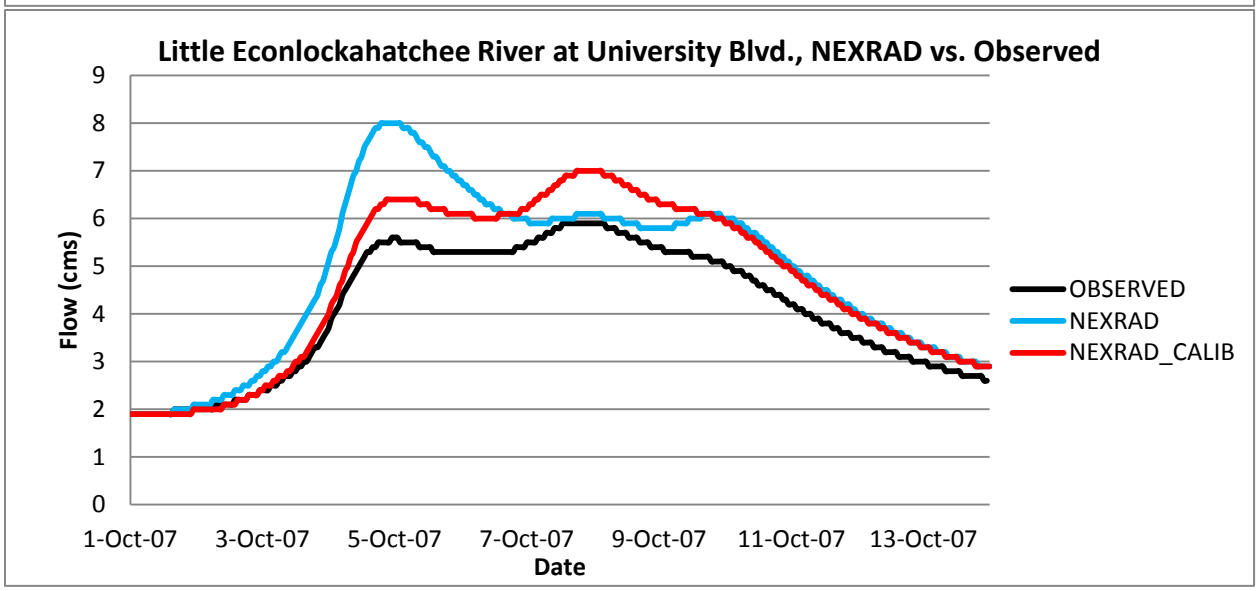

Figures 13a and 13b - Little Econlockhatchee River at University Blvd. 2007 Validation Results
USGS Gauge 02233473

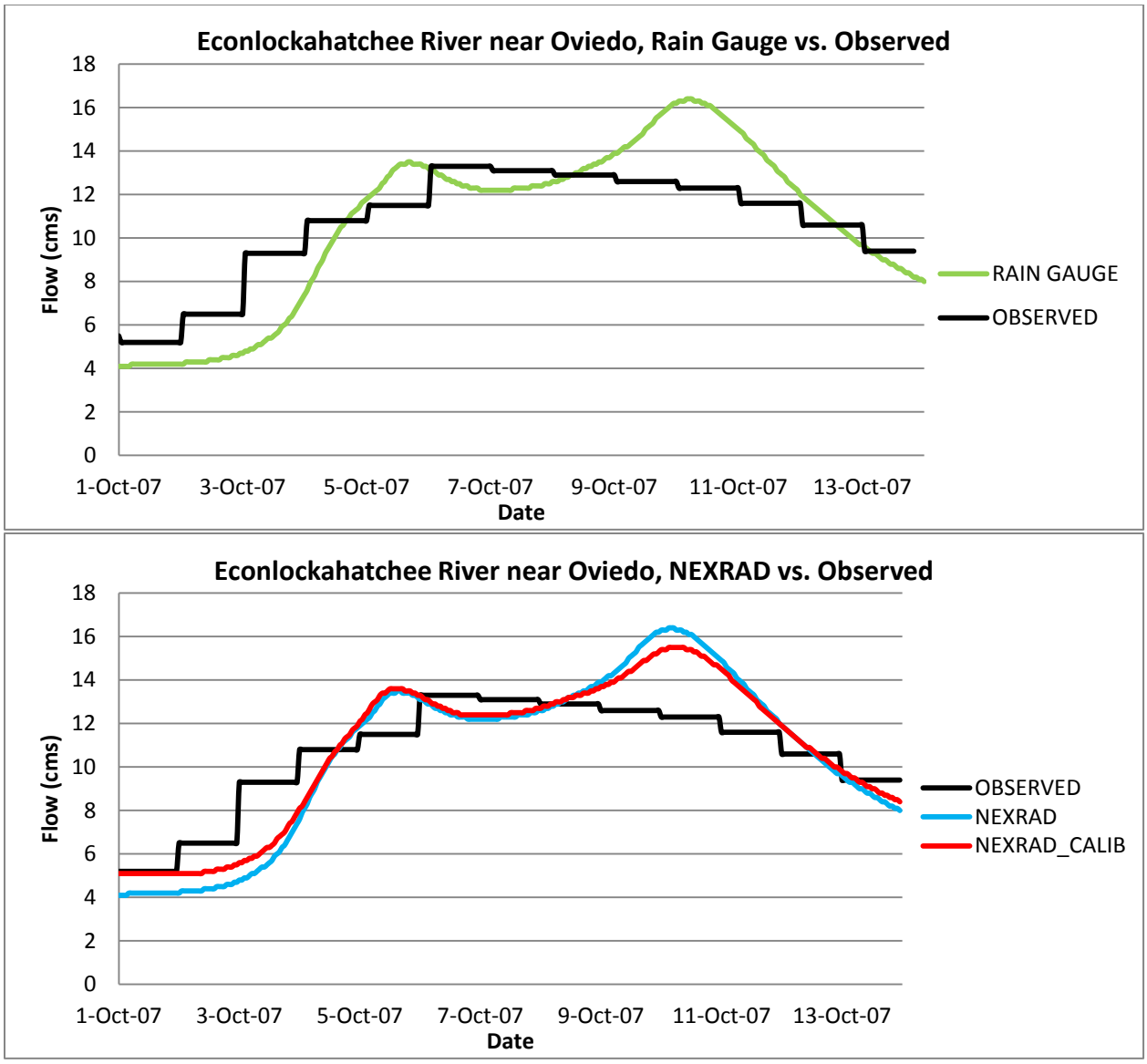

Figures 14a and 14b - Econlockhatchee River near Oviedo 2007 Validation Results USGS Gauge 02233484

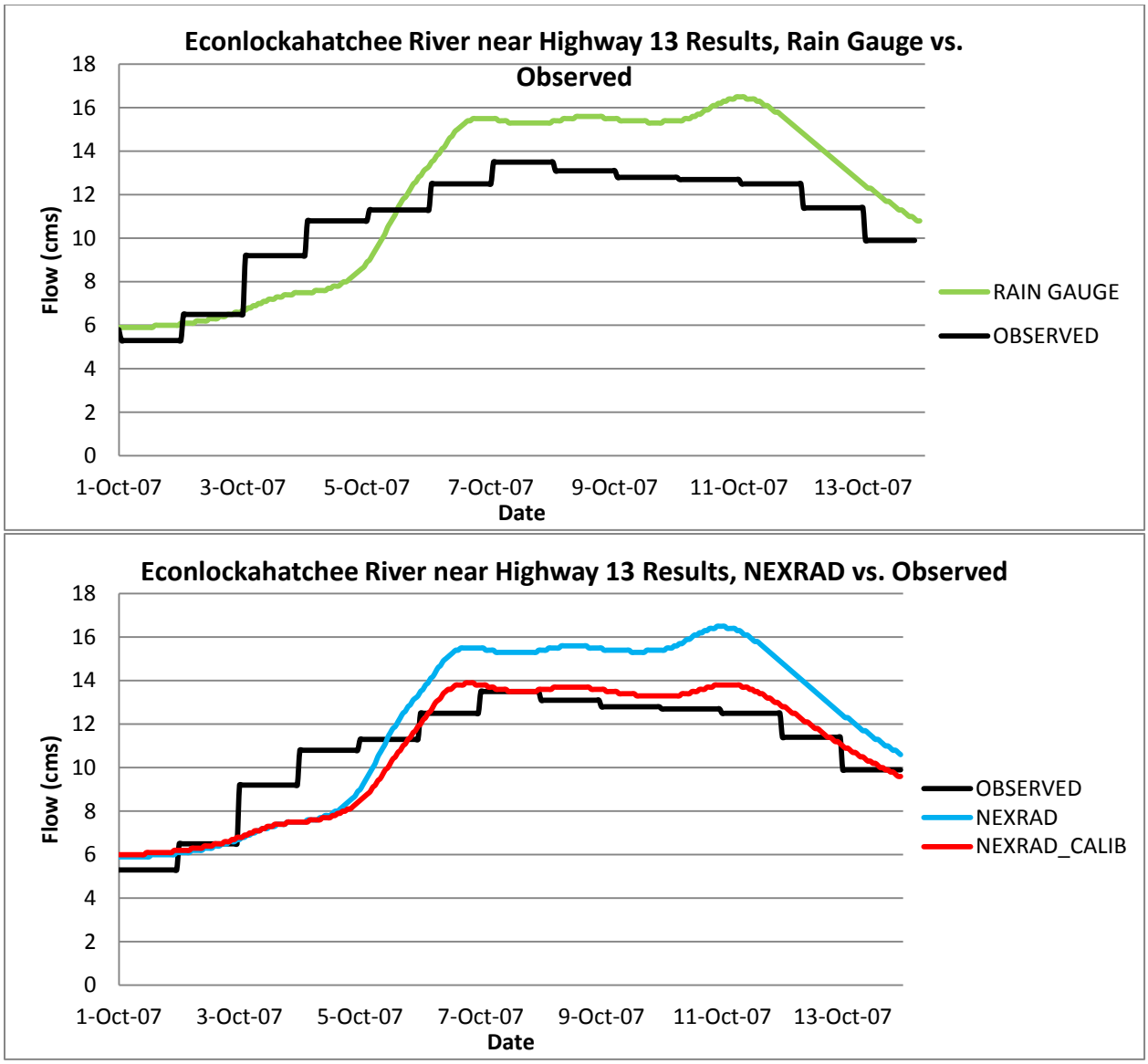

Figures 15a and 15b - Econlockhatchee River near State Highway 13 2007 Validation Results
USGS Gauge 02233500

APPENDIX C

March 2010 Validation Model Results

Subbasin	I. A. (mm)	C. N.	Lag Time (min.)	Subbasin	I. A. (mm)	C. N.	Lag Time (min.)
Barney Green	42	72	1560	Lake Poinsett Rainfall North	18	83	3300
Barry Groves	24	81	2646	Lake Poinsett Rainfall South	37	74	3450
BC East Rainfall	14	88	3351	Lake Price Outlet	47	68	1000
BCMCA Rainfall	27	79	7500	Lake Proctor	81	51	550
BC West Rainfall	23	82	1700	Lake Wash 1 Rainfall	13	89	4500
Bird Lake Combined	30	78	1800	Lake Wash 2 Rainfall	13	89	3850
Bird Lake Ditches	31	78	1200	Lake Wash 3 Rainfall	13	89	2900
Bithlo Branch	26	80	650	Lake Wilson Outlet	27	79	2361
Blue Cypress Creek	35	60	3500	Lake Winder Rainfall	25	86	5800
Broadmoor Marsh	32	76	1370	Little Creek	38	72	2000
Bull Creek	36	75	1300	Little Econlock River	51	66	2000
Buscombe Creek	15	87	1000	Little Econlock Tributary	43	70	2100
C25 Ext	43	71	2130	Long Branch	23	75	650
C54 Retention Area	10	92	1163	Mary A Groves	15	87	715
Cabbage Slough	31	76	2300	Mary A Groves Res Rain	29	79	500
Caine Farms	18	85	1250	Mary A Groves Restoration	6	95	574
Christmas Creek	14	89	1500	Mary A Rainfall	37	74	1400
Clark Lake Outlet	30	78	3100	Mills Creek	27	80	1550
Cocoa Canals	21	84	2500	Mitchell Creek	15	88	1285
Cowpen Branch	28	79	750	Moccasin Isl 1	40	73	7600
Cox Creek Lower	30	71	1400	Moccasin Isl 2	17	86	3000
Cox Creek Res Rainfall	31	73	990	Moccasin Isl 3	21	83	2500
Cox Creek upper	25	78	1800	Moccasin Isl 4	26	80	2000
Crane Strand Drain	55	68	1500	Moccasin Isl 5	35	75	1800
Cross Triangle	32	77	1900	Moccasin Isl 6	47	69	3300
Delespine Grant	34	76	1400	Padgett Branch	28	79	2405
Delta Farms	64	63	1240	Pennywash Creek	15	65	1350
Delta Farms Res Rain	20	84	735	Pressley Ranch	40	73	1282
Deseret 1	10	91	720	Pressley Ranch South	33	76	869
Deseret 2	21	84	662	Rdd Primary Canal	33	76	1650
Deseret East	24	81	1525	Roberts Branch	30	77	1600
Deseret Farms	40	73	2240	Rockledge	50	68	2129

Figure 1 - Calibration Parameters for March 2010 Simulation Event with Rain Gauge and NEXRAD (not re-calibrated) Input

Subbasin	I. A. (mm)	C. N.	Lag Time (min.)	Subbasin	I. A. (mm)	C. N.	Lag Time (min.)
Deseret Farms South	41	72	1400	Rollins Ranch	40	73	955
Econlock 1	35	73	1600	Rollins South A	41	72	1143
Econlock 2	50	60	1600	Rollins South B	40	73	1143
Econlock 3	53	65	2500	Rollins South C	40	73	1143
Econlock 4	44	70	2150	Sartori East	40	73	1459
Econlock 5	50	67	1700	Sartori Farms	16	87	1797
Econlock River Swamp	56	64	3000	Savage Creek	16	87	1000
Econlock River Trib 1	36	74	1000	Second Creek	27	80	1700
Econlock River Trib 2	36	74	1000	Sixmile Creek	26	80	2000
Evans Grove	31	77	1190	Sixmile Restoration Area	35	75	1131
FDMCA Rainfall	27	79	2770	Sixmile Tributary	26	80	745
FF PS1	36	75	1970	SJR Cone	20	84	2100
FF PS2	36	75	1720	SJR Harney	12	89	1650
FF PS3	18	85	1265	SJR Puzzle	12	92	2500
FF PS4	34	76	1525	SJR State Road 46	29	79	1300
FF PS5	15	87	875	SJR State Road 50	25	84	3300
FF PS6	38	74	1751	SJWMA Rainfall	40	73	1681
FF PS7	33	76	1593	SN Knight (Kenansville)	16	86	130
Fort Drum Creek	45	75	2400	South Lake Outlet	35	75	1200
Fourmile Creek	45	74	3000	St Johns Imp Dis	37	74	7054
Goupher Slough	19	85	2074	St Johns Imp Dis Res Rain	37	74	1516
Green Branch	32	76	650	St Johns Trib 1&2	21	83	2500
JG Bull Creek	35	72	3000	St Johns Trib 3	17	86	850
JG Crabgrass Creek	30	64	3500	St Johns Trib 7	22	82	1200
JG Creek	39	73	2984	St Johns Trib 9	38	74	3500
JG Tributary	37	74	2563	Taylor Creek	25	82	1600
Jim Creek	32	77	2700	Taylor Creek Res Rainfall	41	72	2511
Jim Creek North	41	72	1800	Tenmile Creek	41	72	2272
Jim Green Creek	33	76	2125	Tootoosahatchee Creek	38	74	1500
Joshua Creek	19	84	2200	Tucker Rainfall	34	76	669
King Street	36	75	2200	Turkey Creek	38	73	1150
Knight Creek	13	89	1483	Underhill Slough	17	86	836
Lake Berge Outlet	44	70	1000	Union Park Canal	55	69	1600
Lake Hell n Blazes	41	72	1200	Wolf Creek	68	64	1400
Lake Irma Outlet	60	68	1200	Wolf Creek North	15	76	1500

Figure 1a - Calibration Parameters for March 2010 Simulation Event with Rain Gauge and NEXRAD (not re-calibrated) Input

Subbasin	I. A. (mm)	C. N.	Lag Time (min.)	Subbasin	I. A. (mm)	C. N.	Lag Time (min.)
Barney Green	42	72	1560	Lake Poinsett Rainfall North	18	83	3300
Barry Groves	24	81	2646	Lake Poinsett Rainfall South	32	74	3450
BC East Rainfall	14	88	3351	Lake Price Outlet	47	68	1000
BCMCA Rainfall	27	79	7500	Lake Proctor	81	51	550
BC West Rainfall	23	82	1700	Lake Wash 1 Rainfall	13	87	5900
Bird Lake Combined	30	78	1800	Lake Wash 2 Rainfall	13	87	3850
Bird Lake Ditches	35	78	1200	Lake Wash 3 Rainfall	13	87	3900
Bithlo Branch	26	80	650	Lake Wilson Outlet	27	79	2361
Blue Cypress Creek	46	60	3500	Lake Winder Rainfall	15	83	5800
Broadmoor Marsh	32	76	1370	Little Creek	38	72	2000
Bull Creek	36	75	1300	Little Econlock River	56	66	2000
Buscombe Creek	15	87	1000	Little Econlock Tributary	48	70	2100
C25 Ext	43	71	2130	Long Branch	28	75	650
C54 Retention Area	10	92	1163	Mary A Groves	15	87	715
Cabbage Slough	31	76	2300	Mary A Groves Res Rain	29	79	500
Caine Farms	18	85	1250	Mary A Groves Restoration	6	95	574
Christmas Creek	14	89	1500	Mary A Rainfall	37	74	1400
Clark Lake Outlet	30	78	3100	Mills Creek	27	80	1550
Cocoa Canals	21	84	2500	Mitchell Creek	15	88	1285
Cowpen Branch	33	79	750	Moccasin Isl 1	40	73	7600
Cox Creek Lower	30	71	1400	Moccasin Isl 2	17	86	3000
Cox Creek Res Rainfall	31	73	990	Moccasin Isl 3	21	83	2500
Cox Creek upper	25	78	1800	Moccasin Isl 4	26	80	2000
Crane Strand Drain	60	68	1500	Moccasin Isl 5	35	75	1800
Cross Triangle	32	77	1900	Moccasin Isl 6	47	69	3300
Delespine Grant	34	76	1400	Padgett Branch	28	79	2405
Delta Farms	64	63	1240	Pennywash Creek	33	65	1350
Delta Farms Res Rain	20	84	735	Pressley Ranch	40	73	1282
Deseret 1	10	91	720	Pressley Ranch South	33	76	869
Deseret 2	21	84	662	Rdd Primary Canal	33	76	1650
Deseret East	24	81	1525	Roberts Branch	30	77	1600
Deseret Farms	40	73	2240	Rockledge	50	68	2129

Figure 2- Re-Calibration Parameters for March 2010 Simulation Event with NEXRAD Input

Subbasin	I. A. (mm)	C. N.	Lag Time (min.)	Subbasin	I. A. (mm)	C. N.	Lag Time (min.)
Deseret Farms South	41	72	1400	Rollins Ranch	40	73	955
Econlock 1	35	73	1600	Rollins South A	41	72	1143
Econlock 2	50	70	1600	Rollins South B	40	73	1143
Econlock 3	53	65	2500	Rollins South C	40	73	1143
Econlock 4	49	70	2150	Sartori East	40	73	1459
Econlock 5	50	67	1700	Sartori Farms	16	87	1797
Econlock River Swamp	56	64	3000	Savage Creek	16	87	1000
Econlock River Trib 1	46	74	1000	Second Creek	25	80	1700
Econlock River Trib 2	46	74	1000	Sixmile Creek	35	80	2000
Evans Grove	31	77	1190	Sixmile Restoration Area	35	75	1131
FDMCA Rainfall	27	79	2770	Sixmile Tributary	26	80	745
FF PS1	36	75	1970	SJR Cone	20	84	2100
FF PS2	36	75	1720	SJR Harney	12	89	1650
FF PS3	18	85	1265	SJR Puzzle	12	92	2500
FF PS4	34	76	1525	SJR State Road 46	29	79	1300
FF PS5	15	87	875	SJR State Road 50	20	84	3300
FF PS6	38	74	1751	SJWMA Rainfall	40	73	1681
FF PS7	33	76	1593	SN Knight (Kenansville)	16	86	130
Fort Drum Creek	45	66	2400	South Lake Outlet	35	75	1200
Fourmile Creek	45	74	3000	St Johns Imp Dis	37	74	7054
Goupher Slough	19	85	2074	St Johns Imp Dis Res Rain	37	74	1516
Green Branch	37	76	650	St Johns Trib 1&2	21	83	2500
JG Bull Creek	35	66	3000	St Johns Trib 3	17	86	850
JG Crabgrass Creek	30	64	3500	St Johns Trib 7	23.5	82	1300
JG Creek	39	73	2984	St Johns Trib 9	38	74	3500
JG Tributary	37	74	2563	Taylor Creek	23	82	1600
Jim Creek	32	77	2700	Taylor Creek Res Rainfall	31	72	2511
Jim Creek North	35	72	1800	Tenmile Creek	41	72	2272
Jim Green Creek	33	76	2125	Tootoosahatchee Creek	38	74	1500
Joshua Creek	19	84	2200	Tucker Rainfall	34	76	669
King Street	36	75	2200	Turkey Creek	38	73	1150
Knight Creek	13	89	1483	Underhill Slough	17	86	836
Lake Berge Outlet	44	70	1000	Union Park Canal	60	69	1600
Lake Hell n Blazes	41	72	1200	Wolf Creek	65	66	1400
Lake Irma Outlet	60	68	1200	Wolf Creek North	35	77	1500

Figure 2a- Re-Calibration Parameters for March 2010 Simulation Event with NEXRAD Input

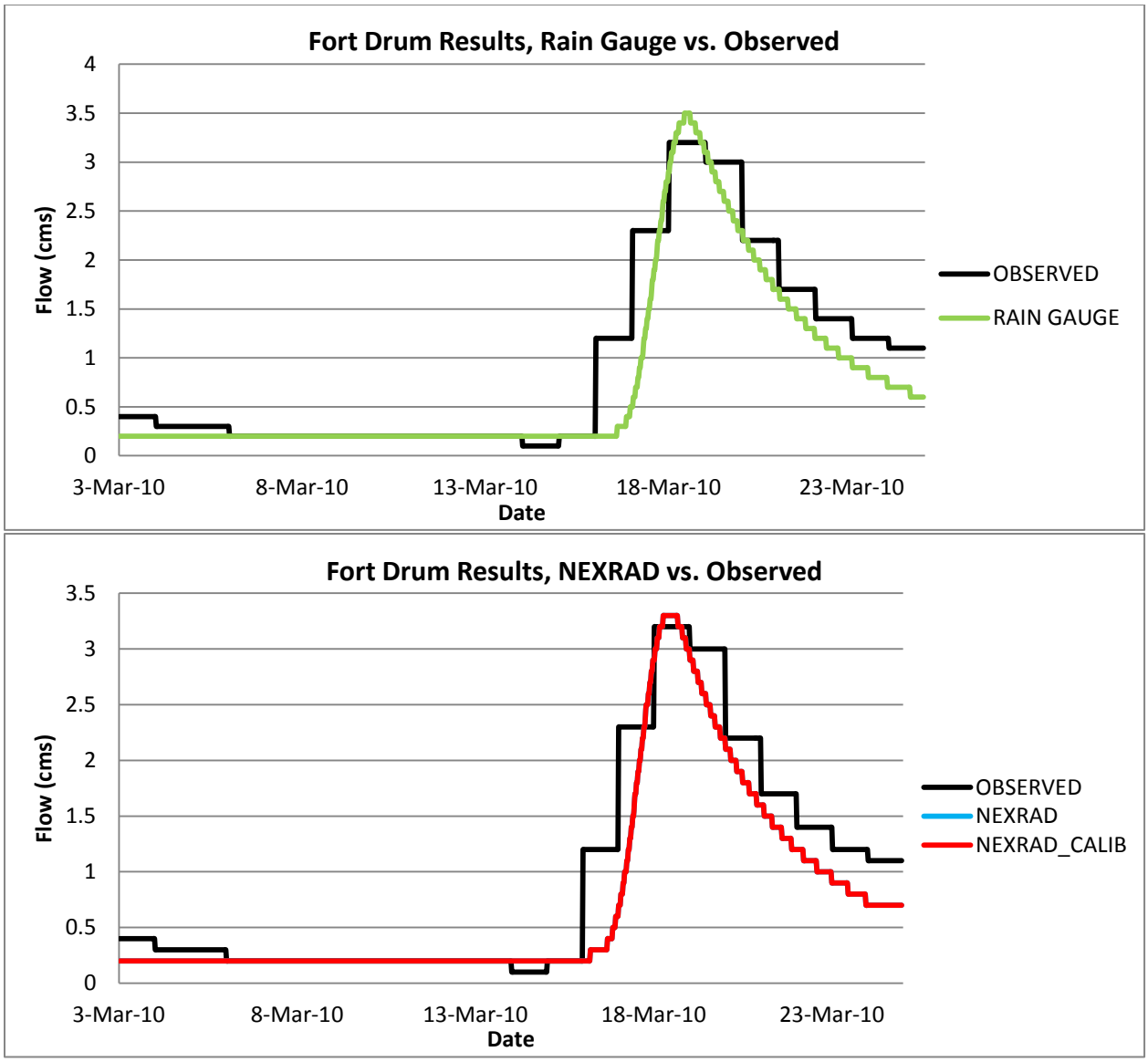

Figures 3a and 3b - Ft. Drum Creek 2010 Validation Results, USGS Gauge 02231342

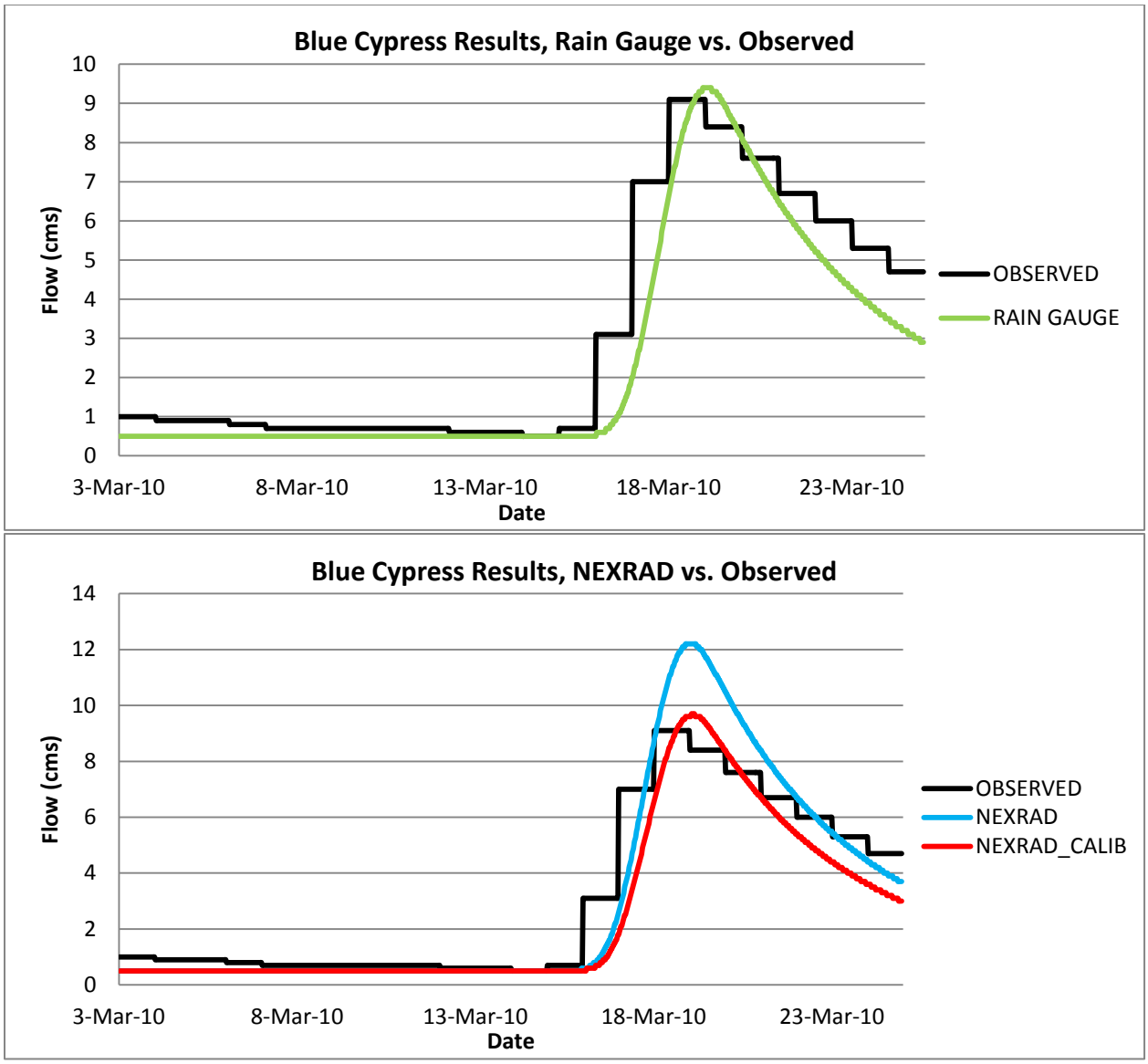

Figures 4a and 4b - Blue Cypress Creek 2010 Validation Results USGS Gauge 02231396

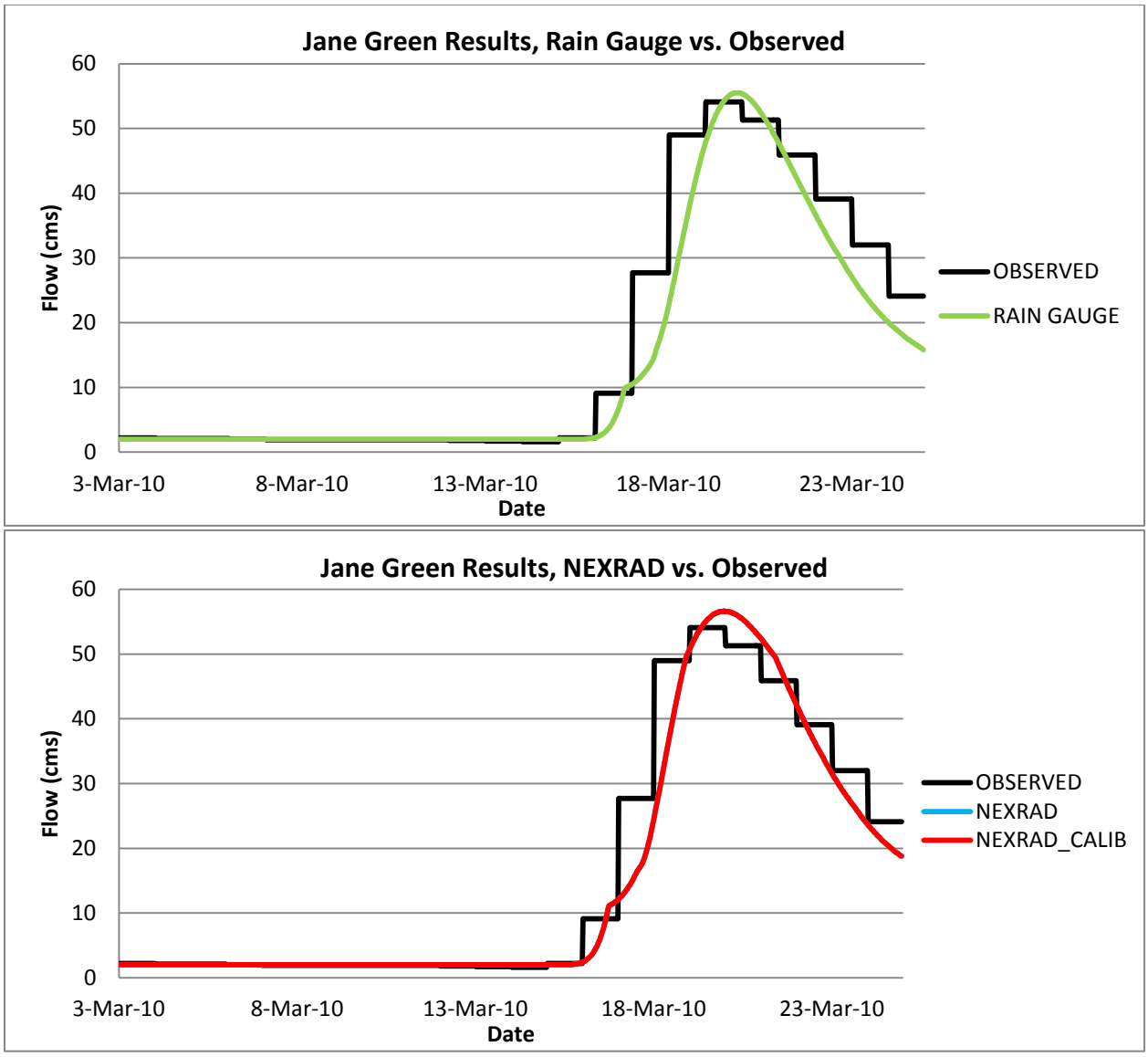

Figures 5a and 5b – Jane Green Reservoir 2010 Validation Results USGS Gauge 02231600

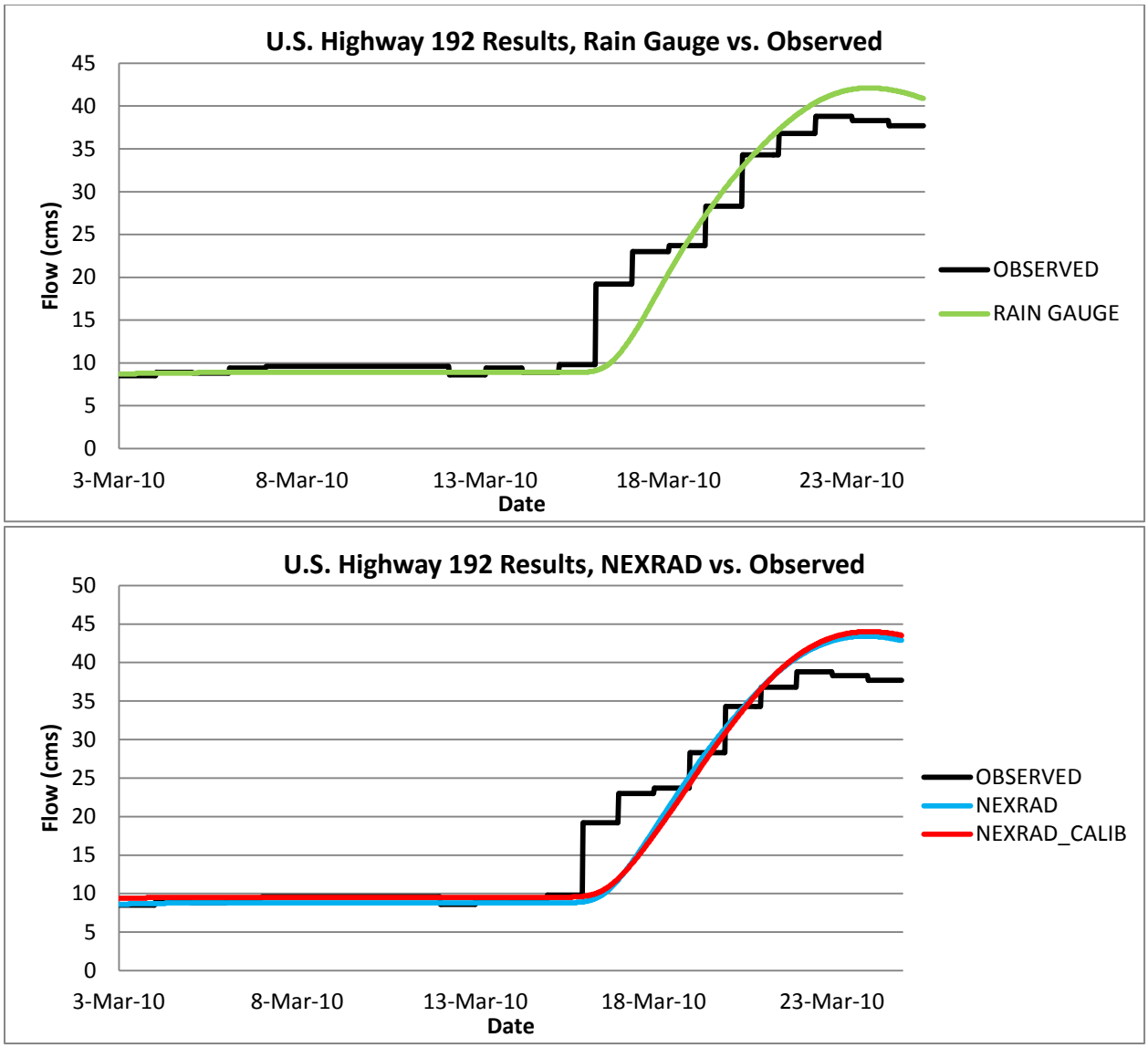

Figures 6a and 6b – St. Johns River at U.S. Highway 192 2010 Validation Results USGS Gauge 02232000

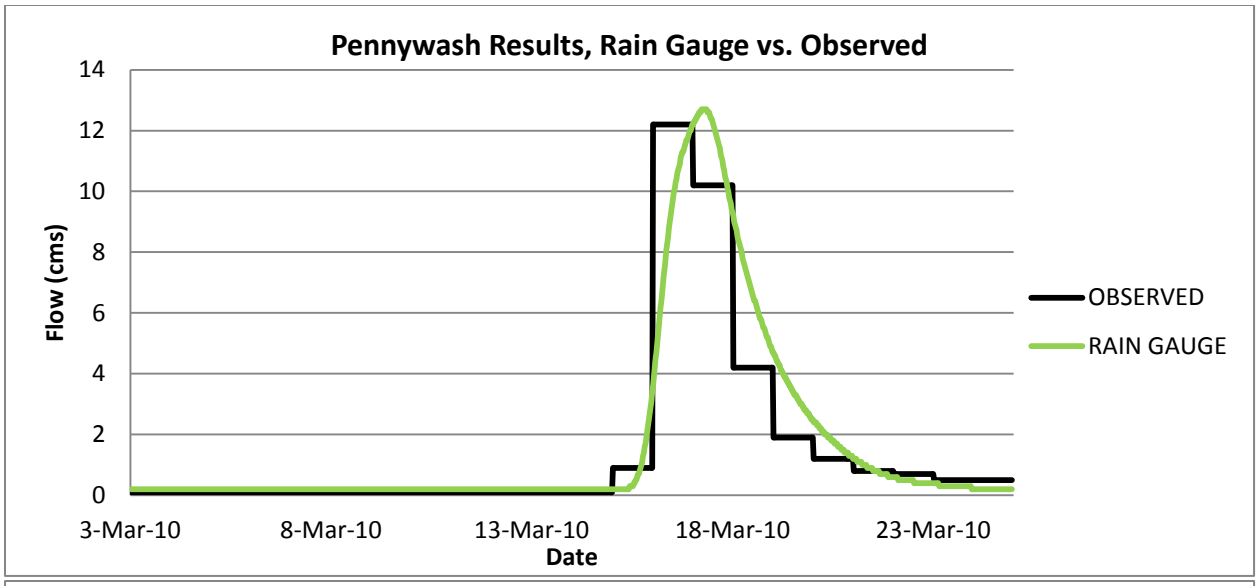

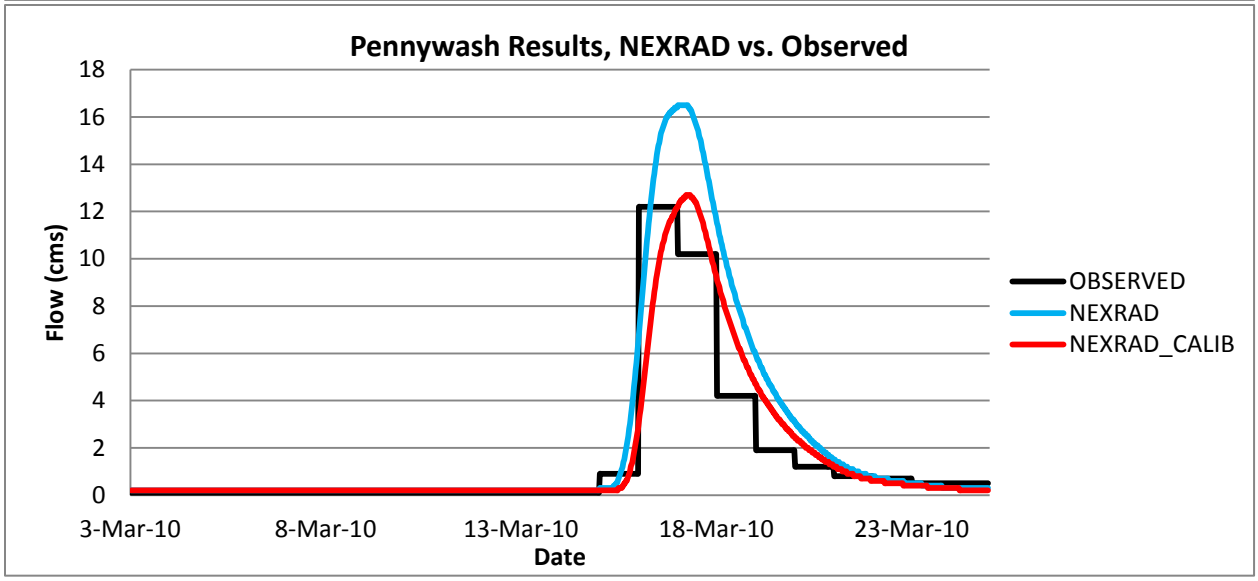

Figures 7a and 7b – Pennywash Creek 2010 Validation Results USGS Gauge 02232155

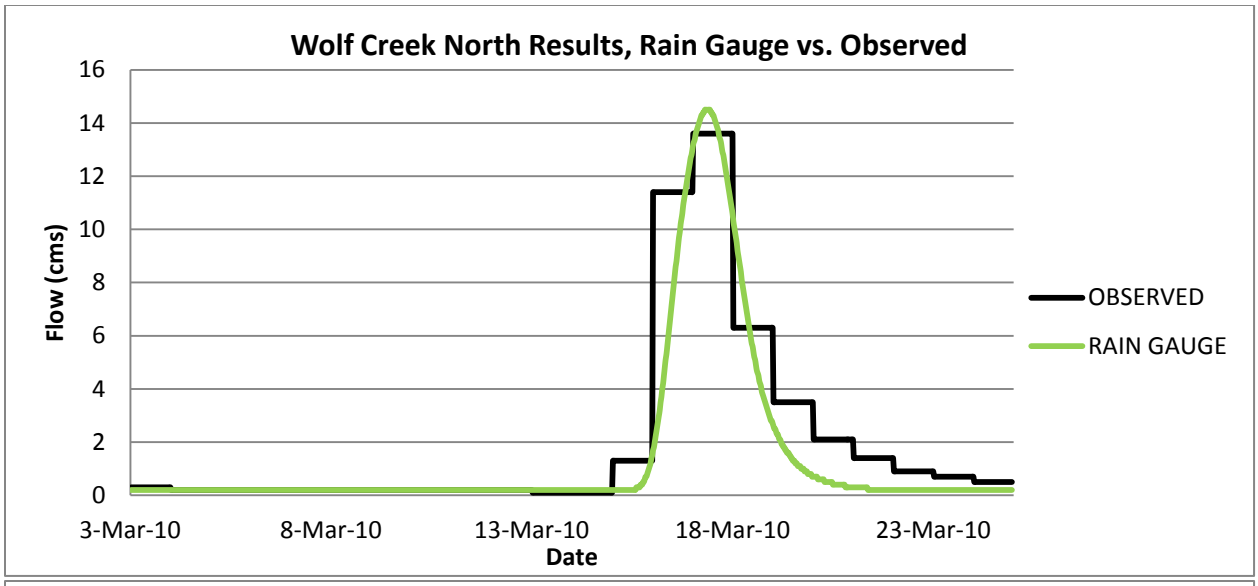

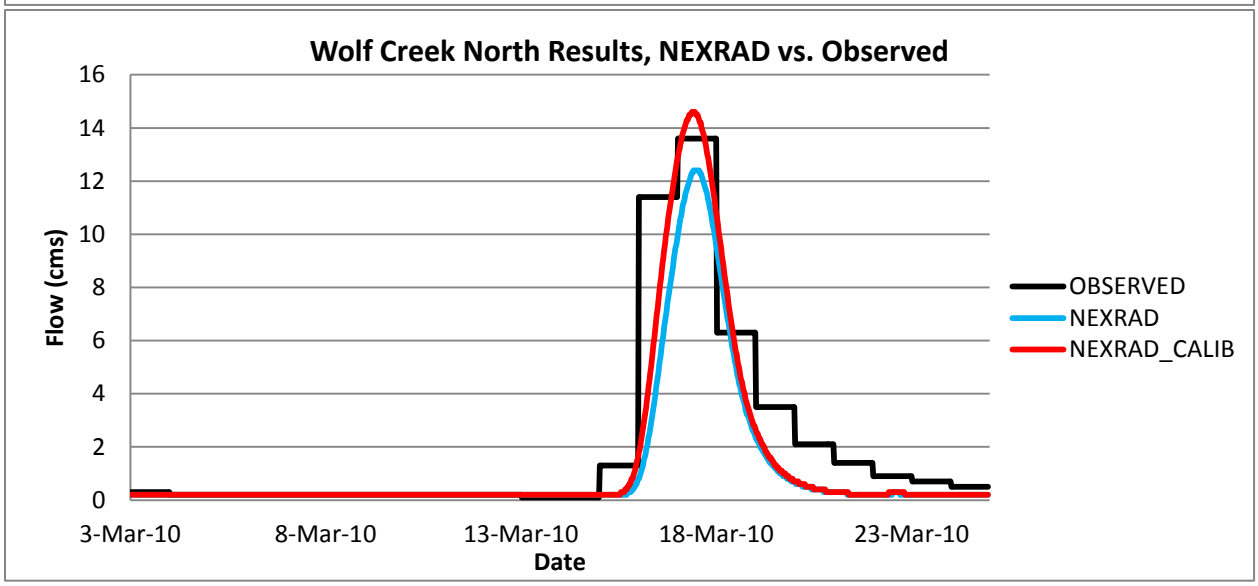

Figures 8a and 8b – Wolf Creek North 2010 Validation Results USGS Gauge 02232200

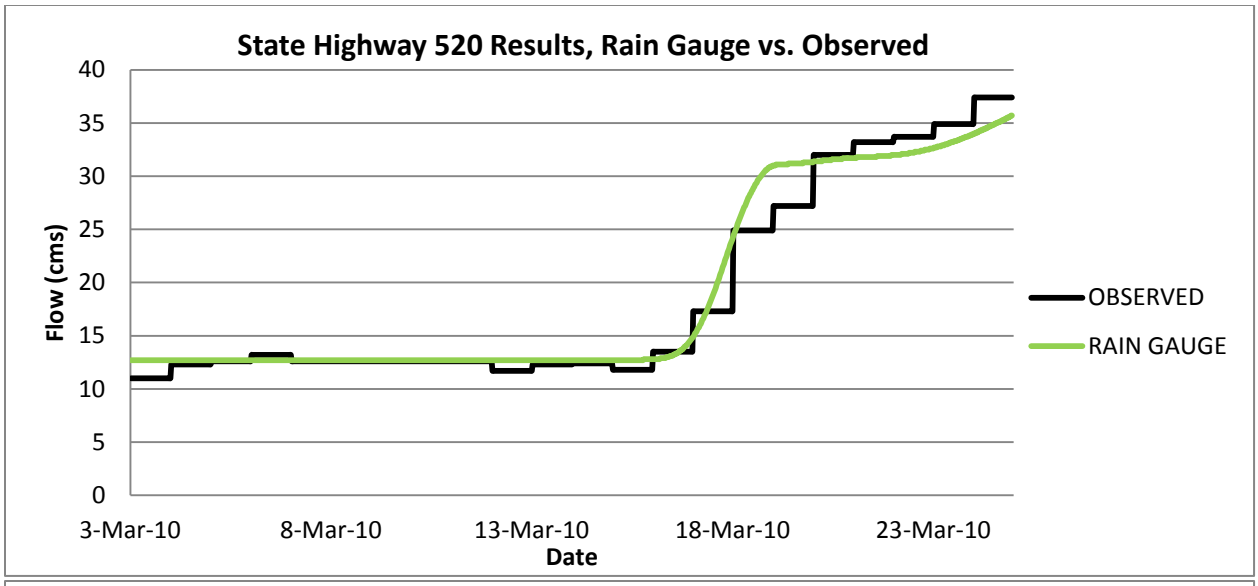

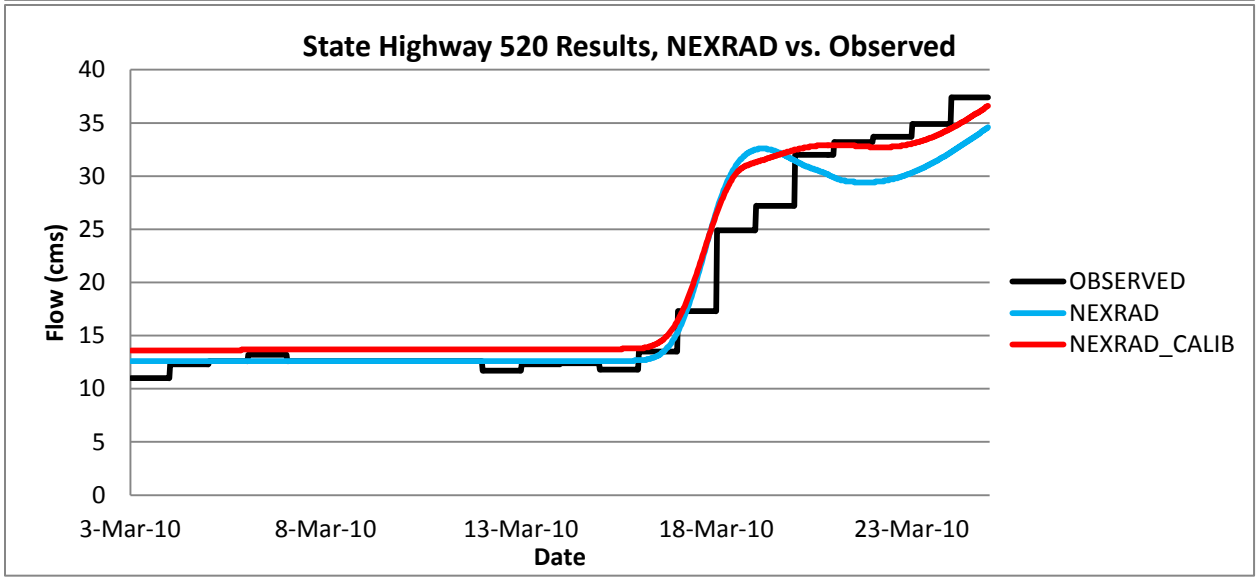

Figures 9a and 9b – St. Johns River at State Highway 520 2010 Validation Results USGS Gauge 02232400

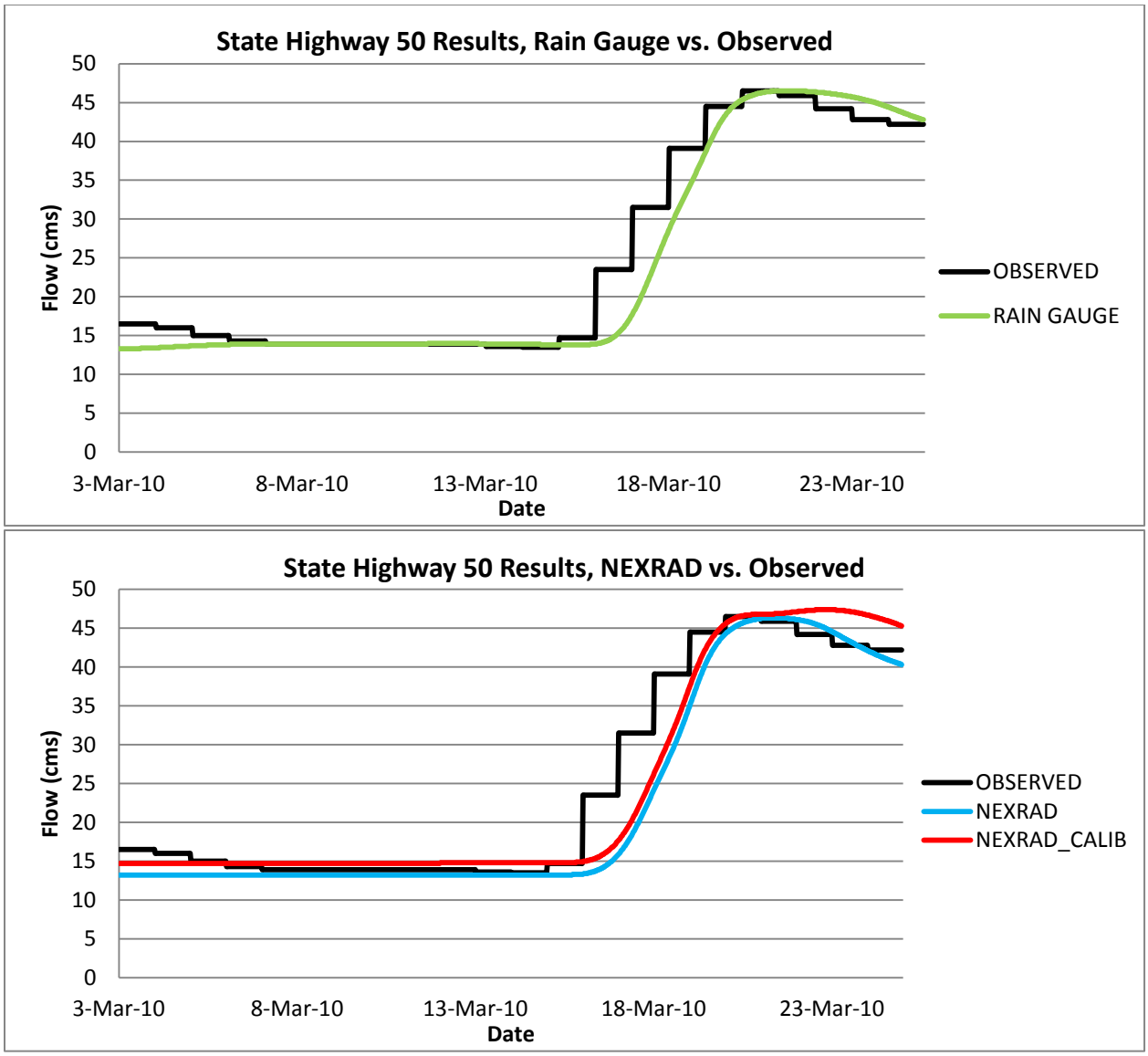

Figures 10a and 10b - St. Johns River at State Highway 50 2010 Validation Results USGS Gauge 02232500

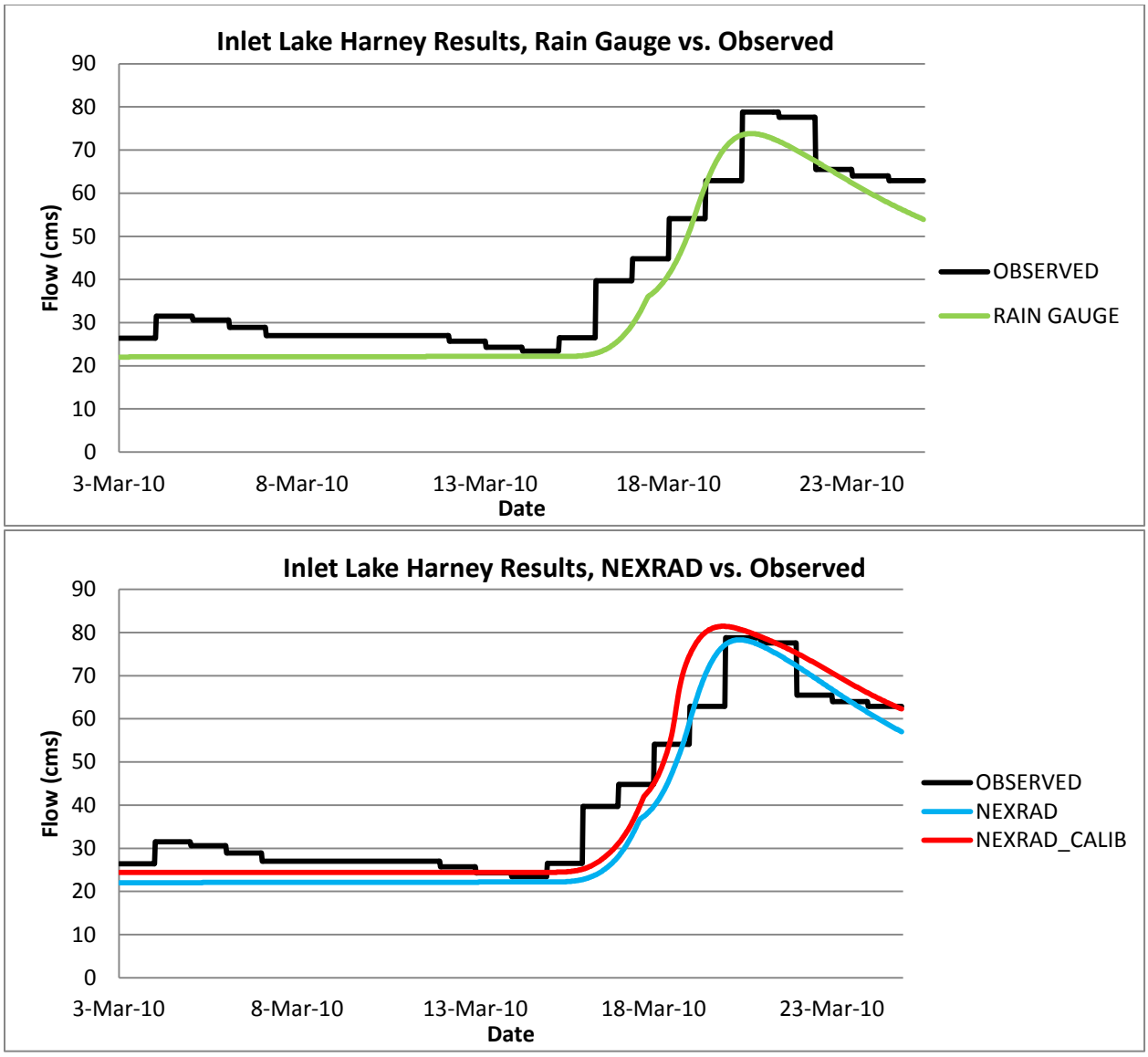

Figures 11a and 11b - St. Johns River at Inlet of Lake Harney 2010 Validation Results USGS Gauge 02234000

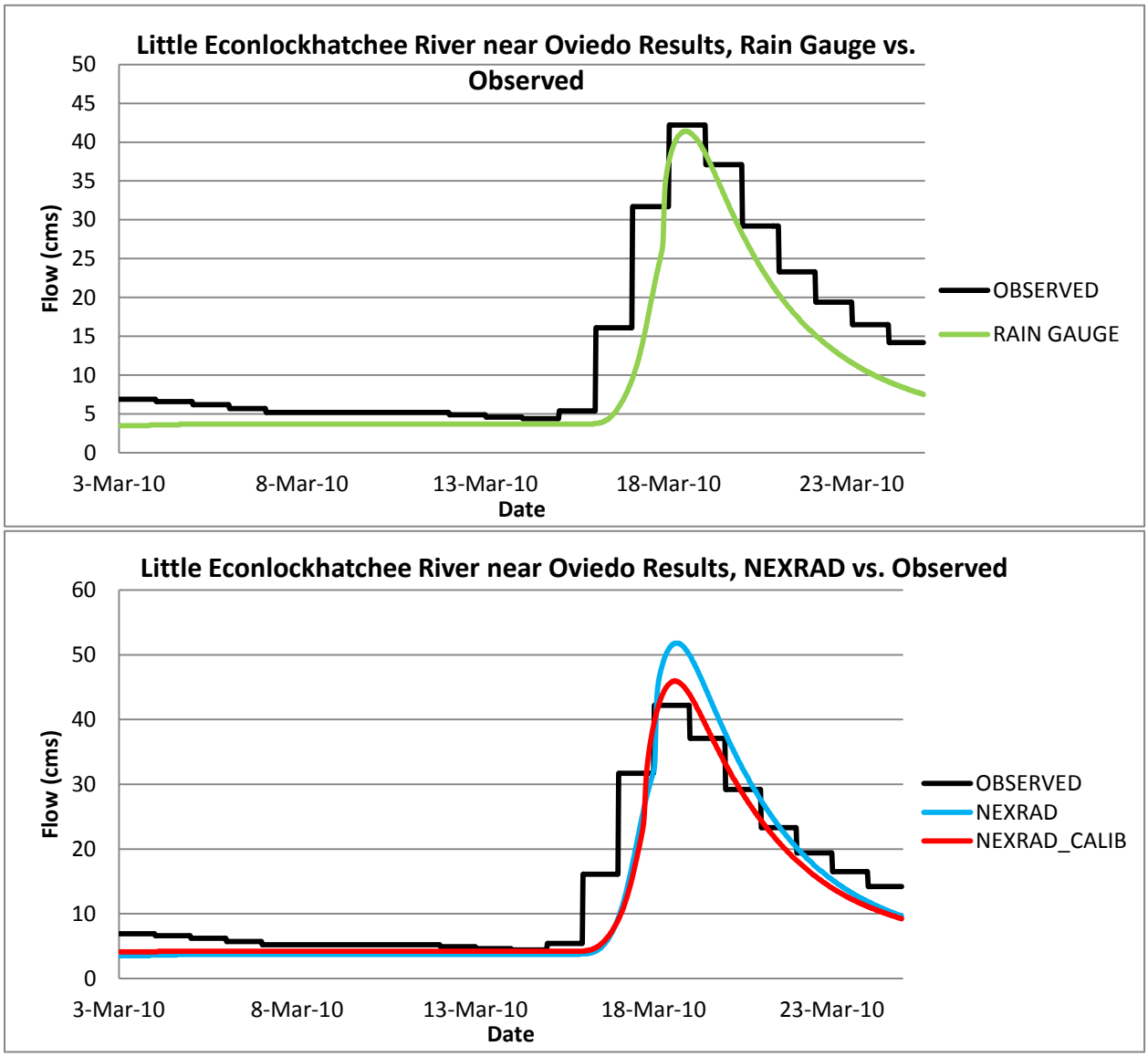

Figures 12a and 12b - Little Econlockhatchee River near Oviedo 2010 Validation Results USGS Gauge 02233484

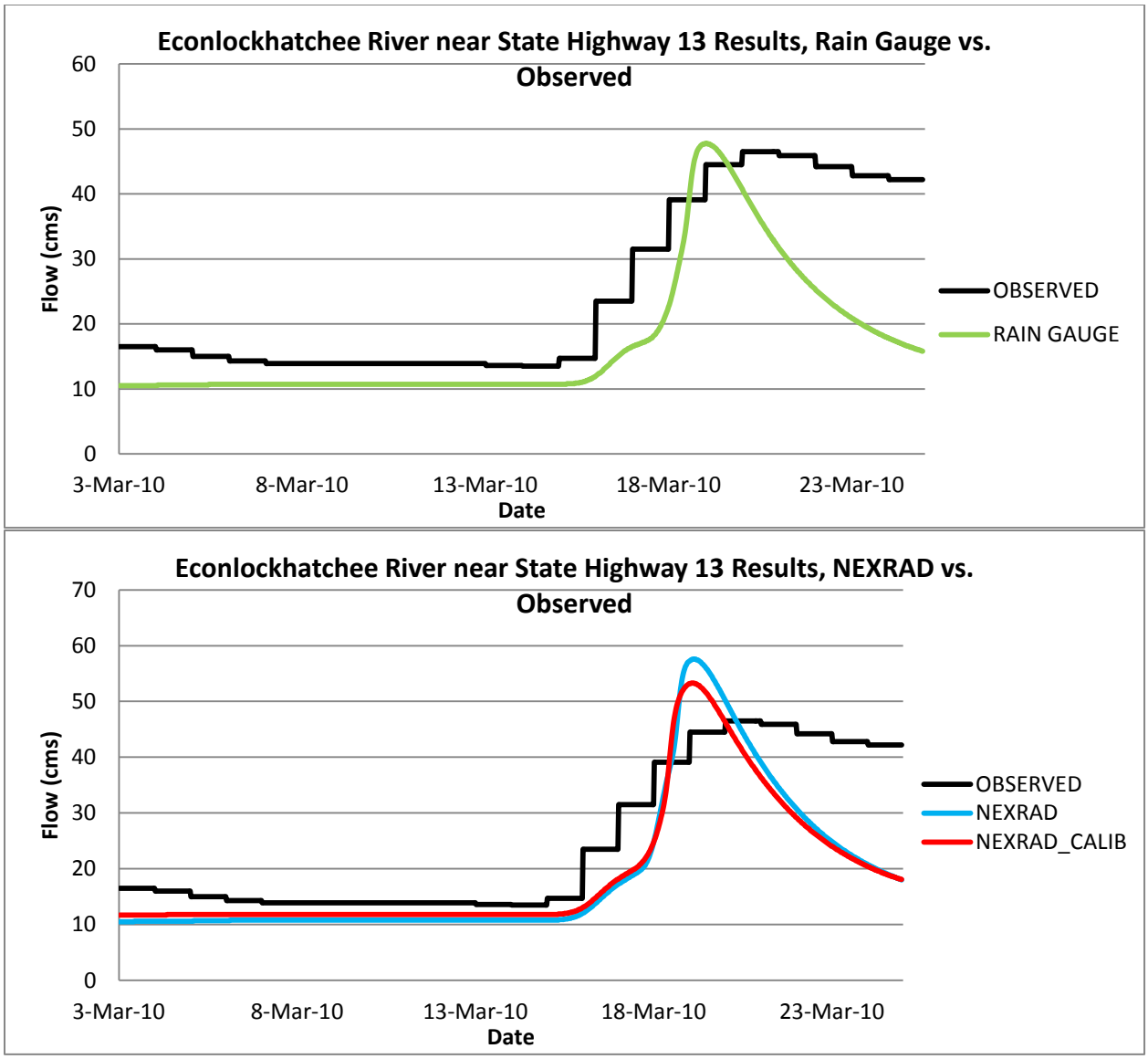

Figures 13a and 13b - Econlockhatchee River near State Highway 13 2010 Validation Results
USGS Gauge 02233500

APPENDIX D

October 2011 Validation Model Results

Subbasin	I. A. (mm)	C. N.	Lag Time (min.)	Subbasin	I. A. (mm)	C. N.	Lag Time (min.)
Barney Green	42	72	1560	Lake Poinsett Rainfall North	37	83	3300
Barry Groves	24	81	2646	Lake Poinsett Rainfall South	18	74	3450
BC East Rainfall	14	88	3351	Lake Price Outlet	47	68	1000
BCMCA Rainfall	27	79	7500	Lake Proctor	81	51	550
BC West Rainfall	23	82	1700	Lake Wash 1 Rainfall	16	87	5900
Bird Lake Combined	30	78	1800	Lake Wash 2 Rainfall	16	87	3850
Bird Lake Ditches	31	78	1200	Lake Wash 3 Rainfall	16	87	3900
Bithlo Branch	26	80	650	Lake Wilson Outlet	27	79	2361
Blue Cypress Creek	80	60	3500	Lake Winder Rainfall	22	83	5800
Broadmoor Marsh	32	76	1370	Little Creek	38	72	2000
Bull Creek	36	75	1300	Little Econlock River	51	66	2000
Buscombe Creek	15	87	1000	Little Econlock Tributary	43	70	2100
C25 Ext	43	71	2130	Long Branch	23	75	650
C54 Retention Area	10	92	1163	Mary A Groves	15	87	715
Cabbage Slough	31	76	2300	Mary A Groves Res Rain	29	79	500
Caine Farms	18	85	1250	Mary A Groves Restoration	6	95	574
Christmas Creek	14	89	1500	Mary A Rainfall	37	74	1400
Clark Lake Outlet	30	78	3100	Mills Creek	27	80	1550
Cocoa Canals	21	84	2500	Mitchell Creek	15	88	1285
Cowpen Branch	28	79	750	Moccasin Isl 1	40	73	7600
Cox Creek Lower	41	71	1400	Moccasin Isl 2	17	86	3000
Cox Creek Res Rainfall	31	73	990	Moccasin Isl 3	21	83	2500
Cox Creek upper	30	78	1800	Moccasin Isl 4	26	80	2000
Crane Strand Drain	55	68	1500	Moccasin Isl 5	35	75	1800
Cross Triangle	32	77	1900	Moccasin Isl 6	47	69	3300
Delespine Grant	34	76	1400	Padgett Branch	28	79	2405
Delta Farms	64	63	1240	Pennywash Creek	24	65	1350
Delta Farms Res Rain	20	84	735	Pressley Ranch	40	73	1282
Deseret 1	10	91	720	Pressley Ranch South	33	76	869
Deseret 2	21	84	662	Rdd Primary Canal	33	76	1650
Deseret East	24	81	1525	Roberts Branch	30	77	1600
Deseret Farms	40	73	2240	Rockledge	50	68	2129

Figure 1 - Calibration Parameters for October 2011 Simulation Event with Rain Gauge and NEXRAD (not re-calibrated) Input

Subbasin	I. A. (mm)	C. N.	Lag Time (min.)	Subbasin	I. A. (mm)	C. N.	Lag Time (min.)
Deseret Farms South	41	72	1400	Rollins Ranch	40	73	955
Econlock 1	35	73	1600	Rollins South A	41	72	1143
Econlock 2	50	70	1600	Rollins South B	40	73	1143
Econlock 3	53	65	2500	Rollins South C	40	73	1143
Econlock 4	44	70	2150	Sartori East	40	73	1459
Econlock 5	50	67	1700	Sartori Farms	16	87	1797
Econlock River Swamp	56	64	3000	Savage Creek	16	87	1000
Econlock River Trib 1	36	74	1000	Second Creek	27	80	1700
Econlock River Trib 2	36	74	1000	Sixmile Creek	26	80	2000
Evans Grove	31	77	1190	Sixmile Restoration Area	35	75	1131
FDMCA Rainfall	27	79	2770	Sixmile Tributary	26	80	745
FF PS1	36	75	1970	SJR Cone	20	84	2100
FF PS2	36	75	1720	SJR Harney	12	89	1650
FF PS3	18	85	1265	SJR Puzzle	12	92	2500
FF PS4	34	76	1525	SJR State Road 46	29	79	1300
FF PS5	15	87	875	SJR State Road 50	20	84	3300
FF PS6	38	74	1751	SJWMA Rainfall	40	73	1681
FF PS7	33	76	1593	SN Knight (Kenansville)	16	86	130
Fort Drum Creek	70	66	2400	South Lake Outlet	35	75	1200
Fourmile Creek	45	74	3000	St Johns Imp Dis	37	74	7054
Goupher Slough	19	85	2074	St Johns Imp Dis Res Rain	37	74	1516
Green Branch	32	76	650	St Johns Trib 1&2	21	83	2500
JG Bull Creek	54	66	3000	St Johns Trib 3	17	86	850
JG Crabgrass Creek	52	64	3500	St Johns Trib 7	23.5	82	1300
JG Creek	39	73	2984	St Johns Trib 9	38	74	3500
JG Tributary	37	74	2563	Taylor Creek	23	82	1600
Jim Creek	36	77	2700	Taylor Creek Res Rainfall	25	72	2511
Jim Creek North	41	72	1800	Tenmile Creek	41	72	2272
Jim Green Creek	33	76	2125	Tootoosahatchee Creek	38	74	1500
Joshua Creek	19	84	2200	Tucker Rainfall	34	76	669
King Street	36	75	2200	Turkey Creek	38	73	1150
Knight Creek	13	89	1483	Underhill Slough	17	86	836
Lake Berge Outlet	44	70	1000	Union Park Canal	55	69	1600
Lake Hell n Blazes	41	72	1200	Wolf Creek	65	66	1400
Lake Irma Outlet	60	68	1200	Wolf Creek North	24	77	1500

Figure 1 continued - Calibration Parameters for October 2011 Simulation Event with Rain Gauge and NEXRAD (not re-calibrated) Input

Subbasin	I. A. (mm)	C. N.	Lag Time (min.)	Subbasin	I. A. (mm)	C. N.	Lag Time (min.)
Barney Green	42	72	1560	Lake Poinsett Rainfall North	37	83	3300
Barry Groves	24	81	2646	Lake Poinsett Rainfall South	22	74	3450
BC East Rainfall	14	88	3351	Lake Price Outlet	47	68	1000
BCMCA Rainfall	27	79	7500	Lake Proctor	81	51	550
BC West Rainfall	23	82	1700	Lake Wash 1 Rainfall	16	87	5900
Bird Lake Combined	30	78	1800	Lake Wash 2 Rainfall	16	87	3850
Bird Lake Ditches	31	78	1200	Lake Wash 3 Rainfall	16	87	3900
Bithlo Branch	26	80	650	Lake Wilson Outlet	27	79	2361
Blue Cypress Creek	80	60	3500	Lake Winder Rainfall	22	83	5800
Broadmoor Marsh	32	76	1370	Little Creek	38	72	2000
Bull Creek	36	75	1300	Little Econlock River	51	66	2000
Buscombe Creek	15	87	1000	Little Econlock Tributary	43	70	2100
C25 Ext	43	71	2130	Long Branch	23	75	650
C54 Retention Area	10	92	1163	Mary A Groves	15	87	715
Cabbage Slough	31	76	2300	Mary A Groves Res Rain	29	79	500
Caine Farms	18	85	1250	Mary A Groves Restoration	6	95	574
Christmas Creek	14	89	1500	Mary A Rainfall	37	74	1400
Clark Lake Outlet	30	78	3100	Mills Creek	27	80	1550
Cocoa Canals	21	84	2500	Mitchell Creek	15	88	1285
Cowpen Branch	28	79	750	Moccasin Isl 1	40	73	7600
Cox Creek Lower	41	71	1400	Moccasin Isl 2	17	86	3000
Cox Creek Res Rainfall	31	73	990	Moccasin Isl 3	21	83	2500
Cox Creek upper	30	78	1800	Moccasin Isl 4	26	80	2000
Crane Strand Drain	55	68	1500	Moccasin Isl 5	35	75	1800
Cross Triangle	32	77	1900	Moccasin Isl 6	47	69	3300
Delespine Grant	34	76	1400	Padgett Branch	28	79	2405
Delta Farms	64	63	1240	Pennywash Creek	24	65	1350
Delta Farms Res Rain	20	84	735	Pressley Ranch	40	73	1282
Deseret 1	10	91	720	Pressley Ranch South	33	76	869
Deseret 2	21	84	662	Rdd Primary Canal	33	76	1650
Deseret East	24	81	1525	Roberts Branch	30	77	1600
Deseret Farms	40	73	2240	Rockledge	50	68	2129

Figure 2- Re-Calibration Parameters for October 2011 Simulation Event with NEXRAD Input

Subbasin	I. A. (mm)	C. N.	Lag Time (min.)	Subbasin	I. A. (mm)	C. N.	Lag Time (min.)
Deseret Farms South	41	72	1400	Rollins Ranch	40	73	955
Econlock 1	35	73	1600	Rollins South A	41	72	1143
Econlock 2	50	70	1600	Rollins South B	40	73	1143
Econlock 3	53	65	2500	Rollins South C	40	73	1143
Econlock 4	44	70	2150	Sartori East	40	73	1459
Econlock 5	50	67	1700	Sartori Farms	16	87	1797
Econlock River Swamp	56	64	3000	Savage Creek	16	87	1000
Econlock River Trib 1	36	74	1000	Second Creek	27	80	1700
Econlock River Trib 2	36	74	1000	Sixmile Creek	26	80	2000
Evans Grove	31	77	1190	Sixmile Restoration Area	35	75	1131
FDMCA Rainfall	27	79	2770	Sixmile Tributary	26	80	745
FF PS1	36	75	1970	SJR Cone	20	84	2100
FF PS2	36	75	1720	SJR Harney	12	89	1650
FF PS3	18	85	1265	SJR Puzzle	12	92	2500
FF PS4	34	76	1525	SJR State Road 46	29	79	1300
FF PS5	15	87	875	SJR State Road 50	20	84	3300
FF PS6	38	74	1751	SJWMA Rainfall	40	73	1681
FF PS7	33	76	1593	SN Knight (Kenansville)	16	86	130
Fort Drum Creek	70	66	2400	South Lake Outlet	35	75	1200
Fourmile Creek	45	74	3000	St Johns Imp Dis	37	74	7054
Goupher Slough	19	85	2074	St Johns Imp Dis Res Rain	37	74	1516
Green Branch	32	76	650	St Johns Trib 1&2	21	83	2500
JG Bull Creek	54	66	3000	St Johns Trib 3	17	86	850
JG Crabgrass Creek	52	64	3500	St Johns Trib 7	23.5	82	1300
JG Creek	39	73	2984	St Johns Trib 9	38	74	3500
JG Tributary	37	74	2563	Taylor Creek	23	82	1600
Jim Creek	36	77	2700	Taylor Creek Res Rainfall	25	72	2511
Jim Creek North	41	72	1800	Tenmile Creek	41	72	2272
Jim Green Creek	33	76	2125	Tootoosahatchee Creek	38	74	1500
Joshua Creek	19	84	2200	Tucker Rainfall	34	76	669
King Street	36	75	2200	Turkey Creek	38	73	1150
Knight Creek	13	89	1483	Underhill Slough	17	86	836
Lake Berge Outlet	44	70	1000	Union Park Canal	55	69	1600
Lake Hell n Blazes	41	72	1200	Wolf Creek	65	66	1400
Lake Irma Outlet	60	68	1200	Wolf Creek North	14	77	1500

Figure 2 continued - Re-Calibration Parameters for October 2011 Simulation Event with NEXRAD Input

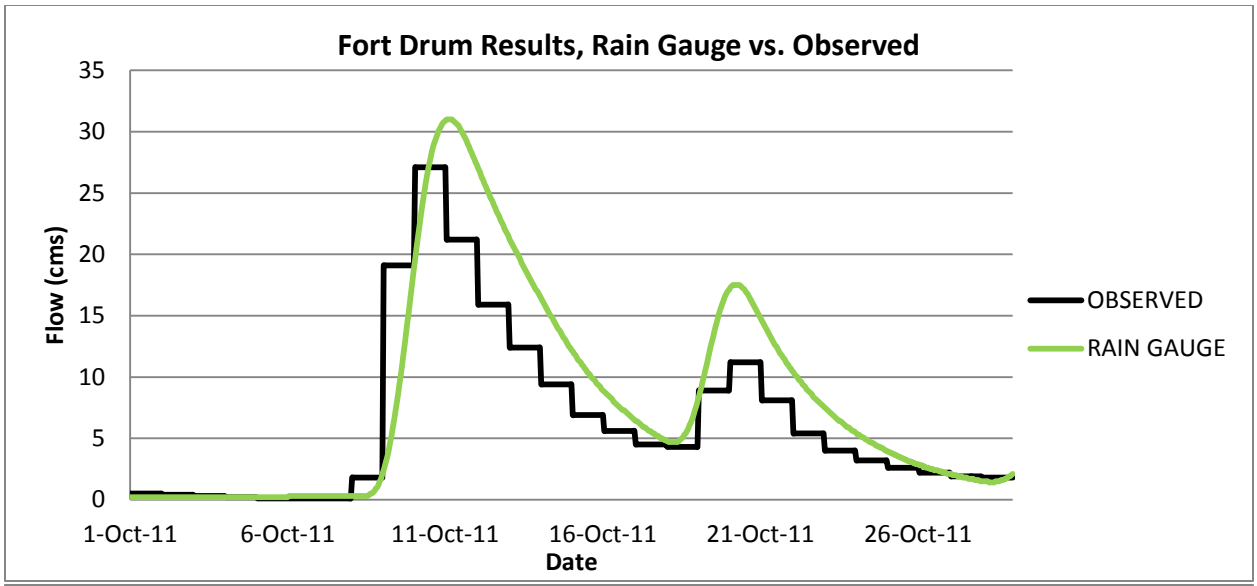

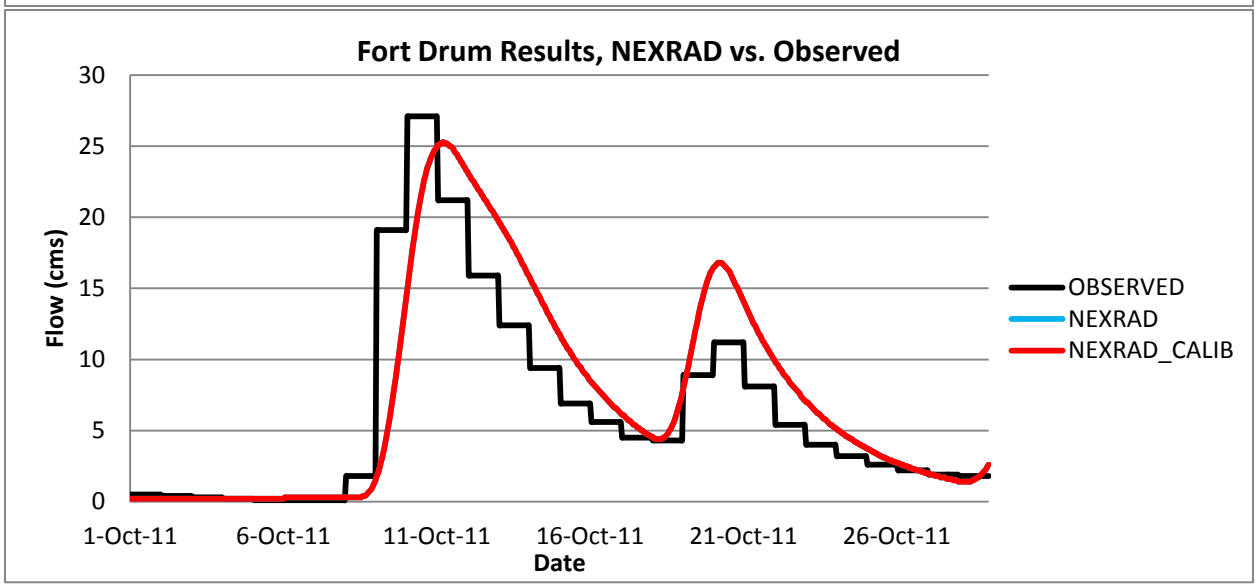

Figures 3a and 3b - Ft. Drum Creek 2011 Validation Results, USGS Gauge 02231342

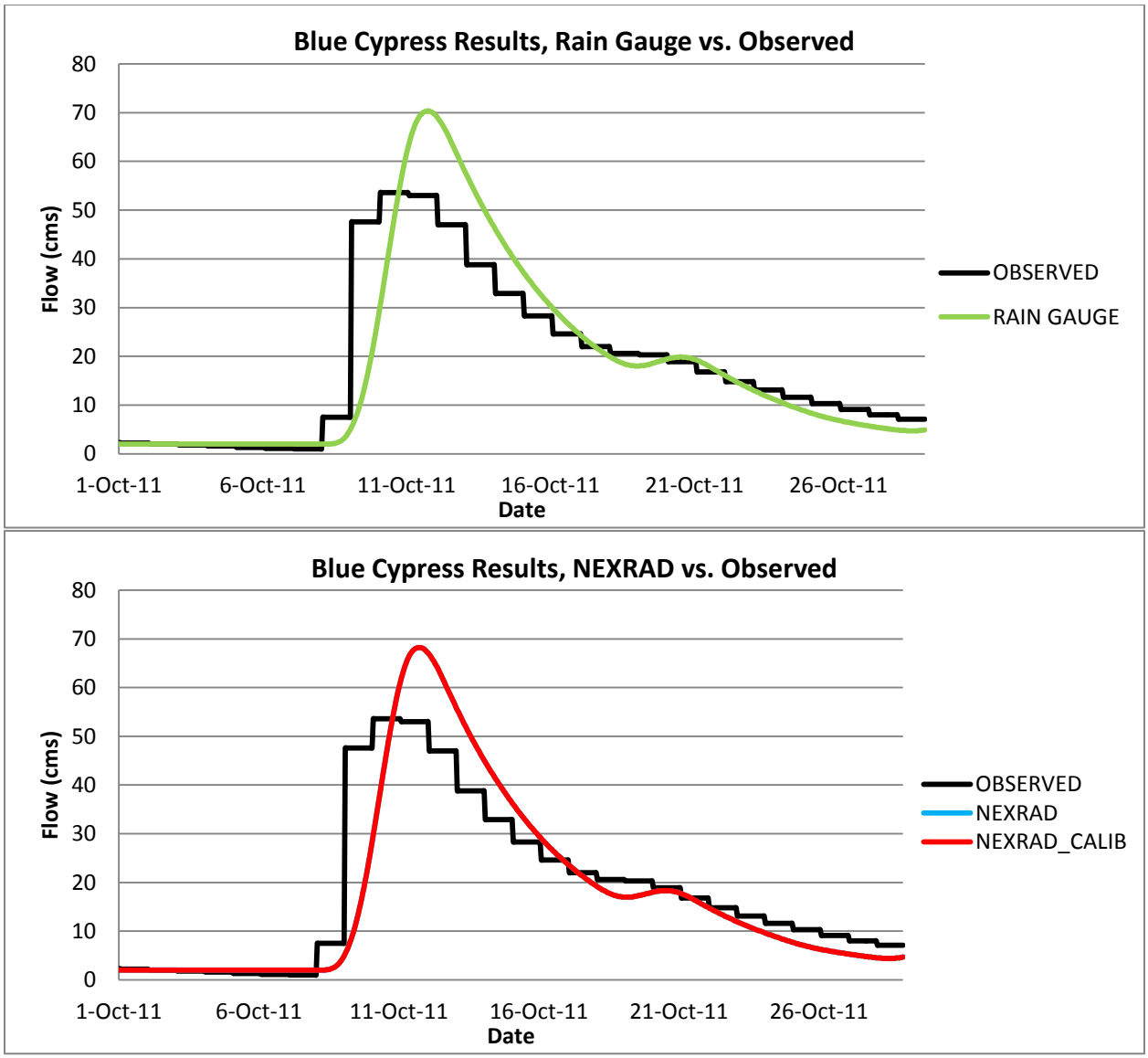

Figures 4a and 4b - Blue Cypress Creek 2011 Validation Results USGS Gauge 02231396

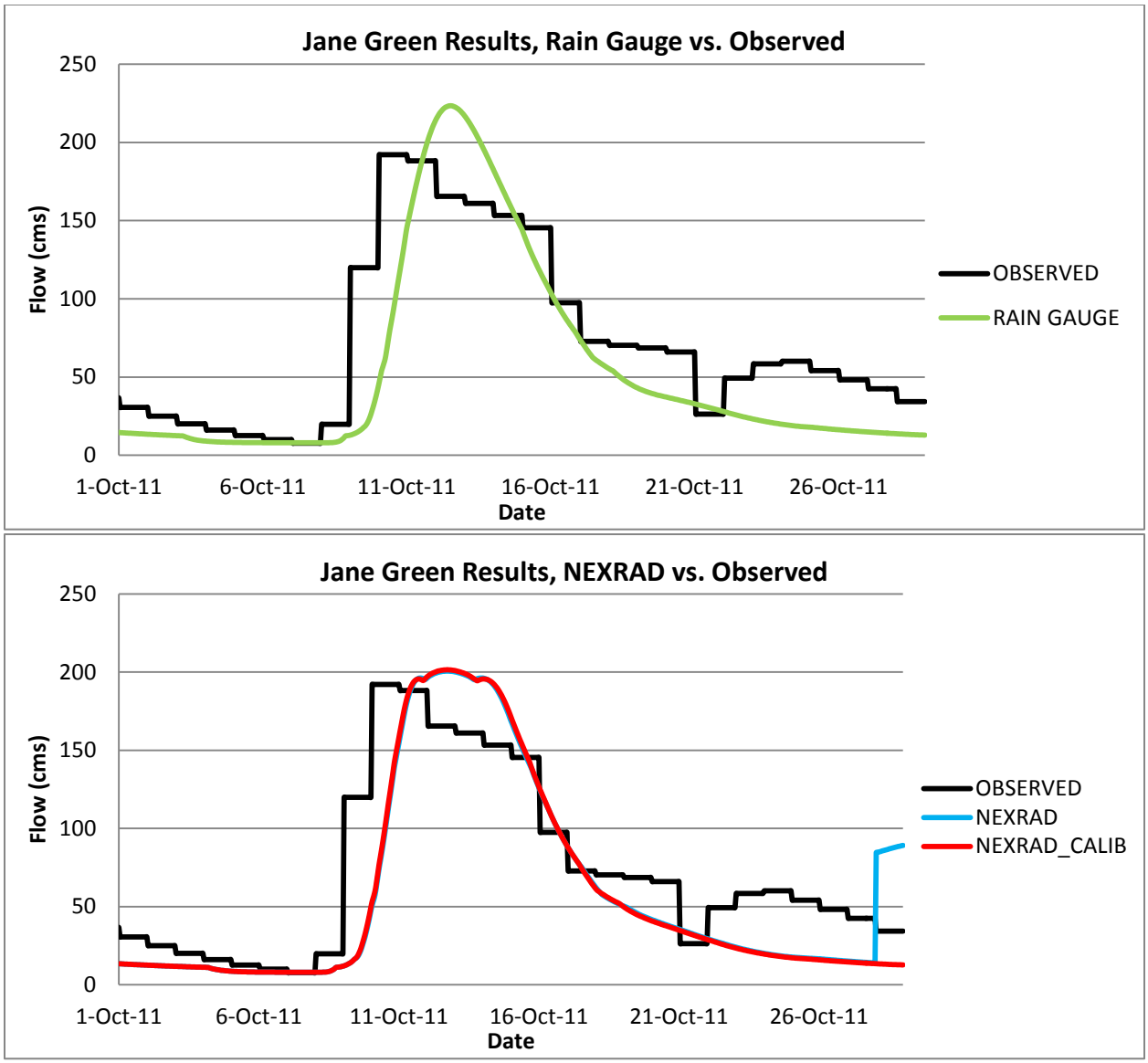

Figures 5a and 5b – Jane Green Reservoir 2011 Validation Results USGS Gauge 02231600

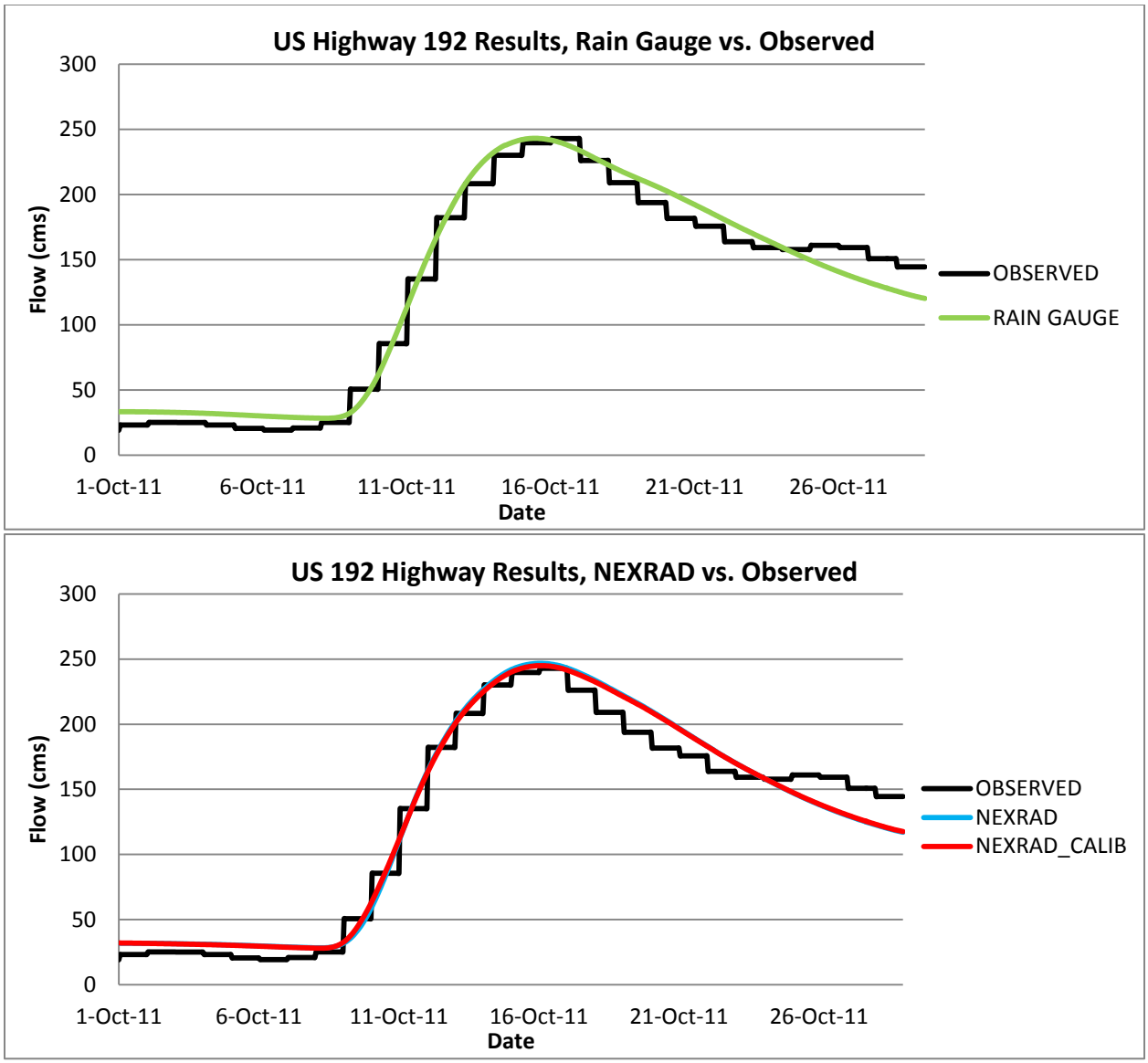

Figures 6a and 6b – St. Johns River at U.S. Highway 192 2011 Validation Results USGS Gauge 02232000

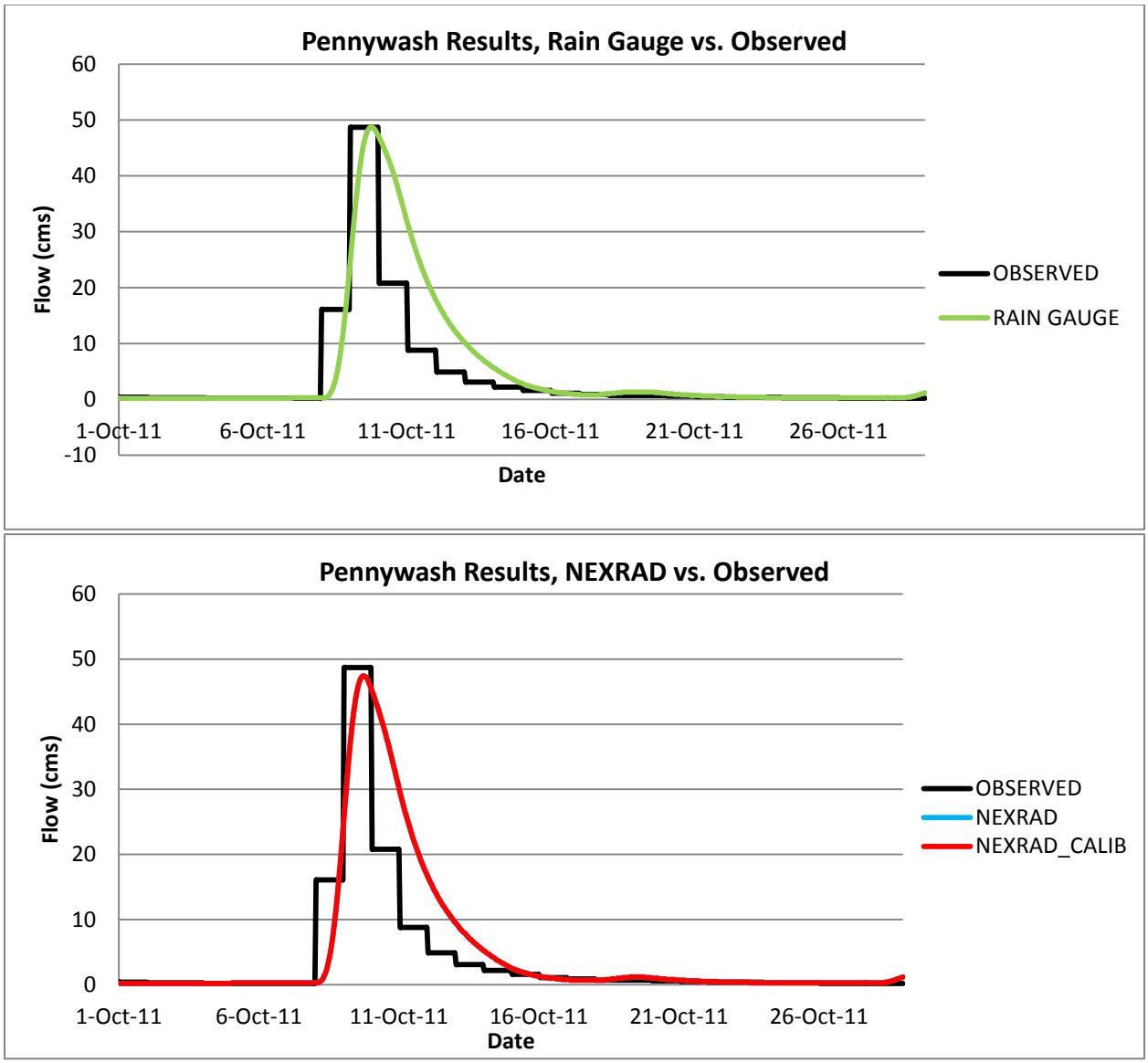

Figures 7a and 7b – Pennywash Creek 2011 Validation Results USGS Gauge 02232155

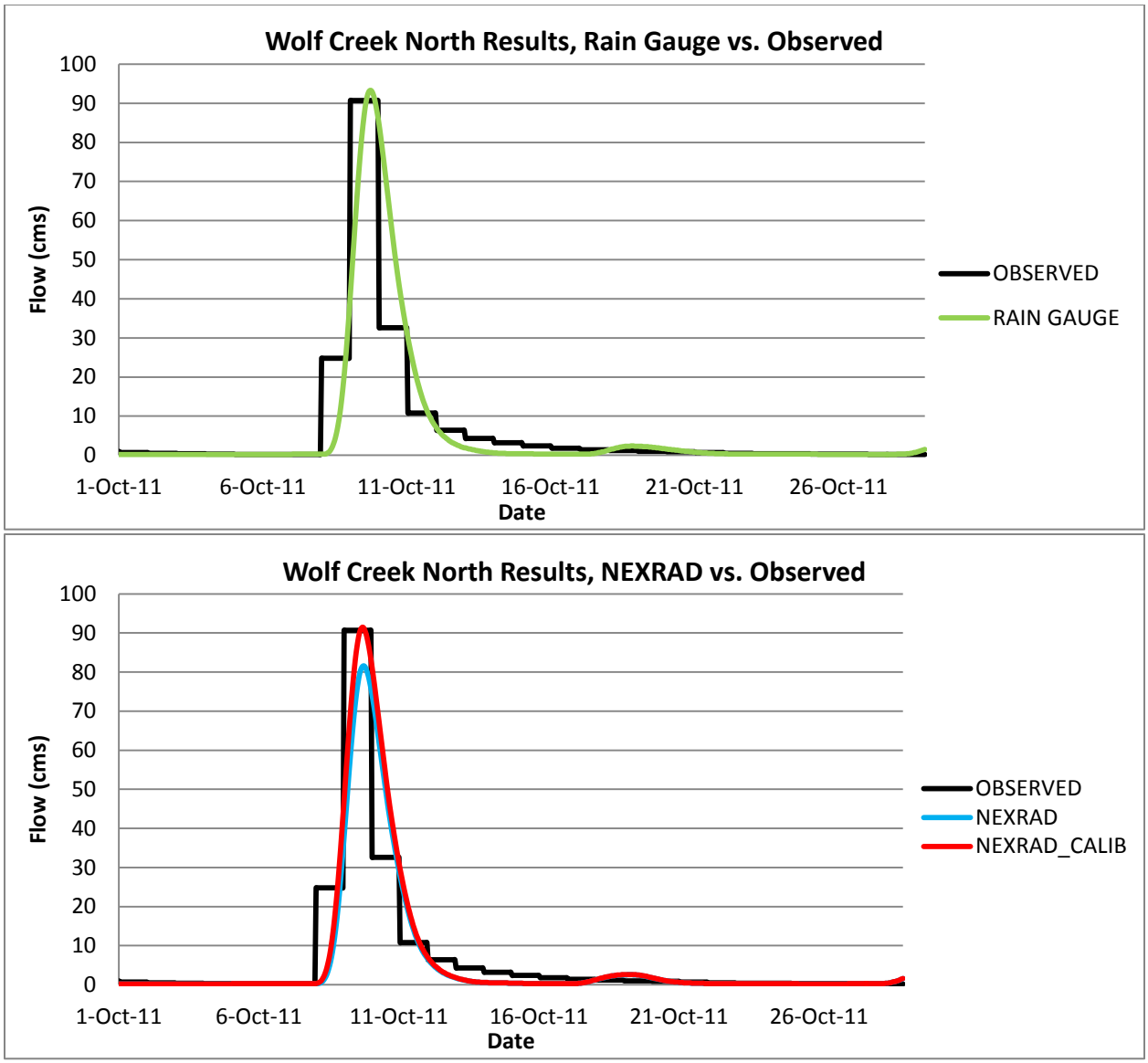

Figures 8a and 8b – Wolf Creek North 2011 Validation Results USGS Gauge 02232200

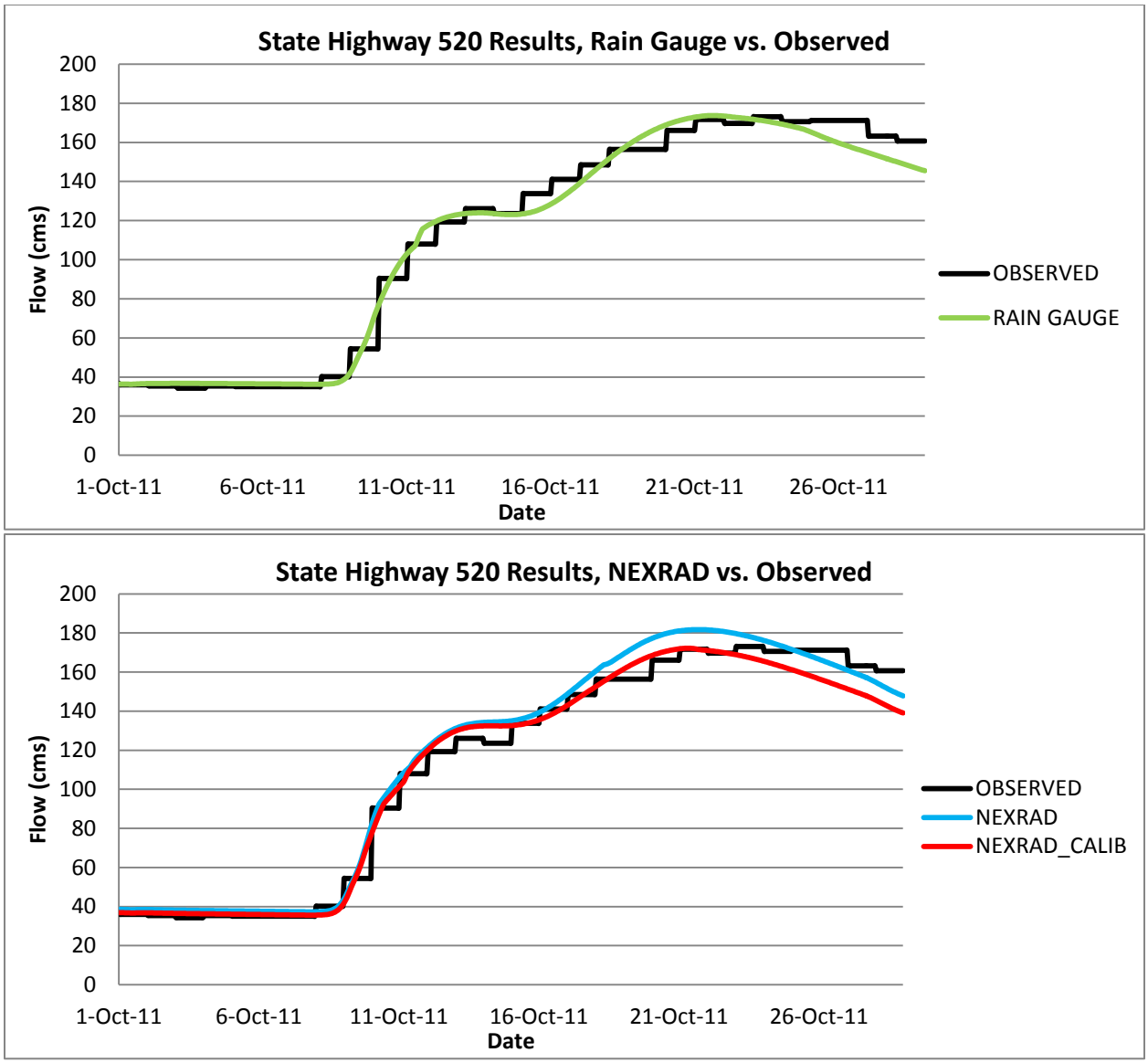

Figures 9a and 9b – St. Johns River at State Highway 520 2011 Validation Results USGS Gauge 02232400

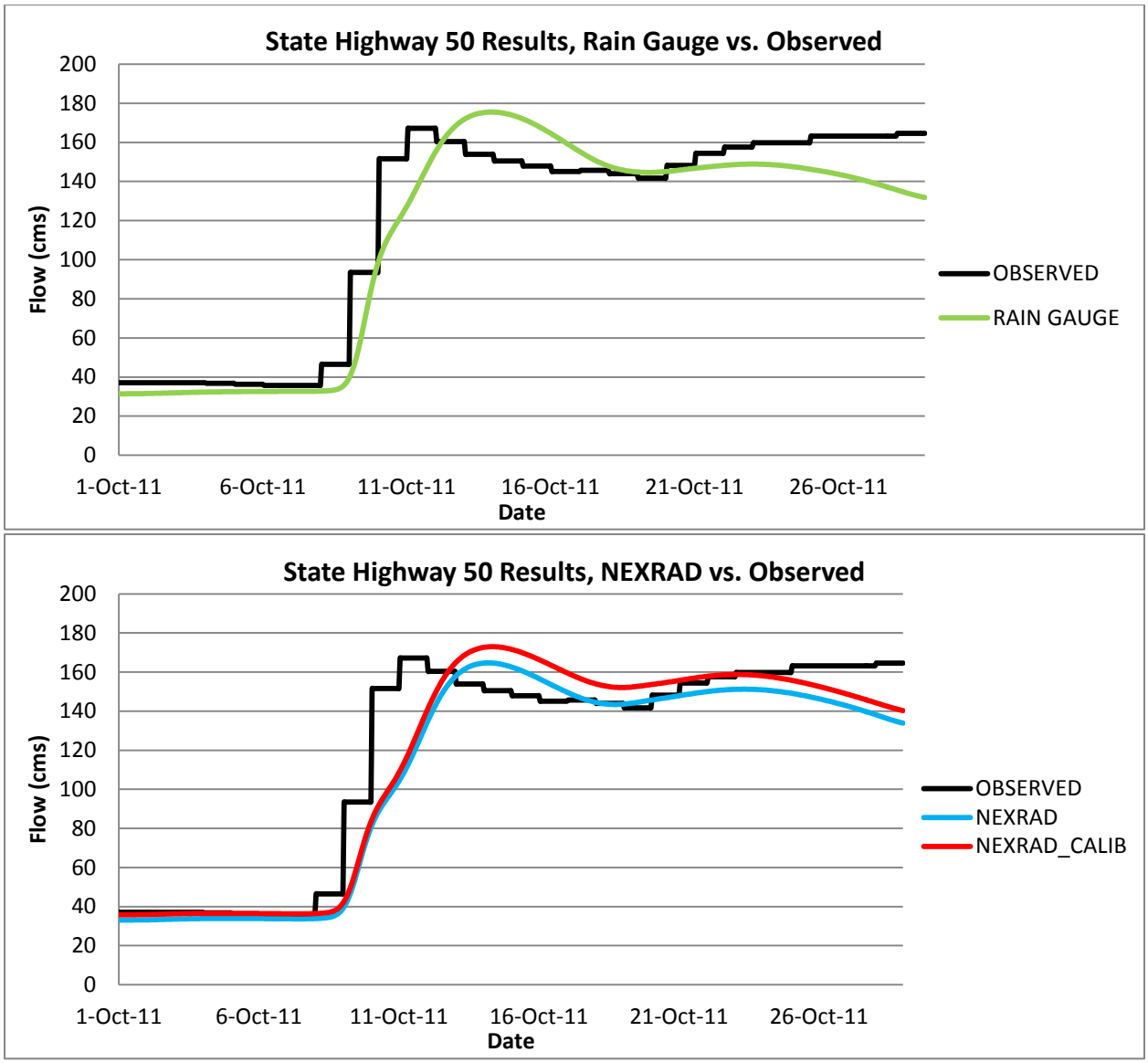

Figures 10a and 10b - St. Johns River at State Highway 50 2011 Validation Results USGS Gauge 02232500

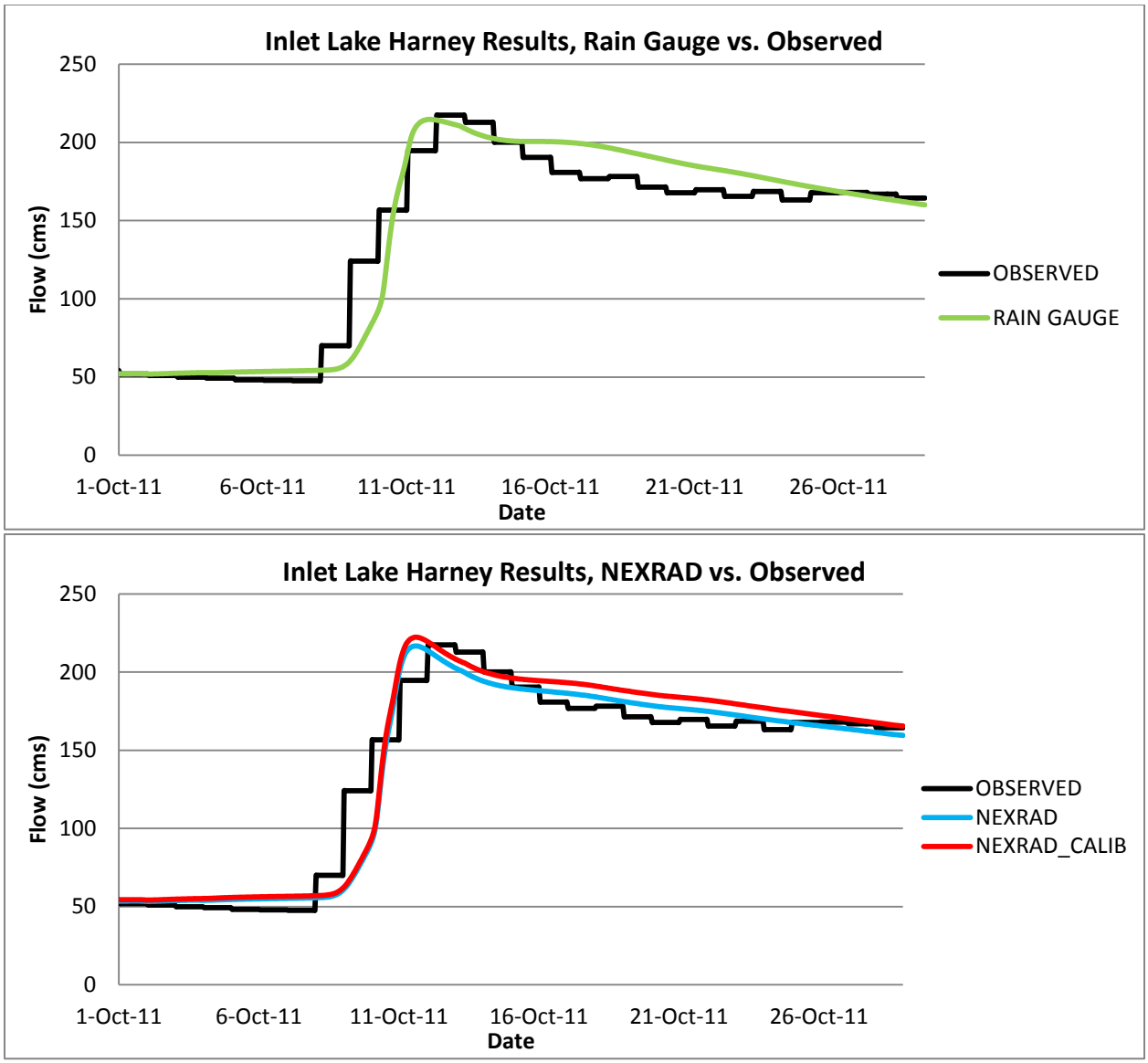

Figures 11a and 11b - St. Johns River at Inlet of Lake Harney 2011 Validation Results USGS Gauge 02234000

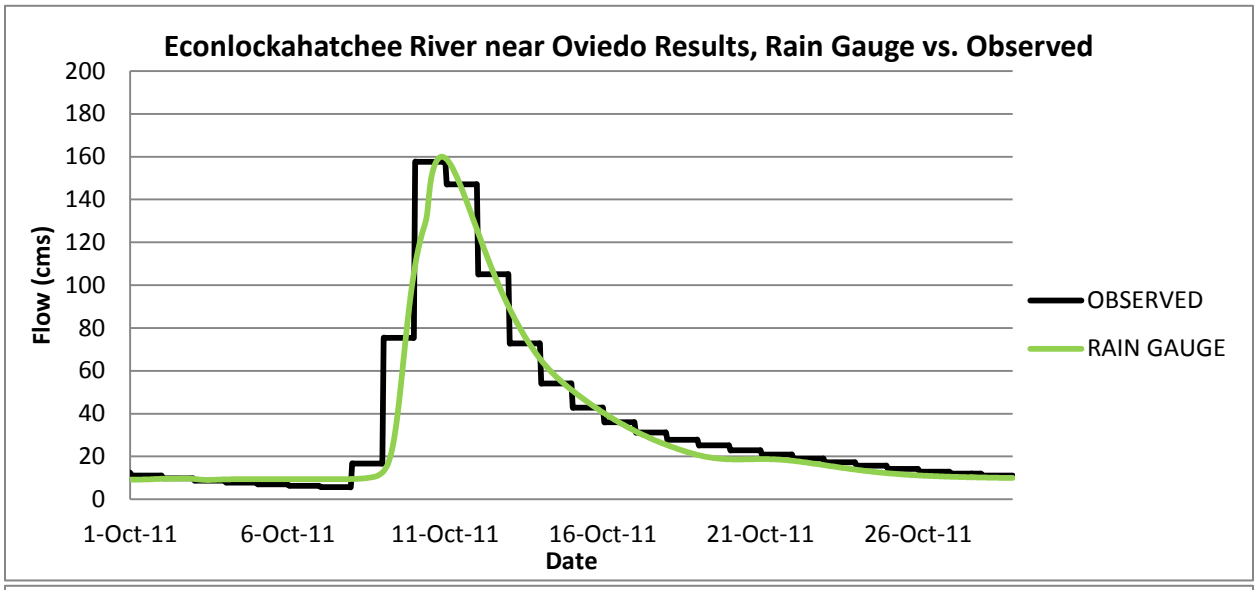

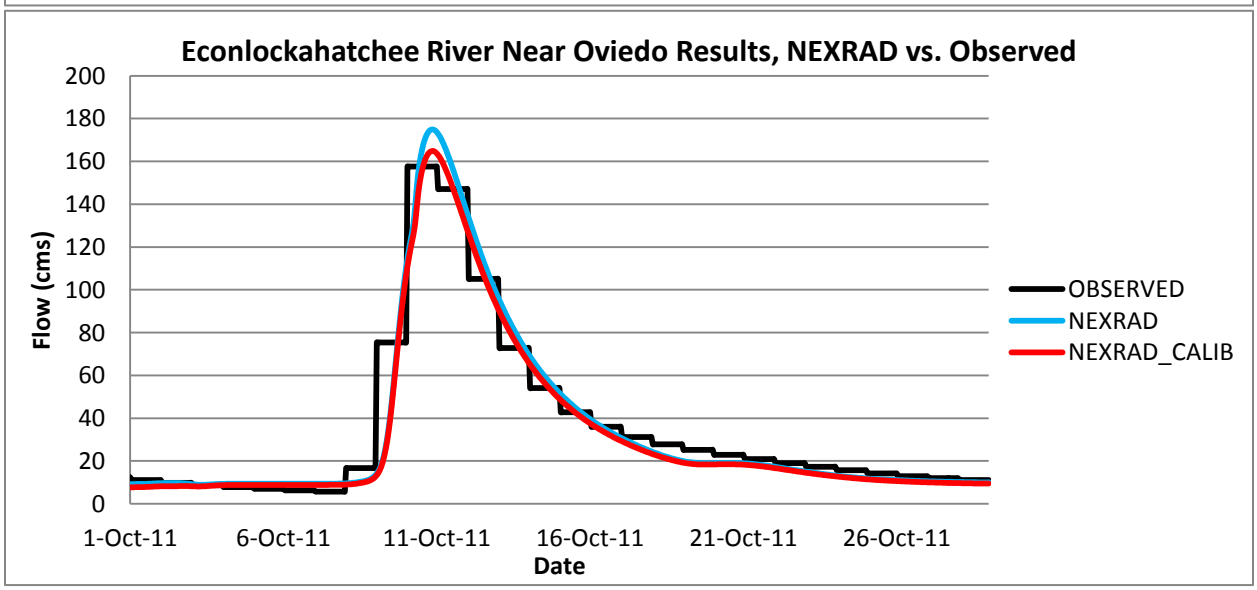

Figures 12a and 12b - Little Econlockhatchee River near Union Park 2011 Validation Results
USGS Gauge 02233460

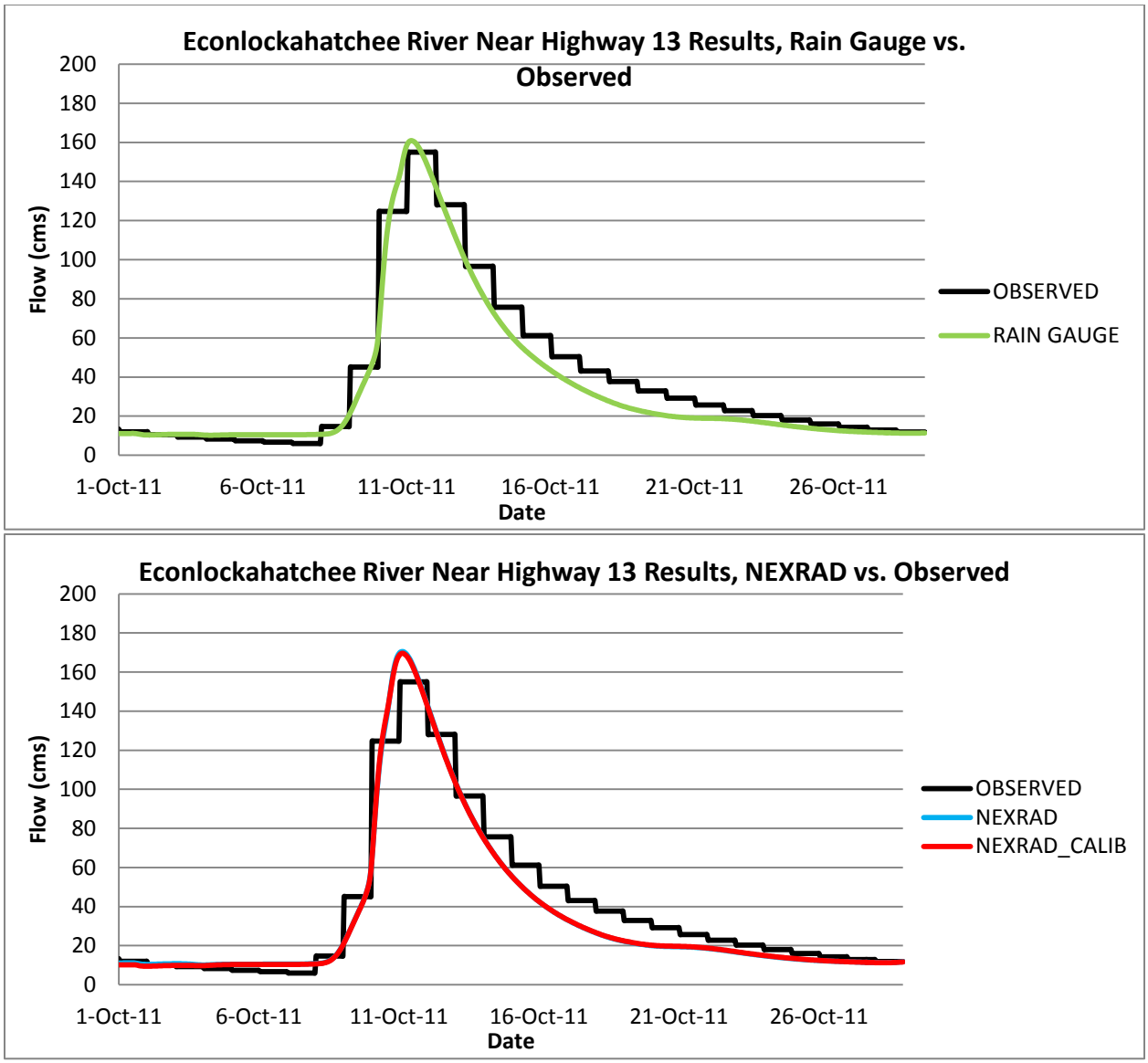

Figures 13a and 13b - Econlockhatchee River near State Highway 13 2011 Validation Results
USGS Gauge 02233500

REFERENCES

Armstrong, D. R. (2001, April). Project Works, the Physical Mechanisms of Water Management. St. Johns River Water Management District.

Ayres Associates. (2001, August). Hillsborough River Watershed Management Plan.

Ball, J. E., & Luk, K. C. (1998). Modeling spatial variability of rainfall over a catchment. *Journal of Hydrologic Engineering*, *3*(2), 122-130.

Bayraktar, H., Turalioglu, F. S., & Sen, Z. (2005). The estimation of average areal rainfall by percentage weighting polygon method in Southeastern Anatolia Region, Turkey. *Atmospheric Research*, *73*(1-2), 149-160. http://dx.doi.org/10.1016/j.atmosres.2004.08.003

Burcea, S., Cheval, S., Dumitrescu, A., Antonescu, B., Bell, A., & Breza, T. (2012). COMPARISON BETWEEN RADAR ESTIMATED AND RAIN GAUGE MEASURED PRECIPITATION IN THE MOLDAVIAN PLATEAU. *Environmental Engineering and Management Journal*, *11*(4), 723-731.

CH2M Hill. (1997). Water supply needs and sources assessment alternative water supply strategies investigation artificial recharge of the floridan aquifer through drainage or injection wells in Orange and Seminole Counties (Publication No. SJ97-SP14). Palatka, FL: St. Johns River Water Management District.

Charbonnier, S. F., & Genta, J. L. (2000). The antecedent soil moisture condition of the curve number procedure. Hydrological Sciences- Journal, 45(1).

Cheng, C.-D., Cheng, S.-J., Wen, J.-C., & Lee, J.-H. (2012). Effects of Raingauge Distribution on Estimation Accuracy of Areal Rainfall. *Water Resources Management*, *26*(1), 1-20. http://dx.doi.org/10.1007/s11269-011-9898-7

City and County of Sacramento. (1996, December). Drainage Manual Volume 2: Hydrology Standards, Chapter 7 Lag Time. Retrieved October 18, 2014, from http://www.waterresources.saccounty.net/DrainageManual_Volume2/V2_Chap07.PDF

Di, J. J., Smith, D., Lippincott, C., & Marzolf, E. (2010). Pollutant Load Reduction Goals for Newnans Lake (Publication No. SJ2010-1). Palatka, FL: St. Johns River Water Management District.

Diaz-Ramirez, J. N., McAnally, W. H., & Martin, J. L. (2012). Sensitivity of Simulating Hydroloigc Processes to Gauge and Radar Rainfall Data in Subtropical Coastal Catchment. *Water Resources Management*, *26*, 3515-3538. http://dx.doi.org/10.1007/s11269-012-0088-z

Florida Geological Survey. (2004). Bulletin No. 66: Springs of Florida. Tallahassee, Fl.

Habib E, Larson B, Graschel J. 2009b. Validation of nexrad multisensor precipitation estimates using an experimental dense raingauge network in south Louisiana. Journal of Hydrology 173: 463–478.

Harmel, R., Cooper, R., Slade, R., Haney, R., & Arnold, J. (2006). Cumulative uncertainty in measured streamflow and water quality data for small watersheds. Transactions of the ASABE, 49(3), 689–701.

Hawkins, R. H., Hjelmfelt, A. T., and Zevenbergen, A. W. (1985). "Runoff probability, storm depth, and curve numbers." J. Irrig. Drain. Eng., 10.1061/(ASCE)0733-9437(1985)111:4(330), 330–340.

Huebner, S.R., Pathak, C. and Hoblit, B.C., 2003. Development and Use of a NEXRAD Database for Water Management in South Florida. ASCE EWRI World Water and Environmental Resources Congress Proceedings. ASCE, Reston, Virginia.

Inwood Consulting Engineers. (2009, November). Stormwater master plan, Hydrological & Hydraulic Model Summary Report. Retrieved October 10, 2014, from http://www.alachuacounty.us/Depts/PW/engineering/stormwaterManagementProgram/SWMasterPlan/Pages/FinalHydrologicalandHydraulicModel.aspx

Jain MK, Mishra SK, Babu PS, Venugopal K, Singh VP (2006) Enhanced runoff curve number model incorporating storm duration and a nonlinear Ia-S relation. J Hydrol Eng 11(6):631–635.doi:10.1061/(ASCE)1084-0699(2006)11:6(631)

Jayakrishnan, R., Srinivasan, R., & Arnold, J. G. (2004). Comparison of raingage and WSR-88D Stage III precipitation data over the Texas-Gulf basin.*Journal of Hydrology*, *292*(1), 135-152.

KBN Engineering and Applied Sciences. (1993, June). SJ93-SP7: A Wetland Management Strategy for the St. Marys River Basin

Kalin, L., & Hantush, M. M. (2006). Hydrologic Modeling of an Eastern Pennsylvania Watershed. *Journal of Hydrologic Engineering*, *11*(6), 555-569. http://dx.doi.org/10.1061/ASCE1084-0699200611:6555

Kang, K., & Merwade, V. (2014). The effect of spatially uniform and non-uniform precipitation bias correction methods on improving NEXRAD rainfall accuracy for distributed hydrologic modeling. *Hydrology Research*, *45*(1), 23-42.

Kimrey, J. O., & Fayard, L. D. (1984). Geohydrologic reconnaissance of drainage wells in Florida.

Li, M.-H., & Chibber, P. (2008). Overland Flow Time of Concentration on Very Flat Terrains. Journal of the Transportation Research Board No. 2060, 133-140. http://dx.doi.org/10.3141/2060-15

Looper, J. P. and Vieux, B. E. (2012) An assessment of distributed flash flood forecasting accuracy using radar and rain gauge input for a physics-based distributed hydrologic model. Journal of Hydrology, 412-413(0), 114-132.

Ly, S., Charles, C., & Degre, A. (2013). Different methods for spatial interpolation of rainfall data. *Biotechnol. Agron. Soc. Environ.*, *17*(2), 392-406.

Mao, L.M, M.J. Bergman and C. Tai (2002). "Evapotranspiration Measurement and Estimation of Three Wetland Environments in the Upper St. Johns River Basin, Florida". Journal of the American Water Resources Association, 5(38), 1271- 1285.

Mays, L. W. (2011). Water resources engineering (2nd ed.). John Wiley & Sons, Inc.

Mazari, N., Xie, H., Zeitler, J., & Sharif, H. O. (2013). Validation of the NEXRAD DSP product with a dense rain gauge network. *Journal of Hydrologic Engineering*, *18*(2), 156-167.

Mohamoud, Y. (2004, September). Comparison of Hydrologic Responses at Different Watershed Scales. Research Triangle Park, NC: U.S. Environmental Protection Agency.

Nash, J.E. and J.V. Sutcliffe, 1970. River Flow Forecasting Through Conceptual Models: Part I. A Discussion of Principles. J. of Hyd. 10:282-290

Neary, V. S., Habib, E., and Fleming, M. 2004. "Hydrologic modeling with NEXRAD precipitation in middle Tennessee." J. Hydrol. Eng., 95, 339–349.

Pathak, C., Curtis, D., Kitzmiller, D., & Vieux, B. (2013). Identifying and Resolving the Barriers and Issues in Using Radar-Derived Rainfall Estimating Technology. *Journal of Hydrologic Engineering*, *18*(10), 1193-1199.

Ponce, V. M., & Hawkins, R. H. (1996). Runoff Curve Number: Has It Reached Maturity? Journal of Hydrologic Engineering, 1, 11-19.

Price, K., Purucker, S. T., Kraemer, S. R., Babendreier, J. E., & Knightes, C. D. (2014). Comparison of radar and gauge precipitation data in watershed models across varying spatial and temporal scales. *Hydrological Processes*,*28*(9), 3505-3520.

Rendon, S. H., Vieux, B. E., & Pathak, C. S. (2013). Continuous Forecasting and Evaluation of Derived Z-R Relationships in a Sparse Rain Gauge Network Using NEXRAD. *Journal of Hydrologic Engineering*, *18*(2), 175-182.

Rumenik, R. P. (1988). Runoff to Streams in Florida [Map]. Tallahassee, FL.

Scharffenberg, W. A., & Fleming, M. J. (2010, August). Hydrologic Modeling System HEC-HMS User's Manual. Davis, Ca: U.S. Army Corps of Engineers, HEC.

Sepúlveda, Nicasio, Tiedeman, C.R., O'Reilly, A.M., Davis, J.B., and Burger, Patrick, 2012, Groundwater flow and water budget in the surficial and Floridan aquifer systems in east-central Florida: U.S. Geological Survey Open-File Report 2012–1132, 195 p., plus appendixes.

Sexton, A. M., Sadeghi, A. M., Zhang, X., Srinivasan, R., & Shirmohammadi, A. (2010). Using NEXRAD and Rain Gauge Precipitation Data for Hydrologic Calibration of SWAT in a Northeastern Watershed. *American Society of Agricultural and Biological Engineers*, *5*(3), 1501-1510.

Sharifi, S., & Hosseini, S. M. (2011). Methodology for Identifying the Best Equations for Estimating the Time of Concentration of Watersheds in a Particular Region. Journal of Irrigation and Drainage Engineering, 137(11), 712-719.

Skinner, C., Bloetscher, F., and Pathak, C. (2009). "Comparison of NEXRAD and Rain Gauge Precipitation Measurements in South Florida." *J. Hydrol. Eng.*, 14(3), 248–260.

State of Florida Department of Transportation, Drainage Handbook (Office of Design, Drainage Section, Comp.). (2012, February). Tallahassee, FL.

St. Johns River Water Management District. (2012, July). St. Johns River Water Supply Impact Study (Publication No. SJ2012-1).

St. Johns River Water Management District. (2014). Land Cover / Land Use 1994-95 - SJRWMD [Map]. Retrieved from GIS data download table database.

St. Johns Water Management District (SJRWMD). (2015). Radar Rainfall. Retrieved February 5, 2015, from http://webapub.sjrwmd.com/agws10/radrain/index.htm

Suphunvorranop, T. (1985, July). A Guide to SCS Runoff Procedures (Publication No. 85-5). Palatka, FL: St. Johns River Water Management District.

Tabios G.Q. & Salas J.D., 1985. A comparative analysis of techniques for spatial interpolation of precipitation. Water Resour. Bull., 21, 265-380.

U.S. Army Corps of Engineers, Hydrologic Modeling System HEC-HMS, Rep. No. CPD-74B, at 145 (2000).

U.S. Army Corps of Engineers, Preliminary Water Control Manual Upper St. Johns River Basin, Doc. (1991).

U.S. Department of Agriculture Natural Resources Conservation Service, National Engineering Handbook, Chapter 15, Time of Concentration, 2010.

U.S. Department of Agriculture Soil Conservation Service, National Engineering Handbook, Section 4, Hydrology, available from U.S. Government Printing Office, Washington, DC, 1972.

U.S. Department of Commerce, Rainfall Frequency Atlas of the United States, Doc., at 61 (1961).

USGS Water Resources. (2014). USGS Current Water Data for the Nation. Retrieved November 3, 2014, from USGS Current Water Data for the Nation website: http://waterdata.usgs.gov/nwis/rt

Wang, W. C., Chau, K. W., Cheng, C. T., & Qiu, L. (2009). A comparison of performance of several artificial intelligence methods for forecasting monthly discharge time series. *Journal of hydrology*, *374*(3), 294-306.

Wilcoxon, F. (1945). Individual comparison by ranking methods. Biometrics 1, 80–83.

Wyzga, B. (1999). Estimating mean flow velocity in channel and floodplain areas and its use for explaining the pattern of overbank deposition and floodplain retention. Geomorphology, 28(3-4), 281-297. http://dx.doi.org/10.1016/S0169-555X(98)00110-X

Zhijia, L., Wenzhong, G., Jintao, L., & Kun, Z. (2004). Coupling between weather radar rainfall data and a distributed hydrological model for real-time flood forecasting/Couplage de données pluviométriques issues de radars météorologiques et d'un modèle hydrologique distribué pour la prévision de crue en temps réel. *Hydrological sciences journal*, *49*(6).

VITA

The author, Amanda Tancreto, began studying Civil Engineering at the University of North Florida (UNF) in 2008. In 2011 she began her career at the U.S. Army Corps of Engineers as a Civil Engineering Student Co-op in the Project Management Division for Water Resources. She received a Bachelor of Science in Civil Engineering from UNF in the spring of 2012. After graduation, she was accepted into the UNF Graduate School, Civil Engineering Department with a concentration in Water Resources Engineering. During this time she also became a Department of Army Engineer Intern, where she was afforded the opportunity to work in multiple different sub-disciplines of civil engineering for the Corps of Engineers. In 2014 she became a hydraulic engineer in the Water Resources Engineering branch of the Corps. She anticipates graduating from UNF with a Master of Science in Civil Engineering in July, 2015.